Hybrid Biocomposites with Starch Derived Nanoparticles and Cellulose Fibers

by

Injla Khan

A thesis
presented to the University of Waterloo
in fulfillment of the
thesis requirement for the degree of
Master of Applied Science
in
Chemical Engineering

Waterloo, Ontario, Canada, 2017

AUTHOR'S DECLARATION

I hereby declare that I am the sole author of this thesis. This is a true copy of the thesis, including any required final revisions, as accepted by my examiners.

I understand that my thesis may be made electronically available to the public.

ABSTRACT

The use of natural polymers such as starch and cellulose in composites has gained significant popularity due to two main reasons: i) biopolymers increase the ratio of biodegradable and renewable content in most fossil-based polymer matrix composites and ii) their low density and high specific strength allows for a multitude of tailored material properties which can cater to industries such as automotive, biomedical and food packaging, construction etc. The purpose of this work was to evaluate composites the use of cellulose fibers, starch granules and novel starch-based biopolymer nanoparticles as fillers in polyolefins matrices and to investigate their mechanical and thermal properties. Several formulations were prepared and evaluated in order to further understand the effect of these fillers and matrices. Two types of cellulose fibers were used, regular ground cellulose pulp and Cellulose Fiber Type 2 pulp. Two grades of linear low-density polyethylene (LLDPE) and one grade of polypropylene (PP) were used as matrices and two types of native starch granules and two grades of amorphous starch-based biopolymer nanoparticles were used.

The aim of this research was to determine individual and synergistic effect of formulation components on the mechanical properties, with special attention to flexural modulus, flexural strength and impact strength. The effect of filler on the polymer flow was evaluated by measuring melt flow index (MFI). The thermal properties were evaluated by measuring glass transition and melting temperatures. The effect of the fillers on the crystallinity was also measured. The morphology was studied using microscopy (SEM) and crystallinity of composites measured by X-ray diffraction (XRD) and calorimetry (DSC).

ACKNOWLEDGEMENTS

I would like to express my sincerest gratitude to Dr. Leonardo C. Simon, my supervisor, for providing me with the opportunity of research and for all his assistance, guidance and supervision through my graduate research.

I also would like to thank Dr. Boxin Zhao and Dr.Michael Tam, my thesis committee members, for accepting to be readers of my thesis, and for all their help and guidance.

I would also like to thank my friends in Dr. Simon's lab, for all their support and help, and to the co-op students, Amrita Gill, Khadija Asad and James Kim who helped with many parts of the experimentation. I would especially like to thank Dr. Charles dal Castel, for his mentorship, training and wise insights throughout the course of my work.

Furthermore, I would like to acknowledge the financial support and assistance provided by the project sponsors, ECOSYNTHETIX Inc. for their financial assistance as well as for their guidance and valuable input. As well as financial support from Natural Science and Engineering Council Canada (NSERC).

Lastly, I would like to thank my family and friends in Pakistan, and here in Canada, for their love and encouragement that has enabled me to get through this time. Without the balance their affections have given to my life, I would not have been able to do my work with such zeal and commitment.

DEDICATIONS

To Umar, my husband and friend, for the love,

For the jokes and laughter,

And most of all, for paving the way for me.

TABLE OF CONTENTS

LIST OF FIGURES

LIST OF TABLES

LIST OF ABBREVIATIONS

A
ASA: Alkenyl Succinic Anhydride
Abs: Acrylonitrile Butadiene Styrene

B
BPE: Bio Derived Linear Low Density Polyethylene
BSD: Back Scatter Display
BKP: Bleached Kraft Wood Pulp
BNP: Biopolymer Nanoparticle Derived From Starch

C
CF1: Cellulose Fibers Type 1
CF2: Cellulose Fibers Type 2 (Freeze Dried)
CNC: Cellulose Nanocrystals
CNW: Cellulose Nanowhiskers

D
DSC: Differential Scanning Calorimetry
DTA: Differential Thermal Analysis
DP: Degree of Polymerization

E
EAA: Ethylene Acrylic Acid (Eco-compatibilizer)
EVOH: Ethylene Vinyl Alcohol (copolymer)
EPDM: Ethylene Propylene Diene monomer

F
FTIR: Fourier-Transform Infrared

H
H-BNP: Hydrophobic BNP
HDPE: High Density Polyethylene

L
LDPE : Low Density Polyethylene
LLDPE: Linear Low Density Polyethylene

M
MA: Maleic Anhydride
MWCNT: Multi-Walled Carbon Nanotubes
MW: Molecular Weight
MFI: Melt Flow Index
MI: Melt Index (same thing as MFI)
MMT: Montmorillonite Clay
MPa: Mega Pascal

N
NMR: Nuclear Magnetic Resonance

O
OSA: Octenyl Succinic Anhydride
OH: Hydroxyl

P
PA 6,66: Polyamide 6,66
PBAT: Poly Butylene Adipate-co-Terephthalate
PBS: Polybutylene Succinate

PCL: Polycaprolactone
PE: Polyethylene
PET: Polyethylene Terephthalate
PEG: Polyethylene Glycol
PE-*g*-MA: Polyethylene-*graft*-Maleic Anhydride
PE-*g*-MA (H): Polyethylene-*graft*-Maleic Anhydride with High Maleic Anhydride Content
PHBV: Poly(3-hydroxybutyrate-*co*-3-hydroxyvalerate)
PHA: Polyhydroxy Alkanoate
PP: Polypropylene
PLA: Poly Lactic Acid
PP-*g*-MA: Polypropylene-*graft*-Maleic Anhydride
PPGBE: Poly(propylene glycol) monobutyl ether
PTHF: Polytetrahydrofuran
PI: Phenyl Isocyanate
PVC: Polyvinyl Chloride
PPC: Polypropylene Carbonate
PVOH: Polyvinyl Alcohol

R

RPE: Injection Molding Grade Polyethylene

S

SEM: Scanning Electron Microscopy
SNP: Starch Nano Particle
SNC: Starch Nanocrystals

T

TGA: Thermo-Gravimetric Analysis
TPS: Thermoplastic Starch

U

UV: Ultra Violet
UTS: Ultimate Tensile Strength

W

WAXD: Wide Angle X Ray Diffraction

X

XRD: X Ray Diffraction

1. INTRODUCTION

1.1 MOTIVATIONS

The fluctuations in crude oil costs directly affect the cost of petro-derived polymers in the 80's & 90's. This uncertainty of costs pushed the industry to search for alternative materials that are more sustainable and are derived from agricultural or natural origins reducing the dependency on fossil fuels. Moreover, European countries and USA, amongst others, have now implemented a government push by providing tax incentives on the use of biobased polymers and biocomposites, and have introduced new taxes and stringent regulations on petroleum derived polymers. USA Department of Energy has set goals of increasing the share of renewable sourced chemicals to 10% by 2020 and to 50% by 2050. The use of natural fibers and fillers in composite materials has thus been widely researched after the introduction of this subject in the United Nations Conference on Trade in 1996. And the work on 'biocomposites' has continued to flourish as a viable alternative to fossil-derived, unsustainable, environmentally unfavorable materials for applications in all walks of life. [1]

A complete life cycle analysis performed by VanDam and Bos in 2004 showed that an overall efficiency advantage in using natural fibers vs synthetic fiber can be achieved while expending only 10-15% of the energy used for manufacturing PP or glass fibers. With over thirty five thousand research articles published on biocomposites, this is a budding field in material sciences possessing massive prospects and potential for mass commercialization. [1]

In addition to the established applicability of biocomposites in the automotive, construction and structural industries, relevant research in the near future in the area of nanoparticles and biocomposites can enable further applications, like food packaging for example, by increasing preservation for fresh foods like vegetables and fruits. More specifically, in addition to increasing the barrier properties and strength of the packaging, the nano-structure of the fillers can prevent bacterial contamination. Furthermore, it is expected that smart packagings will indicate to the consumer when the product has expired. The complete horizon of possible applications of biocomposites and nano-biocomposites is limitless given the infinite material combinations. [1]

1.2 RESEARCH CHALLENGES

1.3 OBJECTIVES

Natural fibers and fillers have been successfully applied as reinforcements and dispersants in polymeric composite materials. The purpose of using bio-based dispersants in composites ranges from mechanical property enhancements, improvement of thermal, electrical, barrier properties to inducing biodegradability or compostability, and often times only to offset the ratio of fossil derived to natural raw materials to achieve a more 'green' material.

Due to their global abundance, natural fibers and starch have been the most widely tested and used raw materials for use as biocomposite reinforcements. They are often used in their natural state, and sometimes modified to suit a variety of applications or to fit certain property profiles. Amongst these modifications are physical and chemical treatments, grafting, and functionalization through replacement of hydroxyls on the saccharide unit. One of the more recent approaches, still under exploration, is the modification of these raw materials to a nanoscale and to study their effect in and interaction with various matrix materials. Cellulose nanofibers and nanowhiskers have been reported as effective fiber dispersants for mechanical reinforcements as well as for improvement of other properties such as thermal stability

and so on. Starch nanocrystals have also been used in rubber and thermoplastic matrices and have been reported as effective fillers.

The research on establishing concrete property relationships with this 'nano' approach is still underway and a wide array of interpretations is found in literature. It appears from most works that this correlation is highly dependent on the type of fillers used, the method of extraction of the nanoparticles, and more so on the type of base matrix used and the type of co-additives used in the nanocomposite. This forms a complex situation where testing different materials in different combinations is of value due to possible synergistic property enhancements. The reason this is different from most macro-scale composites, is because the interphase of the dispersants and matrix has long been assumed to have a unique set of characteristics, different from those of the matrix or the filler itself. By using nanofillers this interphase ratio in the composite increases many folds, and is thus predicted to have unique material properties which may effect, greatly, the way different fillers interact within the composite.

This brings us to the prime objectives of this current work. The foremost objective was to investigate the effect of using fully amorphous starch derived nanoparticles in a thermoplastic base matrix, which has not been assessed so far. As mentioned by many experts in the field, amorphous starch derived nanoparticles have been mostly limited for use as binders in paper manufacturing while starch nanocrystals have dominated the bio-composites research market as fillers, and it is of essential value to study both in the other application. This current work studies the effect of using starch nanoparticles derived from a regenerated route in polyolefin matrices such as LLDPE and PP. The use of different, conventionally accepted, compatibilizers was studied and these composites were also compared with composites using granular starch to find the feasibility of using a nano sized filler instead. Moreover, since it is an established challenge to achieve good dispersion of hydrophilic fillers in hydrophobic matrices, effective ways to achieve nano-dispersion of the hydrophilic polysaccharide starch nanoparticle filler aggregates was investigated. The mechanical and thermal properties of the bio-nanocomposites was investigated and their morphological characterization was performed to obtain better understanding of the nanofiller-matrix behavior.

The second objective of this work was to investigate the synergistic or co-performance of these starch nanoparticles with softwood cellulosic pulp. The reason of studying this is twofold, first is based on a new approach or theory presented in literature which predicts the possible effect of nanofillers as 'selective dispersants' or 'phase compatibilizers' between the components of a multi-phase blend or composite. This, at surface value, seems a viable approach considering the chemical similarity of cellulose and starch, and as such starch based nanofillers may behave as either phase compatibilizers or dispersant, or both, for cellulose fiber reinforced polyolefin composite where cellulose aggregation is encountered as a common challenge in the manufacturing of natural fiber-polyolefin composites. The second is to study the performance of the composite with both, a particulate nanofiller and a fiber in conjunction. Few works have been reported where natural fibers and starch filler were used together in a thermoplastic matrix and it is of value to study the use of both reinforcements in formulations together. These hybrid composites were also studied for mechanical performance, thermal properties and for morphology to develop a sound understanding of the individual and synergistic effect in the composite.

1.4 STRUCTURE OF DOCUMENT

Chapter one discusses the motivations and objectives of the research work.

Chapter two is a summary of relevant literature, a bird's eye view of biocomposites and their relevance, a thorough study of the components especially materials used in this work, processes and properties that are also to be used in this research, and discussion of similar works. The understanding from this chapter is later extended in observing results of the research conducted.

Chapter three lists all materials and equipment used in the course of this work and also explains all the procedures used in the experiments carried out.

Chapter four present all results from experiments, and discusses these results to obtain relevant understanding.

At the end of the document a short conclusion and recommendations for future work are presented.

2. LITERATURE REVIEW

2.1 BIOCOMPOSITES: INTRODUCTION AND APPLICATIONS

The planet's depleting fossil fuel reservoirs and the ever fluctuating costs of petroleum and petrochemical products has resulted in a global drive towards sustainability in manufacturing practices. The materials industry has an increased interest in alternative materials that can provide competitive properties at lower costs whose resource is sustainable and available in abundant supply. Composites utilizing bio-based renewable reinforcements in synthetic polymer matrices are rising as a viable solution since these fit the criteria and allow for environmental compatibility in the design framework. An illustrative example is the successful application of natural fiber filled PE and PP composites in the automotive interiors industry. According to a study 250 million barrels of crude oil can be saved just by reducing a vehicles weight by 25%, in turn reducing carbon dioxide emissions by 220 billion pounds per annum. Wood based plastic composites are also a very popular example of biocomposites where they are used in structural applications such as decking, fencing, bridge constructions etc. [2]

The most successful application of biocomposites (natural fiber reinforced) has been in the automotive industry. Kenaf and bamboo filled composites have been used successfully as tire covers and tailgate trims respectively. The notion of a car developed with fully bio-based materials is not far from reality. The 'Agri-car' was developed at University of Akron and Ohio University with a 90% biodegradable materials. [1]

Cellulose and starch are the two most abundant organic [compounds/materials] in the world, and naturally they have been the subject of immense research and development to fulfill the material industry's changing needs in the 20th century. Cellulose has been widely recognized as a reinforcing fiber due to its structural integrity and the mechanical properties it provides, while starch has been studied both as a particulate filler as well as a matrix material in the gelatinized state. Both materials are extremely light weight, low cost and are readily available worldwide. Also, owing to their inherent structure, they both are easy to modify chemically. The area of constant research and improvement with these materials is their high moisture sensitivity, low compatibility with hydrophobic polymers and their low thermal stability. The addition of cellulose fibers and cellulose microfibrils in PP matrix has been successfully marketed as odorless, moldable and colorable composites to be used in a wide range of applications from packaging, to automotive, to construction etc. Some commercial products are NCell by GreenCore Composites that uses 40% cellulosic microfibrils in PP, UPM's ForMi that comes in different grades in granule form and Thrive by Weyerhaeuser also available in a multitude of grades, some using recycled PP as well. Other uses of cellulose based biocomposites include structural construction material, stay in place bridges, furniture, window and door fixtures [3].

Nanocomposites comprise of nanoscale fillers and/or fibers; and have been the topic of attention in the recent times. With smaller sizes, the interfacial area between phase increases and the distance between particles becomes smaller imparting a unique enhancement in the macroscopic material properties due to particle-particle interactions. Compared with micrometer scale reinforcements, better property enhancements are possible without compromising impact properties and elongation at break when smaller amount of nano-scale reinforcements are used.

However, the commercial unavailability of nano-scale natural reinforcement materials and their tendency to aggregate when used in higher loadings in more hydrophobic matrices limits the scope to research experimentation or specialized applications. One such niche application was in the works at LEIPMI

(Laboratoire d'Electrochimie et de Physico-chimie des Materiaux etdes Interfaces) using cellulose nanoparticles in electrolytic nanocomposites for lithium batteries. Cellulose nano-fiber composites also have much scope in applications such as optical devices, magnetic strips and biosensors due to the ability of attaining desired morphological orientation under the influence of magnetic field, and the ease of chemical modification. These composites can also be used as flexible, biodegradable electrical devices. Optically active films made out of cellulose nano-fibers can also find use in security papers, passports, currency, electoral cards etc. [2]

Nanoparticles derived from cornstarch have been identified as potential replacements of carbon black and silica used as filler in automotive tires. Novamont (Italy) and Goodyear Tire and Rubber are now collaborating to develop tires filled partially with these starch nanoparticles to reduce the pollution resulting from the use of carbon black.[1]

Chemical modification of starch and cellulose with siloxanes, isocyanates, carboxylic anhydrides and epoxides can provide functionalities on the starch and cellulose surface via reaction with the hydroxyl groups, such functional modification can theoretically improve the interface bonding, and potentially improve barrier and mechanical properties. [4][2]

Biocomposites made of matrix derived from an agricultural/biological source and reinforced by natural fibers or fillers are called 'green composites', they are fully degradable, sustainable and environmentally friendly. These composites are very suitable for consumer products with a short lifecycles such as food packaging since they can easily degrade after disposal, minimizing waste associated with these applications.[5] Cassava starch based films are used as food packaging and are odorless, colorless, non-toxic and fully biodegradable. Another attractive option is the use of polysaccharide nano-fillers in biocomposites, due to their high surface area to mass ratio they generally tend to degrade faster and bring all the advantages of using a natural vs fossil derived polymer. [1]

Biocomposites, of nano scale in particular find extensive use in the food industry. As packagings they are not only non-toxic and biodegradable, but also aid in extending the shelf life of the packaged food and also enhance its properties. They also carry important functions like the delivery of antioxidants and antimicrobials. Another application of biobased materials, biocomposites and starch based biocomposites is in the agriculture industries where they can be successfully used as mulches, silage films, bale wraps etc. Successful experiments have been conducted with these materials as mulches for growing of strawberries, melons, maize and cotton. This promotes environmental sustainability, reduces the waste associated with disposal, or the pollution from burning mulches, in addition to reducing soil contamination.[1]

The following figure gives a good visual summary of the performance, competitiveness, sustainability and applications of natural fiber reinforced biocomposites and this can be extended to starch filled biocomposites as well:

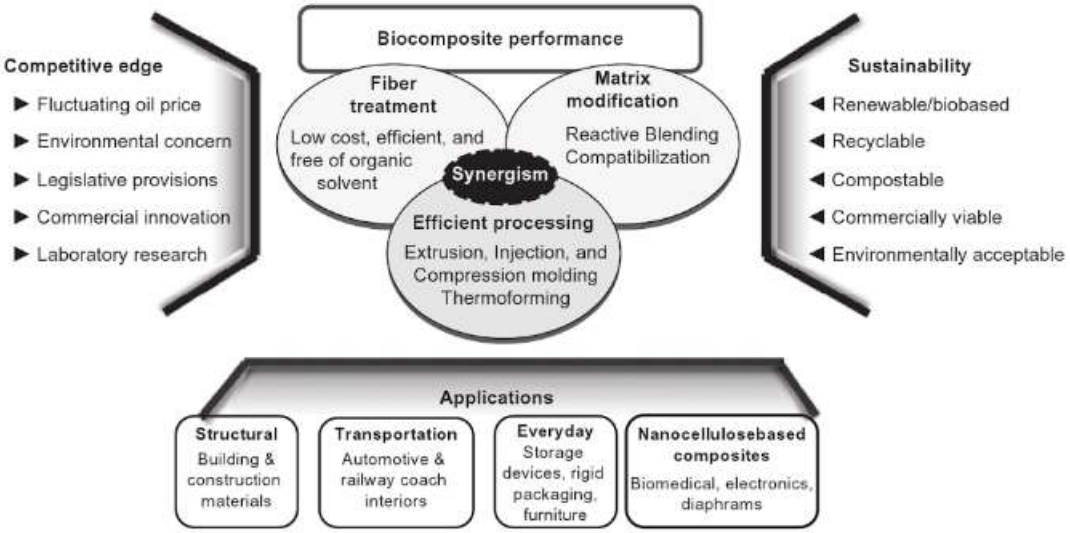

Figure 2-1 Performance, Competitiveness, Sustainability and Applications of Biocomposites [2]

2.2 BIOCOMPOSITE PROPERTIES

Biocomposites present a viable solution for effective reduction and eventually elimination of non-degradable waste in landfills and water bodies. The incorporation of biodegradable reinforcements in non-biodegradable matrices helps controls the overall environmental impact of the composite and keeps the costs low that are needed to meet market demands. The global market of biocomposites has grown substantially over the years, from 771 million kg in 2002 to 8.7 million tons in 2011 [2]. This climbing interest in biocomposites has in turn spiked the research being done in this field in the past decade.

Biocomposites, or composites, in general are composed of two phases, the continuous phase, termed as the 'matrix', and the discontinuous phase, often called the 'reinforcement' or the 'dispersant'. Usually the mechanical properties of the composites are higher than the matrix phase, but the dispersants are not always present for reinforcements, these could added to promote other properties or features of the composite such as biodegradability, optical properties etc. The undeniable advantage that composites present is the opportunity of tailorability of properties to fit niche application requirements while keeping costs and processing complexities to a minimum.

The following chart gives a good description of the common raw materials of biocomposites and their biodegradability and the renewability of their sources:

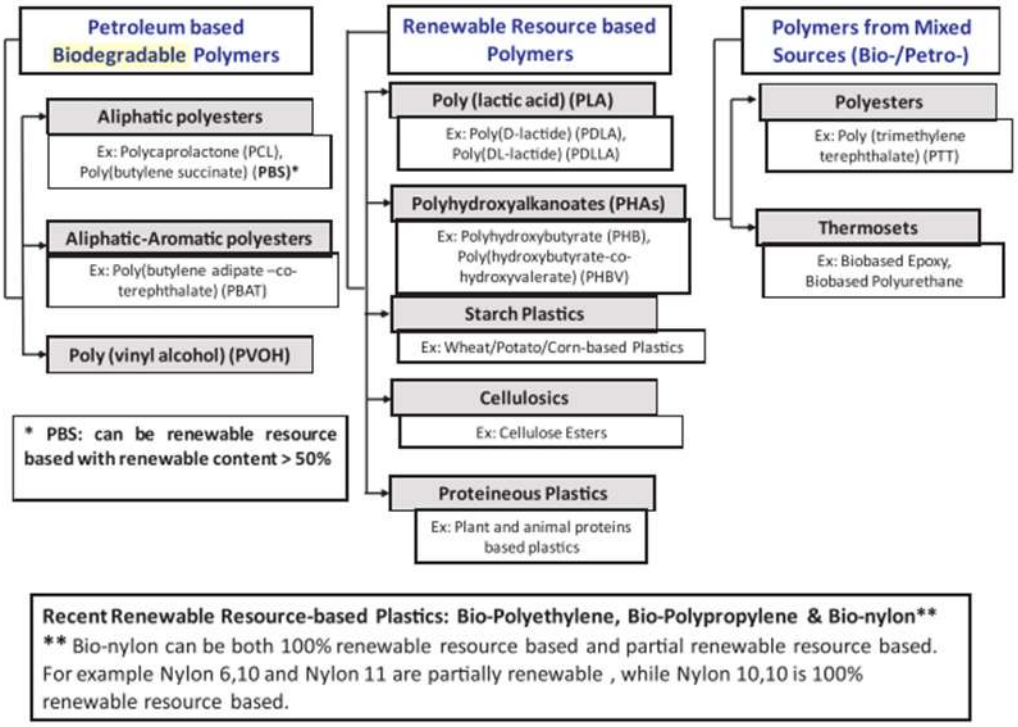

Figure 2-2 Common Base Raw Materials for Biocomposites. [6]

The properties of composites often follow a rule of mixtures, while at times there are synergistic effects on the overall properties owing to unique interactions between the phases and this effect is more enhanced or noticeable in nanocomposites.

Biocomposites are termed as nano-biocomposites or simply nanocomposites when the size of one or all the fillers/fibers goes from a macro to a nano scale. In order for a composite to be considered a nanocomposite, at least of dimension of the particle must be of the 1-100nm scale range. The interfacial area of the matrix-dispersant increases hugely when the fillers are that small, up to 700m^2/gram for fully exfoliated phyllosilicates for example, and therefore this phenomenon predicts the materials macro-properties and behavior which is often times not truly representative of either of the components independently. [2] Another advantage that nanocomposites have over macro composites is the favorable balance of strength and toughness which is often compromised with rigid macro-reinforcements. The small size of the fillers allows modulating properties of a neat polymer such as, barrier performance, thermal stability, biocompatibility, biodegradability, and melt viscosity which are also lost with macrofillers. They also provide better property enhancements at relatively low loading levels.

Very little work has been reported however, using reinforcements of two or more different types, and fibers of different lengths. It has been shown that longer fibers lend to improved modulus and strength but compromise the elongation at break while shorted aspect ratio favors the better offset on impact properties and toughness. Thus by using a combination of fiber types, an optimal region of property enhancement could be attainable in what may be considered hybridized composite systems [2].

Due to the inherent light weight of natural fibers and fillers, biocomposites reinforced with natural fibers or fillers have a light weight, high specific strength and the advantage of being mostly biodegradable,

compostable or recyclable. They find use in applications such as automotive parts, packagings, furniture, construction, decking, electrical housings, household and consumer goods and musical instruments.

The disadvantages associated, with mostly natural fiber/filler, based biocomposites lie in poor moisture resistance, low thermal stability, low temperature processing, and mostly in the poor wettability with most commodity plastic matrices that have hydrophobic surface characteristics. This low interaction between phases is a barrier towards achieving the maximum mechanical benefit derivable from the composites and is therefore a prime focus of research and development.

2.2.1 MATRIX PHASE

The matrix is the continuous phase of the polymer composite and contributes to macro-scale properties such as appearance, environmental susceptibility, and durability. It acts as the binder for the dispersed phase of the composite. It also controls the processing conditions such as the extrusion/molding temperature.

2.2.1.1 Thermoplastics

The most common matrix materials used in biocomposites are petroleum-derived commodity plastics such as PE, PP, and PS etc. which represent 80% of the entire plastics markets. Companies are now developing 100% bio-based Polyethylene, the Green PE by Braskem is the most relevant commercially available PE that is made from ethylene monomer that comes from ethanol derived from sugarcane biomass, widely available in Brazil. The properties of the PE are identical to fossil derived PE, it is recyclable and can be manufactured in the same way and in many different grades (topology/MW etc.).

Polyethylene has been used as matrix material with a number of different natural fiber reinforcements such as rice hull fibers, soya powder, carua, rice straw, hemp, bagasse etc. [7] It has also been used with starch, chitosan, chitin and other natural particulate filler reinforcements. A more extensive discussion on PE based biocomposites and their properties is presented in the later sections.

There has been extensive work using PP as matrix material reinforced with wheat straw. Fatoni, Sardashti and other have reported extensive properties; mechanical, thermal and morphological, as well as the effect of various co-fillers such as clay and different compatibilizers and treatments of the fibers for improved composite performance [8][9]. Oduola and Akpeji tested PP as matrix with tapioca starch as filler between 5 and 50%, they reported improvement in flexural modulus and Impact strength with optimum loading being 30% starch, while elongation at break and MFI of the composite were negatively affected. [10]

2.2.1.2 Bioplastics

The term Bio-polymers covers all polymeric materials that are derived from renewable biological resources or are biodegradable; whether derived from renewable and bio-based resources or not, or both. Bioplastics are biopolymers that can be processed like plastics. The trend of using bioplastics as reinforced (matrix) phase in composite materials is continuously increasing. A rapid growth of bioplastics production in the market is forecasted, it is expected that the production volumes would have increased from 0.36 million metric ton in 2007 to 2.33 million metric ton in 2013 and will continue to rise to 3.45 million metric tons in 2020. [7]

Table 1 gives a list of biodegradable polymers that can be used as matrices in bio-composites.[5]

Table 1 List of Polymer Matrix Materials [5]

Natural and biodegradable matrices	
Biodegradable polymer matrices	
Natural	Synthetic
1. *Polysaccharides*	1. Poly(amides)
Starch	2. Poly(anhydrides)
Cellulose	3. Poly(amide-enamines)
Chitin	4. Poly(vinyl alcohol)
2. *Proteins*	5. Poly(vinyl acetate)
Collagen/gelatin	6. Polyesters
Casein, albumin, fibrogen, Silks	6.1 Poly(glycolic acid)
3. *Polyesters*	6.2 Poly(lactic acid)
Polyhydroxyalkanoates	6.3 Poly(caprolactone)
4. *Other polymers*	6.4 Poly(orthoesters)
Lignin	7. Poly(ethylene oxides)
Lipids	8. Poly(phosphazines)
Shellac	
Natural rubber	

PHA's are a family of thermoplastic polyesters which have properties similar to PP but with drawbacks such as brittleness, low processing temperature range and thermal stability. These problems can be overcome by copolymerization with other polyesters. This however makes the cost of the material much higher than the commodity plastic PP, and the high cost does not offset the biodegradability advantage.

Thermoplastic starch, PLA and PHA are considered as the highest volume production bioplastics [7]. PLA possesses the ease of processing via conventional processes such as extrusion, injection molding, casting, blow molding etc. and can be used for applications such as food packaging, compostable bags, textiles and pharmaceutical applications as well. PLA composites have also been used to develop model kayaks, laptop and phone bodies and turbine rotors [2]. PBAT is another thermoplastic polyester often used as a suitable thermoplastic matrix in biocomposite given its biodegradable nature. It has similar processing and mechanical properties as PE but is more expensive, it possesses good thermal and excellent toughness. The biodegradability of PBAT is similar to PLA but much higher than natural polymers like starch.[11]

PBAT, PBS and PCL are biodegradable but derived from fossil fuels, and owing to their biodegradability are considered bioplastics. PBS is a semi-crystalline material and is an attractive bioplastic due to its thermal stability, ease of processing, and mechanical properties similar to polyolefins. It is commonly used in film based applications such as mulches, bags, laminates etc. PBAT is also used in similar applications as PBS. Both these thermoplastics are often used as matrix materials in composites to either improve poor qualities; example water permeability, or due to their inherent functionality which makes them suitable for fillers like starch and cellulose to provide strong interfacial attraction within the material. [2]

Starch is also used in its plasticized or gelatinized form (TPS) very commonly as a matrix in biocomposites, often with natural fibers, cellulose and sometimes clay and carbon-based nano fillers. TPS based starch composites find use in applications such as food packaging, compostable packaging, agricultural applications such as pots, mulches, pegs etc., personal hygiene products and personal care applications.[2]

2.2.2 REINFORCEMENT/DISPERSED PHASE

The reinforcement phase is the discontinuous or the dispersed phase in the composite. The reinforcements are either in the form of longitudinal fibers, whiskers or rods while particulate fillers may be spherical, platelets, layered, or irregular shaped particles with smaller aspect ratios.

The most effective reinforcement in composites is achieved when the reinforcing fibers or fillers are well dispersed and have good adhesion with the matrix phase. Better distribution and dispersion of reinforcements throughout the matrix lead to better and more uniform modulus values. Orientation of dispersants that have high aspect ratios also provides higher mechanical properties in the direction of orientation compared to the transverse direction. The adhesion between the reinforcements phase and the matrix determines the efficacy of stress transfer between the phases, a stronger bonding between two supplies better properties and voids or debonding of the interphase leads to poor mechanical strength and impact properties due to inefficient stress-transfer or crack propagation.

Other aspects of the reinforcement phase that effect the macro-properties of the composite include size and shape of the dispersed phase. A smaller reinforcement will generally show better impact properties and toughness than larger sizes. Regular shaped particles will generally exhibit better tear properties in film composites. Moreover, these aspects also effect moisture barrier, degradation and more. Composites having reinforcements with more complex morphologies such as layered silicates, will have properties heavily dependent on the extent of exfoliation of clay galleries, bonding etc. Reinforcements with smooth surfaces often favor unique phenomena like transcrystallization that skew the properties of a composite away from a nominal values based on the rule of mixtures.

Nano scale reinforcements bring a peculiar set of properties in composites. The interface of matrix-filler where stress transfer takes place increases drastically at a much lower loading level. Due to the small size the crystalline structure and order of crystallinity are also changed. Formation or disruption of intermolecular bonds and steric hindrance due to rigid nanoparticles are also some of the unique characteristics of nanocomposites. If the size of the reinforcement is less than 200nm, smaller than the wavelength of visible light, the composite will tend to have better optical clarity. [1]

2.2.2.1 Fiber Reinforcement

Fiber reinforced polymeric materials date back to 1908 when cellulose fibers were used in phenolics, then urea and melamine. Today the fiber-reinforced materials make up a multi-billion dollar industry. These materials find applications in fields like automotive, construction, marine and electronic components.[5] Up to 50% of the matrix can be replaced with natural fibers to improve the ratio of environmentally friendly components of the composites, for injection molded processes and even more than 50% for compression molded composite. [2]

Glass Fibers are the most commonly used reinforcements for polymeric composites, they are cheap compared to the higher performing aramid or carbon fibers and have fairly decent mechanical performance. They are largely used in applications such as sporting goods, aerospace, automotive and construction applications. However, due to very strict disposal regulations for glass filled materials in many countries and the ban on mineral fibers like asbestos, natural fibers can be a suitable alternative in many applications. They are often cheaper, and not abrasive compared to synthetic fibers that cause much wear to processing equipment, and are also CO_2 neutral. They also eliminate the dermal contact hazards and respiratory irritation associated with glass fibers providing a safer manufacturing

environment. Natural fibers possess high specific strength and moduli while their density is lower than E-glass fibers, and the light weight of the resulting composites is an added advantage in certain applications like the automotives where light weight translates to better fuel consumption. The works of many authors have shown that the specific mechanical properties of natural fiber filled composites is relatively comparable to E-glass reinforced composites; hemp, kenaf and sisal in particular have been shown to have comparable tensile strength, modulus and impact properties [12]. Some sources cite that flax and soft wood fibers come closest to the physical properties of glass fibers.[13] The mechanical properties of fibers depends on a variety of factors such as age of plant, origin, growing conditions such as soil, climate and weather and also on processing conditions such as spinning, cutting etc. The range of mechanical properties is very wide and is reported extensively in literature for different natural fibers.

Fibers derived from a natural source can be classified as softwood, hardwood or non-wood fibers. A detailed classification of natural fibers and some examples is visualized in Figure 2-3 [14]

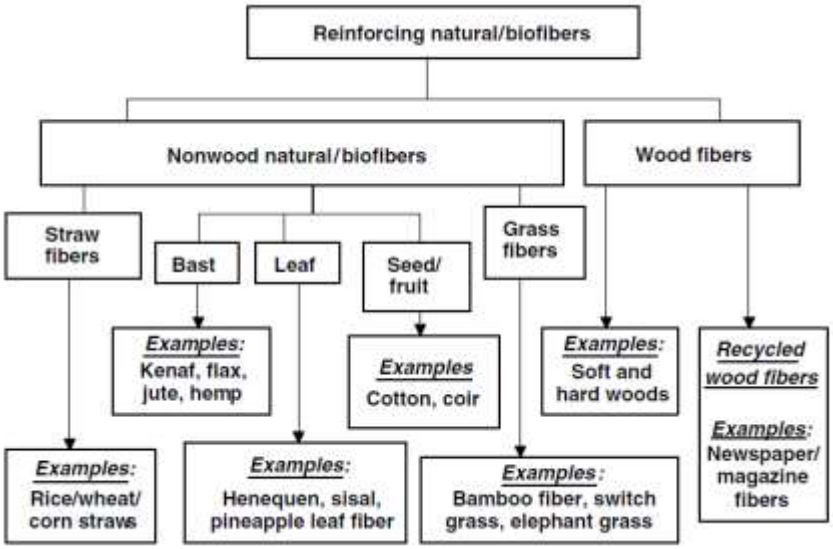

Figure 2-3 Classification of Reinforcing Natural Fibers [14]

Natural fibers in themselves are composites with cellulose being the reinforcing crystalline microfibrils (Fig 2.5-1), lignin acts as a matrix; it is a high molecular weight phenolic polymer that provides the structural support to plants and cements the cellulose and hemicellulosic polymer. The hemi-cellulosic are amorphous polysaccharide units with DP 50-300 and highly branched chains. When used in composites, each component of the natural fiber is responsible for a different characteristic, hemicellulose for example determines the composites moisture absorption and biodegradability, lignin is thermally stable but makes the composite susceptible to UV degradation [3]. The ratio of cellulose in natural fibers depend on the plant origin and has defining effect on final mechanical properties. Due to this inherent variation in plant matter it becomes a challenge to maintain accurate consistency in natural fiber filled composites. The other challenges associated with natural fibers are their compatibility with synthetic polymer matrices, low temperature range of processing and high moisture uptake and UV sensitivity. They are also more susceptible to microbial attack and rotting. [5] Some physical and chemical treatments that fibers often undergo to overcome one or more of these challenges are; surface fibrillation, corona treatment, electric discharge, steam treatment and alkalization, silanization,

acrylation, peroxide graft copolymerization and other forms of changing chemical functionality respectively. [2]

Amongst other factors, as mentioned earlier, the shape and the length of fibers also has a relationship with tensile strength and modulus, up to a certain length after which the two become constant. The fiber length also effects the impact strength of the composites, but contradictory relationships have been shown by researchers where some show a shorter fiber length to provide better impact properties while others relate longer lengths with better impact properties (up to a certain length after which the property plateaus out) [3].

2.2.2.2 Filler Reinforcement

The most abundantly used inorganic filler in composites is calcium carbonate and has proved to be an effective mechanical reinforcement for a number of thermoplastic matrices. In comparison to inorganic fillers, however, natural fillers have a lower density and enable light weighted composite while being environmentally safe and renewable. [2]

Various shapes of fillers are used in composites ranging from spherical, layered, tubular, rod, tridimensional and irregular. The addition of rigid fillers or those that have strong interaction networks also increases the overall T_g of composite materials due to hindered chain mobility within the matrix material. Inorganic fillers such as MWCNT and clay tend to increase thermal stability of organic matrix composites since they tend to act as barriers and insulator to the transport of volatile compounds generated during decomposition. [1]

The use of nanomaterials as reinforcements shows improved material performance even at very low loading levels. Some nano-filler reinforcements include layered silicates popular due to their availability and the versatility of properties they bring to composites, carbon nanoparticles like carbon nanotubes, graphite and fullerene are common ones used to achieve high performance and specialized functions. The addition of nano fillers not only provides mechanical property enhancement but due to their unique properties and interaction mechanisms can also improve physical properties such as fire retardancy and permeability. [1]

The distribution and dispersion of nano-fillers is of significance for mechanical, thermal and morphological properties of the matrix. The shape, size, concentration, surface chemistry, functionality and interaction mechanism between filler and matrix determine how well it disperses in a given matrix. For examples, Cao et al. investigated the dispersion of MWCNT in a PS matrix and found that at any concentration>2%, large aggregates were formed when there were none at 1% loading. Similar trend was observed by Chang et al. who fabricated composites using chitin nanocrystals (with sizes in the range 50-100nm). A good dispersion was achieved at low filler loading (2%), however at higher ratio (5%) a distinguishable aggregation and agglomeration was obvious. [1]

The investigation of natural polysaccharide nanocrystals and nanoparticles of starch, chitin, chitosan, cellulose etc. is also popular in composites due to their renewability, sustainability and biodegradability in addition to the reinforcement effect they may produce. Starch has been used as a filler reinforcement with biodegradable plastics like PLA for over twenty years. [1]

Due to the high density of hydroxyl groups on such fillers a unique feature is the formation of a filler-filler attraction creating a percolating network of particles that extends the reinforcement properties. The

presence of an impenetrable network structure in nanofillers can greatly enhance the mechanical properties of the material. [1]

2.2.2.3 Other Additives: Plasticizers

Glycerol is a common plasticizer used in processing of starch thermoplastics and composites. Garcia et al. used SNC as filler in glycerol plasticized waxy maize starch and compared this with similar formulation using un-plasticized starch as matrix. The results from SEM done for cryofractured surfaces showed that the unplasticized samples had a smooth fractured surface while plasticized starch samples showed rougher, more fibrillar structure. This was attributed to a high degree of interaction between the glycerol and the SNC.

The mechanical properties of composites with plasticizers in their formulation also depend quite a lot on the humidity levels, it was shown that this effect is even more actualized with composite systems with nanosized reinforcements. The presence of glycerol in composite formulation reinforced with cellulose whiskers effected the otherwise strong network of interactions such as hydrogen bonds between the whiskers and thus reducing the reinforcement effect of the fibers. [1] However, Angelier et al. used SNP to reinforce TPS matrix and reported improved reinforcement with increased plasticizer (glycerol or sorbitol) content. The explained that the strong affinity of the plasticizer with both the matrix and the filler may have induced co-crystallization in phases and led to the reinforcement. [15]

Results have shown that the incorporation of fibers more than 50% loading levels in thermoplastic composites caused problems such as agglomeration of fibers and increased in MFI posing challenges in the melt processing during extrusion or injection molding. In order to aid processing external lubricants were added in the formulation, most often waxes, these are chemical that diffuse out of the melt and localize at the equipment-melt boundary to ease flow [2].

2.3 MATRIX: POLYOLEFINS

For biocomposites filled with naturally derived plant fibers, or agricultural biomass, or biobased particulate fillers such as starch that degrade at relatively low temperatures (~200°C) are most suitable used with a matrix that can be melt processed at lower temperatures. And thus, due to their low temperature processing range, diverse qualities and low cost make polyolefins ideal candidates for matrix material. The challenge lies in the hydrophobicity of polyolefins when mixed with natural fillers that are strongly hydrophilic. This challenge is the focus of most research around biocomposites made of polyolefin matrix [2].

2.3.1 POLYETHYLENE

Polyethylene is one of the most hydrophobic polymers with no polar groups in its structure (see Fig 2-4) and therefore, as a matrix material for biocomposites using fillers with highly polar groups such as hydroxyls on starch and cellulose, leads to very low interaction between the phases. The mechanism of stress transfer from the PE matrix to the fibers or fillers is poor, which accounts for low improvement in mechanical properties with failure mostly occurring at the inefficient junction of phases. Many researchers have studied the properties of PE based biocomposites and significant improvements have been made and are continued to be under investigation due to the highly favorable cost of PE and its exceptional and universal properties etc.

Kakroodi et al. studied the morphology of PE and flax biocomposites under an SEM and found gaps and voids between the two phases, they also observed fiber pullout all indicating the lack of interfacial

adhesion. This was translated in mechanical properties; although the properties increased up to 30% loading but tensile properties declined at further increment. Poor tensile properties are often associated with compatibility and stress concentration at the phase junction. The low compatibility of PE and natural fiber such as kenaf also proved disadvantageous to the process of transcrystallization; a phenomenon that further increases mechanical properties, as shown by Chen and Porter [2]. Extensive work has thus been done and has shown to improve this surface compatibility by either treatment of the fibers, by chemical modifications or by inclusion of additives that act as modifiers. A very comprehensive list of such work and the approaches used for compatibilization is presented the literature [2].

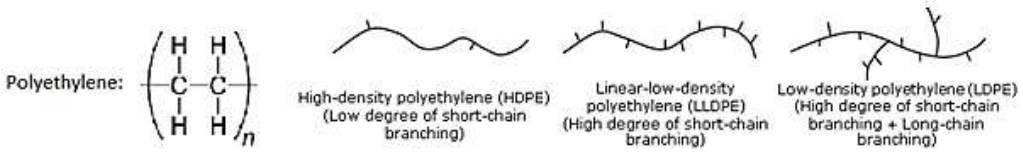

Figure 2-4 Chemical Structure of Polyethylene. Topology of HDPE, LLDPE, and LDPE

The grade of Polyethylene used in blends or as matrix in composites containing hydrophobic polymers such as starch or cellulose has also shown to effect the overall properties of the composite. Pierre et al. formulated sheets using starch gelatinized with 33% glycerol and 19% water and mixed them with two grades of PE; an LDPE with MFI of 12 g/10min and LLDPE of 6g/10min MFI. The results showed that the dispersed starch had a smaller particle size in the higher viscosity LLDPE compared to LDPE. The dispersed phase remained in a spherical particle shape in the LLDPE, due to longer chains not allowing enough coalescence of the dispersed phase, which was the case in LDPE at higher loading ratios where the form factor reduced to 0.7 (1 for sphere) and permitted biaxial deformation. The LLDPE also provided for a more homogenized dispersion. Another unexpected observation from this study was that the elongation at break for the sheets was maintained, contrary to the classical understanding of reduced elongation at break upon addition of a dispersed phase, even without a compatibilizer [16].

The introduction of fibers and fillers in a PE based composite leads to embrittlement and also compromises the otherwise exceptional impact properties of the virgin PE. In order to retain the impact properties, researchers like Oksman et al. and Clemons, used elastomeric copolymers such as EPDM and SEBS to act as impact modifiers in the composite and noted significant improvement in properties. It is predicted that virgin elastomers may function by encapsulating the fibers and thereby acting as surface modifiers. More work has also been done on using waste tire derived rubber as filler in conjunction with hemp fibers in a compatibilized PE composite resulting in considerable improvement in impact properties but also reduced the moisture uptake of the composite [2].

2.3.2 POLYPROPYLENE

PP is a semi-crystalline polymer with a hydrophobic chemical structure (see Figure 2-5), it is a non-degradable thermoplastic and unlike PE cannot be derived from environmentally sustainable raw materials. PP is however very cost effective and possesses very versatile mechanical properties, with high strength, modulus and good toughness while being very easy to process. It has been used as a matrix extensively with natural fibers to achieve very high mechanical properties and can thus be used in semi-structural applications, in automobiles and more.

The addition of biomass fillers in PP also gives rise to the transcrystallization behavior, the fillers are explained to localize in the amorphous regions of the PP chains and can act as nucleating sites increasing crystallinity. PP based wood plastic composites are widely used in outdoor applications such as decking boards, and so factors such as moisture barrier, thermal stability, UV susceptibility etc. have to be considered and are optimized by the use of additives and compatibilizers. PP composites have been fabricated with wheat straw, doum fibers, chicken eggshells, pineapple leaf fiber, flax and kenaf, chitosan, lignin and more such natural fillers [2].

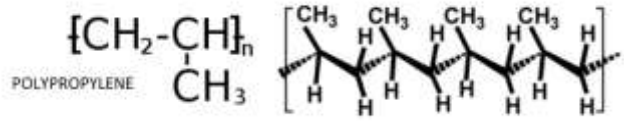

Figure 2-5 Chemical Structure of Polypropylene, Isotactic Conformation of most commercial PP products

2.4 STARCH

In terms of chemical structure (see Fig 2-6) starch is a polysaccharide consisting of D-glucose units also known as glucopyranose or homoglucan. The starch granule; obtained from the seeds, tubers and roots of various plants, is about 2-100μm in diameter and occurs in the form of alternating amorphous and semi-crystalline 'growth rings'. It is the main source of carbon and energy storage in plant matter. The two main chemical components of starch are amylose and amylopectin.

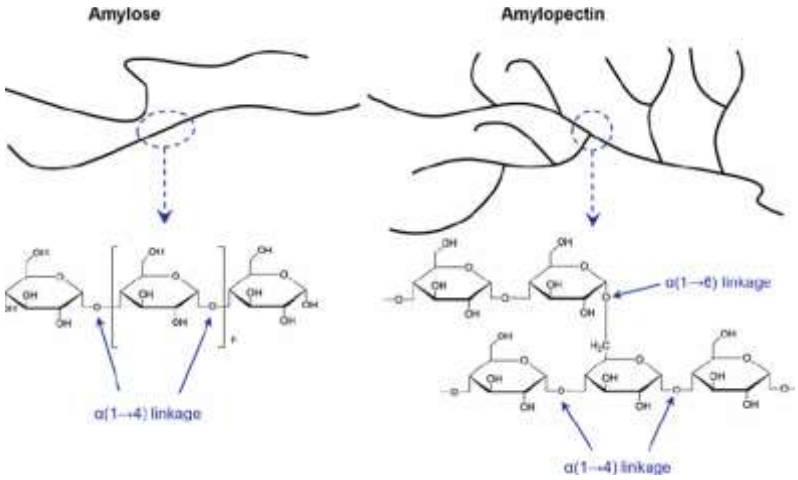

Figure 2-6 Chemical Structure of Starch, and distinction between Amylose and Amylopectin Chains

Starch also contains some degree of phosphorous and lipids that are capable of altering the properties during processing. The amylose is a highly linear structure with α(1-4) links with a molar mass of 10^5-10^6 g/mol and DP of around 600 and forms single or double helix semi-crystalline structure turning at every six glucose units. Amylopectin on the other hand is a largely branched structure and consists of 95% α (1-4) and 5% α (1-6) links. Branching points are at every 22-27 units and the resulting pendant chains have an appx. DP of 15 and are the main source of crystallinity in starch. Depending on the botanical source of the plant, starch granules have a crystallinity of 15-45% [2]. The crystal structure of starch is that of a double helix, with three types of configurations; A, B and C. The A type structure is that of tightly packed helices with water molecules in between, while the B type is formed by six double helixes surrounding

water molecules in the middle, the C configuration is a mix of A and B.[1] Figure 2-7 gives a detailed description of the components of the starch granule:

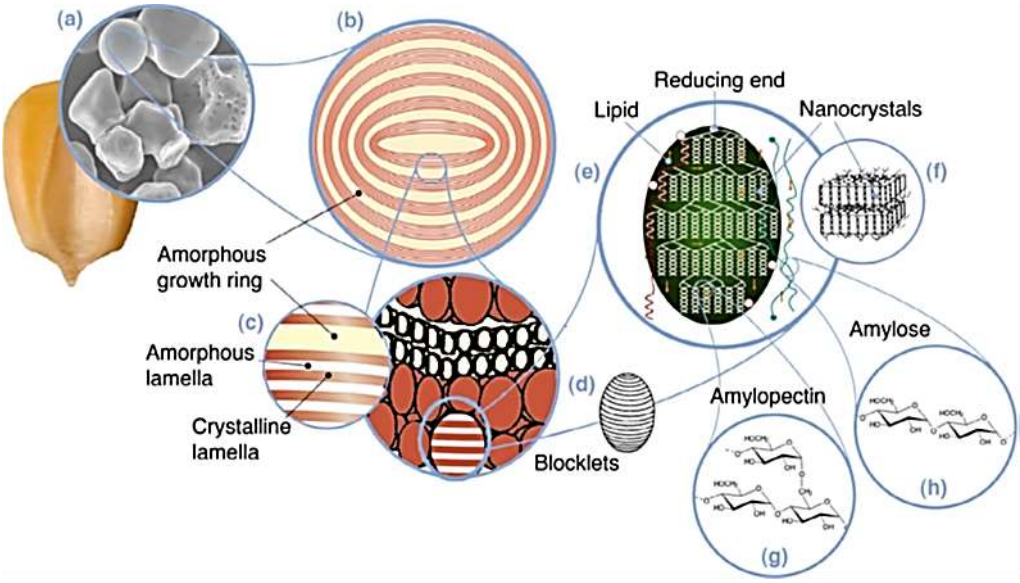

Figure 2-7 Starch multi-scale structure. (a) Starch granules from normal maize (30 µm), (b) amorphous and semicrystalline growth rings (120–500 nm), (c) amorphous and crystalline lamellae (9 nm): magnified details of the semi crystalline growth ring, (d) blocklets (e) amylopectin double helices forming the crystalline lamellae of the blocklets, (f) nanocrystals: other representation of the crystalline lamellae called SNC when separated by acid hydrolysis, (g) amylopectin's molecular structure, (h) amylose's molecular structure (0.1–1 nm). [1]

Starch is a biodegradable, inexpensive and non-abrasive material which comes from sustainable and renewable sources such as potato, wheat, rice, corn, maize, cassava etc. Addition of thermoplastic (gelatinized) starch in blends with other plastics and as particulate filler in composites improves the biodegradation characteristics, lowers cost and can enhance mechanical moduli of the final material. [1][17]Some of the disadvantages associated with starch based materials including water sensitivity, low heat distortion temperature, high gas permeability, low melt viscosity, brittleness, etc. can be overcome by blending starch with other materials, graft copolymerization and addition of fillers such as lignin, cellulose, fibers, clay and carbon nanotubes. [1][17]

In order to be able to process starch like other thermoplastics, it must be gelatinized. The following image provides a very comprehensive visual explanation of the process of gelatinization [2]:

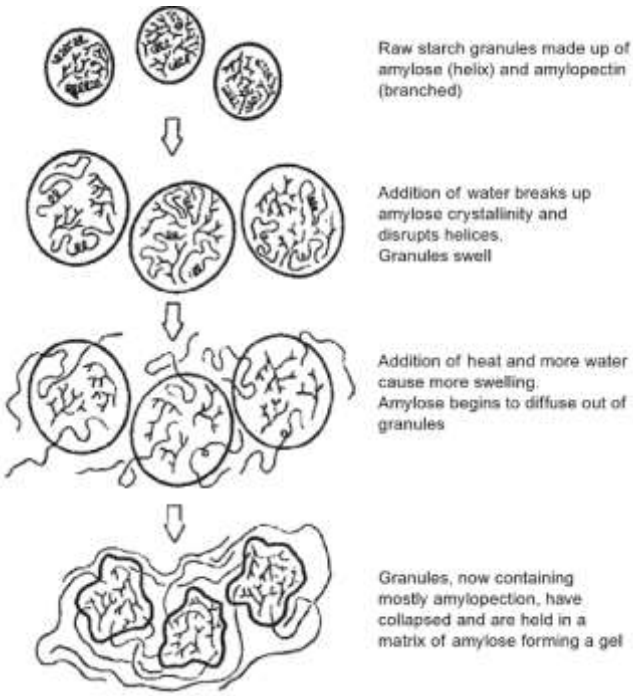

Figure 2-8 Gelatinization Mechanism of Starch [2]

Plasticizers such as water or glycerol are used regularly in the industry for gelatinization so that they can be processed using conventional thermoplastic processing equipment. At water levels 30-60%, starch gelatinization is incomplete and thermograms show a double peak. Several explanations have been put forward to explain this phenomenon; partial melting and recrystallization, amorphous ring swelling and crystallinity, differential melting of crystalline regions and then breakdown of amylose structures etc. [18] The plasticizers act as inhibitors to crystallization in the structure thereby preventing rigidity and brittleness of starch [2].

It is easy to modify starches to achieve certain desired characteristics example film formation, digestibility and solubility or to minimize the negative aspects such as high viscosity, degradation at process temperatures and retrogradation. Acid modified starched using HCl or sulphuric acid have been used conventionally for applications such as gum candy production, sizing agent in paper production etc. [18]

Acid hydrolysis of the amorphous regions of starch produces starch nano-crystals of sizes ranging from 30-100nm depending on the source of native starch. However, this method is not feasible at a commercial scale due to its negative environmental impact and mostly limited to laboratory synthesis. A more economic and efficient way is to use gamma irradiation to generate free radicals that are capable of hydrolyzing the bonds and break the particles into smaller fragments of dextrin. Ma et al. produced starch nanoparticles by precipitating a gelatinized solution of starch in ethanol and dried the suspension at 50°C to remove ethanol after centrifuging to remove water. [18]

The preparation of starch nanoparticles is limited commercially, only a handful of companies have patents on the commercial production; these include Ecosynthetix Inc. that market their Biopolymer nanoparticles, Ecosphere as biolatex and paper sizing agent and Novamont's Mater-Bi that finds

application as filler in tires (BIOTRED). Both these grades are prepared by the regeneration route which consists of gelatinizing the starch and then 'regenerating' it with a process like solvent precipitation or crosslinking [11][18].

The comparison of starch nanocrystals (SNC) and regenerated starch nanoparticles indicates the difference in crystallinity, the SNC's have a much higher crystallinity than native starch due to elimination of amorphous regions, while SNP's are produced in melt or from gelatinized starch and may have 2-4% crystallization due to retrogradation (V-type Crystal structure) and are mostly completely amorphous. SNC are shaped like platelets and SNP are obtained as spherical particles (when dispersed). This difference in shape is predicted to give SNC better barrier properties than SNP. [1].

The presence of ester bonds due to crosslinking in SNP's breakdown at a lower temperature thus reducing its degradation temperature. At present the majority of work involves SNC to be used as reinforcement in composites while SNP are used as binder/adhesive replacements for latex in paper manufacturing and such, there are no references of work focused on using amorphous SNP in composites [1].

A detailed diagram of the different routes of obtaining starch nanocrystals and starch nanoparticles is shown in Figure 2-9 [20].

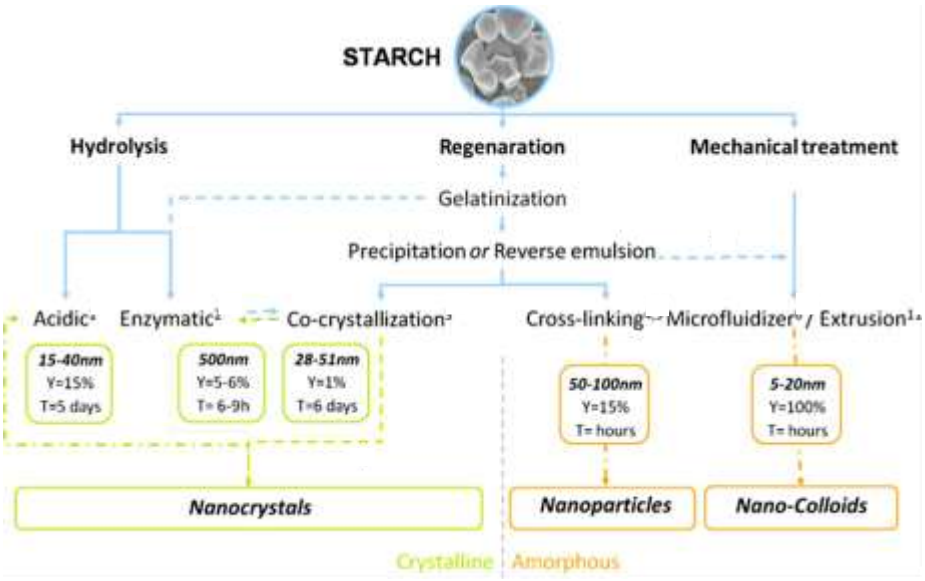

Figure 2-9 Routes of Starch Nanoparticle Production [20]

The retrogradation of starch in composites changes some mechanical properties and is reason for some concern. Retrogradation is the recrystallization phenomenon of amylose chains present in an already gelatinized starch. This formation of crystalline structure in food and thermoplastic materials containing starch can happen due to melting or due to loss of a plasticizer due to evaporation or drying (removal of water). This can cause the material to become hardened, dried out or brittle and crack.

Another interesting phenomenon was explained by Ma et al., who used winceyette fibers in a composite of TPS, urea and formamide as plasticizer, according to them the addition of low contents of the fiber, below 20%, suppressed the formation of crystals due to retrogradation while higher level of fiber allowed small crystallinity peaks. These factors can be effectively manipulated to control the retrogradation and to achieve required mechanical properties [1]. The native starch granule is a stiff material, the tensile

modulus of starch is approximately 25% of that of cellulose but almost 5-10 times larger than semi-crystalline polymers such as PET and Nylon [21].

2.4.1 STARCH BASED COMPOSITE MATERIALS

Starch granules added to thermoplastics such as LDPE give the characteristics of a conventional filler in composites, increasing the modulus and strength while reducing the elongation at break due to its rigid particulate structure [16]. One of the early works using starch granules in polyolefin composites was done by J.L Willett in 1994 who used starch in LDPE matrix with ethylene acrylic acid as compatibilizer. He reported no effect of compatibilizer on tensile strength and elongation at break and a reduction in these properties at higher loading level of starch. The tensile modulus however, increased with compatibilization versus no compatibilzation and also with increased loading levels of starch. He explained that the compatibilizer reduced 'slippage' between the starch granules and the matrix, and also improved interfacial adhesion. He also reported that larger potato starch granules compared with the smaller granules of corn starch provided better tensile moduli and strength, but this size did not contribute significantly to the elongation at break. A detailed comparison of obtained results is shown with the then prevalent theoretic models for composites which are no longer used commonly in composite studies today [21].

As mentioned previously, starch can be used in the gelatinized state as 'TPS' in blends with other polymers. Experiments done by Sailaja and Chanda (2002) showed that the addition of thermoplastic starch improves phase compatibility, biodegradability and homogenous distribution in a blend with LDPE resin when compared with native granular starch [22]. Similar work by several others in the field has shown, however, that mechanical properties such as tensile modulus, strength and strain at break are compromised when plasticized starch (rice, corn, tapioca) is used with PE in blends. Figure 2-10 shows the result of experiments by Sabetzadeh showing a drop in mechanical properties upon incorporation of TP corn starch:[23]

Tensile Modulus of the LDPE–TPCS Blends

TPCS content (wt %)	Young's modulus (MPa)
0	250
10	231
20	214
25	200
30	160
40	140

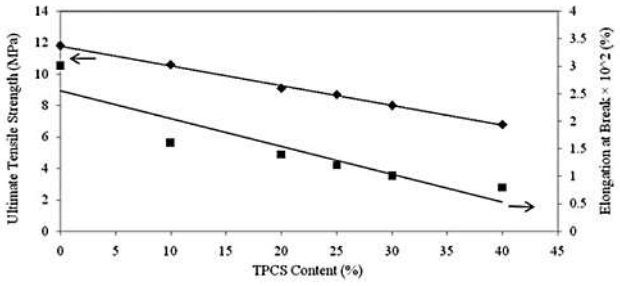

Figure 2-10 Reduced Modulus, UTS and Strain at break on increasing TPS content [23]

Starch has also been used in the plasticized state as the matrix material with cellulose fibers serving as reinforcements, over 20 research papers can be cited studying the various effects this combination produces and all show improved mechanical properties with increased filler loading. Some show a property enhancement based on a simplistic mixing-law, while others show synergistic improvement owing to very high matrix-filler interactions and transcrystallization. However, the authors Xie et al. also cite that the improvements observed in macrocomposite research studies is of a smaller scale compared with nano-filler based composites utilizing TPS as matrix. Common nanofillers include phyllosilicates, polysaccharides, carbonaceous compounds, metalloid oxides, metal phosphates and others that have a variety of nano structures ranging from nanotubes, nanolayers, to nanoparticle. Since improved

properties are observed with improved matrix-filler interactions and with good dispersion, the same is applicable to nano fillers. The common strategies to improve dispersion and interaction in starch matrix-nanofiller composites include surface modification and in-situ synthesis of nanofiller in the starch matrix [2].

It is common to see TPS used in blends with other thermoplastics to enhance certain properties and also to make the blend more environmentally friendly. In a study of a blend of TPS, gelatinized with 10% water and 15% glycerol, with EVOH (Polyethylene-*co*-vinyl alcohol) showed reduced modulus and tensile strength at break and an elongation at break almost as good as pure EVOH. However, the extent of gelatinization determines the trend of physical properties. This was exhibited in an experiment by Otey et al. who used starch plasticized with only 5-10% moisture and obtained a film blend with EAA and LDPE as matrix, ammonium hydroxide as compatibilizer and urea. The reduced elongation at break and improved UTS concluded that in this case the starch acted as a rigid filler in the films rather than a co-continuous blend component [16].

Modification of starch granules or modification of other polymers with starch are also done to improve the compatibility of the phases or to induce certain unique properties such as biodegradability. Kim and Lee showed were able to crosslinking native starch without disrupting its granular structure using less than 2% epichlorohydrin. The fabricated LLDPE composite films by melt extrusion and then casting with these crosslinked granules as fillers and showed improved tensile and elongation properties in comparison to films that had native starch granules while the crystallinity and morphology remained the same, this indicates that crosslinking can have a reinforcing effect on composite film properties by improving intermolecular chemical bonding [24]. Starch grafted polyethylene films were tested for biodegradability and results showed a continuous weight loss of the sample in soil (up to 88%) and even better (90%) in urea enriched soil, the number of microorganism colonies also continued to increase. The degradation products were also tested for plant toxicity and found to have no negative impact on the growth of new plants in that soil [25].

2.4.2 STARCH NANOCOMPOSITES

Starch nanocomposites can be composed of starch as the matrix phase in the gelatinized state with nanofillers, but also of starch nano-particles or nano-crystals as filler in other polymeric matrices. Starch is often used as filler in biodegradable matrices such as PVA, PHA, PLA, PCL and aliphatic polyesters with the aim of reducing cost at acceptable property thresholds. However the main challenge in using nanofillers is that they tend to aggregate during fabrication and it is difficult to obtain efficient dispersion which is important for maintaining good thermal, mechanical and optoelectronic properties of the material.

As the size of the starch filler decreases, mechanical properties such as young's modulus, UTS and yield strength increase, while elongation at break for composites has been shown to either increase or decrease when particles of sizes 33-480µm and 0.02-0.2µm were studied. In LLDPE films, Lim et al. concluded from experiments that increasing granular size of starch decreased the tensile strength as well as the elongation at break [21].

SNC as fillers have been the subject of extensive work since 2006 in matrix polymers like waterborne polyurethane, TPS, pullulan, PLA, PBS and soy protein isolate as well as in elastomeric matrices like polystyrene-*co*-butyl acrylate. The general trend observed is that the addition of SNC increases the Young's modulus and strength while strain at break is compromised. However in some formulations such

as with pea starch SNC and waterborne polyurethane it was seen that a filler loading of more than 5% caused a drop in modulus and strength values (compared with lower loadings not neat matrix) and was explained to be the result of aggregation and extensive phase separation. In some composites the strength and strain at break seemed to lower after a certain loading level but the modulus continued to increase [1].

The reinforcing effect of starch nanocrystals is much less in comparison to cellulose or chitosan nano-crystals. The difference in size and shape of the obtained crystals is an evident reason; starch nanocrystals are extracted as platelets, approximately 5nm thick and 20-50nm wide, whereas both chitosan and cellulose are shaped as rigid rods with dimensions of 3-20nm x 100-2000nm [4].

Seligra et al. successfully applied the concept of improving phase interaction using hydrophilic nano fillers in TPS/PBAT films where starch nanoparticles produced by gamma irradiation was used as compatibilizing filler. The results from SEM and DTA indicated that the starch grains of TPS which were not fully gelatinized initially were broken down to smaller grain, and improved gelatinization and a shift of gelatinization temperature to a lower value was observed. The authors also concluded improved interaction of the TPS and PBAT with SNP, based on results from NMR showing a wider and intensified band for CH_2 stretching. The modulus and stress at break values for these composite films also increased by 20% at a loading of only 0.6% of SNP in TPS/PBAT blend films proving the reinforcement capability of nano-fillers [11]. The addition of starch in thermoplastic composites effects the morphology of the inherent plastic as well. For PLA starch composites, starch increased the crystallization rate of PLA [13].

A detailed collection of research presented in the review paper by Le Corre et al. shows the use of starch nano crystals as filler in various types of matrix materials. The paper concludes that for rubber matrices the introduction of the SNC increases the storage modulus and stress at break while reducing the strain at break. The tensile modulus continued to increase exponentially from 0.64MPa to 77.8MPa at 0-30% loading. To achieve optimum properties of strength, modulus and decent strain at break in natural rubber 30% was the most favorable loading level. They present a viable case for SNC as a replacement of carbon black in the filling of tires with superior stiffening properties compared with carbon black; a fossil derived filler [18].

It is shown by Angelier et al. and Viguei et al. that the content of starch nanocrystals in a TPS matrix film composite improves mechanical properties between 0-15% the Modulus, and Tensile strength continued to increase however the elongation at break was compromised. [2] In addition to the enhancement in mechanical properties, addition of SNC to polymer matrices in a composite can decrease water and oxygen permeability and increase diffusion path tortuosity due to platelet like structures, thereby enhancing composite's barrier properties. For thermoplastic matrices some common trends were observed, self-aggregation and severe microphase separation at higher filler loadings (usually >30%) was observed. Introduction of PCL chains on pea-starch nanocrystals using the grafting from strategy by Yu et al. showed to improve the uniformity of SNC dispersion and reduced the aggregation, thus improving strain at break (10% to 135%) and tensile strength(42 to 58MPA) but inversely affected the Young's Modulus. The source of SNC was also of significance, waxy maize SNC performed better than pea SNC, and this was attributed to a higher aspect ratio of waxy maize SNC. The mechanical reinforcement in thermoplastics was also better than in rubbers, perhaps due to a crystallization at the filler matrix interface [18]. The addition of SNC in rubber matrices exhibit good dispersion, mechanical properties and results of XRD analysis show that the crystalline structure of the starch was intact. SNC have also been

used as reinforcement in biopolymer matrices such as cyclodextrin/polymer inclusions for alignate microsphere drug carriers and hydrogels; and these present the advantage of sustained drug release in addition to the reinforcement effect [1].

The reinforcing effect of nano-sized starch depends greatly on the interactions at the interphase between matrix and filler in addition to the good dispersion of filler. Both these factors depend on the similarity or difference of the two materials. SNC reinforcement of a TPS of waxy maize showed greatly improved mechanical properties due to the similarity in chemical structure which lead to strong interfacial adhesion and miscibility. SNC can also act as nucleating sites for nanocrystals and for the formation of a percolating network of secondary bonding, this effect was actualized in a PBS based nanocomposite with 5% SNC, showing a simultaneous enhancement of strength and elongation compared to the neat matrix. On the other hand, lack of good bonding at the filler matrix interface can lead to a decline in properties, such a trend was observed in PVOH nanocomposite filled with SNC where the tensile strength and elongation break decreased rapidly as the filler content was increased up to 40% [1].

The dispersion of TPS in PE matrices have been mostly shown to be at a micrometer size scale, however, the works or Cercle et al. has shown possibly the smallest dispersion morphology of TPS in PE at a size of 600nm. Their results also indicate a good mechanical outcome at a nanoscale dispersion of starch, with impact properties comparable to the neat matrix and the elongation at break at about 800% [2]. This leads to the understanding that a nanoscale starch based filler in PE matrix may lend to exceptional property enhancements not otherwise attainable with macrocomposites.

2.5 CELLULOSE

Natural fibers can be either derived from plants or animals; animal derived fibers consist of proteins while cellulose is the main component of natural plant derived fibers. Cellulose can be obtained from different parts of plants; leaves, stems, wood, seed, fruit, roots etc. Cellulose fibrils are oriented in a lignin matrix with hemicellulose and small amounts of pectin and waxes are also present as unaligned additives. The amount, crystallinity and type of cellulose in the natural fiber determines the mechanical properties it lends to a composite. Higher cellulose content generally increases the Young's modulus and tensile strength of the natural fibers. The cellulose microfibrils exist in the shape of slender rigid rods (monoclinic sphenoid), their high amount of crystallinity provide the tensile and flexural strength to the natural fiber and a higher aspect ratio of the fibers provides good stress transfer. The chemical structure of cellulose (Fig2-11) is that of a polysaccharide with 1, 4-β-D-glycosidic linkage, the degree of polymerization of cellulose is of the order of 10,000 but is usually decreased to the order of 2500 after purification and processing [26]. Cellulose is easily hydrolyzed by acids but has good resistance towards alkalis and oxidizing agents [5].

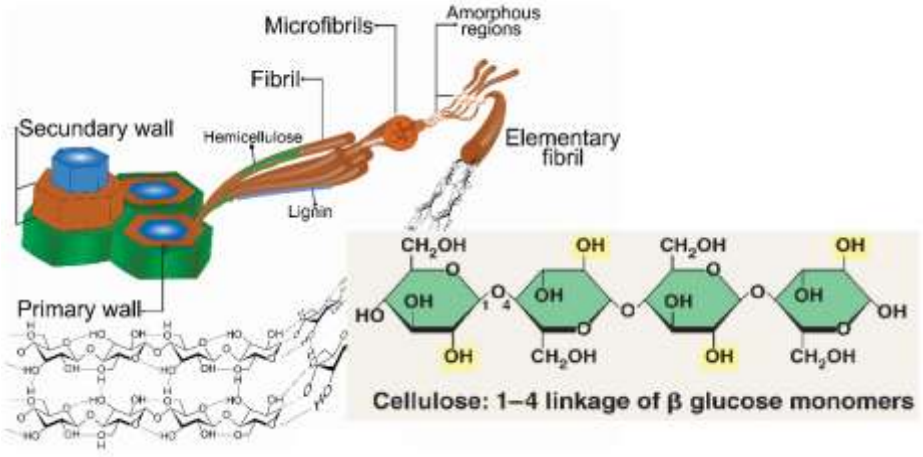

Figure 2-11 Cellulose Structure and Presence inside the Plant cell wall [26]

Cellulose fibers are known to have very high strength, stiffness and low density. They are amongst the fibers whose properties are more comparable to E-glass fibers, such as hemp. Kraft wood pulp fibers (softwood pulp) which is basically natural fibers, bleached to remove lignin and hemicellulose, is known to have an elastic modulus of 40GPa, compared to an approximate of 10Gpa of bulk natural fiber like wood. Theoretical calculations have shown that micro fibrils of cellulose could have a modulus of up to 70GPa and that of cellulose chains individually is 250GPa [3].

The shape of fibers effect the reinforcing effect observed in composites despite these being from the same source and of the same chemistry. This is the case between cellulose whiskers and cellulose micro fibrils, the whisker is rather stiff and straight while the microfiber is hair like and tends to entangle due to the inherent flexibility. Therefore in formulations with micro fibrils there is the reinforcing effect of entanglements in addition to a strong percolating network of secondary bonding while the whiskers may only have the later [1]. A higher aspect ratio in general also favors higher mechanical properties, this makes the reinforcement by fibers more effective than by particulate fillers.

2.5.1 NATURAL FIBER AND CELLULOSE BASED PLASTIC COMPOSITES

Cellulose and other natural fibers have been effectively used as fiber reinforcement in thermoplastics like PLA, polyolefins, PBAT etc. However, they have recently been tested with gelatinized starch matrix and the results provide good understanding of the interaction between starch and cellulose. Keshk and Al-Sehemi formulated composites of mercerized cellulose from paper waste and gelatinized corn starch and studied the properties of the resulting composites [13].

Shibata et al. produced a green composite filled with regenerated cellulose fibers from lyocell fabric and biodegradable polyesters; PHBV, PBS and PLA and studied their properties. They found the tensile modulus and strength increased with increased fiber content [5].

The incorporation of fibers in PP and PLA matrices were investigated by Bledzki et al. Al and the effect on flexural and tensile properties was reported. The composites were extruded and then injection molded. A 30% addition of cellulose fiber and 30% abaca fiber in PLA and PP matrix was compared, the mechanical results are summarized in the following figure [7] :

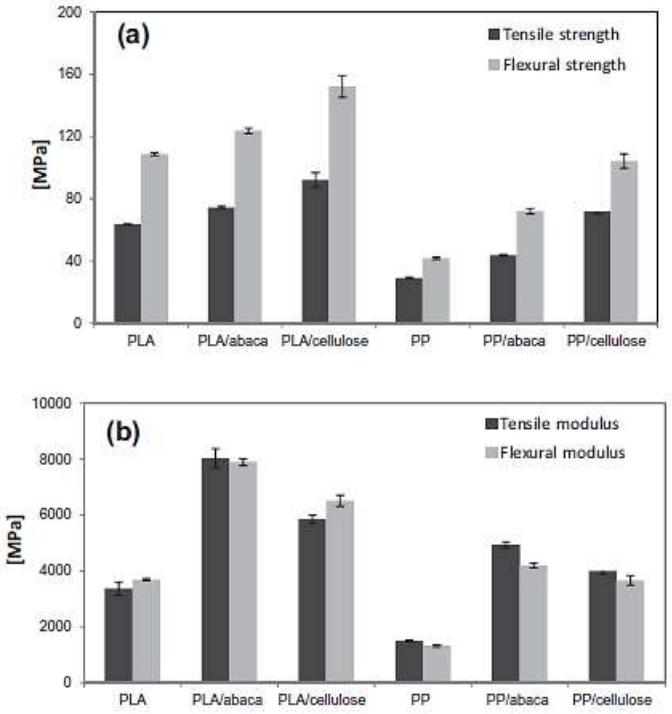

Figure 2-12 Effect of adding Abaca and Cellulose Fibers in PLA and PP Matrices on Mechanical Strength and Modulus [7]

A comparison of PP composites was done for Bleached Kraft Fibers (BKP, Cellulose Fiber Type 1s) versus flax, hemp and woodflour, Fig 2-13. In terms of mechanical properties the bleached kraft fibers performed best and the lowest values of tensile modulus and strength were observed for woodflour. This again can be attributed to the fiber length and aspect ratio. The apparent difference in properties between the bleached kraft fibers and hemp or flax fibers was due to fiber length reduction of flax and hemp fibers due to the high shear of PP melt. A lower shear keeps the fiber length of the two intact but compromises on homogenous dispersion [7].

Fiber type	BKP	Flax	Milled hemp	Core hemp	Wood hour
Tensile (MPa)	50	42	42	29	35
Tensile modulus (GPa)	3.0	3.2	3.0	2.3	2.9
Flexural (MPa)	78	67	70	52	59
Flexural modulus (GPa)	3.3	3.4	3.5	2.6	3.0
Notched Izod (J/m)	40	44	42	20	28
U-notched Izod (J/m)	205	150	145	100	105

Figure 2-13 Effect of different natural fibers on mechanical properties of PP composite [7]

Table 12 in the appendix gives an incredibly comprehensive analysis of work done on PE based composites using natural fibers and the different methods of optimization used and their results [2].

2.5.2 NANO-CELLULOSE BASED COMPOSITES

Cellulose nanocrystals are obtained after delignification and removal of other hemicellulosic by acid hydrolysis. CNC have recently been the subject of many research papers studying their effect if various matrix materials. In a similar study, flax cellulose nano crystals obtained from acid hydrolysis were used in a TPS matrix by Cao et al. and films were made by casting a homogenized suspension. Since starch and cellulose are extremely close in terms of chemical nature and due to strong –OH interactions their phase adhesion is almost ideal which also allows for exceptional fiber dispersion and uniform distribution in the starch matrix. AFM results done on these casted films confirm these hypothesis. This further translated in the mechanical test results showing a 20x increase in Young's Modulus, triple the tensile strength while the strain at break was compromised when CNC loading of 0-30% were used respectively [17].

Cao et al. concluded from FTIR results that some interactions (-OH) were reduced within the starch and that some intensified –CO peaks could mean strong secondary bonding between CNC-starch matrix [17]. Similar experiments were done by Kaushik et al. who used steam exploded, acid treated wheat straw fibers in a corn TPS matrix and studied mechanical, thermal and morphological properties [26].

Chen et al. reported that the aspect ratio of CNW had a positive correlation with mechanical properties such as tensile strength and elongation at break. They tested CNW with TPS matrix and concluded that a higher aspect ratio corresponds to superior properties. They also reported that the mechanical properties of the nanocomposites were better than the corresponding macro-composite. [2]

2.6 PHASE COMPATIBILITY

In order for the any heterogeneous material system to have superior mechanical properties, it is essential that there exist near ideal stress transfer from one component of the mixture to another. Such a problem, of poor stress transfer, often occurs in blends of two or more polymers or a composite of multiple phases where the surface chemistry of the components is dissimilar and they are immiscible. In other words, when the blend or composite is composed of hydrophobic and hydrophilic components, the interphase of these components is not meshed well and prevents complete stress transfer between the phases. Compatibilization is an approach to reduce surface tension and to improve adhesion by either the addition of a surface modifier; also called a coupling agent, or by the chemical modification of the components to improve molecular interactions between phases [2].

2.6.1 COUPLING AGENTS

Coupling agents are surface modifiers that improve interfacial adhesion by having mutual affinity for the immiscible phases of a composite or blend. They form secondary bondings with polar groups on the hydrophilic phase such as dipole-dipole interactions or hydrogen bonds, and entangle with the chains of hydrophobic phases, thereby providing a strong intermeshing between the matrix and the dispersed phase [2].

The most widely used surface compatibilizer for fiber reinforced thermoplastic composites are maleated polyolefins. Numerous studies have been published reporting the superior effect of using maleated coupling agents on mechanical properties of composites. A common example of maleated compatibilizer is Polyethylene-*graft*-Maleic Anhydride. The fairly hydrophilic maleic anhydride is often considered as a polar head with a hydrophobic PE tail. The polar head is able to form hydrogen bonds, dipole-dipole

interaction with the hydrophilic filler or even sometimes form a covalent ester bond with some of the hydroxyl groups in the filler/fiber, and the tail is capable of entangling and often co-crystallizing with the hydrophobic matrix thereby tying together two incompatible or immiscible phases. Some commercial maleated polyolefins marketed as compatibilizers include FUSABOND®, INTEGRATE® and POLYBOND® [7].

Flexural strength, modulus and water absorption resistance are all positively enhanced by the addition of MA coupling agents in composites using hemp, sisal, jute and other fibers. The strong fiber-matrix adhesion also reduces energy loss due to an impact stress, and the impact strength can be increased up to 30%. An optimum concentration of maleated coupling agents showed an increase of flexural properties by up to 60% for PP and jute or flax fiber composites [7].

The works of Sailaja et al. show improved modulus, strength and impact strength when using HDPE-*g*-MA as compatibilizer in Starch-HDPE composites compared with uncompatibilized composites. However, the compatibilizing effect was not as pronounced for TPS-PE blends as it was for discontinuous phase composites in terms of Modulus and Tensile strength. A higher improvement in impact strength was observed in blends than in composites upon addition of 25% HDPE-*g*-MA as compatibilizer. Same was the case for elongation at break, where addition of both granular starch in composite and TPS in blends decreased elongation at break compared with virgin HDPE, but the addition of just 5% HDPE-*g*-MA at 40% TPS loading increased the elongation at break to the value for virgin HDPE, this was not the case for composites filled with granular starch [22].

J L Wilet studied the effect of EAA on LDPE/Starch composites and concluded that although EAA did not significantly affect the tensile strength and strain at break but a sharp increase in the tensile modulus occurred upon addition of EAA in the composite [21].

A comparison of coupling agents was performed with respect to their effect on impact properties of PE based composites filled with agricultural fibers such as bagasse. Maleated PE, carboxylated PE and a titanium based mixture were used for the comparison. While all the coupling agents enhanced the impact propertied compared with uncompatibilized composites, the maleated PE performed best and also aided in dispersion [2] [7]. The chemical structure effects the capability of compatibilizer to enhance the phase interface. Rigidity of pendant groups on the compatibilizer can reduce effective stress transfer between the filler-matrix interfaces. Panthapulakkal et al. studied the effect of four different compatibilizers on rice husk filled HDPE intended for use in a structural application. They looked at properties like tensile and flexural moduli and strengths, and impact strength of 65% filled PE with 2.5% compatibilizer. The compatibilizers were based on ethylene-(acrylic ester)-maleic anhydride and ethylene-(acrylic ester)-methacrylate. While all the compatibilizers showed enhanced flexural, tensile and impact properties compared to uncompatibilized composites, the best results were those of methacrylate terpolymers instead of maleic anhydride terpolymers. The compatibilization reduced the extrusion as well as the water uptake in composites, explained by increase tortuosity in structure disallowing water molecules to easily seep in [27].

For a blend of two homopolymers that are thermodynamically immiscible, maleated polyolefin compatibilizers help decrease the interfacial tension between the two polymers. Eastwood et al. found that the most effective form of compatibilization is the use of sequential copolymers as interfacial modifiers (Di-block, triblock, pentablock etc.). By spacing the polar interacting moieties on the copolymer chain they were able to achieve pseudo-miscible blends. The copolymer was able to tie in with the two phases better and create entanglements in form of multiple loops, knitting the immiscible phases together

as shown in Figure 2-14. According to them, this may prove to be a relevant strategy for nano-composites as well [28].

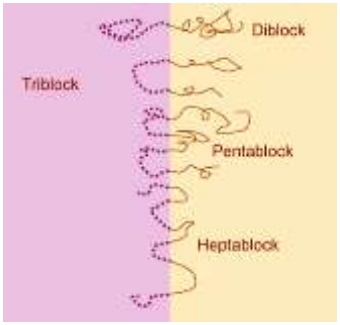

Figure 2-14 Multi-block Copolymers acting as surfactant at a sharp phase separation between two hompolymers in blend [28]

Coupling agents can have other effects on material properties than improvement of phase adhesion, dispersion etc. The effects of lysine based isocyanide (LSI) were studied by Lee and Wang, and they found that this coupling agents improved tensile properties and water resistance in PLA, PBS and bamboo fiber composites but reduced thermal flow due to crosslinking between matrix and fibers. It also delayed degradation of the composite [5].

Citric Acid and stearic acid are often used when blends of hydrophobic and hydrophilic polymers like TPS and PBAT are formulated. The hydrophilic carboxylic group (-COOH) in the acids interacts with the hydroxyls (-OH) in starch through secondary bonding and improves its compatibility with hydrophobic materials. Succinic anhydride was shown to be a suitable coupling agent for Poly(propylene carbonate) PPC and granular cornstarch composites by Ma et al. and improved the interaction between matrix and filler [5].

Another interesting approach listed in literature towards increasing compatibility in blends of hydrophobic-hydrophilic mixtures is the addition of hydrophilic nanofillers. The nano hydrophilic filler like starch nanoparticles is rich in surface –OH groups and these can interact with the other hydrophobic filler/additive through hydrogen bonds hence improving its dispersion in the hydrophobic polymer [11].

2.6.2 CHEMICAL MODIFICATION

The alternative approach to compatibilization is the chemical modification of one or more of the components to improve their miscibility or interaction with the other components. The most common methods of chemical modification include modification of one or more of the functional groups on the polymer chain with reagents (sodium hydroxide, peroxides, maleic anhydride, permanganates, organosilanes, isocyanates and so on), introduction of grafts that will increase interfacial bonding, or the addition of chemicals that will provide reactive compatibilization. Reactive compatibilization is most commonly implied with immiscible blends with an additive such as dicumyl peroxide, an anhydride or a methacrylate that is capable of forming chemical bonds, via esterification for example, with one or both the components that will aid mutual miscibility [2].

Since SNC and SNP are often used as fillers in incompatible thermoplastic matrix like polyolefins, several surface modifications are carried out to prevent aggregation and agglomeration that can render the size advantage futile. The three main methods are i) functionalization, ii) grafting onto, and iii) grafting from. As mentioned before, the presence of sufficient –OH groups on the starch surface provide ample

opportunity for chemical reactions (functionalization). Esterification of this hydroxyl group with an anhydride group, an isocyanate to transform into a urethane and the acetylation of starch have been common methods of altering the functionality of the nanofiller to make it more compatible with hydrophobic matrices. Fig 2-15 shows the most common chemical modifications performed for starch nanocrystals using either the functionalization or grafting approach [18]

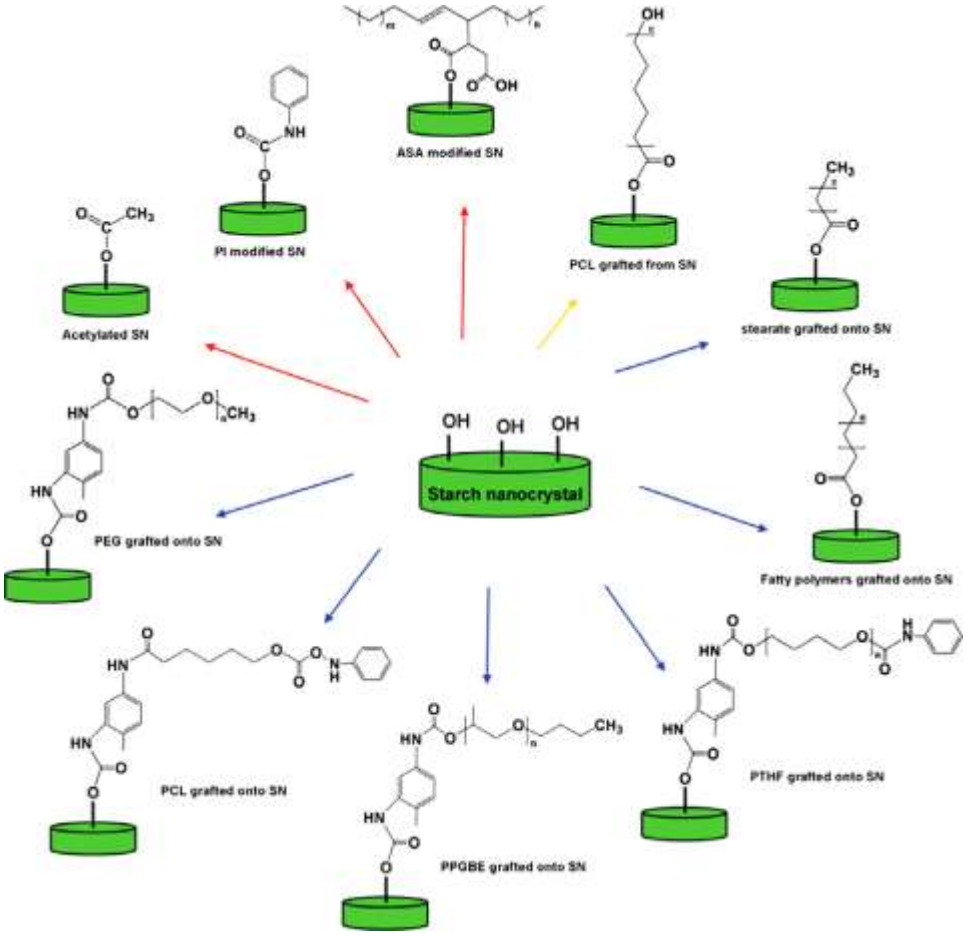

Figure 2-15 Common chemical modifications of SNC [18]

The final properties of the filler and the resulting composite depend greatly on the degree of substitution of these –OH groups. However, a high degree of functionalization reduces the three dimensional percolating network of filler-filler interactions, resulting in a sharp decrease in mechanical properties. [18] Such a downward trend in mechanical properties was observed in nanocomposites of rubber filled with crabshell chitin nanowhiskers. Other composites of natural rubber filled with SNC which were functionally modified with ASA and PI also showed that the interaction at the filler-matrix level increased but this compromised the filler-filler interaction; a higher swelling rate was observed in toluene, this was also ascribed to increased interaction between modified filler and toluene vs unmodified SNC with toluene [1].

The modification of native starches with alkenyl anhydrides particularly octenyl succinic anhydride has been in practice for several years in the food industry. Due to the eight carbon unit molecule of OSA the functionalization can perform more like a short chain graft by entanglement with the matrix. The

introduction of bifunctional groups allows starch to be used as an effective emulsifier. This OSA Starch has been employed as emulsion stabilizer additive in puddings, sauces, baby food etc. for over 30 years [29].

The modification via grafting introduces long chained branches onto the starch backbone by either grafting a polymeric substance on the chain or by introducing monomers and initiator to polymerize onto the starch to give long chained grafts. Effective stress transfer at the interface of the matrix and filler is an advantage of grafting longer chains, spaced out on the starch, and due to entanglement of these grafted chains and the matrix. They also possess the advantage of retaining a strong percolated network of filler-filler secondary bonding.

Song et al. introduced polystyrene grafts on SNC, and these were shown to have good amphiphilic properties and dispersed well in polar and non-polar solvents due to adapting conformation of the polystyrene chains on the starch backbone depending on the type of solvent [1].

Kaur and Gautam successfully grafted starch onto polyethylene to improve biodegradation. Benzoyl peroxide initiator abstracted hydrogens from starch and active macro-oxy radicals were produced by gamma irradiation of PE. The radicals combined via an ether linkage and the resulting structure consisted of pendant branches of starch on the PE backbone [25]. Another successful 'grafting-onto' compatibilization was shown by Ma et al. who polymerized methyl acrylate onto starch initiated by ceric ammonium nitrate. This was used to reinforce PPC and improved the modulus and strength of the composite significantly while also improving thermal stability [5].

Promising results were produced by Habibi and Dufresne who modified SNC with different molecular weight grafts of PCL using the 'grafting onto' technique and then used these with a PCL matrix at different loading levels. The results showed that while the modulus values for unmodified SNC films were only slightly higher, the modified SNC films had a much higher strain at break and strength, making the compromise between modulus vs much more optimum. This was attributed to an undisturbed percolated network of hydrogen bonds on the surface of SNC which is compromised with functionality modification, chain entanglements between the filler-matrix due to the grafts, and potentially co-crystallization at the interphase [30].

The chemical modification of starch widens the scope of applications both as fillers in nanocomposites by improving the phase adhesion and dispersion, and also other than as a filler. The amphiphilic nature of the modified starch and the controllability makes it ideal in the pharmaceuticals as a drug delivery, and controlled release vehicle; for example stearate modified starch nano-platelets have excellent water absorption and retention properties and can be used as absorbents, in agricultural and sewerage applications, as emulsion stabilizers, etc [18].

2.7 PROCESSING TECHNIQUES

The most common processing techniques for fiber and filler reinforced biocomposites include mixing, extrusion, casting, injection molding, resin transfer molding and compression molding. These techniques have been developed over a long time and accumulated experience ensures successful application and reproducible results.

Some common processing methods for starch based bionanocomposites include solution casting, melt intercalation and in situ polymerization. For water soluble polymer solution casting is a favorable option where the polymer solution is heated with nanofillers. Composites using plasticized starch with nano

cellulose and layered fillers are fabricated by this technique providing a homogenous dispersion (confirmed by SEM results of fractured surfaces) and distribution of fillers leading to improved modulus and tensile strength. In-situ polymerization is a sophisticated technique whereby the filler is dispersed in liquid monomer or monomer solution and polymerization takes place consequently with the aid of heat or radiation. This method is more commonly used in composites using layered fillers so that the matrix in well intercalated between the layers of the fillers as the monomers polymerize throughout the medium forming strong links between matrix chains and filler (tethering effect). This was successfully applied to nylon-MMT, PE/layered silicate composites [1].

2.7.1 COMPOUNDING

In melt intercalation, the composite is processed above the softening temperature of the matrix and allows for homogenous mixing of fillers and fibers inside under the presence of shear. The polymer chains of the matrix more easily diffuse between aggregated nano-fillers and also eliminate the need of removing solvents as in solution casting. Extrusion is a commercially viable melt intercalation technique for the compounding of polymer biocomposites and nanocomposites [1].

Extrusion is used to produce pellets or often continuous geometries like pipes, tubes and wire coatings. In case of composites, twin screw extruders are often implied to provide better mixing, co-rotating and counter rotating screw mechanisms are both used to either supply better dispersion and mixing of component or for providing a higher shear to materials that are susceptible to degradation at higher temperatures, respectively. The parameters used during extrusion effect the overall properties of the material. The temperature, residence time, pressure generated by the screws and thus the screw speed has a major impact. It was found that the strain at break was enhanced for screw speeds over 300 rpm for PE composites and over 350 rpm for PP composites [7]. The residence time in the extruder also determines the number of bonds formed between the matrix and filler due to the coupling agent, the more the bonds the better the properties [31]. Higher shear in the extruder can also aid in better dispersion and distribution of the fillers that eventually impacts the macro-properties of the composite. High shear rates also reduce agglomerate size of fillers and the size of fibers, and can also orient the fibers longitudinally in the direction of flow [32].

Joseph et al. performed an extensive study observing the effect of processing parameters on tensile properties of PP/Sisal composites and their results are summarized in the Fig 2-16. It can be interpreted that there is an optimum for all processing parameters, at unsuitably higher temperatures and shears the fiber undergoes degradation which negatively effects the mechanical performance [33].

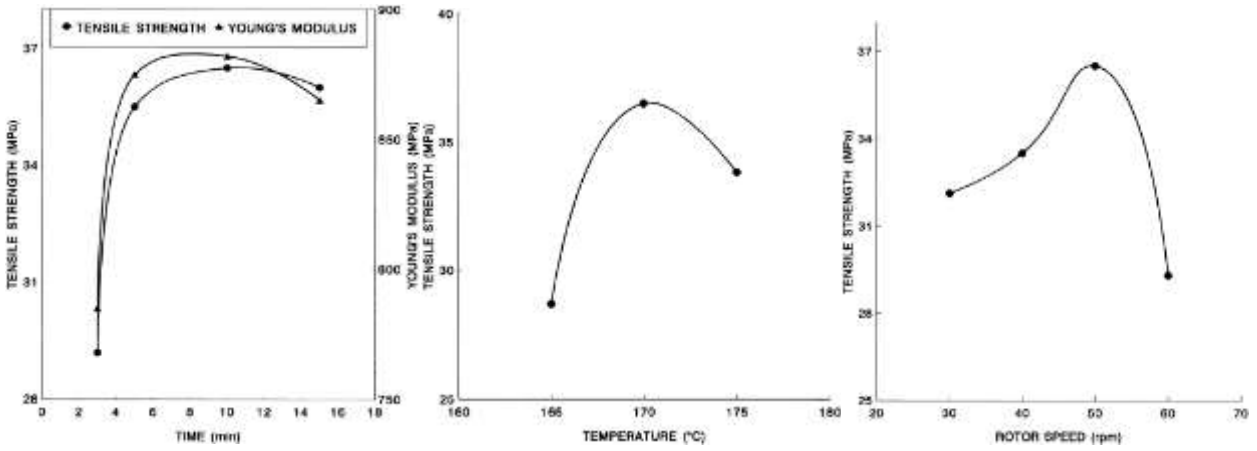

Figure 2-16 Effect of residence Time, melt temperature and Rotor speed on Tensile Properties [33]

2.7.2 MOLDING

Physical properties of materials are effected by the type of molding process employed. As such, it was noted that compression molding resulted in a higher percentage crystallinity than injection molding but the tensile strength was better and water absorption was also lower for injection molding [13].

Compression molding uses the principle of pressure to fill molds while injection molding uses much higher temperatures and lower piston pressures. The advantage of injection molding is that of higher production rates, low shrinkage and warpage. A high complexity of mold shapes is achievable with injection molding and minimum finishing is required with final product.

Molding techniques offer a unique property of fiber orientation in the matrix as the hot melt is filled directionally in a mold, this orientation provides for enhances properties in the direction of melt flow [7].

2.8 PROPERTIES

2.8.1 MECHANICAL PROPERTIES

Tensile and Flexural Properties:

The tensile and flexural properties are two very universal measures to assess material's mechanical properties. Tensile strength measures strength, modulus of elasticity and strain at break while the material is under a tensor stress while flexural test measure these properties while the material is under a deforming flexing (bending) stress. The difference between the two is that the tensile test measures average properties across the thickness of the sample while the flexural test is influenced by the top and bottom surfaces. Moreover in a tensile test the applied stresses are equally distributed through the cross-sectional thickness while in a flexural test the stresses are zero at center of the thickness and maximum at the top and bottom surfaces [7]. The flexural test is however more commonly reported for stiffer composites and it models both compressive (top surface) and tensile (bottom surface) behaviors in the material. It measures the extent of deformability in stiff composites and is based on two main properties, the elastic modulus and the moment of inertia that depends on the cross-sectional geometry of the composite.

For tensile tests, a higher crosshead rate (rate of deformation) causes the material to behave in a more brittle manner. Other factors that affect tensile strength and modulus include type and content of reinforcement, moisture, processing conditions etc. Since the Modulus is calculated on the linear portion

of the stress-strain curve and represents the initial response of the material where the stress transfer from matrix to fillers is minimum, its values depend greatly on the dispersion of the reinforcements. On the other hand, strength is calculated at the maximum of the curve at highest fiber stress conditions, and is therefore more dependent on the extent of adhesion between the matrix and the efficiency of stress transfer at the interphase [31].

In multiphase composites with starch as filler, the plasticizer content or the extent of gelatinization of the starch being used has a direct proportionality with properties such as elongation at break and ductility. While the modulus and strength is highest for dry granular starch as the filler. At a much higher level of gelatinization, the mixtures of thermoplastics and starch behave as classical blends with a co-continuous phase morphology.

The elongation at break is directly related to the interfacial adhesion of phases. Therefore the addition of surface modifiers in immiscible blends and composites positively effect this property [16].

Impact properties:

Impact properties depict a materials capability to resist fracture under the influence of a high speed stress. Impact properties depend heavily on the interfacial adhesion of the filler/fiber and matrix. The crack propagation most often takes place along a weak interface. This is one of the properties where bio based fibers lack behind glass fibers. The Impact properties of natural fiber reinforced composites is almost 20-25% of that of glass reinforced composites. It is widely accepted that the addition of reasonable compatibilizer can improve the impact properties by preventing a loss of energy at the interface by debonding, fiber pullout or effects of friction. Longer fibers are known to provide better impact properties than shorter whisker like geometries. [3]. Mulinary et al. however reported improved impact strength when using cellulose fibers in an HDPE composite and observed increasing impact strength with increased amount of fiber when compared with neat matrix, they also showed further improvement by chemical modification of the fiber surfaces to reduce the interfacial tension [34].

The micro aggregation of organic fillers like starch particles in granular as well as plasticized blends of starch with PE can act as stress concentrators and thus reduce impact strength of the composite/blend materials [23]. In general a higher loading of reinforcement reduces the impact strength in matrices like PE, PP, and PLA that have good intrinsic impact properties compared with the stiffer fibers or fillers.

2.8.2 THERMAL PROPERTIES

The addition of nanoparticles can greatly effect thermal characteristics of materials. They can influence the formation of imperfect crystals, act as nucleating sites and even prohibit crystal growth by restricting chain mobility and folding capacity. The shape and size of particles plays an important role, smoother and flatter particles like CNC with rod like structures can act as nucleating sites, while irregular amorphous starch particles may distort crystalline structure or hinder lattice growth.

Consequently, an increased glass transition temperature in composites indicates stronger fiber/filler-matrix interactions. A reduced thermal stability indicates strong plasticizer-filler interaction.

The addition of starch nanoparticles produced by gamma irradiation showed a lowered T_c for PBAT/TPS blends corresponding to reduced crystallinity in the stiffer BT segments of the polymer caused perhaps by the hindrance due to the nanoparticles [11]. The properties of PLLA filled with hemp fibers was investigated by Masirek et al. Their TGA results showed that the onset of degradation started earlier in

fiber filled systems than in neat PLLA [5]. It is also been established that cellulose content of fibers effects the thermal properties of fiber reinforced composites. The cellulose crystallite size and amount of crystallinity shifts the thermal decomposition to higher temperatures [35].

2.8.3 PROCESSABILITY

The flow properties of olefinic polymers upon addition of starch change; decrease MFI and increase melt stability. In the case of LDPE and starch, macroalkyl and macroalkoxy radicals formed due to thermomechanical shear in an extrusion process cause the formation of crosslinks in LDPE chains, leading to a rise in the MFI. Figure 2-17 shows the shear-viscosity relationship at increasing starch content in TPS/LDPE blends, as experimented by Sabetzadeh et al. [23].

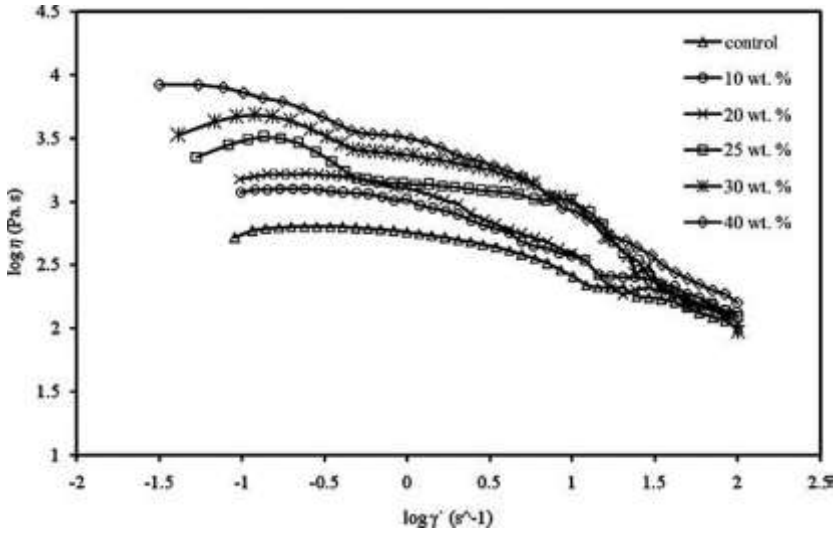

Figure 2-17 Apparent Viscosity vs Shear Rate, effect of increasing cornstarch wt. % of TPS in TPS/LDPE Blend [23]

The presence of anhydride compatibilizers such as PE-*g*-MA improve interaction between dissimilar phases and arguably enhance chemical linkages between –OH of starch and anhydride groups, this enhanced bonding also increases the MFI. The addition of plasticizers such as glycerol or using TPS instead of native starch improves macromolecular mobility thereby reducing MFI.

Increasing the amount of fibers naturally increases the viscosity as well. Sardashti reported reduction in MFI of PP reinforced with ground wheat straw, Ng also reported similar trend when formulating PP composites with agricultural waste fibers [8] [36].

The MFI of the matrix material used also has a significant impact on the final properties of the composite. A high MFI (low molecular weight) matrix provides better wettability of the dispersed fillers or fibers and due to shorter chains, also allows easier distribution, on the other hand a low MFI (high molecular weight) matrix provides more shear in melt processing which helps in dispersion of aggregates and also helps in orienting longer geometries of dispersants, such as fibers or straws, in the direction of flow in injection molding [37].

2.8.4 MORPHOLOGY

The morphology of the composites is greatly affected by the type of filler/fiber, and the extent of distribution, dispersion, interfacial interactions etc. The morphological behavior is often directly translated into mechanical and thermal behavior. In order to study morphology, Scanning Electron

Microscopy of fractured surfaces is observed to determine the extent of dispersion, agglomeration and the nature of the interphase bonding of separation. X-ray Diffraction gives results on the type of crystallinity of virgin materials and then compared with XRD of composites, significant conclusions on structure change, exfoliation (increased d spacing), shifting of peaks indicating crystal size change, and transcrystallization can be made. The percentage crystallinity, although a morphological measure, is more conveniently measured through the DSC results by calculating the enthalpy of melting during a heating cycle.

Uncompatibilized composites of PE and starch often exhibit poor mechanical properties due to poor adhesion and agglomeration of the hydrophilic fillers. A dispersed morphology of hydrophilic fillers in a hydrophobic matrix is supplemented by the use of a compatibilizer like PE-g-MA. The maleic anhydride groups of the compatibilizer are able to form ester bonds with the starch hydroxyl groups. This interaction is further strengthened by the PE chains of the PE-g-MA which entangle and interact with the matrix chains, thereby improving the morphology by dispersing the fillers and also preventing phase separation [38].

SEM images provide a very clear understanding of the dispersion or agglomeration phenomenon in composites. Sabetzadeh et al. studied the effect of increasing the cornstarch content of TPS in a blend with LDPE and found that increasing the starch reduced the distribution and dispersion of the starch in the hydrophobic LDPE. This property of bad distribution can be directly linked with the decline in observed mechanical properties mentioned in section 2.4.1. Figure 2-18 shows the inhomogeneity as the starch content is increased [23].

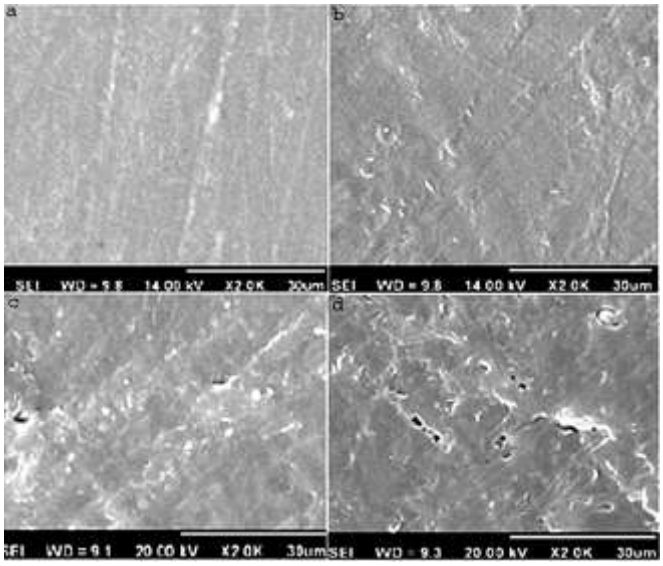

Figure 2-18 Effect of 0, 10, 25 and 40% Cornstarch in TPS/LDPE blend [23]

The crystalline structure of cellulose is a type B while that of native granular starch is a type A, XRD results of a composite of TPS and paper-waste cellulose show that the crystallinity index of the composite was higher than the crystallinity index (up to 83%) of the individual components (62 & 51%) accompanied by a shift in peaks. Keshk et al. explained their results as an increased intermolecular interaction between the starch and cellulose and a consequent enhancement in crystal stacking in the gelatinized starch phase [13].

Matzino et al. showed the XRD of starch in comparison to TPS which had been processed with glycerol and the results (Fig 2-19) show the expected lack of crystallinity of the TPS compared with the semi-crystalline granule having a characteristic A-type spectrum. TPS was compounded with LDPE and the XRD spectra of the composite containing 30% TPS were also, shown in Figure 2-19, and it can be seen that the TPS peaks at 13.5 and 23 degree are overlapped with a classical PE spectrum, the peak at 13.5 is also fainter which was explained by the authors as diminished crystallinity due to additional mechanical strain by compounding, injection molding and blowing of the composite films [38].

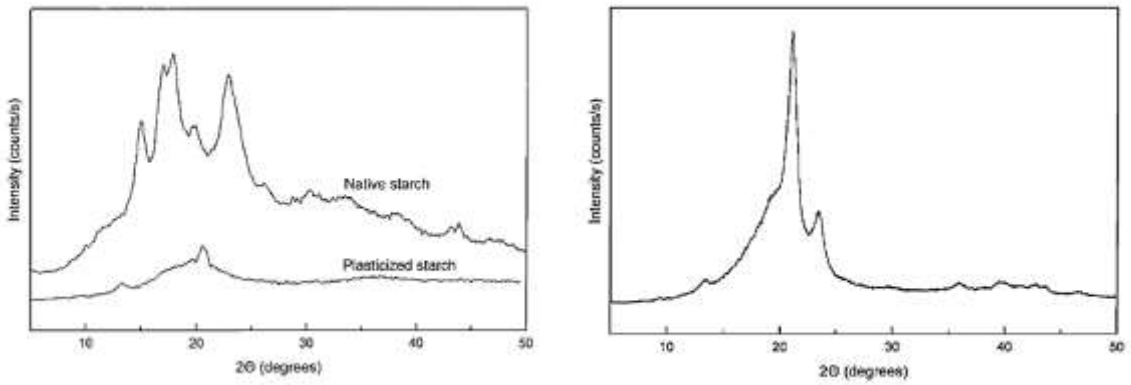

Figure 2-19 XRD Spectra of Native and Plasticized starch, XRD Spectrum of LDPE/TPS Composite [38]

Shi et al. looked at the Wide angle X ray Diffraction (WAXD) of cornstarch films with and without starch nanoparticles derived by emulsion crosslinking (regenerated route) and therefore mostly amorphous in nature; they found results displayed here in Figure 2-20, and can be interpreted as having destroyed the inherent peaks of the corn starch observed at 16°, 20° and 21° of 2theta [39]:

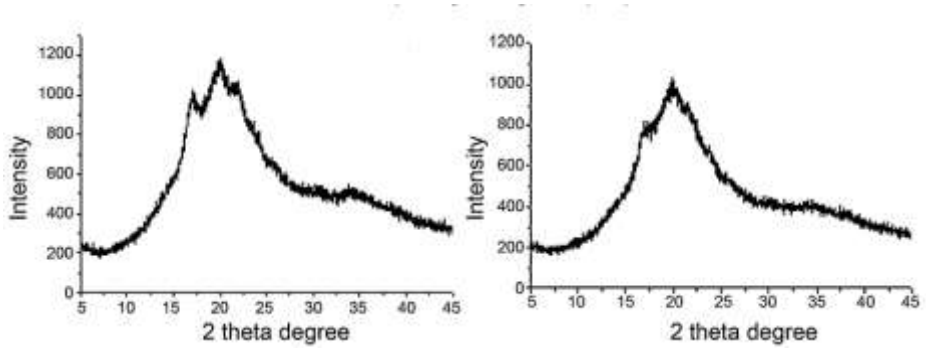

Figure 2-20 XRD of Cornstarch Film compared to XRD of Cornstarch/SNP Composite Film [39]

The addition of semi crystalline fibers often induces a phenomenon called transcrystallization; surface induced crystallization. The fiber surfaces act as nucleation sites for crystallization for matrix chains and the crystals formed via transcrystallization; or on the surface of the fibers have a structure that is different from the crystal structure of the neat matrix or the individual fibers themselves. This phenomenon is mostly common for flat, tape like or rod like fiber structures than for spherical or irregular shaped particulate fillers. The XRD is a powerful tool to identify these transcrystals in a composite and enable differentiation between the crystals corresponding to the additives and the crystals formed at the fiber surface [40]. Han et al. looked at XRD spectra of PP, kenaf fibers and their composites at different loading of kenaf fiber and observed the formation of the peculiar β crystals in the composites which were not

present in either the PP or the Kenaf (Fig 2-21), this indicates transcrystallization and thus improved crystallinity, and also improved toughness and impact strength due to the better properties of β crystals versus α crystals [41].

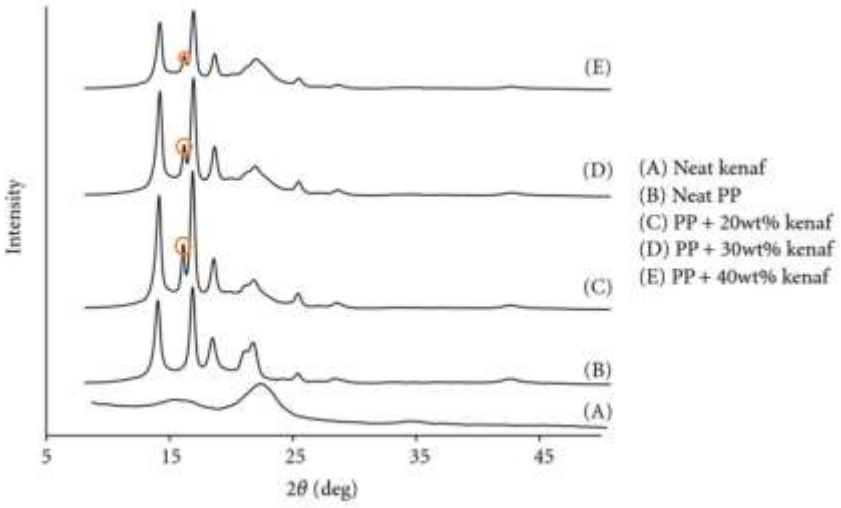

Figure 2-21 XRD Spectra of Neat PP, Neat Kenaf Fibers and their Composites [41]

This phenomenon was also supported by XRD data, in the works of Keshk et al., which shows the sharpest crystallinity peak and by DSC data obtained on composites of 2:1 ratio of starch to cellulose that showed a lowered heat capacity and thermal expansion and increased thermal stability; due to more crystallinity, in the composite compared with the TPS alone [13]. However, a similar study by Cao et al. showed wide angle XRD of CNC-TPS casted films and concluded that the diffractogram of the composite was merely a superposition of the constituent two materials confirming no inter-dependency in the crystallization phenomenon in their case [17].

3. MATERIALS AND METHODS

3.1 MATERIALS AND INSTRUMENTS

In this work composites were formulated with three different types of base matrices, varieties of starch and starch derived nanoparticles as filler and two types of cellulose fiber reinforcements while maleated polyolefins were used as surface modifiers. The compositions were compounded, molded and then tested for mechanical, thermal and morphological properties. Table 3.1 and 3.2 list the materials and equipment used in this course of experiments:

Table 3-1 List of Chemicals and Materials Used

Material	Supplier/Manufacturer
Base Polymer	
Polyethylene (BPE)	Braskem
Polyethylene (RPE)	Unknown
Polypropylene (PP)	Braskem
Filler	
Corn Starch	Ingredion
Cassava Starch	Ingredion
Starch derived Biopolymer Nanoparticle (BNP) (Research Grade)	Ecosynthetix Inc.
Hydrophobic Starch derived Biopolymer Nanoparticle (HBNP) (Research Grade)	Ecosynthetix Inc.
Fiber	
Cellulose Fiber Type 1	N/A
Cellulose Fiber Type 2	N/A
Coupling Agent	
Polyethylene-*graft*-Maleic Anhydride	Clariant
Polyethylene-*graft*-Maleic Anhydride	Clariant
Polypropylene-*graft*-Maleic Anhydride	Eastman
Ethylene Acrylic Acid	N/A

Table 3-2 List of Equipment Used

Equipment	Manufacturer
Analytical Balance AB304-S	Mettler Toledo
Minilab Haake Extruder	Thermo Electron Corporation
Grinding Mill	
Injection Molding Machine RR/TSMP	Ray Ran, UK
Minitec 120 Q1000	TestResources, USA
Specimen Notch Cutter Type XQZ I	Chengde Jinjian Testing Instruments Co, Ltd.
Monitor Impact Tester 43-02-01	Testing Machines Inc
MFI Dynisco Polymer Test D4001 DE	Alpha technology
DSC Q2000	TA Instruments
TGA Q500	TA Instruments
TZero Aluminium Pan and Lid	TA Instruments

FESEM Gold Coating Unit Desk II with Argon Gas	Denton Vaccuum, USA
QuantaFEG 250 E-SEM	FEI, Thermo Fischer Scientific

3.2 FORMULATION

Composites were first formulated by weighing out different proportions of dried polymer, powdered starch filler, cellulose fiber and compatibilizers in the Analytical Balance AB304-S. Prior to this, the cellulose pulp and the Cellulose Fiber Type 2 were both ground in the [blue grinder] to convert the solid chunks of the cellulose into a more fluffy, fibrous form that would be easier to mix in the dry mix formulation before it was compounded. The formulation mixtures were hand mixed thoroughly in plastic ziplock bags to achieve some level of homogeneity. Table 4-1 gives the composition of all the formulations made and tested.

3.3 COMPOUNDING

The dry blends were compounded in a co-rotating twin screw extruder (Minilab Haake Extruder) where the composites were melt processed to give a homogenized extrudate. The powder was fed through the hopper and pumped through manually using a rod and maintaining a near-constant torque of [40-60J]. Extra care was exercised to incorporate equal ration of components in each feed through the hopper since the pellets of polymer were much larger in size compared to the starch powder and fibrous cellulose. The contents entered the chamber consisting of the conical rotating screws and heated top and bottom plates with an integrated backflow channel. The temperature used for the extrusion was 160°C for PE composites containing low loadings of additives while 190°C was used for very high loading of fiber and filler. For PP composites the temperature used was 200-220°C. Exact values of processing for each formulation is listed in Table 3-3. The pressure inside the chamber was maintained under 500MPa. The screw rotation speed was 100 RPM, and residence time of 1 minute was set. After being melted and mixed in the chamber the extrudate exit through the horizontal rod die in the form of a continuous spaghetti. This was wound manually and later ground in the mill [insert name] to produce a coarse powder which could be used for injection molding.

3.4 INJECTION MOULDING

The ground composite from the mill was then molded into rectangular bars in an injection molding equipment by Ray Ran. The material was fed in the barrel through an inbuilt funnel and allowed a melting time of approximately 15 minutes. After the material was molten in the barrel the extrudate was injected in a mold using a pneumatic piston attached to a high pressure air transducer. The piston was held in place for about 10 seconds to ensure complete filling of the mold and to prevent mold shrinkage. After this the molds were removed from the tool plate and molded bar was detached by cutting it at the gate with a sharp cutting tool. The sprue and runner was cut off from the bar using pliers. The temperatures of barrel and mold were set based on the loading capacity and type of base polymer used which is listed in Table 3-3. The mold used produced bars of the following dimension shown in Table 3-4dictated by the ASTM D256 and D790 needed for subsequent flexural and impact testing of reinforced plastics.

Table 3-4 Dimensions of Injection Molded Specimens

Length	63.5±0.2 mm
Width	12.7±0.2mm
Thickness	3.3±0.2mm

3.5 CHARACTERIZATION TECHNIQUES

3.5.1 FLEXURAL PROPERTIES

The bars obtained from the injection molding process were conditioned for 48 hours at room temperature before they were subjected to flexural testing according to the method described in ASTM 790-15 (Type I) on the *TestResources Minitec 120 Q1000* universal testing apparatus which has been force calibrated according to the ASTM E4. Procedure B (strain rate of 0.1mm/mm/min) was chosen after an initial test with Procedure A, confirming that sample does not break or yield within 5% of strain limit. The specimen was placed flat on two support cylinders and its center was deflected by a vertically oriented load cell attached to a cylindrical nose moving down on the specimen until the maximum strain was reached. Simultaneous load-deflection data was recorded based on the crosshead motion (13.9mm/min-7mm/min). The apparatus was connected to a computer where the results of the test were transferred and properties like flexural modulus (Secant 1%), flexural strength and strain at break were calculated using this load-position data and the specimens recorded span, thickness and width.

The Secant modulus is recorded as the slope of the stress-strain curve at 1% strain in the center of the specimen. The strain at break on the other hand is the maximum value of strain on the stress-strain curve, but since the experiment is not carried out to break therefore a maximum strain at 5% is recorded. For each composition 5 or more samples were tested and an average was recorded along with the standard deviation.

3.5.2 IMPACT PROPERTIES

In order to measure the impact resistance properties of the composites, Izod Pendulum Impact Resistance tests were performed according to the ASTM D256-10. The rectangular bars obtained from the injection molding process were first notched using the Jinjian Notch Cutter Lathe such that the distance from the notch to the other end of the specimen (width-wise) was 10.16 mm. Other dimensions of the notch were followed as described in ASTM D256 for Izod Specimens. The specimens were then conditioned at room temperature for 48 hours before the experiment. Method A of the experimental procedure was chosen since the expected value of impact resistance was more than 27 J/m (this was confirmed by the actual test). The notched specimen was clamped vertically as a cantilever beam using a wedge to ensure that the notched face was parallel to the clamping vise-jaws. It was then broken by a single swing of a pendulum of capacity 1 Ft.Lbs.

The potential energy difference between when the pendulum is allowed to swing without the specimen and then with the specimen is recorded inside the equipment and then divided by the width of the notched face (thickness of specimen), previously entered in, and reports the impact strength in units of J/m on the digital display. This value is the amount of energy loss in breaking the sample in the direction of impact and across the width of the impacted surface.

The type of break for each sample was also recorded.

3.5.3 THERMAL PROPERTIES

3.5.3.1 Differential Scanning Calorimetry (DSC)

Thermal properties such as the T_g, melting and crystallization temperatures, and percentage crystallinity were calculated by conducting DSC on the *TA Instruments Q2000* combined with an *RCS90* Cooling system. A computer connected to the instrument serves as the interface which allows the user to control an experiment by choosing a set of parameters. This instrument uses the mechanism of heat flux DSC to measure the differential heat flow to an enclosed reference pan and sample pan. These pans are placed inside the DSC cell on two platforms connected to thermocouples that measure difference in heat flow for the reference pan and the sample pan which is based on the heat capacity of the sample in the sample pan. A third thermocouple placed directly in between the reference and sample pan allows for accountability of all thermal losses due to cell imbalances between the reference and sample sides, this allows for flat baselines and a very sensitive differential analysis.

The equipment is calibrated as per the Tzero Method where a first experiment is run without any reference or sample pans and a second with 95mg sapphire disks on both sample and reference platforms. This is done at a high heating rate and the complete program consists of heating at a constant rate, an equilibration, holding at an isotherm and then cooling at a ramp.

For experiments with the samples, Tzero Aluminum pans and Tzero aluminum lids were used, the sample pans consisted of 5±1mg of sample and were then sealed with the lid in a Tzero DSC Sample encapsulating press. The purge gas in the cells was nitrogen at a flow rate of 50 ml/min. Flange temperature was maintained at around -90°C. The procedure consisted of two heating cycles, one to remove thermal history of the samples and a second one to observe the endothermic process associated with the melting transition and a cooling cycle to observe the exothermic, crystallization phase transition. The method used for all samples was:

Equilibrate at 30°C
Ramp 10°C/min to 175°C
Isothermal for 5 minutes
Ramp 10°C/min to 30°C
Mark End of cycle 0
Equilibrate at 30°C
Ramp 10°C/min to 175°C
Mark End of Cycle 0

The analysis of crystallinity was performed in the TA Universal Analysis software, the melting peak was integrated between 80-140°C for all LLDPE samples and between 80-200°C for PP samples to ensure a comparative analysis could be made.

Multiple sample pans were loaded onto the auto-sampler, and sample mass and pan position was entered into the software, at a time for unattended operation. The results were analyzed using the *TA Instruments Universal Analysis 2000* program. [1][2][3]

3.5.3.2 Thermal Gravemetric Analysis (TGA)

In order to determine the thermal stability and the onset temperature of degradation for each sample TGA experiments were conducted in *TA Instruments Q500* apparatus connected to a computer for user control and analysis. The instrument is operated with platinum pans which are first tared on a vertical thermobalance inside a furnace housing the thermocouple for a temperature-compensated environment which can provide very accurate weight measurements from ambient to up to 1000°C. The thermobalance system operated on a 'null-balance' principle which eliminated the need for complicated base line measurements and only required the tared weight of pans. The pans are loaded on an autosampler which allows for automatic taring until all pans are preweighed. The samples are then loaded onto the pans in a 10±1mg weight range.

The calibration of the equipment was done using the Curie Temperature Standards which works on the principle of magnetic transition of ferro-magnetic materials. In this particular apparatus nickel was the chosen ferromagnetic material and was heated on a tared pan inside the furnace in the presence of a strong magnet until the curie point was reached. At Curie point the material transitions from diamagnetic to para-magnetic (loses its magnetic properties). This is accompanied by a weight loss at a sharp temperature. The equipment corrects any deviation recorded from the documented true Curie point of Nickel.

For the experiment, nitrogen was used as the balance gas at 60 ml/min and air for the furnace at 40 ml/min where the sample was heated at a rate of 10°C/min until 600°C. The weight loss was recorded as a function of time. The results were retrieved on the computer and analyzed on the *TA Instruments Universal Analysis 2000* software. [4] Sample of appx. 10mg was loaded on the aluminum pans. For samples showing degradation under 100°C, moisture content was analyzed and the degradation temperature was determined at 5% weight loss after the moisture had evaporated, for samples without any moisture onset of degradation was calculated at 5% weight loss of the total sample.

3.5.4 MORPHOLOGY

3.5.4.1 Scanning Electron Microscopy (SEM)

In order to study the surface characteristics; dispersion, distribution of fillers and particle/fiber sizes in the composites, SEM of samples and individual fibers and starch nanoparticles was done in the *QuantaFEG250* equipped with a field emission column. The operation principle of an SEM is that it uses electrons to illuminate a surface and projects its image on a detector. Since the wavelength of a beam of electrons is much smaller than the wavelength of a light photon, a resolution of up to 0.1 nm can be achieved vs 200nm; which is the highest resolution theoretically possible for optical microscopes. The QuantaFEG250 has a resolution of 1-3nm.

The sample preparation consisted of some impact fractured samples to observe the fiber pullout phenomenon while other samples (injection molded bars) were cryo-fractured in liquid nitrogen and then extracted in water at 50°C for a minimum of 4 hours with constant stirring to ensure that all the starch particles had migrated from the fractured plane. The extraction would allow for a higher contrast due to the holes left behind on the surface by the removed starch and the cryo-fracturing provides a smoother surface to observe. A small piece of these samples were cut and attached onto the aluminum stubs using double sided conductive tape with the fractured surface facing up. Since none of the components of the composite are good electrical conductors they were sputter-coated with a thin layer of gold (≈10nm) on the surface using the *FESEM Gold Coating Unit Desk* to provide a better resolution of images and minimum charging.

The SEM was operated in a high vacuum mode, electron beams at 15kV were incident on the fractured surface and the image was casted by two detectors; an electron back scattering diffractor (BSD) and a secondary electron (SE) detector. Images at various magnifications (65X-10,000X) were saved and then analyzed on the *ImageJ* application. The BSD gives a better contrast and is thus more suitable to observe features of the surface, while the SE gives a better visual of depth and height and is thus better for determining the surface morphology.

3.5.4.2 X-Ray Diffraction (XRD)

The Bruker D8 Focus instrument was used for obtaining XRD results on composites. The instrument was operated at 40kV and 40mA with a Cu Kα radiation source. The pattern was recorded between 10 and 40 degree of 2θ values with a step size of 0.02, the scan time was 1 second and a step scan was used. The composite test samples were prepared as films in a hot press and then placed on the sample holder, while the BNP powder was pressed into the sample holder using a glass slide. The 0.1mm slit was used for the incident beams at the X-ray source while 0.6mm slit was used for the diffracted beam at the X-ray detector. The XRD recorded the scattering intensity at every diffraction angle.

3.5.5 FLOW PROPERTIES

3.5.5.1 Melt Flow Index

To measure the MFI of all composite formulations the Dynisco D4001DE MFI Tester was used. The extrudate samples were ground to small coarse powder in the mill and then tested according to the parameters defined in the ASTM D1238. Method A was chosen for MFI of thermoplastics.

The plastometer equipment consisted of a thermostatically controlled heated steel cylinder with a vertical cavity and a die positioned at the bottom end. The die chosen for this method was 8mm long with a bore 2.95 mm in diameter. A piston with dead-weight attachments was used to force sample melt through the bore of the die.

Approximately 5g of sample was fed in the heated cylinder through a wooden funnel when a stabilized set temperature was reached, the feeding was managed to be completed within a 1 minute mark to allow equal residence time to the entire sample bulk added. The set temperature was 190°C for LLDPE composites and 230°C for PP samples. The material was allowed to melt in the cylinder for 360 minutes. After this the piston and weight was inserted and the material was allowed to flow through the die under the influence of a 2.16 kg load (piston and weight) for both LLDPE and PP samples. 4 to 5 extrudate cuts

were taken and the time duration for flow of each of these cuts was recorded using a stop watch. The cuts were weighed and then mathematically manipulated to give the result in g/10minutes.

4. RESULTS AND DISCUSSIONS

4.1 FORMULATIONS

The following naming convention has been implied to aid better understanding of results presented later in this section:

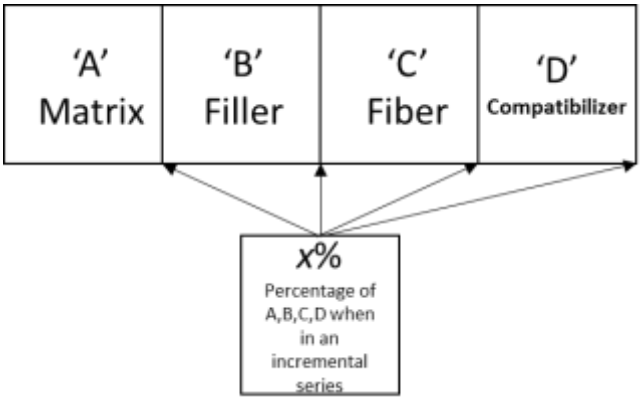

Figure 4-1 Formulation Naming Convention

Where;

'A'	B	BPE
	R	RPE
	p	PP
'B'	S	Starch Derived Bionanoparticle (BNP)
	S_H	Starch derived hydrophobic Bionanoparticle (HBNP)
	C	CORN
	V	CASSAVA
'C'	F	CF2
	P	CF1
	G	GLYCEROL
'D'	M_L	PE-*g*-MA (Low MA content)
	M_H	PE-*g*-MA (High MA content)
	E	Ethylene Acrylic Acid

Table 2 List of Formulations, Compositions and Processing Temperatures Using BPE as Matrix

Sample	Formulation (%)				Injection Molding Temperatures		Extrusion Temperature
	BPE	HBNP	CF2	PE-*g*-MA	Barrel	Tool	
$BS_H0M_L0.5$	79.5	20	X	0.5	200	40	190
BS_H0M_L1	79	20	X	1	200	40	190
BS_H0M_L2	78	20	X	2	200	40	190
BS_H0M_L5	75	20	X	5	200	40	190
BS_H0FM_L	83	X	15	2			
BS_H5FM_L	78	5	15	2	200	40	190
BS_H10FM_L	73	10	15	2	200	40	190
BS_H15FM_L	68	15	15	2	210	45	190
BS_H20FM_L	63	20	15	2	210	45	190
BS_HF5M_L	78	15	5	2	200	40	190
BS_HF10M_L	73	15	10	2	200	40	190
BS_HF15M_L	68	15	15	2	210	40	190
BS_HF20M_L	63	15	20	2	200	40	190
	BPE	**HBNP**	**CF1**	**PE-*g*-MA**			
BS_HP20M_L	63	15	20	2	200	40	190

Table 3 List of Formulations, Compositions and Processing Temperatures Using RPE as Matrix

Sample	Formulation (%)				Injection Molding Temperatures		Extrusion Temperature
	RPE	Cassava	Cellulose	PE-*g*-MA	Barrel	Tool	
RV00	70	30	X	X	195	40	160
	RPE	**Corn**	**Cellulose**	**PE-*g*-MA**			
RC00	70	30	X	X	200	40	160
	RPE	**BNP**	**Cellulose**	**PE-*g*-MA**			
RS00	70	30	X	X	190	40	160
	RPE	**Cassava**	**Cellulose**	**PE-*g*-MA**			
$RV0M_L$	68	30	X	2	190	40	160
	RPE	**BNP**	**Cellulose**	**PE-*g*-MA**			
$RS0M_L$	68	30	X	2	195	40	160
	RPE	**Corn**	**Cellulose**	**PE-*g*-MA**			
$RC0M_L$	68	30	X	2	200	40	190
	RPE	**HBNP**	**CF2**	**PE-*g*-MA**			
$RS_H0M_L0.5$	78	20	X	0.5	190	40	190
RS_H0M_L1	73	20	X	1	190	40	190
RS_H0M_L2	68	20	X	2	190	40	190
RS_H0M_L5	63	20	X	5	190	40	190
RS_H0FM_L	83	X	15	2	190	40	190
RS_H5FM_L	78	5	15	2	190	40	190
RS_H10FM_L	73	10	15	2	190	40	190

RS_H15FM_L	68	15	15	2	190	40	190
RS_H20FM_L	63	20	15	2	190	40	190
RS_HF5M_L	73	20	5	2	190	40	190
RS_HF10M_L	68	20	10	2	190	40	190
	RPE	**HBNP**	**GLYCEROL**	**PE-*g*-MA**			
RS_HG10M_L	68	20	10	2	160	40	180
	RPE	**HBNP**	**CF2**	**PE-*g*-MA**			
RS_HF15M_L	63	20	15	2	190	40	190
$RS_H15F20M_L$							
RS_HF20M_L	58	20	20	2	190	40	190
	RPE	**HBNP**	**CF1**	**PE-*g*-MA**			
RS_HP20M_L	58	20	20	2	190	40	190

Table 4 List of Formulations, Compositions and Processing Temperatures Using BNP as Nanofiller and CF1 as fiber

Sample	**Formulation (%)**				**Injection Molding Temperatures**		**Extrusion Temperature**
	BPE	**BNP**	**CF1**	**PE-*g*-MA (H)**	**Barrel**	**Tool**	
$BS20M_H$	78	20	X	2	190	40	160
$BP20M_H$	78	X	20	2	190	40	160
$BP15M_H$	83	X	15	2	190	40	160
	BPE	**BNP**	**CF1**	**EAA**			
BP15E	83	X	15	2	190	40	160
BS20E	78	20	x	2	190	40	160
	BPE	**BNP**	**CF1**	**PE-*g*-MA**			
$BP15M_L$	83	X	15	2	190	40	160
$BS20M_L2$	78	20	X	2	190	40	160
$BS20M_L0.5$	79.5	20	X	0.5	190	40	160
$BS20M_L1$	79	20	X	1	190	40	160
$BS20M_L5$	75	20	X	5	190	40	160
$BP15M_L0.5$	84.5	X	15	0.5	190	40	160
$BP15M_L1$	84	X	15	1	190	40	160
$BP15M_L5$	80	X	15	5	190	40	160
$BS5PM_L$	79	5	15	1	190	40	160
$BS10PM_L$	74	10	15	1	190	40	160
$BS15PM_L1$	69	15	15	1	190	40	190
$BS20PM_L$	64	20	15	1	190	40	190
$BSP5M_L$	74	20	5	1	190	40	160
$BSP10M_L$	69	20	10	1	190	40	160
$BSP20M_L$	59	20	20	1	190	40	190
$BSP15M_L2$	63	20	15	2	190	40	190
$BSP15M_L5$	60	20	15	5	190	40	190

Table 5 List of Formulations, Compositions and Processing Temperatures Using PP as Matrix

Sample	Formulation (%)				Injection Molding Temperatures		Extrusion Temperature
	PP	BNP	CF2	PP-*g*-MA	Barrel	Tool	
pS15FM$_L$	63	15	20	2	220	45	190
pS20FM$_L$	58	20	20	2	220	45	200

4.2 MECHANICAL PROPERTIES

4.2.1 COMPATIBILIZATION

The positive effect of compatibilizers on starch and polyolefin blends/composites has been shown extensively in literature. The most commonly use compatibilizers for PE based composites are PE-g-MA, Ethylene Acrylic Acid, and also copolymer of ethylene vinyl acetate. Prinos et al. studied the effect of ethylene vinyl acetate as compatibilizers on starch/LLDPE blends [42] Willett showed the effect of EAA on LDPE/starch composite [21] and Matzinos et al. conducted similar work on LDPE/starch blends with PE-g-MA and compared results with the previous two studies, stating that PE-g-MA is the more suitable compatibilizers for most cases [38]. It has been observed from a thorough literature review that EAA and similar random copolymers were the preferred compatibilizers of the research conducted in the 90's, and this trend has skewed in favor of grafted maleic anhydride compatibilizers in the past decade.

4.2.1.1 Effect of Compatibilizer and Type of Starch in Starch-Based Composites

So far, to the best of our knowledge, effect of starch nanoparticles (other than fully crystalline SNC) in composites has not been reported [1]. The following graphs show a comparison of native starch granules (Cassava starch and cornstarch), and the novel bionanoparticle derived from starch BNP in terms of the mechanical properties of their composites in a PE matrix. The results of flexural modulus and strength show almost no difference between the granular starch and the nanoparticles when uncompatibilized. Slight increase can be seen when PE-g-MA is used as a compatibilizers. The absence of a considerable difference can be attributed to the large aggregates of the BNP, which does not fully disperse to a nanoscale filler in the hydrophobic PE matrix. However, the trends of impact strength show a clear superiority of BNP over native starch, which at similar modulus values gives a better offset on impact properties.

Since the modulus values are measured at low loading conditions at the dispersant-matrix interface and strength at much higher break loads where the stress has transferred to the interface, therefore the presence of a coupling mechanism, an thus, the content of compatibilizers is expected to be more pronounced in flexural strength results than in modulus [31]. This is evident from results shown in Fig 4-2 and 4-3 where the increase in flexural strength is much more than the increase in modulus values between compatibilized and uncompatibilized samples. Moreover, the increase is more evident for starch nanoparticles than for granules due to the higher surface to volume ration due to the aggregates that have dispersed at a nanoscale thereby increasing the coupled surface area.

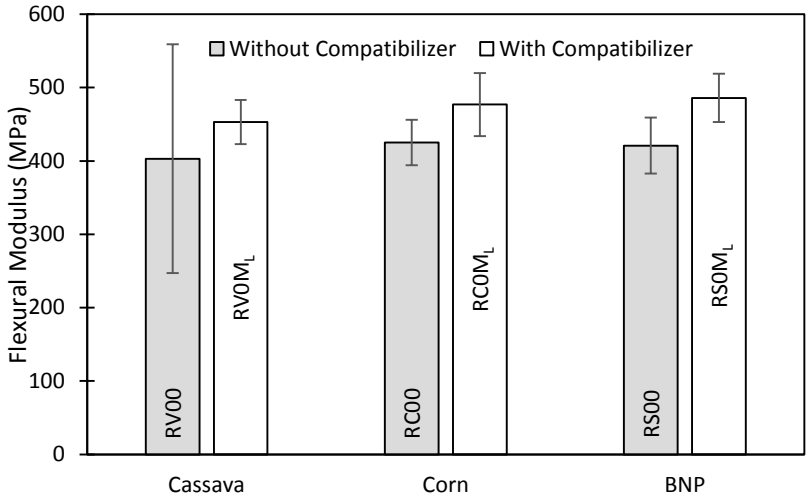

Figure 4-2 Effect of Cassava, Corn, BNP & HBNP on Flexural Modulus of BPE Composite with and without PE-g-MA as compatibilizer

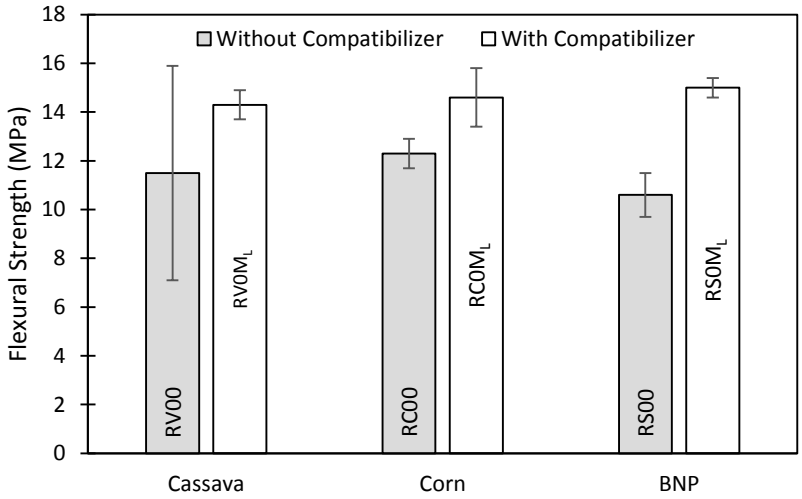

Figure 4-3 Effect of Cassava, Corn, BNP & HBNP on Flexural Strength of BPE Composite with and without PE-g-MA as 48ompatibilizers

The composite samples which have been compatibilized with PE-g-MA seem to have a lower impact strength than uncompatibilized samples as shown in Fig 4-4. This effect is even more pronounced in samples containing BNP than it is for native granular Cassava or Cornstarch for which the difference is either negligible or can be accounted to the high deviation in results. This result is contrary to most published in literature, where the addition of a compatibilizers increases impact strength (Izod Notched Test). Amongst many similar corroborating studies, Sailaja and Chanda's work is closest in nature using tapioca starch as filler in an HDPE matrix who show slightly improved (31%) impact strength upon incorporation of a maleic anhydride compatibilizers at 25%, a styrene-co-maleic anhydride was shown to improve impact strength of a Polystyrene-ZnO composite, similar trend was reported by Chen et al. who used silanes and stearates as compatibilizers in PP-Starch composites and observed improved impact

strength, Lin et al. also observed enhanced impact strength for short fiber glass filled PP composites upon incorporation of PP-g-MA as compatibilizers [22] [43][44][45].

It should be noted however, that none of these studies report on dispersants at a nano-scale and a unique characteristic of the interface of a nanoparticle and matrix may be the reason of this unusual observation.

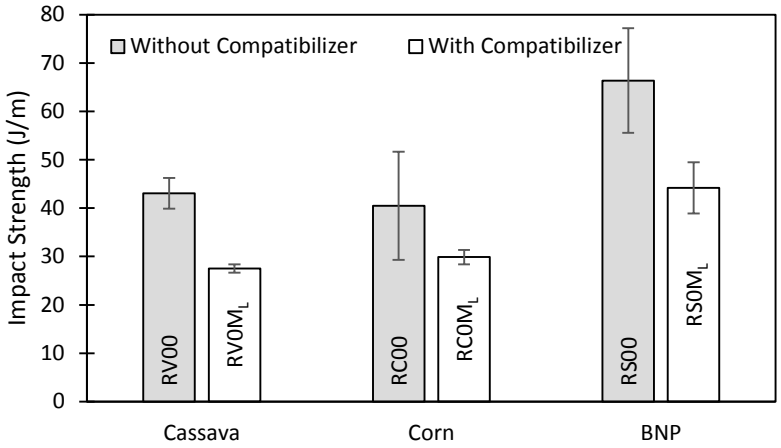

Figure 4-4 Effect of Cassava, Corn, BNP & HBNP on Impact Strength of BPE Composite with and without PE-g-MA as compatibilizers

4.2.1.2 Effect of Maleic Anhydride vs. Ethylene Acrylic Acid as Compatibilizer on Starch and Cellulose Fiber-Based Composites

In the current work, a comparison of three types of compatibilizers was performed in PE composites with BNP as filler or with Cellulose Fiber Type 1s. PE-*graft*-Maleic Anhydride of a high and a low Maleic anhydride grafting percentage, and a random copolymer of Polyethylene-*co*-Acrylic Acid (also called ethylene acrylic acid EAA) were used.

The Flexural mechanical tests show that the low concentration PE-g-MA performs relatively better and lends to the best Modulus (Fig 4-5) and strength (Fig 4-6) metrics compared with the other two while the ethylene acrylic acid provides best results in an Izod impact strength test (Fig 4-7). Between the two types of MA compatibilizers the low content MA compatibilizers performs better but this is almost a negligible difference. Kim et al. tested PP composites filled with rice husk and wheat flour and tested the formulations with five commercial PP-g-MA compatibilizers, they found that between two almost identical M_w Polybond compatibilizers with 0.5 and 1% grafts of MA, the one with 1% MA showed only negligibly better flexural, impact and tensile strength. They also showed that between two identical MA% compatibilizers with M_w 52000 and 9100, the one with higher M_w showed considerably better mechanical strength [46]. This probably means that more entanglement and perhaps co-crystallization of the compatibilizers with the matrix phase effects the mechanical properties more than a difference in grafting level.

Another interesting result to note here is that at 15% fiber loading versus 20% BNP loading, the composites with fiber show much better flexural properties. This is attributed to the aspect ratio, which

is repeatedly mentioned as one of the significant parameters for reinforcement in literature. While the starch nanoparticles have better impact properties than cellulose fiber filled composites.

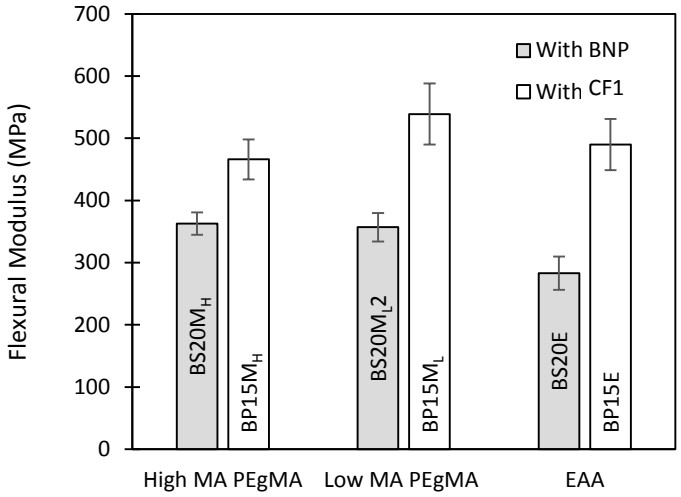

Figure 4-5Effect of three types of compatibilizers on the Flexural Modulus of BNP and CF1 Filled BPE Composites

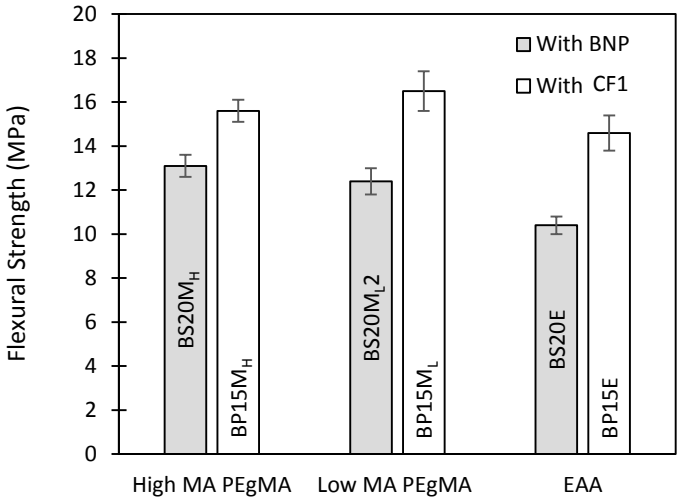

Figure 4-6 Effect of three types of compatibilizers on the Flexural Strength of BNP and CF1 Filled BPE Composites

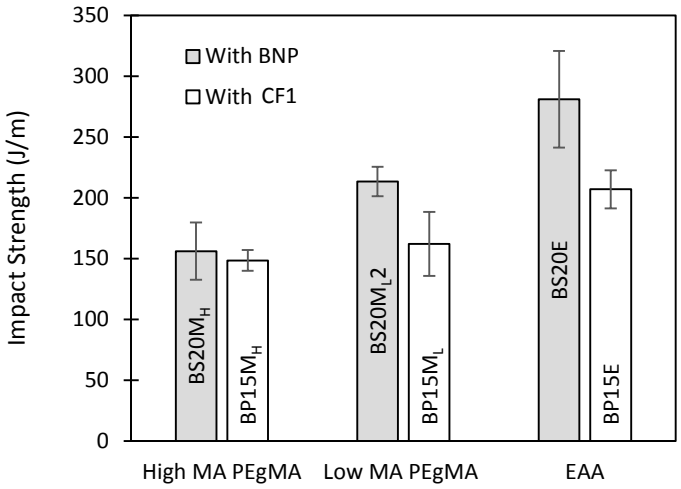

Figure 4-7 Effect of three types of compatibilizers on the Impact Strength of BNP and CF1 Filled BPE Composites

4.2.1.3 Effect of Surface Compatibilizer Content AND Chemical Modification of BNP

Improved adhesion between the matrix phase and the fibers and fillers leads to enhanced mechanical properties. The following graphs compare the improvement in flexural modulus, strength and impact strength upon addition of PE-g-MA as compatibilizers and the use of a hydrophobically modified (functional modification by maleic anhydride) BNP as filler versus the unmodified nanoparticle.

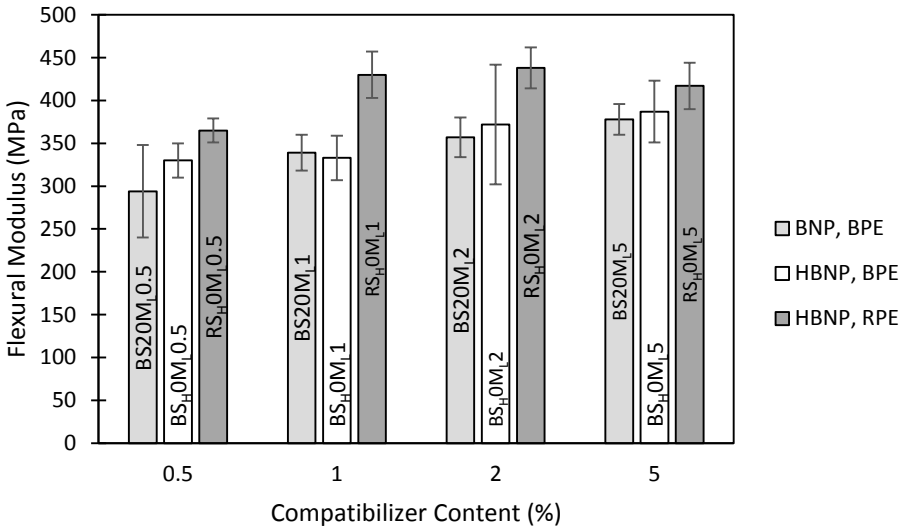

Figure 4-8 Effect of increasing PE-g-MA content on Flexural Modulus of Modified and Unmodified BNP filled BPE Composites

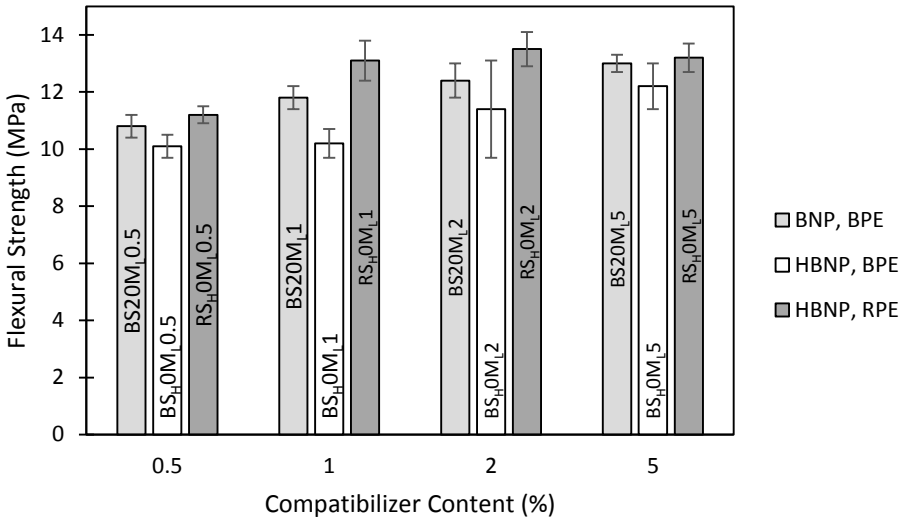

Figure 4-9 Effect of increasing PE-g-MA content on Flexural Strength of Modified and Unmodified BNP filled BPE Composites

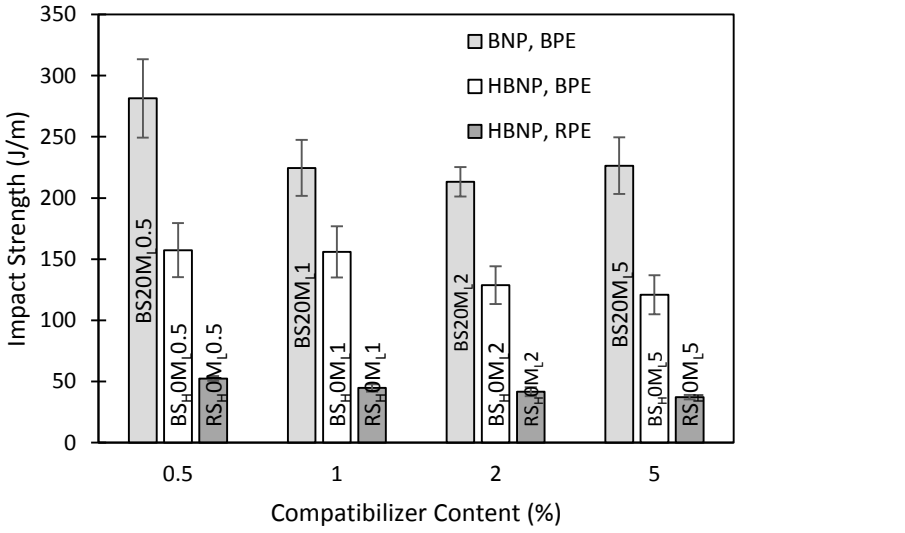

Figure 4-10 Effect of increasing PE-g-MA content on Impact Strength of Modified and Unmodified BNP filled BPE Composites

It can be observed from Figure 4-9 and 4-10 that the flexural and impact strength for formulations using BNP in BPE are slightly higher than formulations using Hydrophobic BNP in BPE at all concentrations of compatibilizers.

The hydrophobic BNP was expected to perform better given the better interface adhesion possible due to modification to increase affinity with hydrophobic and non-polar substance. However, it can be observed from Figure 4-9 and 4-10 that the flexural and impact strength for formulations using BNP in BPE are slightly higher than formulations using Hydrophobic BNP in BPE at all concentrations of compatibilizers. . This was also confirmed through literature in other types of modified products where SNC modified with ASA and another with PI (phenylisocyanate) was used in a natural rubber matrix. The mechanical properties of these composites were compared with composites using unmodified version of

the SNC and the results showed a sharp decrease in the strength and strain at break as well as thermal stability. The reason for this was explained as reduced interaction between filler particles through the hydrogen bonds which were replaced, this destroyed the three-dimensional network of the particles despite the improvement of adhesion at the matrix-filler interface [47]. This result is concurrent with that reported by Angellier et al., who reported reduced mechanical properties when a modified SNC was used as reinforcement in NR compared with unmodified SNC [47]. A very small increase in modulus is observed at 2% compatibilizer content.

Also, for increasing compatibilizers content from 0.1, 1, 2 and 5% it can be seen that the flexural modulus (Fig 4-8) and flexural strength (Fig 4-9) increase, but increasing the concentration to 5% either has no effect or is goes down slightly. For this reason all other formulations were done with the optimum of 2% PE-g-MA content.

Impact strength is reduced with the incorporation of starch nanoparticles, whether modified or unmodified when compared with virgin base material as is established from literature for all rigid particulate fillers. But this decrease is shown to be more enhanced with modified BNP than it is for unmodified, in Fig 4-10. This is contrary to classic composite science. For example the results from Sailaja and Chanda's experiments, using PVOH as compatibilizers in TPS-LDPE composite, showed continually increasing impact strength from 0-25% of compatibilizers content increase [48]. For these experiments (Fig 4-10) the increase of compatibilizer content shows reduced impact strength for all samples between 0.5 to 2% but this increases slightly at 5% but not enough to justify the compromise on flexural properties and cost offset.

Similar results were obtained by Liu et al. who tested cornstarch in LDPE with compatibilizer content ranging from 0 to 35% and reported an increase in tensile strength up to 10% of PE-g-MA, after which the values plateaued indicating there was an optimum quantity which corresponds to a maximum in interfacial adhesion. However, at increasing starch content they observed decreased tensile strength and the addition of compatibilizers again increased this value slightly at high starch loadings [49].

4.2.2 FILLER REINFORCEMENT

Starch, both in granular and plasticized states is a strong and stiff material. With modulus, strength values of the order of 2 GPA and 20MPa respectively, it acts as a reinforcing filler in most polyolefin based composites or blends. In the work presented starch nanoparticles have been used as fillers in LLDPE matrices along with cellulose fibers as co-reinforcement. The following section reviews the capability of starch derived nanoparticles as reinforcement at increasing concentrations.

The majority of work done on starch fillers at a nanoscale in composites has been done for starch nanocrystals and the mechanical properties have been reported for SNC with numerous sources and in a variety of polymer matrices. A detailed paper on this was published by Le Corre and Angellier who list a table with properties of a number of such composites researched by many others [18].

4.2.2.1 Effect of BNP and Modified BNP content

The following figures demonstrate the effect of increasing BNP/ Modified BNP on Cellulose Fiber Type 1/ Cellulose Fiber Type 2 fiber filled composite's mechanical properties. From Fig 4-11 it can be concluded that increasing starch nanoparticle content from 0-20% increases modulus irrespective of type of matrix, fiber and whether the nanoparticle is modified or not. This is similar to many literature citing such as the work by Matzinos et al. who found rising modulus upon addition of plasticized starch from 0-40% in a

compatibilized LDPE matrix [38]. This establishes that nanoparticles derived from starch are viable reinforcing fillers. Upon closer inspection, it can be deduced that the percentage rise in modulus for RPE is much higher than it is for BPE, therefore a lower molecular weight PE with shorter chains allows perhaps for better reinforcement by the nanoparticles, their respective dispersions and distributions will be discussed in the Morphology results later. There is negligible difference between moduli between formulations with modified and unmodified nanoparticles derived from starch, and for these fiber filled composites, modified nanoparticles derived from starch seem to show negligibly better moduli when increased in concentration. This could be attributed to their smaller size, as will be seen in morphological results which can be compared against the results by Taik et al. who showed larger starch granules provided better mechanical properties [50], this difference in trend could be unrelated since it is a comparison of native granule vs amorphous crosslinked nanoparticle aggregates. . Or perhaps due to the reduced interface tension between filler-matrix which enhances the stress transfer between phases.

In terms of flexural strength results shows in Fig 4-12 that the strength increases gradually from 0-15% modified nanoparticles derived from starch in BPE after which it decreases at 20% which is a trend mentioned often in literature for strength of filled composites [31]. However, in a low molecular weight RPE base matrix the strength continued to increase at 20% modified nanoparticle filler. The effect of modified the reinforcement phase in a polyolefin matrix was studied by Mulinary et al. who reduced the number of –OH groups on cellulose fibers used as reinforcement in HDPE matrix and they reported slightly improved mechanical properties. [34] Whereas, for unmodified SNP in RPE, the strength also continued to increase at 20% filler concentration.

Between samples $BP15M_L1$and BS_H0FM_L where there is no nanoparticles filler, and two types of fibers; CF1 and CF2 respectively, it can be argued that the CF2 makes the composite stiffer and stronger than the CF1. But the results in Fig 4-13 show a much better impact strength for composites containing CF1 than those with CF2, giving a better property offset and thus perhaps are more suitable, and more economical as well.

Another interesting phenomenon that must be discussed here is the suspected role of nanoparticles as compatibilizers in non-miscible blends of two polymers or phase separated composites which has been speculated much in literature [51], [52], this was one of the hypothesis questions. This phenomenon is reported to depend on selective localization and dispersion of nanoparticles in the blend, factors such as temperature, processing shear, viscosity and characteristic of the components determine whether the nanoparticle will localize itself at the interface. Some suggest the formation of *in-situ* grafts at the interface where the nanoparticle localizes [53]. And from the results presented below one can deduce that there seems to be little difference in results between formulations with none and low loadings of nanoparticles derived from starch (5%) where a compatibilizing effect may be evident, indicating that such an effect is not translated in mechanical results or it is related to ineffective dispersion of the BNP aggregates in the matrix. The results of morphology discussed later do however, exhibit a unique adhesion of fiber and matrix upon addition of nanoparticles derived from starch.

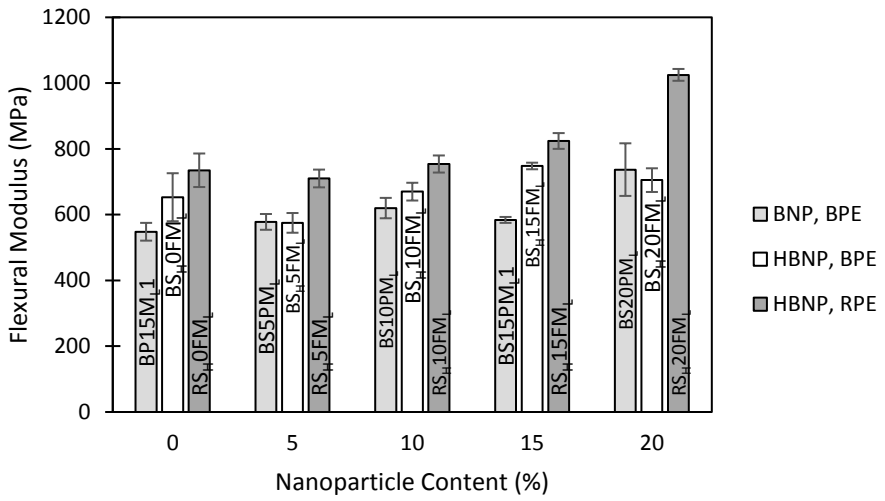

Figure 4-11 Effect of increasing BNP/HBNP content on Flexural Modulus of Composites containing fixed amount of Cellulose Fiber

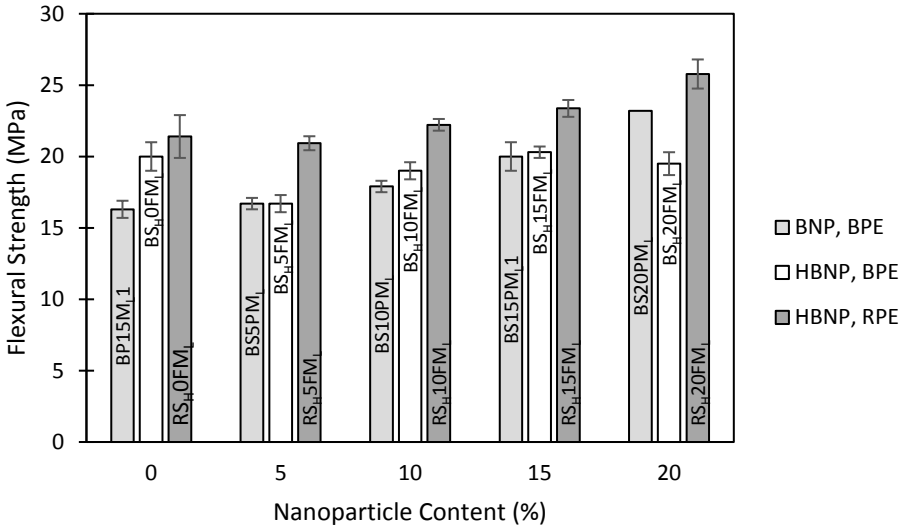

Figure 4-12 Effect of increasing BNP/HBNP content on Flexural Strength of Composites containing fixed amount of Cellulose Fiber

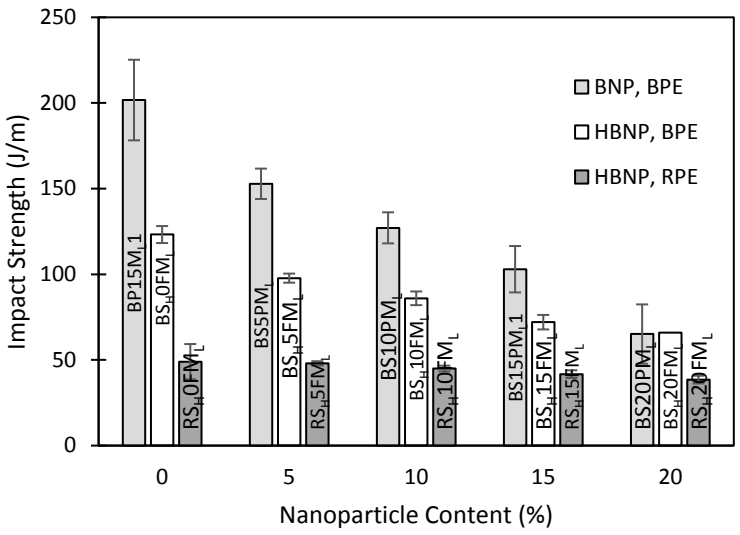

Figure 4-13 Effect of increasing BNP/HBNP content on Impact Strength of Composites containing fixed amount of Cellulose Fiber

4.2.3 FIBER REINFORCEMENT

This section presents and discusses the results of mechanical tests for samples with varying concentrations of fiber, in composites with two different matrix types and filled with two types of SNP's, two types of cellulose fibers are also compared in identical formulations.

4.2.3.1 Effect of Fiber Content

The following figures demonstrate the reinforcing effect of cellulose fibers in two variations, Cellulose Fiber Type 1s and freeze dried pulp fibers. The content of fibers is increased from 5% to 20% in PE matrix filled with modified or unmodified nanoparticles derived from starch.

From the results portrayed in Fig 4-14 it can be inferred that the addition of CF1 and CF2 improves the stiffness of a SNP filled PE composites. The stiffening effect has been presented in literature extensively for various types of fibers-matrix combinations with many approaches for coupling, some very detailed review papers have been reported on the subject as well by Jacob and Thomas, and Manjusri and Misra [54][5].

In comparison the samples with CF1 show the highest rate of increase in Flexural Strength (Fig 4-15) and Flexural Modulus from 12-26 MPa and 446-1041MPa respectively. This property improvement is least prominent with the matrix with highest MFI and with CF2, which is opposite to the trend observed at increasing content of nanoparticles derived from starch. There are multiple studies showing results when it comes to the effect the matrix MFI or molecular weight has on a composite's mechanical properties; Chu et al. for example show that a higher molecular weight HDPE matrix filled with a polar MMT clay nanofiller, shows better modulus enhancement and intercalation than a lower MW HDPE, on account of higher shear stress due to the chains during melt processing [55], Raghavendra et al. also demonstrated similar results for a composite of Polycarbonate matrix-carbon fiber, and measured the interfacial stress transfer between phases for four molecular weights of the matrix, they found that the strength increased upon increasing molecular weight[56].

In the case presented, it can be proposed that due to the tape like geometry of the CF1 and CF2, the fibers were able to orient themselves at a higher degree while injection molding in the low MFI, high MW (BPE) matrix (due to high shear) thus they were able to reinforce the composite more in a directional sense than in the high MFI RPE. However, for the rigid, irregular nanoparticle aggregates, where directional orientation does not play a part, they were able to disperse or distribute more evenly in shorter chains of the high MFI RPE therefore showing a higher increase in properties than in the BPE matrix shown in Section 4.1.2.1.

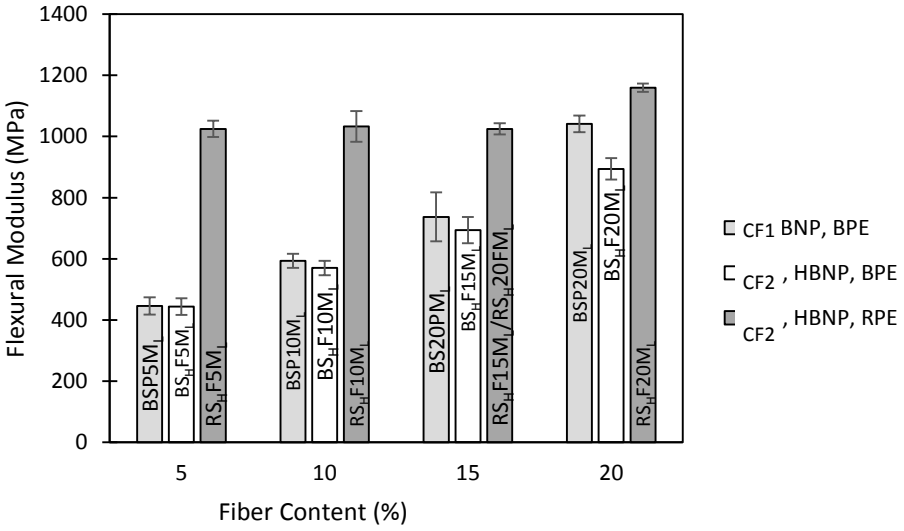

Figure 4-14 Effect of increasing CF1/CF2 content on Flexural Modulus of Composites containing fixed amount of BNP/HBNP

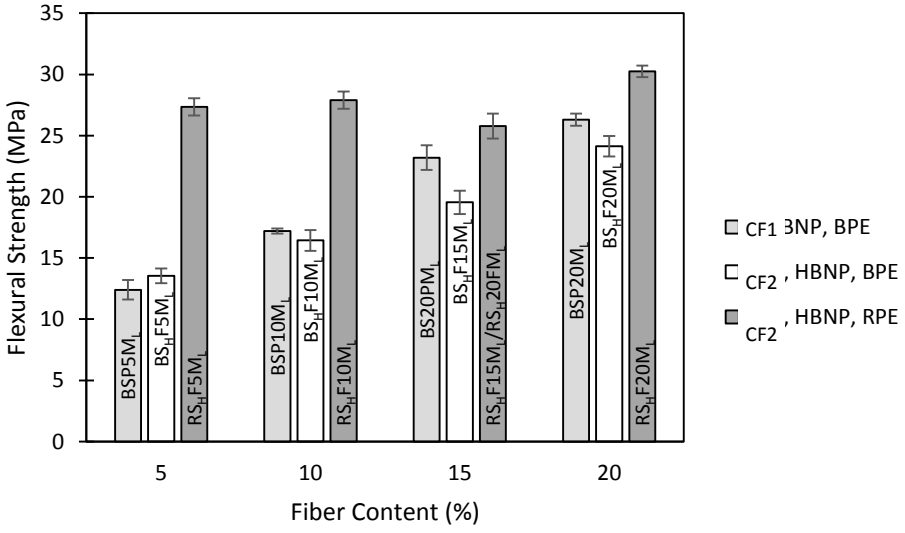

Figure 4-15 Effect of increasing CF1/CF2 content on Flexural Strength of Composites containing fixed amount of BNP/HBNP

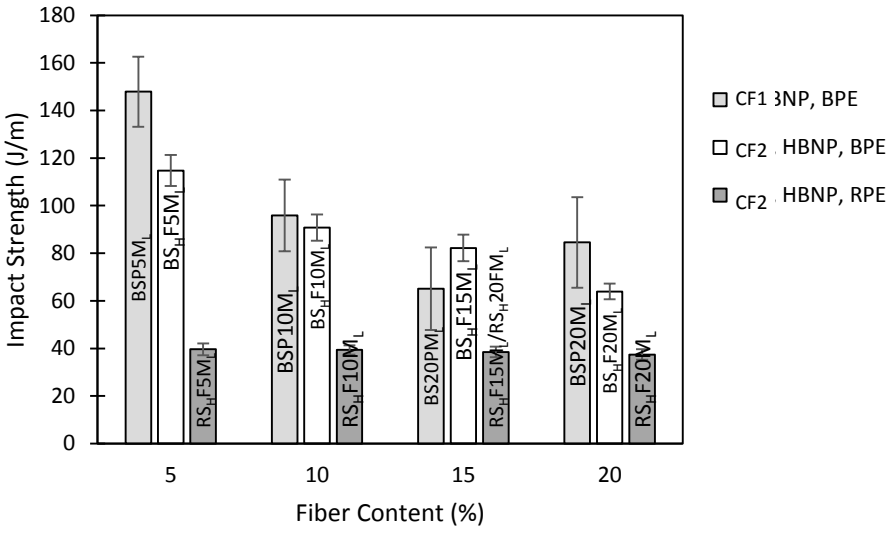

Figure 4-16 Effect of increasing CF1/CF2 content on Impact Strength of Composites containing fixed amount of BNP/HBNP

The impact properties of composites are normally reported to go down upon addition of rigid fibers; such is the observation from the Fig 4-16 where impact strength from an Izod Notch test decays as the fiber content increases. This is in compliance with results presented by Fatoni who observed a decline in impact properties upon addition of wheat straw fibers in PP while its modulus value increased [9] It is interesting to see, that the impact strength decreases much less for samples with CF1 than with CF2 in the same type of matrix, these do have two types of nanoparticles derived from starch though (modified and unmodified). An interesting set of results was presented by Mulinary et al. who showed Flexural and tensile modulus, strength as well as impact strength continued to improve upon addition of very similar Cellulose Fiber Type 1s (both modified and unmodified() in an HDPE matrix from 5 to 40% even without a compatibilizers [34].

4.2.3.2 Effect of Cellulose Fiber Type 2 vs Cellulose Fiber Type 1

The following graphs compare the results obtained with cellulose pulp fibers of different size and aspect ratio. The presence of moisture in composites being generally correlated with poor mechanical properties, the cellulose fibers type 1, received wet, was freeze dried to remove the interference of an excess of water in the final composite material. The figures suggest no improvement of any mechanical property upon moisture removal. The flexural modulus, strength and also impact strength are better for composites with CF1 fibers vs CF2 (Fig 4- 17, 18,19). The size and other aspects of the fiber are the same so it is interesting to see why non-dried fibers perform slightly better, this may mean that the fibers formed sturdier aggregates during the freeze drying or that upon grinding prior to addition to the composite they underwent more strain and deformation. These details will be observed further under the morphological results.

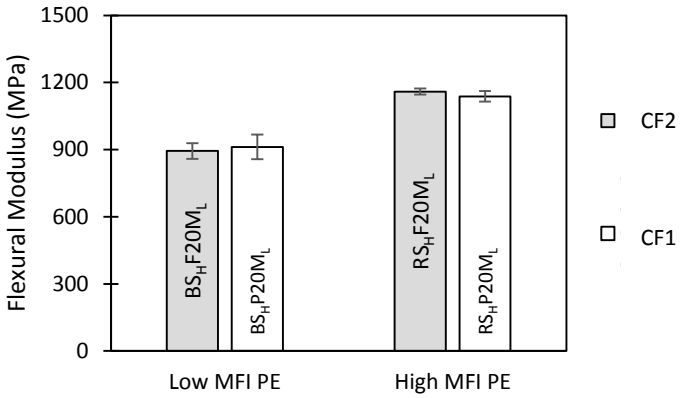

Figure 4-17 Effect of Cellulose Fiber Type 2 vs Cellulose Fiber Type 1 on Flexural Modulus of BPE/RPE composites filled with fixed amount of HBNP

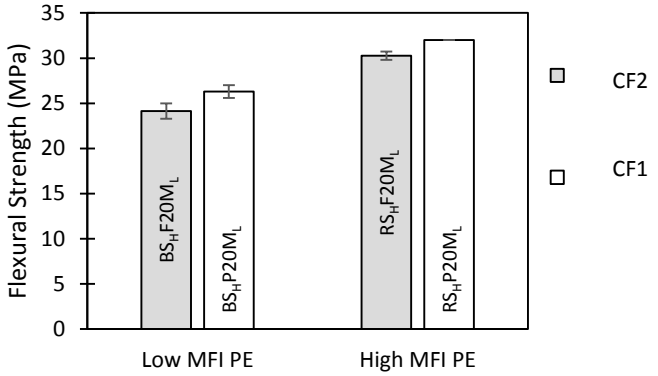

Figure 4-18 Effect of Cellulose Fiber Type 2 vs Cellulose Fiber Type 1 on Flexural Strength of BPE/RPE composites filled with fixed amount of HBNP

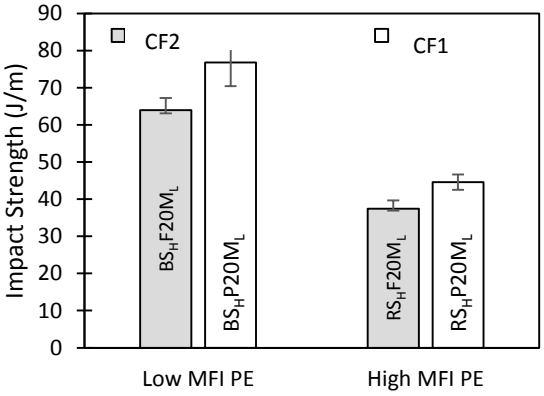

Figure 4-19 Effect of Cellulose Fiber Type 2 vs Cellulose Fiber Type 1 on Impact Strength of BPE/RPE composites filled with fixed amount of HBNP

4.2.4 REINFORCEMENT COMPARISON BETWEEN NANOPARTICLES AND FIBERS

The following Figures give a descriptive comparison of the reinforcement effect of particulate fillers versus fibers in the PE matrix with PE-g-MA as compatibilizers. Both the starch derived BNP and cellulose fibers improve flexural properties of the composite. And in agreement with literature, the aspect ratio of the

filler has a profound correlation with the mechanical properties. Neilson reported in the 70's detailed theoretic models predicting the difference between particulate and longitudinal fillers and concluded that a high degree of directional orientation of fibers provides high mechanical properties to the composites [57]. Later research in the field of composites also supports this effect; higher aspect ratio means better reinforcement [20][58]. From Figures 4-20 and 4-21 it can be seen that the cellulose fibers lead to a higher improvement in flexural modulus and strength, the impact strength however, Fig 4-22, is better for composites containing the BNP. The impact strength is reduced significantly compared to the neat matrix and this could be due to high interfacial tension between the hydrophobic matrix and the hydrophilic fillers which do not allow for ideal stress transfer between the phases and act as stress concentrators.

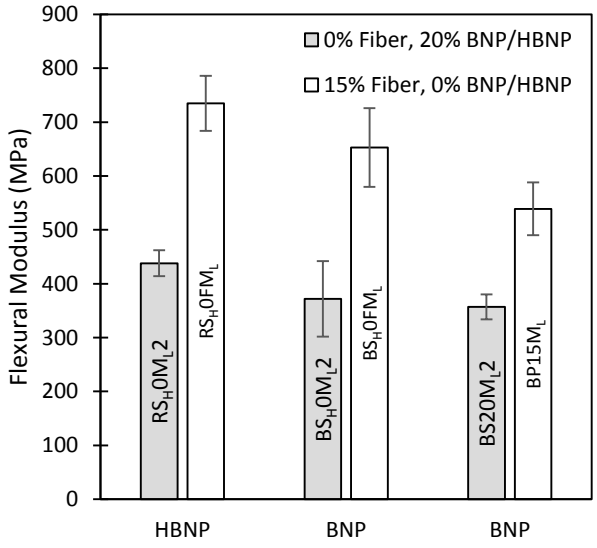

Figure 4-20 Effect of Fiber vs BNP on Flexural Modulus

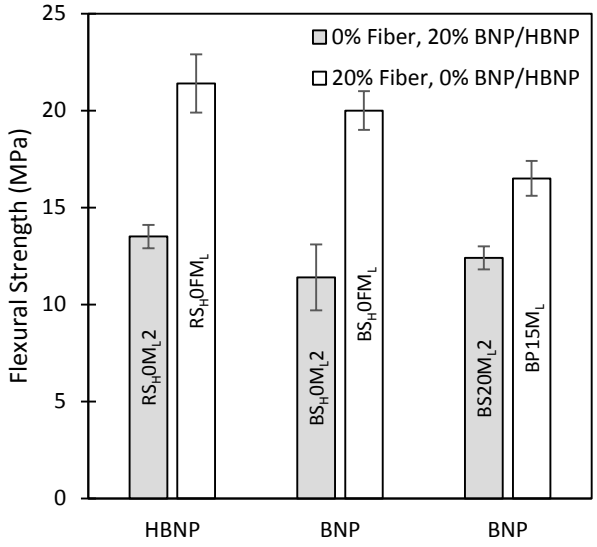

Figure 4-21 Effect of Fiber vs BNP on Flexural Strength

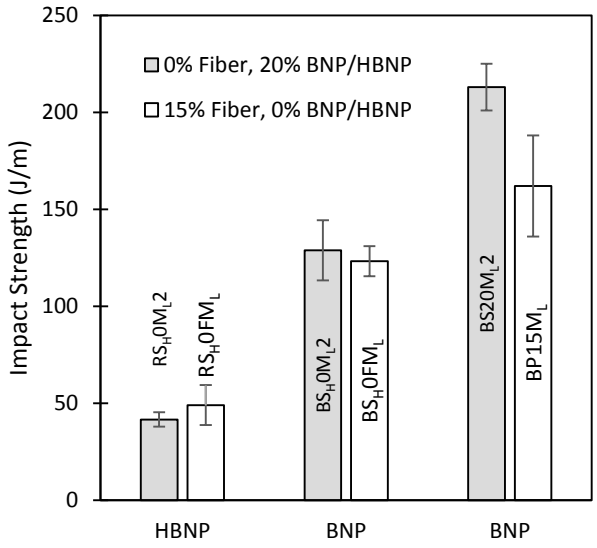

Figure 4-22 Effect of Fiber vs BNP on Impact Strength

Despite this difference, there is still great value in using starch based BNP as reinforcing fillers due to a synergistic effect of the fibers and fillers, due to difference in geometries and similarity in chemical nature as reported by Hemant et al. and Prasad et al. for composite systems studying the effect of shape geometries of reinforcement in composites in work dissimilar to that presented here [59] [60].

4.2.5 MATRIX POLYOLEFIN

4.2.5.1 Effect of using Different Polyolefins as Matrix Material

The following figures present the change in mechanical properties of a base polyolefin matrix upon high loadings of dispersants. The graphs present data of unfilled matrix, and then with 20% cellulose fiber and 15% or 20% of starch nanoparticle in two types of LDPE matrix and in PP matrix as well. Similar comparison of PE and PP matrix material filled with modified nanoparticles has been conducted by Altan and Yildirim [61].

Fig 4-23 shows a Flexural Modulus increase of 360% for RPE, 260% for BPE and 100% for PP, this indicates that the molecular weight as well as the chemical architecture of the matrix polymer effects the level of mechanical improvement achieved by addition of reinforcements. The highest property enhancement is observed for RPE, with a lower molecular weight, this could indicate better wettability or better filler/fiber and matrix interactions. The same trend was shown for a low viscosity PP/Kenaf composite versus high viscosity PLA/Kenaf composite by Han et al. who attributed this difference in property enhancement to a role of matrix MFI. [41]

The work of Aridi et al. on injection molded PP composites filled with rice husk is corroborative in terms that they also observed very little modulus enhancement in PP upon increasing filler loading between 35-55% [62]. Obasi and Igwe tested composites of PP with native cassava starch as filler and compatibilized with PP-g-MA, and also reported the mechanical properties; there was decrease in strength and elongation at break but an improvement in Young's modulus was reported upon increasing starch content from 0-50%, this was still very low in comparison to the many studies done with PE instead of PP [63]. The moduli of the filled RPE and BPE composites are almost better if not equal to the modulus of neat PP,

which is a rigid and stronger polymer than PE. Although the cost of PE and PP have not been very different over decades, but there are no current routes of manufacturing PP from renewable sources, this makes the PE composite much more attractive if environmental concerns and sustainability are kept in view.

The trend in flexural strength (Fig 4-24) is the same as for modulus; i.e., a better property enhancement in LLDPE composites than in PP, the reason for this could be the bulkier methyl pendant group in PP compared with the hydrogen in PE. This increased tortuosity in path might prevent the fillers and fibers to intercalate completely and hinder perfect stress transfer from matrix to fiber or SNP. Another reason could be the temperature at which the composite was processed. In order to prevent the fibers and SNP from degrading the processing temperatures implied were between 190-220°C and this was perhaps not enough for complete melting and blending for the PP with more rigid fillers.

As discussed in previous sections, the addition of rigid reinforcements to polyolefin composites increases the modulus and strength but this comes with a compromise on impact properties; reducing the impact strength. Fig 4-25 shows that the PP composite shows a much lower Impact strength of around 22J/m than the PE composites, but it also shows the least rate of decrease dropping only 4J/m from 26J/m for pure PP. While for PE composites this drop is over 6 times approximately. This drop is less drastic for CF1 fiber and BNP formulations than for CF2 and modified BNP.

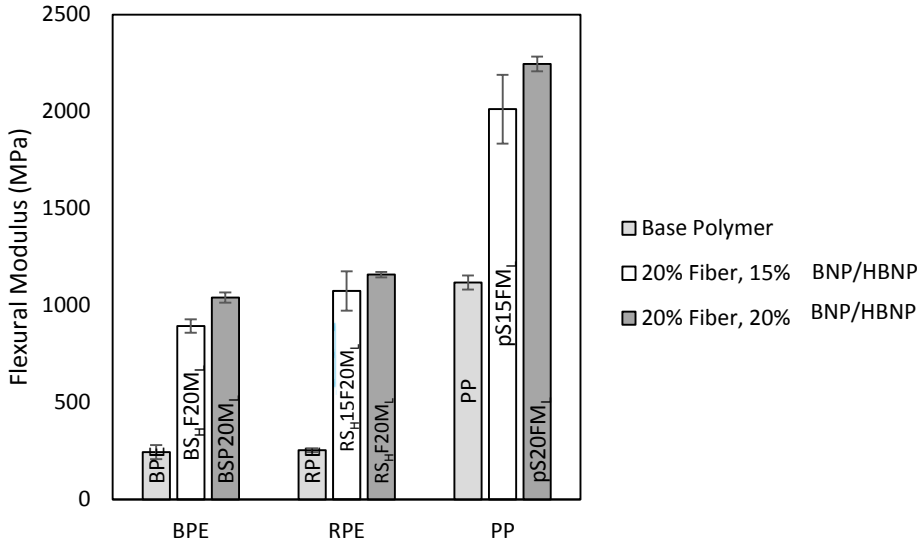

Figure 4-23 Effect of High Loadings of fiber and filler on Flexural Modulus of Composites with three different Matrices

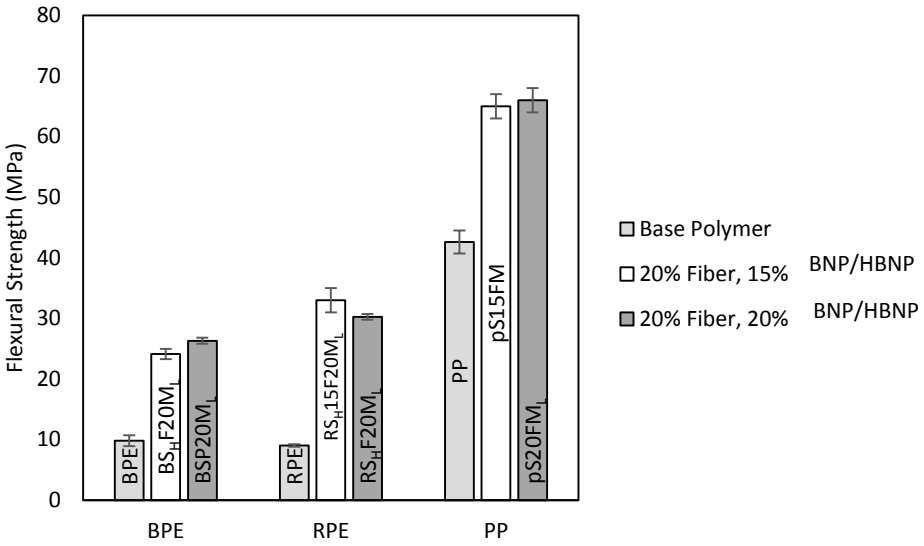

Figure 4-24 Effect of High Loadings of fiber and filler on Flexural Strength of Composites with three different Matrices

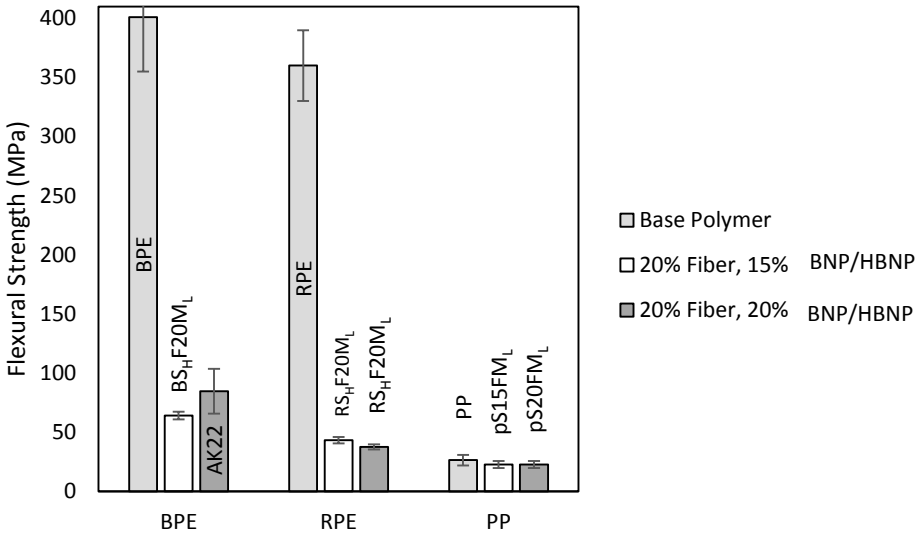

Figure 4-25 Effect of High Loadings of fiber and filler on Impact Strength of Composites with three different Matrices

4.3 FLOWABILITY

4.3.1 MELT FLOW INDEX (MFI)

The effect of adding different fillers, fibers and additives on MFI of the composites was recorded and compared with the neat matrix and between types, and quantities of respective components. These results are discussed categorically in this section.

4.3.1.1 Effect of Increasing Fiber, Filler and Compatibilizer Content on MFI

The effect of adding reinforcing fibers and fillers in neat polymer matrices has universally shown to decrease MFI of the composite owing to the more rigid nature of these reinforcing materials [64][31].

From Table 6 it can be observed that on increasing the compatibilizers content the MFI that drops on addition of filler compared to neat matrix, actually increases, this can be attributed to better mixing, better dispersion that aids in better flow in the melt state as also shown by Gupta and Alam [65].

The increase of HBNO from 0-20% decreases the MFI systematically for RPE matrix composites, for BPE matrix composites the value drops as well but a slight discrepancy is observed between 15 and 20% this can either be attributed to experimental error or some processing non-conformities considering this slight effect is observed in mechanical properties as well (Modulus and Flex strength of BS_H15FM_L is better than BS_H20FM_L counter to the trend Fig 4-11 &12). The increase of MFI upon addition of rigid fillers has been reported in literature, in specific, Tome et al. noted reduced MFI on increasing addition of chitosan in starch matrix and attributed it to higher interactions. The reduced MFI was also paired with higher mechanical properties which is also the case here [66].

The addition of fibers also decreases the MFI of the composite, and it is interesting to note the higher drop (from 16g/10min to 2.1g/10min) on fiber addition compared to a much lower drop for addition of HBNP as shown in the Fig 4-26 and 4-27 for both BPE and RPE composites.

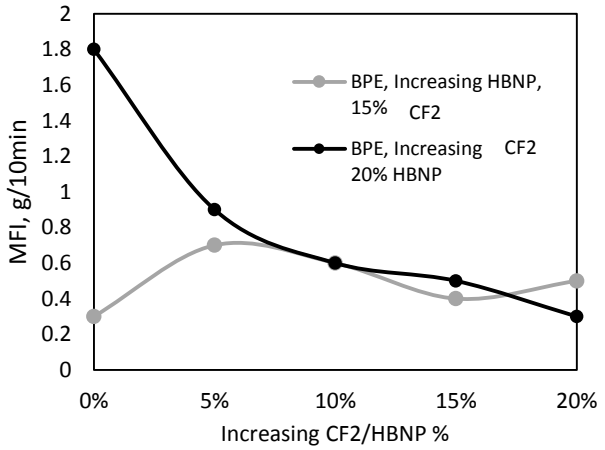

Figure 4-26 MFI drop on addition of CF2 and HBNP from 0-20% in BPE

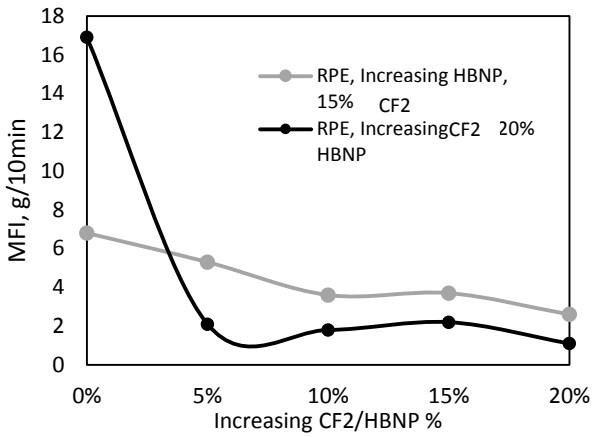

Figure 4-27 MFI drop on addition of CF2 and HBNP from 0-20% in RPE

Table 6 Effect of Increasing Compatibilizer, HBNP and CF2 on composite MFI

	RPE	**Sample**	**BPE**	**Sample**
	33.5	Neat	2.8	Neat
Increasing Compatibilizer Content				
0.50%	15.3	$RS_H0M_L0.5$	1.5	$BS_H0M_L0.5$
1%	17.3	RS_H0M_L1	1.5	BS_H0M_L1
2%	16.9	RS_H0M_L2	1.8	BS_H0M_L2
5%	19.3	RS_H0M_L5	2.1	BS_H0M_L5
Increasing Filler Content				
0%	6.8	RS_H0FM_L	0.3	BS_H0FM_L
5%	5.3	RS_H5FM_L	0.7	BS_H5FM_L
10%	3.6	RS_H10FM_L	0.6	BS_H10FM_L
15%	3.7	RS_H15FM_L	0.4	BS_H15FM_L
20%	2.6	RS_H20FM_L	0.5	BS_H20FM_L
Increasing Fiber Content				
0%	16.9	RS_H0M_L2	1.8	BS_H0M_L2
5%	2.1	RS_HF5M_L	0.9	BS_HF5M_L
10%	1.8	RS_HF10M_L	0.6	BS_HF10M_L
15%	2.2	RS_HF15M_L	0.5	BS_HF15M_L
20%	1.1	RS_HF20M_L	0.3	BS_HF20M_L

4.3.1.2 Effect BNP vs HBNP on MFI

Table 7 gives the list of MFI's for composites formulated with BNP and HBNP. It can be seen that for the same base matrix, at 2% compatibilzation, the BNP shows a lower drop of MFI than does HBNP.

For formulations using 0-20% filler content at a constant fiber concentration, it is clear that both BNP and HBNP cause a drop in MFI from the neat matrix, the drop is however more systematic and observable for HBNP than it is for BNP. This could be due to improved intermolecular interactions between the interfaces causing the restriction in flow.

The drop of MFI upon addition of 15% fiber is drastic compared with 20% filler, 0.3 and 108 g/10min respectively. The addition of HBNP in the formulation with fiber however, increases the MFI slightly compared with only fiber formulation and then falls as content of HBNP is increased, this could indicate that HBNP in small quantities can act as a flow enhancer for fiber formulations.

Table 7 Comparison of the effect of BNP vs HBNP on MFI of Composites with and without Fiber reinforcement

	MFI (g/10min)		**MFI (g/10min)**	
Type of Starch Derived Nanoparticle	**BNP**	**Sample**	**HBNP**	**Sample**
Without Fiber				
20% filler, 2% Compatibilizer	2.3	AK09	1.8	BS_H0M_L2
Increasing BNP/HBNP Content (15% Fiber)				
0%	1	AK07	0.3	BS_H0FM_L
5%	0.7	AK-16	0.7	BS_H5FM_L
10%	0.8	AK-17	0.6	BS_H10FM_L
15%	0.7	AK-18	0.4	BS_H15FM_L
20%	0.6	AK-19	0.5	BS_H20FM_L

4.3.1.3 Effect of type of Compatibilizer on MFI

There is no difference on MFI of composite when using EAA, PE-g-MA (high MA) or PE-g-MA (low MA) as compatibilizers as seen in Table 8. All three compatibilizers show the same value of MFI 2.3 g/10min.

Table 8 Effect of EAA, PE-g-MA (low MA) and PE-g-MA (high MA) on composite MFI

Filler Content 20% BNP, 0% Fiber	**MFI**	**Sample**
EAA (2%)	2.3	BS_H20FM_L
PE-g-MA (low) (2%)	2.3	$BS20M_H$
PE-g-MA (high) (2%)	2.3	BS20E

4.3.1.4 Effect of Native Starch vs BNP on MFI

The addition of native granular starch (corn and cassava) and modified and unmodified starch derived nanoparticles (BNP and HBNP) both reduce the MFI of the composite from 33 g/10min of neat matrix considerable. This is due to the fact that unplasticized starch is rigid with a high molecular weight and the crosslinked nanoparticles are also rigid in a non-polar matrix. The difference between granular starch and BNP aggregates is very negligible.

Table 9 Effect of Types of Filler on MFI

	MFI (g/10min)	**Sample**
Neat Matrix	33.5	RPE
Cassava	18.0	RV00
Corn	17.9	RC00
BNP	17.1	RS00

4.4 THERMAL PROPERTIES

4.4.1 THERMAL PROPERTIES OF PURE MATERIALS

Table 10 lists the thermal data of all the materials used in composites except the compatibilizers. As such, the CF2, CF1, BNP and HBNP do not melt but degrade at higher temperatures and thus their DSC data is not available. The values presented here are essential to the discussion in the following sections.

Table 10 Thermal Properties of Pure Materials

Sample	Thermal Data					
	DSC				TGA	
	Crystallization Temperature T_c (°C)	Melting Temperature T_m (°C)	Enthalpy of Melting ΔH_m (J/g)	Percentage Crystallinity $\%X_c$	Moisture Content %	Onset of Degradation
BPE	110	125	93	37	0.0	340
RPE	107	124	117	29	0.0	371
PP	116	166	77	44	0.7	272
CF2	-	-	-	-	2.2	239
CF1	-	-	-	-	1.3	268
BNP	-	-	-	-	4.5	243
HBNP	-	-	-	-	3.5	227

4.4.2 EFFECT OF INCREASING FIBER, FILLER AND COMPATIBILIZER CONTENT ON THERMAL PROPERTIES

Table 11 presents the DSC and TGA data of composites using BPE and RPE as matrix and HBNP as the filler. CF2 is used as the fiber reinforcement in some but not all formulations presented in this table.

It can be observed for BPE composites that on increasing compatibilizers content the values of Tm, T_c and $\%X_c$ do not change much at all. The similarity is apparent in their thermograms (appendix) which proves that the compatibilizers does not change the thermal properties of the composite with a fixed amount of HBNP when BPE is used as the matrix. However, similar compositions with RPE show a more varied trend, the percentage crystallinity increase upto 2% of compatibilizers, which is shown as the optimum level in previous sections, and decreases on further increase in PE-g-MA, it is interesting also, that at 5% compatibilizers the T_c and Tm also drop, and a double endothermic peak is observed (see thermogram in appendix), this may indicate a difference in crystallization phenomenon due to the PE segments of the compatibilizers and their interactions with the shorter RPE chains of the matrix.

Since the HBNP is an amorphous nanoparticle aggregate, its addition decreases the crystallinity from 38% for no HBNP to 32% for 5% HBNP content in BPE composites. Increasing the HBNP content further up to 20% does not decrease the crystallinity very much. The melting temperature reduces slightly but not significantly. The crystallization temperature increases by up to 7°C from 0% HBNP to 5, 10, 15 and 20%. A similar increase in crystallization temperature was observed by Han et al. who reported on composites of PP/Kenaf and related this to transcrystallization as many other references in literature. [41] For the current work however, it is unfeasible to say that this change in T_c to a higher temperature is due to transcrystallization due to the absence of supporting XRD data and also because a general drop in crystallinity is observed. The effect of nanoparticles has been reported by many to increase the T_c owing to a 'small size effect' [67]

In RPE composites however, the T_c and T_m both decrease on addition of increasing amounts of HBNP as also observed by Liu et al. who reported a decrease in crystallization temperature at increased cornstarch (granular) content in LDPE matrix and this was attributed to hindrance in molecular motion of chains and to a reduced nucleation density [49]. The $\%X_c$ does not follow a regular trend, however a very high, 40% crystallinity is observed at high loadings of filler/fiber (from 29% for Neat RPE) which justifies the enhanced modulus and strength enhancement observed in these samples. This disparity in results on basis of different matrix materials has been reported in literature. Altan and Yildirin reported thermal behavior of PE and PP composites filled with TiO_2 nanoparticles, they showed an increase of crystallization in PE due to a nucleating effect of the silane treated filler, this was opposite for PE where the crystal formation was restricted due to the hindrance of the particles. This emphasizes that the nucleating effect of particles differs from matrix to matrix and what is true for one composite system may not be so for another with different additives. [61]

The addition of increased amounts of CF2 in BPE composites with HBNP filler showed reduction in the $\%X_c$ while a significant increase in $\%X_c$ can be seen for RPE composites.

Increasing the amount of fiber in both RPE and BPE composites does not show an increase in T_c, but reduced or almost unchanged values, this confirms the hypothesis of absence of unique crystals forming at the fiber or filler surfaces as seen in XRD results.

In terms of thermal stability for BPE composites, increasing compatibilizers content reduces the onset of degradation making them less stable at higher temperatures. For RPE composites, the degradation temperature at 2% weight loss does not change significantly from 0% compatibilizer.

HBNP degrades at 227°C (Table 10), which is lower than BPE, RPE and CF2, and therefore the composite's thermal stability goes down with increasing HBNP component in both RPE and BPE composites.

The CF2 is more stable thermally than the HBNP but much less than the neat matrix and therefore the composites for both BPE and RPE, thermal stability is compromised on increasing the content of CF2 but it is not as significant and generally better than for higher HBNP content. However, all samples, with HBNP and CF2 have good thermal stability and can be easily processed at high processing temperature of upto 250°C.

The moisture content in a composite also effects the thermal stability negatively. Even if all other factors are constant, moisture content can be different due to many external factors like the humidity etc. And therefore, formulations with a higher moisture content tend to have a lower onset of degradation temperature.

Table 11 Thermal properties of Composites of RPE & BPE with Increasing Amounts of Fiber, Filler and Compatibilizer

Sample	Thermal Data					
	DSC				TGA	
	Crystallization Temperature T_c (°C)	Melting Temperature T_m (°C)	Enthalpy of Melting ΔH_m (J/g)	Percentage Crystallinity $\%X_c$	Moisture Content %	Onset of Degradation
BPE						
Increasing Compatibilizer Content						
$BS_H0M_L0.5$	118	126	77	35	0.6	292
BS_H0M_L1	118	126	76	36	1.1	284
BS_H0M_L2	117	126	73	36	1.0	281
BS_H0M_L5	117	126	75	34	1.0	271
Increasing Filler Content						
BS_H0FM_L	110	128	74	38	0.2	313
BS_H5FM_L	118	126	84	32	0.4	298
BS_H10FM_L	117	126	83	30	0.6	283
BS_H15FM_L	118	126	74	31	1.1	267
BS_H20FM_L	117	117	74	29	0.7	285
Increasing Fiber Content						
BS_HF5M_L	118	126	67	40	0.8	282
BS_HF10M_L	118	126	121	21	0.4	287
BS_HF15M_L	117	127	69	33	0.7	281
BS_HF20M_L	110	125	69	31	0.8	277
RPE						
Increasing Compatibilizer Content						
BS_HF5M_L	114	124	89	31	0.9	279
BS_HF10M_L	114	123	80	34	0.4	286
BS_HF15M_L	115	124	71	37	0.5	281
BS_HF20M_L	108	121	84	31	0.3	282
Increasing Filler Content						
RS_H0FM_L	115	124	86	33	0.2	290
RS_H5FM_L	112	123	72	37	0.4	278
RS_H10FM_L	111	122	73	34	0.5	276
RS_H15FM_L	111	122	76	31	0.6	269
RS_H20FM_L	111	122	51	42	0.6	272
Increasing Fiber Content						
RS_HF5M_L	114	124	107	23	0.6	271
RS_HF10M_L	110	123	55	42	0.7	267
RS_HF15M_L	111	122	51	42	0.6	272
RS_HF20M_L	114	125	48	41	0.7	269

4.4.3 COMPARISON OF HBNP VS BNP ON THERMAL PROPERTIES

The following Table 12 shows a comparison of thermal properties of similar compositions with the difference of HBNP versus BNP, in general it can be summarized that increasing compatibilizers content in composites with HBNP show higher T_c, T_m and lower $\%X_c$ compared with those with BNP. This can be used to infer that the modification may aid in some level of surface crystallization but reduced lamellae size.Similarly so, the composites showing increased levels of HBNP/BNP, the BNP composites have higher crystallinity and lower T_c too while T_m does not change significantly, compared with HBNP composites.

The same trend is observed in composites with increasing levels of fiber, where BNP filled composites show higher crystallinity and lower T_c.

Table 12 Thermal Properties of HBNP vs BNP Composites

Sample	**Thermal Data**			
	DSC			
	Crystallization Temperature, Tc (°C)	**Melting Temperature, Tm (°C)**	**Enthalpy of Melting ΔHc (J/g)**	**Percentage Crystallinity %Xc**
BNP/HBNP				
Increasing Compatibilizer Content				
$BS_H0M_L0.5$	118	126	77	35
$BS20M_L0.5$	114	124	87	37
BS_H0M_L1	118	126	76	36
$BS20M_L1$	113	124	88	38
BS_H0M_L2	117	126	73	36
$BS20M_L2$	114	125	77	34
BS_H0M_L5	117	126	75	34
$BS20M_L5$	113	125	85	39
Increasing BNP/HBNP Content				
BS_H5FM_L	118	126	84	32
$BS5PM_L$	113	127	80	34
BS_H10FM_L	117	126	83	30
$BP15M_L$	114	125	86	40
BS_H15FM_L	118	126	74	31
$BS15PM_L1$	114	125	83	41
BS_H20FM_L	117	126	74	29
$BS20PM_L$	115	125	76	40
Increasing Fiber Content				
BS_HF5M_L	118	126	67	40
$BSP5M_L$	113	125	60	42
BS_HF10M_L	118	126	121	21
$BSP10M_L$	114	125	60	40
BS_HF15M_L	117	127	76	31
$BS20PM_L$	115	125	76	40
BS_HF20M_L	110	125	69	34
$BSP20M_L$	113	127	49	41

4.4.4 COMPARISON OF CF2 VS CF1 ON THERMAL PROPERTIES

A comparison of thermal properties of composites using CF2 and CF1 is made in the following Table 13. For composites with BPE the properties for CF1 and CF2 formulations are almost identical with no change in T_c, T_m or $\%X_c$ but the onset of degradation is at a higher temperature for CF1 than for CF2. This can be due to the higher content of moisture in the CF2 composite and the lower thermal stability of CF2 vs CF1 (Table 10).

However, for RPE composites, the $\%X_c$ is significantly higher for CF2 samples than for CF1 samples. The T_c is also slightly higher and Tm is not changed considerably.

It is interesting to note that all four samples presented in this table have very high loadings of fiber and filler, yet they have good thermal stability at high temperatures normally encountered in processing.

Table 13 Thermal Properties of CF2 vs CF1 Composites

Sample	**Thermal Data**					
	DSC				**TGA**	
	Crystallization Temperature T_c (°C)	**Melting Temperature T_m (°C)**	**Enthalpy of Melting ΔH_m (J/g)**	**Percentage Crystallinity $\%X_c$**	**Moisture Content %**	**Onset of Degradation**
BPE						
BS_HF20M_L	110	125	69	31	1	277
BS_HP20M_L	112	125	71	30	0	285
RPE						
RS_HF20M_L	114	125	48	41	1	269
RS_HP20M_L	112	124	62	32	1	272

4.5 MORPHOLOGY

4.5.1 XRD

4.5.1.1 Diffraction Patterns of Native Starch vs Starch Derived Nanoparticle Composites

It was shown in Fig 2-19, from open literature we find peaks of granular native starch in between the theta range of 10-30 degrees called a classical A-Type spectrum, while for thermoplastic starch there is not a very strong signal of diffraction. This notion can be used to understand the spectrum showed in Fig 4-28 from results of a PE composite with 30% cornstarch as filler and no other additives. The spectrum obtained is atypical of a PE semicrystalline polymer with signature peaks at 21.3 and 23.8 representing the (110) and (200) crystalline planes of PE, and since the characteristic peaks of the PE structure fall in the 10-30 degree spectrum, the possible peaks from the native granules of cornstarch may be masked under that region/peak. In Fig 4-29 and 4-30 almost identical spectra are obtained as for cornstarch, although these are composites of the starch derived BNP and HBNP filled PE at a 30%. From the manufacturing process of these BNP it is clear that a near complete gelatinization is obtained [68] which suggests there may be a completely amorphous structure unless the crosslinked nanoparticles undergo retrogradation, which will be evident from results discussed later in this section. However, it is sufficient to note at this point that the crystalline structures of the composites containing BNP/HBNP and cornstarch are essentially the

same, the percentage of crystalline regions however, can be assessed from the thermal analysis data of DSC, Table 4.

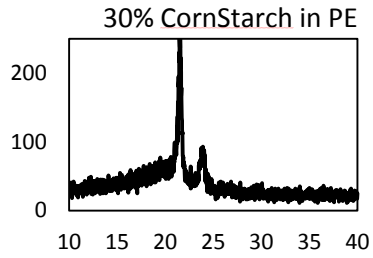

Figure 4-28 XRD of Cornstarch/PE Composite

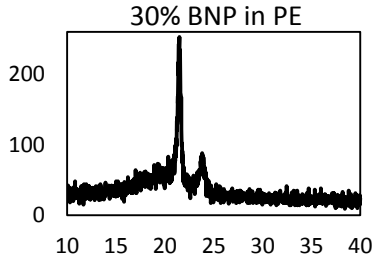

Figure 4-29 XRD of BNP/PE Composite

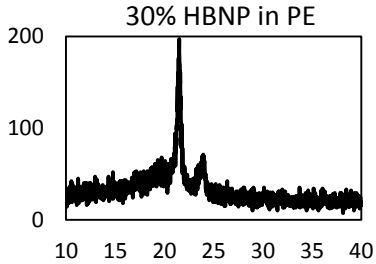

Figure 4-30 XRD of BNP/PE Composite

4.5.1.2 Effect of Compatibilization and Chemical Modification on Diffraction Pattern

The following sets of figures, compare the XRD spectra of composites with and without PE-g-MA compatibilizers in addition to 30% BNP or the chemically modified HBNP in a PE matrix. All four are very similar to typical starch-PE composites. Similar results were obtained by Matzino et al. who studied the blend of TPS and LDPE; and the XRD spectra obtained from a blend of 30% TPS in PE is shown in the literature review Fig 2-19, the only exception to the similarities is the slight overlap of the two faint peaks of TPS in the composite, remnant of the TPS [38]. Whereas, since the BNP/ HBNP filler used here has no absorption peaks Fig 4-29,30, they are also not translated in the composite spectra of Fig 4-31 and Fig 4-23,33.

The composites studied here are composed of a filler that is almost fully amorphous, starch derived crosslinked nanoparticle and therefore does not affect the crystalline structure of the composite. This is corroborative to the WAXD results obtained by Shi et al. who noticed a destruction of peaks inherent to corn starch film upon addition of amorphous starch nanoparticles, confirming that SNP promote destructive diffraction [39].

The addition of compatibilizers on XRD results has been studied in depth my many researchers but for mostly clay nanofillers such as MMT and layered silicates, the addition of TP grafted MA has shown to increase the interlayer spacing (*d* or interplanar spacing) of the nanofiller galleries showing an increased intercalation of the matrix and therefore increased dispersion [69][70]. Moreover Alfadhel et al. investigated the XRD spectra of Pulybutylene/starch/clay nanocomposites and concluded that the addition of a gelatinized starch did not show any absorption peaks on account of its inherent amorphousness, also between compatibilized and uncompatibilized samples, compatibilized samples did have sharper peaks indicating increased crystallinity; this was probably owing to the clay component because with increasing starch content the area under peaks decreased considerably; which also indicated poor dispersion and lowered crystallinity. [71]

This observation can be used to interpret the comparison of results obtained and showed in Fig 4-31, Fig 4-32 and Fig 4-33, Fig 4-34, where no difference in spectra is observed despite compatibilizers; because the BNP nanofiller aggregates are entirely amorphous, the addition of a surface modifier (PE-g-MA) has no effect in crystallinity or co-crystallinity. Moreover, comparing Fig 4-33 and Fig 4-34 it can be safely stated that the functional modification of BNP with maleic anhydride also does not lead to any changes on crystallinity of the composite without fibers.

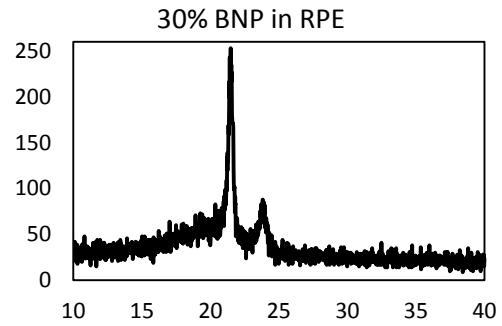

Figure 4-31 XRD of BNP/PE Composite- Uncompatibilized

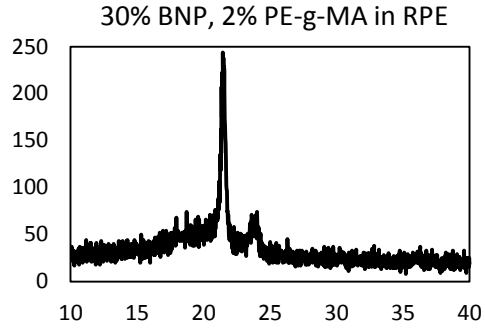

Figure 4-32 XRD of BNP/PE Composite- Compatibilized

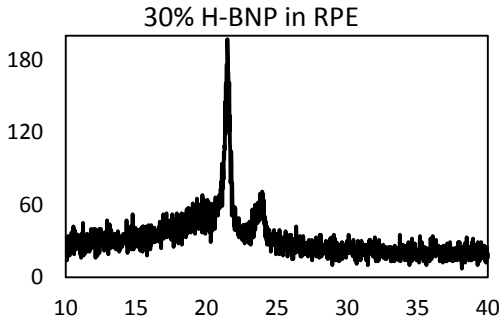

Figure 4-33 XRD of HBNP/PE Composite- Uncompatibilized

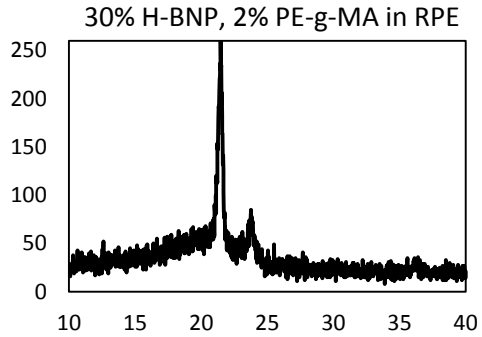

Figure 4-34 XRD of HBNP/PE Composite- Compatibilized

4.5.1.3 Effect of Cellulose Fiber Type 2 vs Cellulose Fiber Type 1 on Diffraction Pattern

Shi et al. presented a strong case of changing diffraction patterns of starch nanoparticles based on the different ways they were dried; freeze dried or spray dried [39]. Since the current work used two cellulose fibers with different size and aspect ratio also dried in different ways; type 2 being freeze dried, their respective XRD spectra were obtained to investigate any possible difference in crystal structure. These are represented in Fig 4-35 and 4-36 and no difference is apparent. These spectra are atypical of cellulosic fibers and for cellulose itself with characteristic peaks at about 2θ of 16° for the (110) crystal plane and at appx. 23° for the (200) planar indices, corresponding to a B-type crystal structure.

Moreover the composites of both CF2 and CF1 fibers with HBNP filler in a compatibilized composite of BPE show no difference in diffraction peaks, as shown in Fig 4-37 and 4-38.

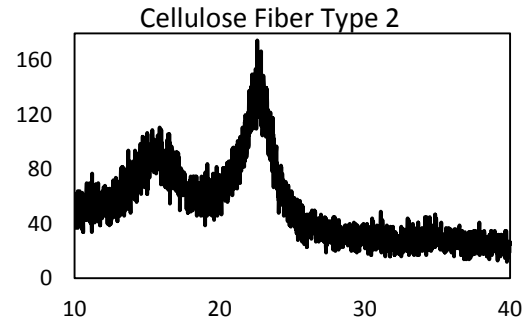

Figure 4-35 XRD of CF2

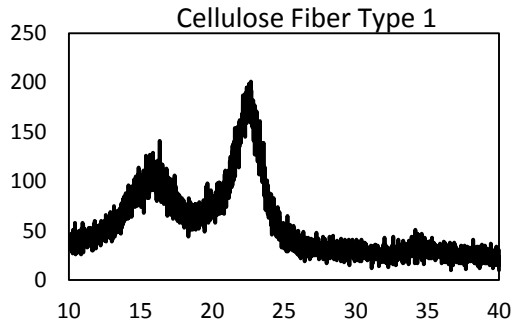

Figure 4-36 XRD of CF1

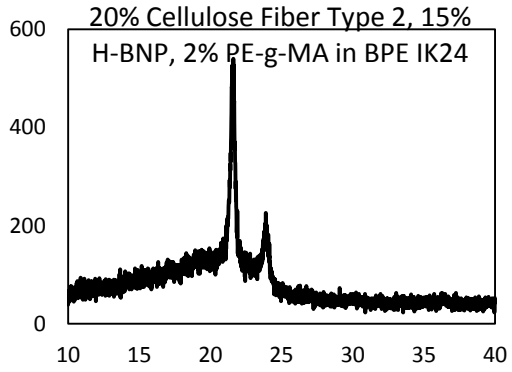

Figure 4-37 XRD of BPE Composite with CF2 and HBNP

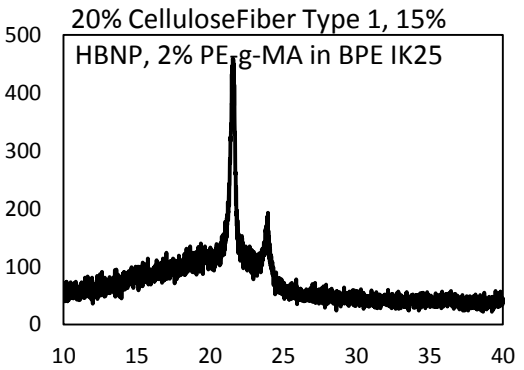

Figure 4-38 XRD of BPE Composite with CF1 and HBNP

4.5.1.4 Effect of CF2 and BNP on Composite Diffraction Pattern:

In order to identify if transcrystallization occurs in the composites upon addition of CF2 fibers, the following spectra were obtained. Unlike Liu et al., and many others, who have observed transcrystallization in PP composites with chitosan and other natural cellulosic fibers respectively [67], no new constructive peaks are found in the composite, the spectrum in Fig 4-39 is identical to the ones observed for the pure PE (Appendix) and also the ones presented above with addition of BNP nanofillers.

This is probably indicative of the absence of the transcrystallization phenomenon in PE biocomposites, as also evident from the lack of transcrystal peaks in the work of Farahbaksh who studied LDPE composites filled with softwood bleached kraft pulp fibers [32], very much like the ones used in the current work.

Fig 4-41 and 4-42 show the XRD spectra of BNP and HBNP fillers and can be seen as almost identical. The synergistic effect of HBNP and CF2 was investigated through Fig 4-43, which is very similar to the spectra obtained so far for these composites with the exception of a short, yet distinct, peak at around 32° of 2θ which are also slightly observable in the spectra of BNP and HBNP at the same position. This peak is not observable in a similar composite with BPE, Fig 4-44, as base matrix instead of RPE.

Moreover, these are also not observed in Fig 4-33 and Fig 4-34 that have only BPE, RPE in compatibilized RPE, and this could be attributed to the low number of counts or to experimental error or to the fact that these composites have no fiber and this phenomenon may be unique to fiber-filler interaction in a low molecular weight PE where they interact easily.

As such there is no concrete explanation, and no similar work is found in literature. However, it is interesting to note that this peculiarity is observed for RPE samples, which also exhibit almost doubled the increase in mechanical (flexural modulus and strength) properties versus the composites of BPE.

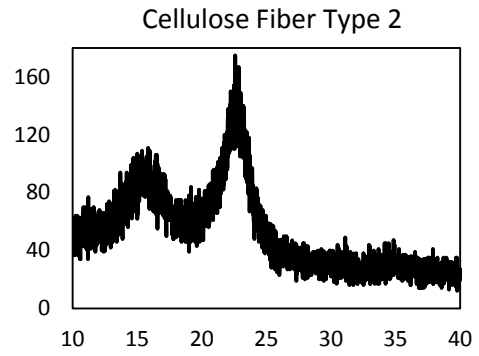

Figure 4-39 XRD of CF2

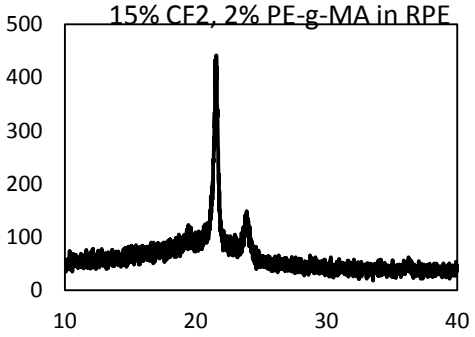

Figure 4-40 XRD of CF2/RPE Composite

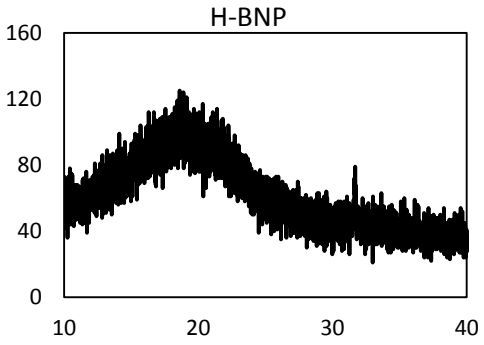

Figure 4-41 XRD of HBNP

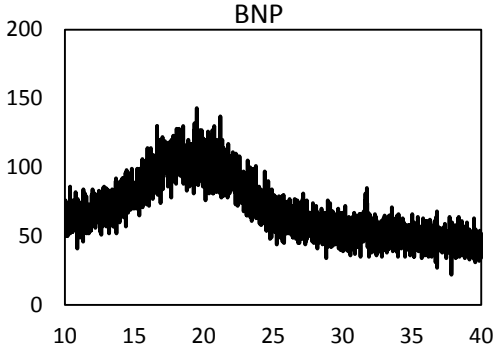

Figure 4-42 XRD of BNP

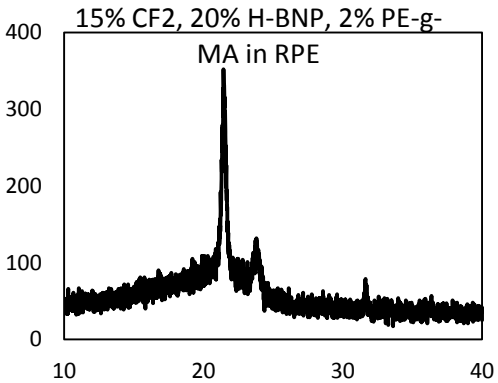

Figure 4-43XRD of HBNP/RPE Composite

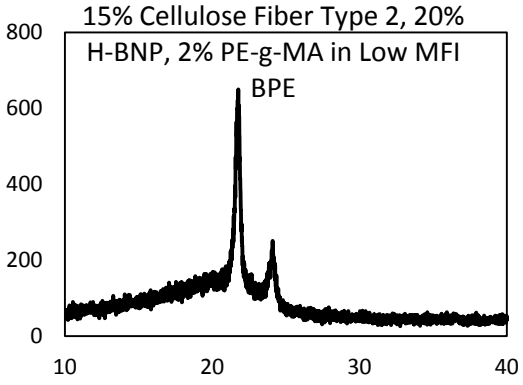

Figure 4-44 XRD of BNP/BPE Composite

4.5.2 SCANNING ELECTRON MICROSCOPY

4.5.2.1 PARTICLE CHARACTERIZATION

PARTICLE SIZE AND SIZE DISTRIBUTION:

Fig 4-45 shows an SEM image of the BNP powder aggregates sprinkled randomly on a dual ended tape. Fig 4-46 is an Image J analysis map of the SEM image based on a particle background contrast and Fig 4-48 shows a graph of the particle size distribution based on the image map. There seem to be two central tendencies at 15 and 150µm. Fig 4-47 shows a magnified image of one of the aggregates showing the irregular, non-homogenous morphology of the particles.

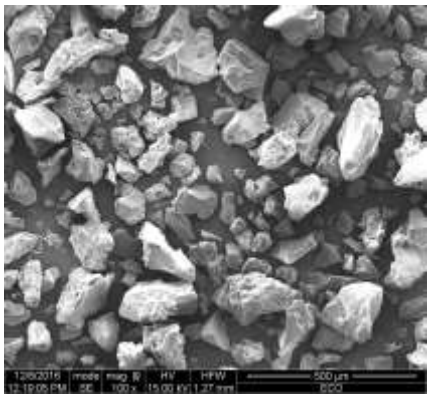

Figure 4-45 SEM of BNP (x100)

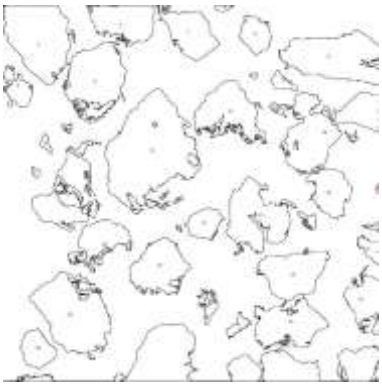

Figure 4-46 ImageJ map of Fig 4.5-14

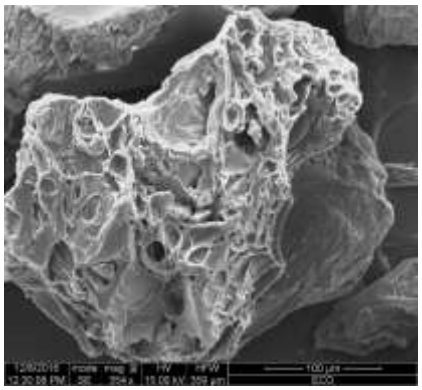

Figure 4-47 SEM of BNP Particle (x354)

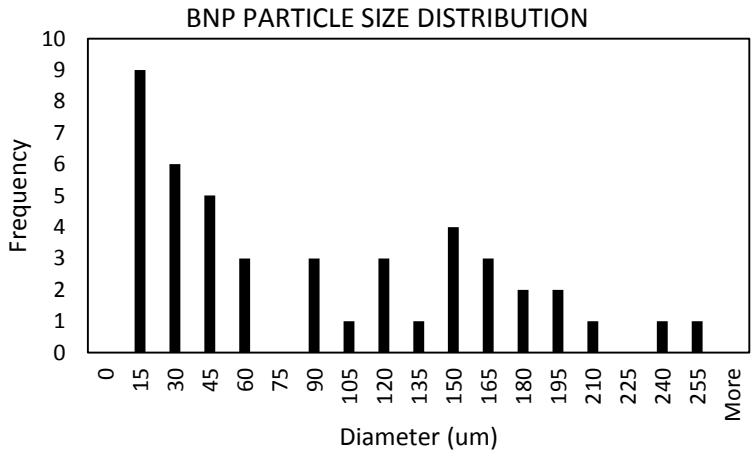

Figure 4-48 Particle Size Distribution of BNP Obtained from ImageJ map of SEM Image

The following Fig 4-49 and Fig 4-50 show the SEM image of the Hydrophobic modified BNP (HBNP) and the ImageJ analysis map of the SEM image respectively. A particle size distribution is plotted and shown in Fig 4-52 based on the ImageJ mapped particle areas and this shows that the mean size tendency is approximately 10 µm. This much smaller aggregate size compared with the BNP indicates a finer grind and has no relationship with the chemical modification of the particles. Fig 4-51 shows a magnified image of one aggregate particle and this seems similar, perhaps slightly smoother, to the BNP in Fig 4-47.

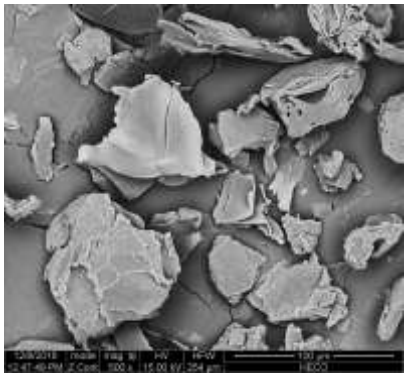

Figure 4-49 SEM of HBNP (x500)

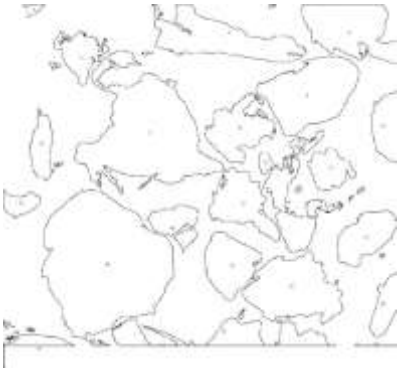

Figure 4-50 ImageJ map of Fig 4.5-18

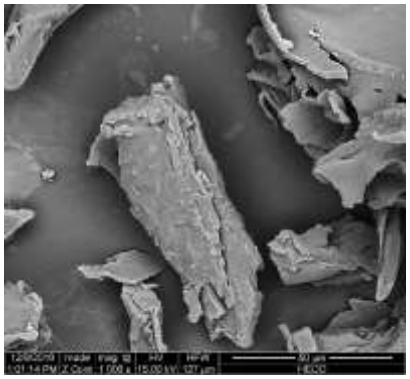

Figure 4-51 SEM of HBNP Particle (x1000)

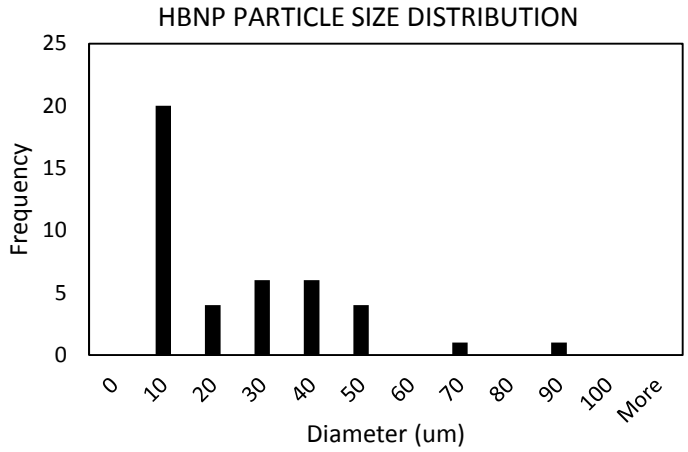

Figure 4-52 Particle Size Distribution of HBNP obtained from ImageJ map of SEM Image

4.5.2.2 CELLULOSE FIBER SIZE ANALYSIS

Cellulose Pulp Fiber Size and Size Distribution:

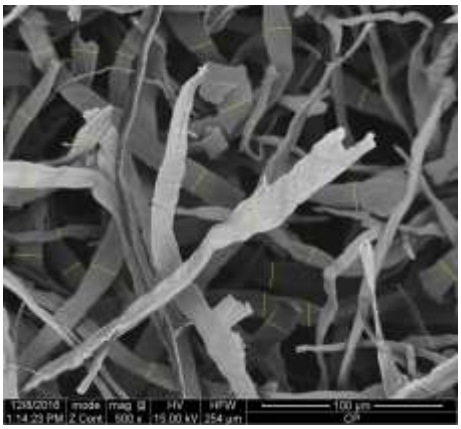

Figure 4-53 SEM of CF2 (x500), Average Width 10.14 µm

Figure 4-54 SEM of CF1 (x300), Average Width 16.545 µm

Fig 4-53 and 54 show a tape like structure of the CF2 and CF1 fibers. A similar tape like, flat structured fibers was presented in SEM results by Mulinari et al. who used Kraft Bleached and unbleached Cellulose Fiber Type 1s of very similar fiber width of 10-30µm. [34]

4.5.2.3 Dispersion of Native Starch in Polyethylene

The works of Sailaja & Chanda and Liu et al., who tested composites of Tapioca Starch-HDPE and Cornstarch-LDPE respectively show poor dispersion, low interface interaction and brittle fractured interfaces in SEM images which were improved considerable upon the addition of PE-g-MA as compatibilizers [22][49]. The weaker interface between granule and matrix in Fig 4-58 and Fig 4-59 and the relatively close bonded and wetted interface shown in Fig 4.-55,56,57 can be interpreted in the same manner. A better particle matrix interface is observable in Fig 4.-56,57.

WITH COMPATIBILIZER:

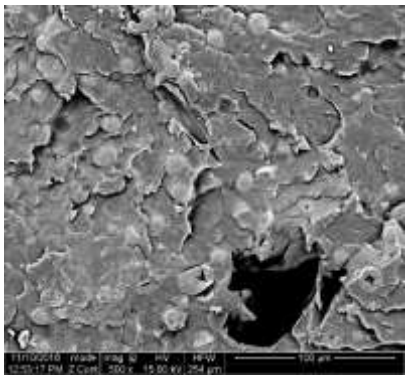

Figure 4-55 SEM of RV0M$_L$ (x500)

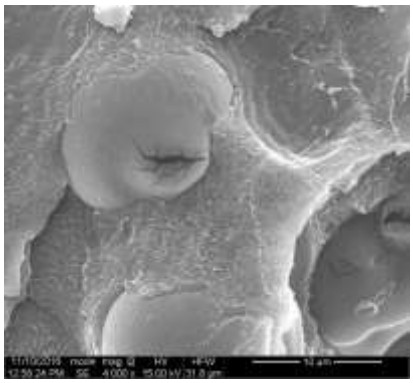

Figure 4-56 SEM of RV0M$_L$ (x4000)

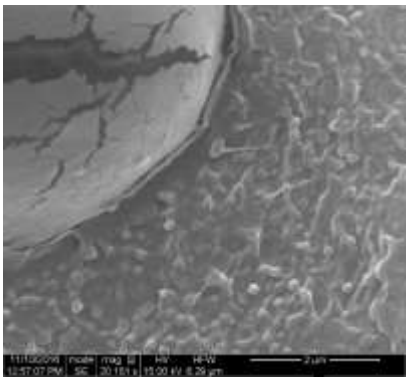

Figure 4-57 SEM of RV0M$_L$ (x20181)

WITHOUT COMPATIBILIZER:

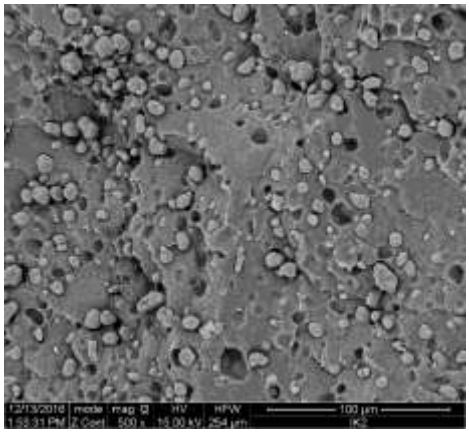

Figure 4-58 SEM of RC00 (x500)

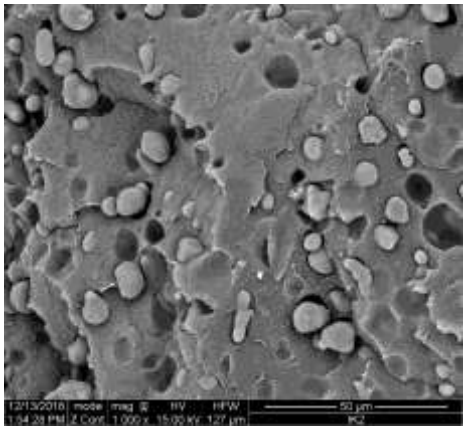

Figure 4-59 SEM of RC00 (x1000)

4.5.2.4 Dispersion of Starch Derived Nanoparticles in Polyethylene

The dispersion of starch granules versus thermoplastic starch can be different, as shown by Sailaja and Chanda, who used 20% TPS in LDPE matrix with and without compatibilizers and studied their morphology through SEM, their images demonstrate a rather co-continuous non-particulate morphology despite the immiscibility of the two phases. [48] However, Wang et al. tested blends of TPS and LLDPE and found that for starch loading less than the LDPE, the TPS formed the disperse phase and SEM images show spherical particles, they suggested that as this balance is offset i.e.; the LLDPE content is lower than the TPS, the TPS will form a continuous phase while the LLDPE will become the dispersed phase. They also showed improved dispersion of the TPS particles with the introduction of PE-g-MA as compatibilizers [74] which is somewhat observable in the difference between Fig 4-60 and Fig 4-63 with respect to the homogeneity of the holes left by the extracted BNP.

There are but few studies in literature covering the dispersion of starch nanoparticles or starch nanocrystals in composite systems. Two such works which are helpful in understanding the results obtained here are by Duan et al. and Wang et al. Duan et al. extracted SNC by acid hydrolysis and used this with Carboxy methyl chitosan to prepare casted composite films. Their SEM results showed that at loadings of SNC under 10% the SNC were not observable and between 10%-30% they appeared as monodisperse white dots. At loadings higher than this however, large aggregates were formed and phase separation was observed between the matrix and the filler similar to the one seen in Fig 4-62. It should

be noted that chitosan has a surface chemistry similar to that of starch, and therefore this aggregation phenomenon must be more pronounced (and at lower loadings) in a matrix like LLDPE, as shown in Fig 4-60 and 63 [75]. Wang et al. on the other hand studied the dispersion of starch derived nanoparticles (uncrosslinked) obtained by suspending plasticized starch past in water with stabilizers and surfactants, in a rubber matrix. The composite was fabricated by first mixing the colloidal nano-starch suspension and the rubber later and later compounded. This produced a homogenized SNP suspension when observed under an SEM [76].

BNP WITHOUT COMPATIBILIZER:

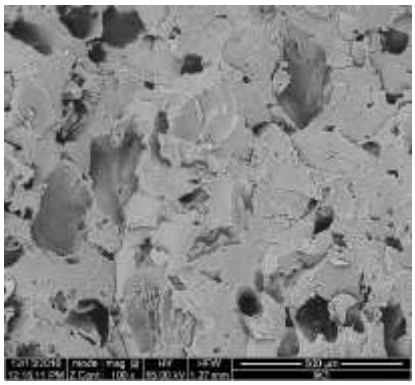

Figure 4-60 SEM of RS00 (x100)

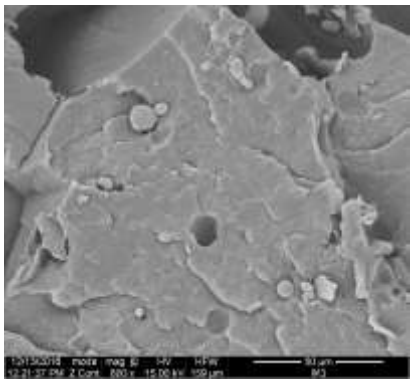

Figure 4-61 SEM of RS00 (x800)

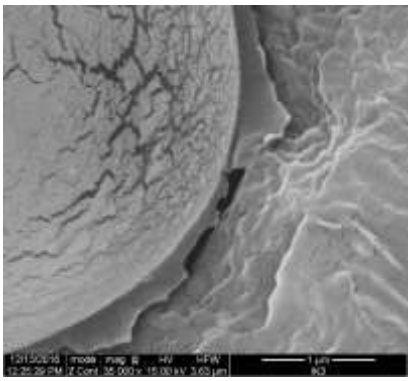

Figure 4-62 SEM of RS00 (x35000)

BNP WITH COMPATIBILIZER:

Gunning et al. fabricated biocomposites of PHB with jute and lyocell fibers they concluded from morphological SEM results that the addition of PE-g-MA as a compatibilizers improved the dispersion of the fibers in the matrix considerably, the surfaces of the compatibilized biocomposites was much more even and smoother than uncompatibilized samples. This can be seen from Fig 4-63 and 65 as well where compatibilized composite fracture surface of BNP with 2% PE-g-MA has a smoother surface compared with uncompatibilized composite (Fig 4-60).

Compatibilization with PE-g-MA allows 30% BNP to disperse to a mean size of 40µm in LLDPE as shown in the particle size distribution plot in Fig 4-64 obtained from the Image J analysis of the image pictured in Fig 4-63. Chemical modification of the BNP however, allows the HBNP to disperse to a mean size of 6µm, Fig 4-65 and 66, this could be attributed to one of the two factors; the functionalization of the BNP which allows for easier disintegration of aggregates, or, to the smaller filler size obtained after grinding of the HBNP.

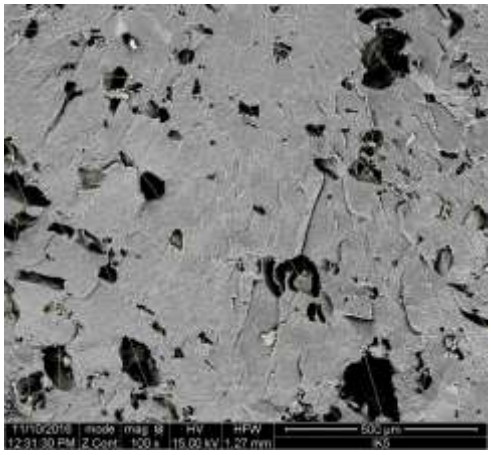

Figure 4-63 SEM of RS0M$_L$ (x100)

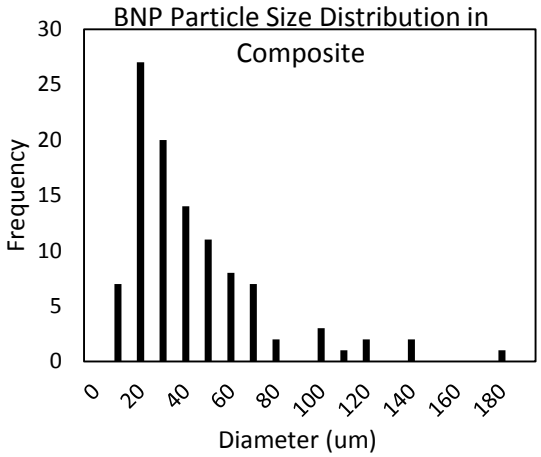

Figure 4-64 Particle Size Distribution of RS0M$_L$, Mean Diameter 40µm

HYDROPHOBICALLY MODIFIED BNP WITH COMPATIBILIZER:

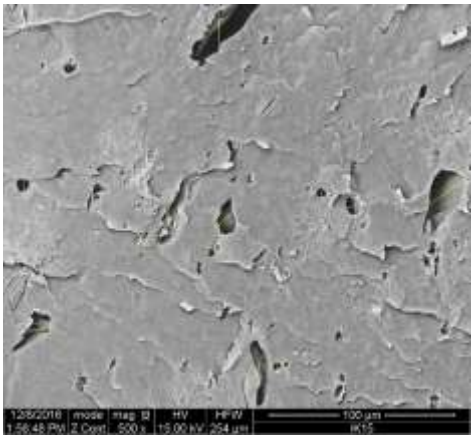

Figure 4-65 SEM of BS$_H$0M$_L$2 (x500)

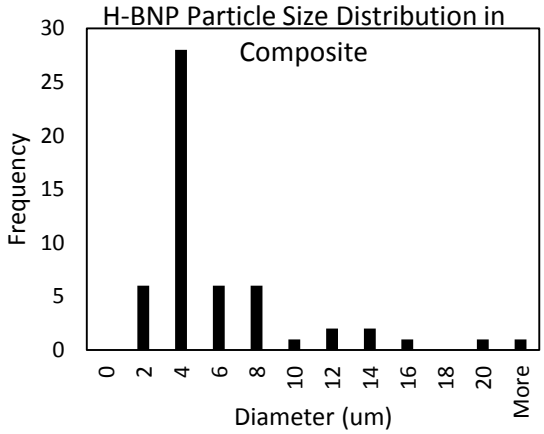

Figure 4-66 Particle Size Distribution of BS$_H$0M$_L$2, Mean Diameter 6µm

It is interesting to note that Angellier et al. observed a reversed trend, of larger aggregates for modified SNC, however this was attributed to the extraction process of the modified SNC (freeze drying of the suspension) which produced a compact powder with larger particles [77]. This result still agree with the results of SEM Figures 4-63 and 65. Since the dry aggregated of BNP were much larger than for Hydrophobic BNP, Fig 4-45 and 47, the resulting dispersion of these show larger particles for unmodified BNP. We can thus deduce that the dispersion of nanoparticulate fillers depends on the respective dry aggregate sizes as well and not only on their chemical characteristic.

WITH EXTERNAL LUBRICANT:

In order to obtain a nanodispersion of the BNP and HBNP in the LLDPE matrix, glycerol was used as a hydrophilic dispersant or an external lubricant. The formulations tested had a 20% loading of BNP in the injection molding grade RPE, 2% PE-g-MA and 10% glycerol. The cryofractured and extracted samples were observed under an SEM and the images obtained shown in Fig 4-67 and 69 show the surface at 100x and 2000x magnification. Compared to Fig 4-63, also at a 100x mag, the drastic reduction in size can be

realized. Further assessment of the image, Fig 4-69, with ImageJ shows a particle mapping shown in Fig 4-70. The particle size distribution is shown in Fig 4-68 where it is clear that the average dispersant size is around 294 nm. This concluded that glycerol is an effective dispersant. A very similar study was conducted by Wang et al. who used native rice starch granules as reinforcing fillers for LDPE, unlike the monodispersity observed with native granules in Fig 4-59, they observed agglomeration of the granules in the matrix with poor interfacial adhesion, to improve this, glycerol was used as a dispersant and the results were very similar to the ones observed here; a great improvement in dispersion was observed and only a few agglomerates were remaining. They also used PE-g-MA as surface modifier/ compatibilizers and observed through SEM that the interfacial bonding increased considerably with the PE-g-MA [78]. The difference however, is that the dispersant size was not below the actual size of rice granules which is of the order of 10 microns in general, and thus the work presented in this thesis is the first observation of dispersing a non-crystalline starch based filler to a nano-scale in a polyolefin matrix.

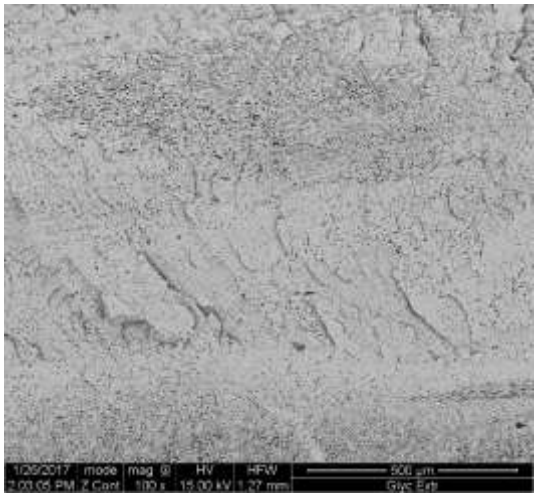

Figure 4-67 SEM of RS_HF10M_L (x100)

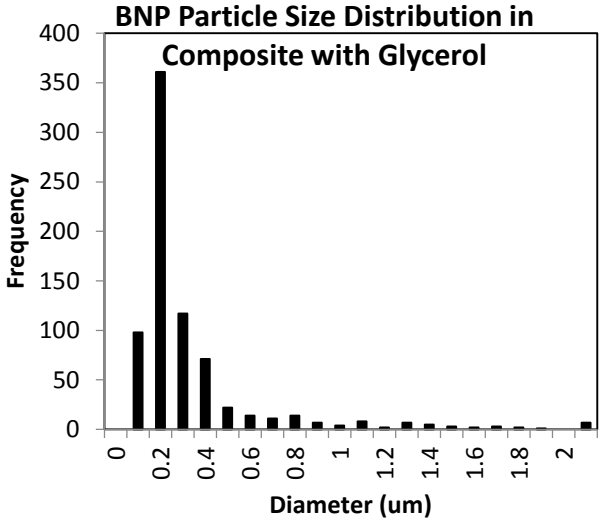

Figure 4-68 Particle Size Distribution of RS_HF10M_L, Average Diameter 294nm

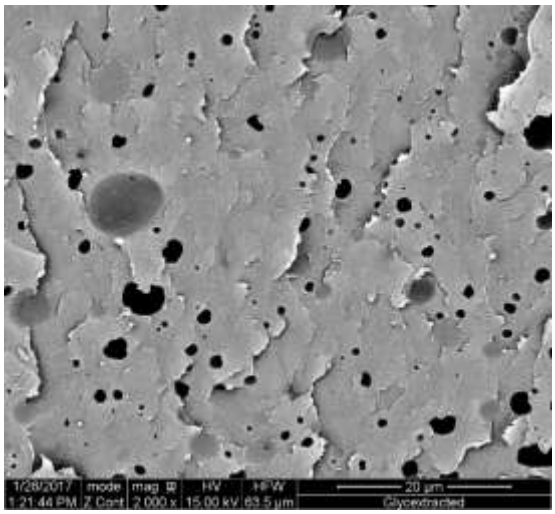

Figure 4-69 SEM of RS_HF10M_L (x2000)

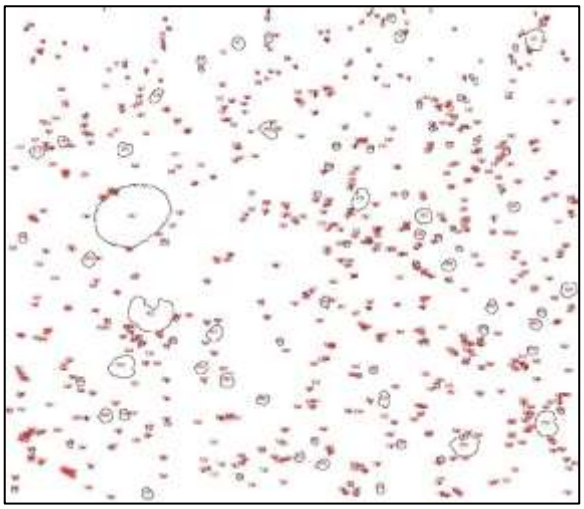

Figure 4-70 ImageJ map of RS_HF10M_L obtained from SEM Image

4.5.2.5 Effect of using SNP in Fiber Reinforced PE Composite

DISPERSION AND ADHESION OF FIBERS IN PE:

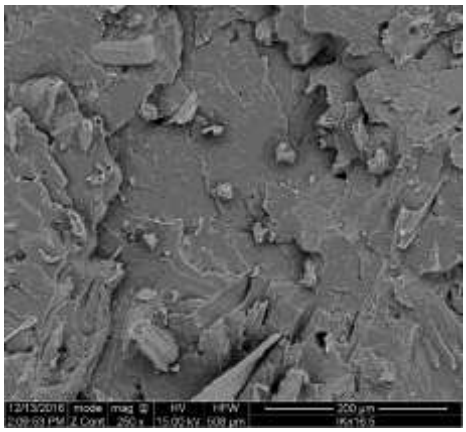

Figure 4-71 SEM of BS_H0FM_L (x250)

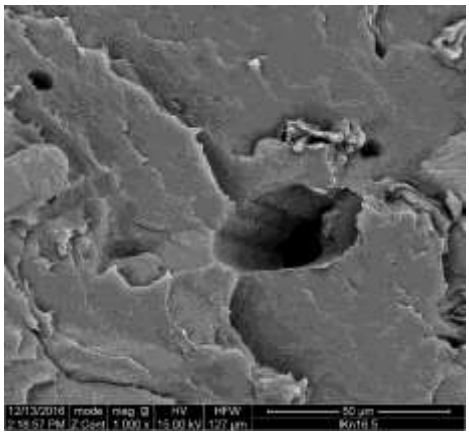

Figure 4-72 SEM of BS_H0FM_L (x1000)

Improved interaction of fibers in matrix was showed in SEM results by Pollanen et al. who used cellulose fiber reinforcements in HDPE matrix, they showed that with the use of PE-g-MA as compatibilizers a better interfacial adhesion was possible, and the fibers looked more strongly attached with the matrix at the fractured surface observed, whereas for uncompatibilized samples there were clear and neat holes and voids around the fiber-matric junctions indicating poor adhesion and fiber pullout [79]. Fig 4-71 and 72 show cryofractured surfaces of composites that have CF2 fibers as filler and PE-g-MA as compatibilizers while these formulations have no BNP or HBNP. The fiber cut off seems efficient in Fig 4-71, however the neat, smooth hole left by a pulled out fiber in Fig 4-72 indicates less than ideal adhesion.

DISPERSION AND ADHESION of FIBER UPON ADDITION OF SNP:

The following figures show cryofractured and extracted surfaces of composites with a high loading of BNP and CF2, 20% each with 2% compatibilizers in BPE and RPE matrices respectively. The loading capacity of filler and fiber often has an optimum value. Mechanical properties increase with increased loadings and strength sometimes suffers negatively after the optimum has been crossed. Since mechanical properties are a direct function of how the fillers or fibers disperse and distribute in the matrix and therefore it is useful to find the ratio of additives and matrix used to provide best results. Experiments by many researchers have shown that an optimum of 30% starch loading in a PBAT matrix gives best dispersion and small particle size distribution[11]

As noted in literature, increased loading levels of fiber and filler favor agglomeration and aggregation, however, as apparent from the following figures (Fig 4-73 and 74), the addition of BNP at higher loading levels of dispersants does not cause too much aggregation or bundling of fibers. This is perhaps one of the reasons why a consistent increase in flexural strength and modulus is observed at up to 40% reinforcement loading.

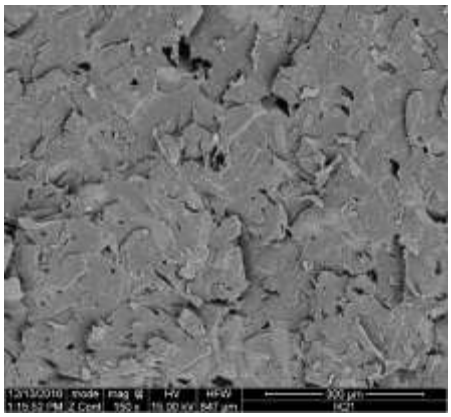

Figure 4-73 SEM of BS_HF5M_L (x150)

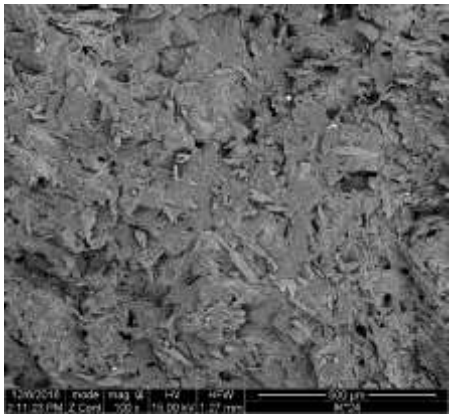

Figure 4-74 SEM of RS_HF20M_L (x100)

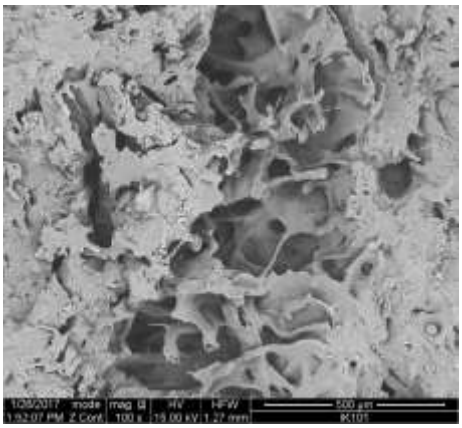

Figure 4-75 SEM of $pS15FM_L$ (x100)

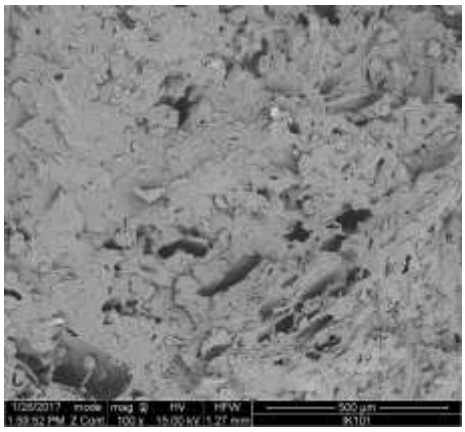

Figure 4-76 SEM of $pS15FM_L$ (x100)

It is commonly reported in literature that at higher loadings of fiber, the number of voids increases and problems such as aggregation are observed in SEM results. Aridi et al. who produced injection molded PP composites filled with rice husk reported more voids and fiber pullout at high fiber loadings of 55% [62]. These results are observed for PP-BNP and CF1 formulations as seen in Fig 4-75 and 76.

It should be noted however, that despite these nonconformities, the mechanical properties were still enhanced. This is corroborative to the results obtained by Gupta and Alam who extruded, molded and tested composites of PP and thermoplasticized potato starch, they observed slight improvement in Tensile, Flexural and Impact strength upon addition of starch and also explain increased adhesion owing to the addition pf PP-g-MA. Their SEM results, however, showed more co-continuous structure rather than a dispersion of starch, unlike the particulate dispersion observed in Fig 4-75 and 76 [65].

Taking a closer look at the surfaces of composites using both BNP and CF1/CF2 fibers in compatibilized LLDPE composites, Fig 4-77 to 82 and comparing them with the images of the fiber only compositions, Fig 4-71 and 72, the following conclusions can be made: the fibers are more strongly adhered to the matrix, the morphology is not as neat and smoothly cut as with the fiber-only samples, and the stretched 'chewing gum' like features seen in Fig 4-79,80,81,82 act as 'bridges; and indicate that the interface provides more efficient stress-transfer from the matrix to the fiber, and fiber pullout or fracture essentially would require a greater force.

It is important to note that this adhesion is visible in samples with BPE and RPE matrices and with CF1 and CF2 samples too (Fig 4-79 & 4-82).

Moreover from Fig 4-78 and 79 it is apparent that a peculiar 'cobweb-like' feature seems to be holding the fibers attached within the BPE matrix, more of this feature is seen and explained in the following figures. A slightly similar observation was put forth by Yang et al. who fabricated nanocomposites with a blend of PPC/PLA and MWCNT's as nanofillers. The observed similar string like features between the spherical fillers and the matrix, they called these, 'nano-bridges' that are suspected to enhance load transfer while maintaining the material's ductility. [2]

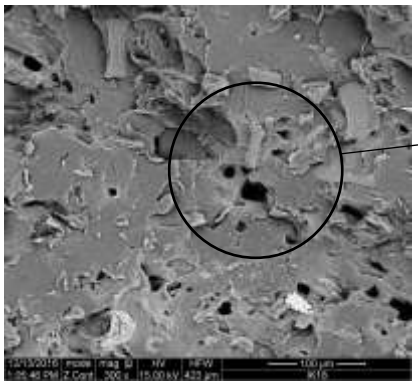

Figure 4-77 SEM of BS_H10FM_L (x300)

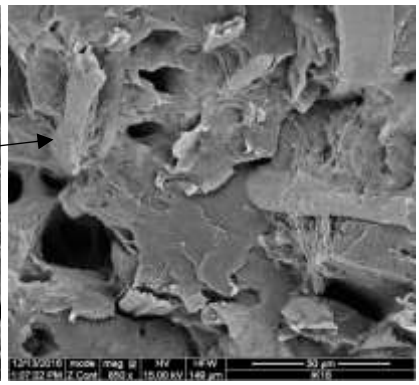

Figure 4-78 SEM of BS_H10FM_L (x850)

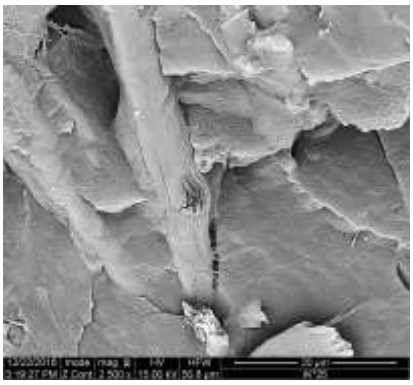

Figure 4-79 SEM of RS_HP20M_L (x2500)

Figure 4-80 SEM of BS_HF5M_L (x2000)

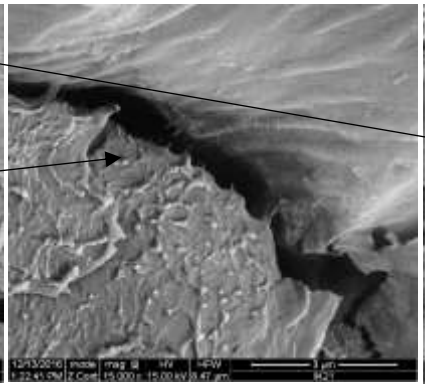

Figure 4-81 SEM of BS_HF5M_L (x15000)

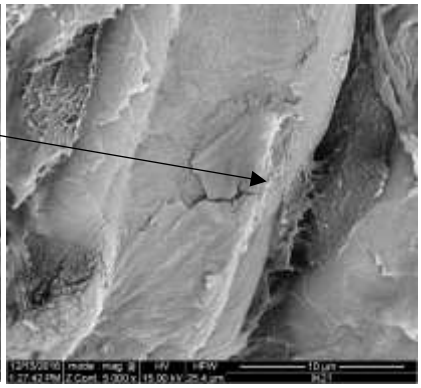

Figure 4-82 SEM of BS_HF5M_L (x5000)

IDENTIFICATION OF A COBWEB STRUCTURE:

More images of this unusual cobweb structure are shown in the following figures. From Fig 4-83,84,85 it can be concluded that this feature is not specific to a grade of PE (RPE or BPE), the type of fiber (CF2 or CF1), or to the type of BNP (BNP or HBNP) and appears systematically in all formulations consisting of fiber and BNP, while not observed in samples with only fiber as the reinforcing dispersant. This is a preliminary hint that these are inherent to either the BNP/HBNP or to the PE which perhaps shears to form micro-necked strings in the presence of the crosslinked rigid nanofiller (BNP). One must note that if this feature is indeed PE, it is not visible in the fiber only sample, Fig 4-71, and thus is unique to formulations with BNP/HBNP.

Figure 4-83 SEM of BS10PM$_L$ (x2000)

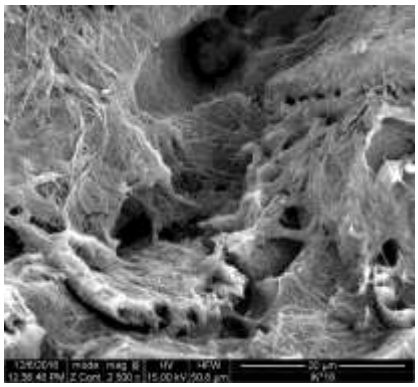

Figure 4-84 SEM of RS$_H$10FM$_L$ (x2500)

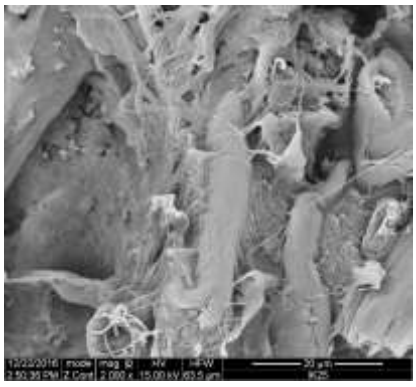

Figure 4-85 SEM of BS$_H$P20M$_L$ (x2000)

The following images, Fig 4-86 & 87, are of samples that contain no fiber and clearly exhibit the same feature observed in mixed composition samples. It might be of value to note that the same features are not present in uncompatibilized samples of BNP and BPE.

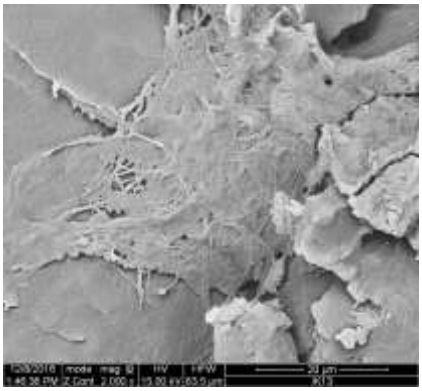

Figure 4-86 SEM of BS$_H$0M$_L$0.5 (x2000)

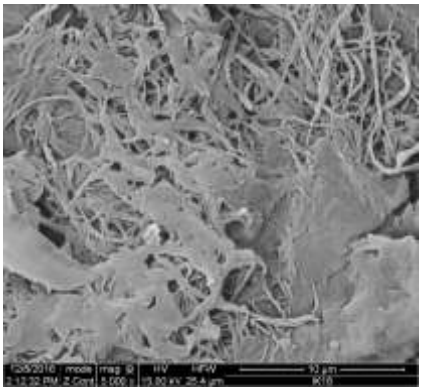

Figure 4-87 SEM of BS$_H$0M$_L$5 (x5000)

The following images, Fig 4-88, 89 & 90 are taken from samples that contain both HBNP and CF2 in a compatibilized RPE composite. These cryofractured samples, extracted at 55°C for up to five hours show granular particles, in Fig 4-88 and 89 it can be seen that a film like layer is exuding out of the granular particle, this could indicate gelatinization of some untreated starch granules in the HBNP. One of the possibilities is that some uncrosslinked plasticized starch in the HBNP mixture enables this sheared cobweb structure.

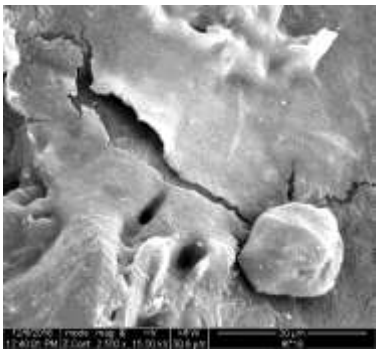

Figure 4-88 SEM of RS_H10FM_L (x2500)

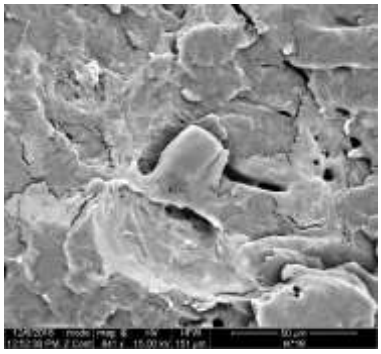

Figure 4-89 SEM of RS_H15FM_L (x841)

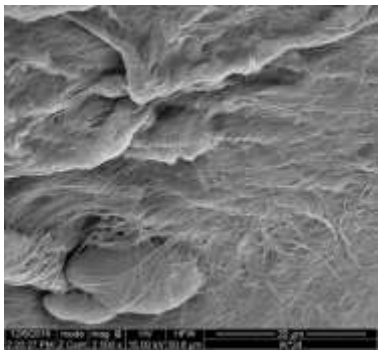

Figure 4-90 SEM of RS_HF20M_L (x2500)

HIGH TEMPERATURE EXTRACTION FOR COBWEB FEATURE:

In order to investigate the nature of these unique cobweb structures the cryofractured samples were extracted at a higher temperature of 80°C for one hour. The hypothesis was; if the features were owing to the matrix Polyethylene or the cellulose fibers the water at 80°C will be unable to extract the structures, while if this was due to the fibrillated starch granules or the BNP/HBNP, then it must migrate from the surface.

Results obtained are presented in Fig 4-91 and 92 and two factors indicate that this feature is most likely owing to the starch derived BNP; the absence of most of the unknown structure, and the small bits of residual clumps reminiscent of the same cobweb structure. Moreover the fiber shafts appear to be much smoother as seen in Fig 4-72 which has no BNP filler. The interface between the fiber and the matrix also seem to be clear and hollow with no adhesion. This concludes that the feature, suspected to be from the BNP/HBNP, aids in the fiber adhesion to the matrix and therefore aids stress-transfer and improves mechanical properties.

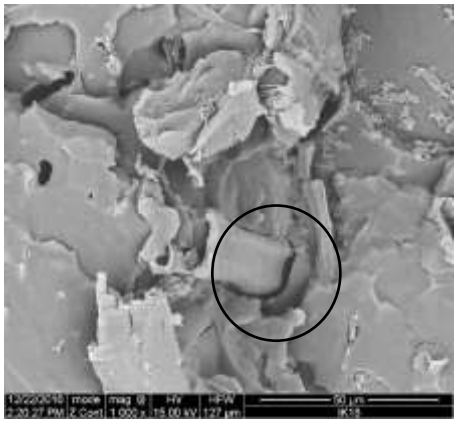

Figure 4-91 SEM of BS_H10FM_L Extracted at 80°C (x1000)

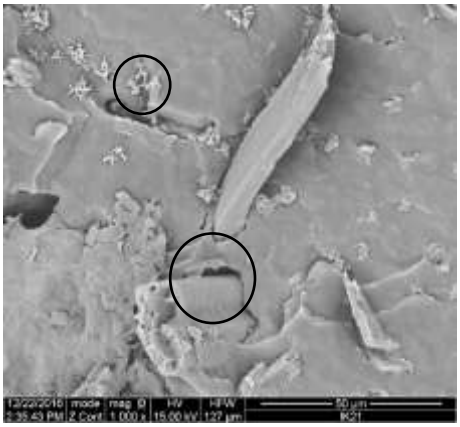

Figure 4-92 SEM of BS_HF5M_L Extracted at 80°C (x1000)

CONCLUSIONS AND RECOMMENDATIONS

The objective of this work was to prepare and analyze composites using nanoparticles derived from starch (BNP) in formulation with polyolefinic matrices (LLDPE, PP) and also in conjunction with cellulose fibers (CF2 and CF1). Mechanical tests, thermal analysis, morphological analysis and flow properties were analyzed to fully characterize over 50 formulations made with these components in different ratios to understand independent and interdependent properties.

The mechanical results, flexural modulus and strength in particular, showed that the use of native starch versus starch derived nanoparticles is not profound, yet with the addition of PE-g-MA as compatibilizers showed enhanced properties of the BNP while no difference was observed for native starch. Moreover, three compatibilizers were tested and all showed improved properties indicating enhanced matrix-filler interaction. Out of the three, PE-g-MA with a low maleic anhydride content showed optimum properties. Increasing compatibilizers content slightly improved properties but increment from 2-5% was not significant hence all other formulations used a constant 2% of PE-g-MA (low MA content). Between BNP and modified HBNP, BNP performed better and showed better flexural and impact properties. Increasing BNP and HBNP content in composites increased the mechanical performance, except for impact properties which were compromised on addition of both fiber and filler. Two types of cellulose fibers were tests, a freeze dried pulp fiber and one not freeze dried, the regular Cellulose Fiber Type 1 showed better property enhancements. Increasing fiber content continued to increase mechanical stiffness and strength. Two grades of LLDPE were used, between which the injection molding grade (low MW, high MFI) showed considerably higher property enhancement than the low MW LLDPE. PP was also tested and although 100% improvement in modulus and flexural strength was observed, the increase was lower compared to LLDPE, the drop in impact strength was also, however, much lower than was for LLDPE.

Thermal test results indicated no transcrystallization. Crystallinity was lowered from neat matrix for BPE composites filed with fiber and filler, while this was increased for RPE composites. Crystallization and melting temperatures remained largely unaffected for BPE composites and were lowered for RPE composites. Percentage crystallinity increased more prominently upon addition of more fibers than for amorphous nanoparticles. Degradation temperature was lowered compared to neat matrix but did not change significantly based on the content of additives rather than the moisture content. No significant changes were observed in XRD data also, indicating there was no change in crystalline structure of the composite. MFI was effected negatively upon addition of both BNP/HBNP and fibers, but it was much more for formulations with CF1 or CF2 than it was for particulate fillers. Compatibilization had no effect on MFI.

Morphological results from SEM showed better matrix-filler junctions for starch derived nanoparticle fillers than for native starch, but dispersion of native starch was better than for BNP. Addition of glycerol resulted in nano-dispersion of the BNP aggregates. Formulations with fiber and BNP/HBNP showed very good fiber matrix interface adhesion, nanobridges were observed at fiber junctions and an unusual ‘cobweb’ film structure was observed, which disappeared at high temperature extraction indicating unique morphology owing to the starch derived nanoparticle filler. Decent dispersion was achieved even at high loadings of fiber and filler.

Based on the results obtained, it can be concluded that the effect of using starch derived nano sized fillers in hybrid composites with cellulose fibers provides synergistically enhanced properties. The composites

developed have potential to be used in automotive interiors, furniture, and glycerol based formulations with nano-dispersion of starch can be used aptly as agricultural films.

Some of the recommendations to increase understanding and to enhance the properties of the biocomposite even further are:

1. to study the effect of glycerol formulations in conjunction with Cellulose Fiber Type 1s
2. to investigate the optimum glycerol content required for nano-dispersion
3. to investigate the results obtained in SEM further via advanced techniques such as chemical mapping that can identify the cobweb structure found in these composites
4. testing of formulations with HBNP and CF1 as these were not incorporated in the design
5. modification of BNP with strategies such as long chain grafting of long chain fatty acids or OSA that are shown in literature [80] [81]
6. more in-depth study of the BNP powder particle size on the composite properties
7. Effect of grinding of the matrix resin to obtain more uniform dispersion during extrusion

REFERENCES

[1] A. Dufresne, S. Thomas, and L. A. Pothan, Eds., *Biopolymer Nanocomposites*, 1st ed. John Wiley & Sons, Inc., 2013.

[2] M. Misra, J. K. Pandey, and A. K. Mohanty, Eds., *Biocomposites: Design and Mechanical Performance*. Woodhead Publishing, 2015.

[3] S. Kalia, Dufresne, A., Cherian, B.M., Kaith, B.S., Avérous, L., Njuguna, J., Nassiopoulos, E., "Cellulose-based bio- and nanocomposites: A review," *Int. J. Polym. Sci.*, vol. 2011, 2011.

[4] W. Thielemans, L. Babacar, A. Dufresne, and N. Belgacem, "Scientific Report of the Laboratory of Pulp and Paper Science and Graphic Arts - UMR 5518 Grenoble - France January 2002-November 2005," 2006.

[5] M. J. John and S. Thomas, "Biofibres and biocomposites," *Carbohydr. Polym.*, vol. 71, no. 3, pp. 343–364, 2008.

[6] M. M. Reddy, S. Vivekanandhan, M. Misra, S. K. Bhatia, and A. K. Mohanty, "Biobased plastics and bionanocomposites: Current status and future opportunities," *Prog. Polym. Sci.*, vol. 38, no. 10–11, pp. 1653–1689, 2013.

[7] O. Faruk, A. K. Bledzki, H. P. Fink, and M. Sain, "Biocomposites reinforced with natural fibers: 2000-2010," *Prog. Polym. Sci.*, vol. 37, no. 11, pp. 1552–1596, 2012.

[8] A. Sardashti, "Wheat Straw-Clay-Polypropylene Hybrid Composites," University of Waterloo, 2009.

[9] R. Fatoni, "Product Design of Wheat Straw Polypropylene Composite by," University of Waterloo, 2012.

[10] M. K. Oduola and P. O. Akpeji, "Effect of Starch on the Mechanical and Rheological Properties of Polypropylene," *Am. J. Chem. Eng.*, vol. 3, no. February, pp. 1–8, 2015.

[11] P. Gonzalez Seligra, L. Eloy Moura, L. Fama, J. I. Druzian, and S. Goyanes, "Influence of incorporation of starch nanoparticles in PBAT/TPS composite films," *Polym. Int.*, vol. 65, no. 8, pp. 938–945, 2016.

[12] P. Wambua, J. Ivens, and I. Verpoest, "Natural fibres: Can they replace glass in fibre reinforced plastics?," *Compos. Sci. Technol.*, vol. 63, no. 9, pp. 1259–1264, 2003.

[13] S. M. A. S. Keshk and A. G. Al-sehemi, "New Composite Based on Starch and Mercerized Cellulose," *Am. J. Polym. Sci.*, vol. 3, no. 3, pp. 46–51, 2013.

[14] A. K. Mohanty, M. Misra, and L. T. Drzal, Eds., *Natural Fibers, Biopolymers, And Biocomposites*. Crc Press, 2005.

[15] F. Xie, E. Pollet, P. J. Halley, and L. Av??rous, "Starch-Based Nano-Biocomposites" *Prog. Polym. Sci.*, vol. 38, no. 10–11, pp. 1590–1628, 2013.

[16] N. St-Pierre, B. D. Favis, B. a Ramsay, J. a Ramsayt, and H. Verhoogt, "Processing And Characterization Of Thermoplastic Starch / Polyethylene Blends" *Polymer (Guildf).*, vol. 38, no. 3, pp. 647–655, 1997.

[17] X. Cao, Y. Chen, P. R. Chang, A. D. Muir, and G. Falk, “Starch-based nanocomposites reinforced with flax cellulose nanocrystals” *Express Polym. Lett.*, vol. 2, no. 7, pp. 502–510, 2008.

[18] D. Le Corre and H. Angellier-Coussy, “Preparation and application of starch nanoparticles for nanocomposites: A review,” *React. Funct. Polym.*, vol. 85, pp. 97–120, 2014.

[19] R. H. Wildi, E. Van Egdob, and S. Bloembergen, “PROCESS FOR PRODUCING BIOPOLYMER NANOPARTICLES,” US 2011/0042841 A1, 2011.

[20] D. Le Corre, J. Bras, and A. Dufresne, “Starch nanoparticles: A review,” *Biomacromolecules*, vol. 11, no. 5, pp. 1139–1153, 2010.

[21] J. L. Willett, “Mechanical properties of LDPE/granular starch composites,” *J. Appl. Polym. Sci.*, vol. 54, no. 11, pp. 1685–1695, 1994.

[22] R. R. N. Sailaja and M. Chanda, “Use of maleic anhydride – grafted polyethylene as compatibilizer for HDPE – tapioca starch blends : effects on mechanical properties,” *J. Appl. Polym. Sci.*, vol. 80, no. 6, pp. 863–872, 2001.

[23] M. Sabetzadeh, R. Bagheri, and M. Masoomi, “Effect of Corn Starch Content in Thermoplastic Starch/ LDPE Blends on their Mechanical and Flow Properties,” *J. Appl. Polym. Sci.*, vol. 126, no. S125, pp. E63–E69, 2012.

[24] M. Kim and S. J. Lee, “Characteristics of crosslinked potato starch and starch-filled linear low-density polyethylene films,” *Carbohydr. Polym.*, vol. 50, no. 4, pp. 331–337, 2002.

[25] I. Kaur and N. Gautam, “Starch Grafted Polyethylene Evincing Biodegradation Behaviour,” *Malaysian Polym. J.*, vol. 5, no. 1, pp. 26–38, 2010.

[26] A. Kaushik, M. Singh, and G. Verma, “Green nanocomposites based on thermoplastic starch and steam exploded cellulose nanofibrils from wheat straw,” *Carbohydr. Polym.*, vol. 82, no. 2, pp. 337–345, 2010.

[27] S. Panthapulakkal, M. Sain, and S. Law, “Effect of coupling agents on rice-husk-filled HDPE extruded profiles,” *Polym. Int.*, vol. 54, no. 1, pp. 137–142, 2005.

[28] E. Eastwood, S. Viswanathan, C. P. O’Brien, D. Kumar, and M. D. Dadmun, “Methods to improve the properties of polymer mixtures: Optimizing intermolecular interactions and compatibilization,” *Polymer (Guildf).*, vol. 46, no. 12, pp. 3957–3970, 2005.

[29] R. Hui, C. Qi-he, F. Ming-liang, X. Qiong, and H. Guo-qing, “Preparation and properties of octenyl succinic anhydride modified potato starch,” *Food Chem.*, vol. 114, no. 1, pp. 81–86, 2009.

[30] Y. Habibi and A. Dufresne, “Highly filled bionanocomposites from functionalized polysaccharide nanocrystals,” *Biomacromolecules*, vol. 9, no. 7, pp. 1974–1980, 2008.

[31] Anatole A. Klyosov, *Wood-Plastic Composites*. John Wiley & Sons, Inc., 2007.

[32] N. Farahbakhsh, “Cotton-based Cellulose Nanomaterials for Applications in Composites and Electronics,” North Carolina State University, 2015.

[33] P. V Joseph, K. Joseph, and S. Thomas, “Effect of processing variables on the mechanical properties of sisal-fiber-reinforced polypropylene composites,” vol. 59, pp. 1625–1640, 1999.

[34] D. R. Mulinari, H. J. Voorwald, M. O. Cioffi, and M. L. da Silva, “Cellulose fiber-reinforced high-

density polyethylene composites--Mechanical and thermal properties," *J. Compos. Mater.*, 2016.

[35] M. Poletto, H. L. Ornaghi Júnior, and A. J. Zattera, "Native cellulose: Structure, characterization and thermal properties," *Materials (Basel).*, vol. 7, no. 9, pp. 6105–6119, 2014.

[36] Z. S. Ng, "BULK ORIENTATION OF AGRICULTURAL FILLER-POLYPROPYLENE by," University of waterloo, 2008.

[37] M. Tabkhpaz Sarabi, A. H. Behravesh, P. Shahi, and Y. Daryabari, "Effect of polymeric matrix melt flow index in reprocessing extruded wood-plastic composites," *J. Thermoplast. Compos. Mater.*, vol. 27, no. 7, pp. 881–894, 2014.

[38] P. Matzinos, D. Bikiaris, S. Kokkou, and C. Panayiotou, "Processing and characterization of LDPE/starch products," *J. Appl. Polym. Sci.*, vol. 79, no. 14, pp. 2548–2557, 2001.

[39] A. M. Shi, L. J. Wang, D. Li, and B. Adhikari, "Characterization of starch films containing starch nanoparticles Part 1: Physical and mechanical properties," *Carbohydr. Polym.*, vol. 96, no. 2, pp. 593–601, 2013.

[40] H. Ishida and P. Bussi, "Surface Induced Crystallization in Fiber Reinforced Semicrystalline Thermoplastics Composites," Ohio, 1991.

[41] Han, S.O., Karevan, M., Sim, I.N., Bhuiyan, M.A., Jang, Y.H., Ghaffar, J., Kalaitzidou, K., "Understanding the reinforcing mechanisms in kenaf fiber/pla and kenaf fiber/pp composites: A comparative study," *Int. J. Polym. Sci.*, vol. 2012, 2012.

[42] J. Prinos, D. Bikiaris, S. Theologidis, and C. Panayiotou, "Preparation and characterization of LDPE/starch blends containing ethylene/vinyl acetate copolymer as compatibilizer," *Polym. Eng. Sci.*, vol. 38, no. 6, pp. 954–964, 1998.

[43] X. Chen, L. Zhou, X. Pan, J. Hu, Y. Hu, and S. Wei, "Effect of different compatibilizers on the mechanical and thermal properties of starch/polypropylene blends," *J. Appl. Polym. Sci.*, vol. 133, no. 17, p. n/a-n/a, 2016.

[44] S. Wacharawichanant, P. Saetun, T. Lekkong, and S. Thongyai, "Effect of Compatibilizer on Impact Strength and Morphology of Polystyrene/Zinc Oxide Nanocomposites," *Adv. Mater. Res.*, vol. 545, pp. 330–334, 2012.

[45] J. H. Lin, C. L. Huang, C. F. Liu, C. K. Chen, Z. I. Lin, and C. W. Lou, "Polypropylene/short glass fibers composites: Effects of coupling agents on mechanical properties, thermal behaviors and morphology," *Materials (Basel).*, vol. 8, no. 12, pp. 8279–8291, 2015.

[46] H. S. Kim, B. H. Lee, S. W. Choi, S. Kim, and H. J. Kim, "The effect of types of maleic anhydride-grafted polypropylene (MAPP) on the interfacial adhesion properties of bio-flour-filled polypropylene composites," *Compos. Part A Appl. Sci. Manuf.*, vol. 38, no. 6, pp. 1473–1482, 2007.

[47] H. Angellier, S. Molina-Boisseau, and A. Dufresne, "Mechanical properties of waxy maize starch nanocrystal reinforced natural rubber," *Macromolecules*, vol. 38, no. 22, pp. 9161–9170, 2005.

[48] R. R. N. Sailaja and M. Chanda, "Use of poly(ethylene-co-vinyl alcohol) as compatibilizer in LDPE/thermoplastic tapioca starch blends," *J. Appl. Polym. Sci.*, vol. 86, no. 12, pp. 3126–3134, 2002.

[49] W. Liu, Y. Wang, and Z. Sun, “Effects of Polyethylene-Grafted Maleic Anhydride (PE-g- MA) on Thermal Properties , Morphology , and Tensile Properties of Low-Density Polyethylene (LDPE) and Corn Starch Blends,” *Polymer (Guildf).*, pp. 2–6, 2002.

[50] S. Lim, J. L. Jane, S. Rajagopalan, and P. A. Seib, “Effect of Starch Granule Size on Physical Properties of Starch Filled Polyethylene Film,” *Biotechnol. Prog.*, vol. 8, no. 1, pp. 51–57, 1992.

[51] A. Taguet, P. Cassagnau, and J. M. Lopez-Cuesta, “Structuration, selective dispersion and compatibilizing effect of (nano)fillers in polymer blends,” *Prog. Polym. Sci.*, vol. 39, no. 8, pp. 1526–1563, 2014.

[52] F. Gubbels, R. Jerome, E. Vanlathem, R. Deltour, S. Blacher, and F. Brouers, “Kinetic and Thermodynamic Control of the Selective Localization of Carbon Black at the Interface of Immiscible Polymer Blends,” *Chem. Mater.*, vol. 10, no. 7, pp. 1227–1235, 1998.

[53] W. Zhang *et al.*, “The use of functionalized nanoparticles as non-specific compatibilizers for polymer blends,” *Polym. Adv. Technol.*, vol. 22, no. 1, pp. 65–71, 2011.

[54] A. K. Mohanty, M. Misra, and G. Hinrichsen, “Biofibres, biodegradable polymers and biocomposites: An overview,” *Macromol. Mater. Eng.*, vol. 276–277, pp. 1–24, 2000.

[55] D. Chu, Q. Nguyen, and D. G. Baird, “Effect of matrix molecular weight on the dispersion of nanoclay in unmodified high density polyethylene,” *Polym. Compos.*, vol. 28, no. 4, pp. 499–511, 2007.

[56] V. K. Raghavendran, M. C. Waterbury, V. Rao, and L. T. Drzal, “Influence of matrix molecular weight and processing conditions on the interfacial adhesion in bisphenol-A polycarbonate/carbon fiber composites,” *J. Adhes. Sci. Technol.*, vol. 11, no. 12, pp. 1501–1512, 1997.

[57] L. E. Nielsen, "Mechanical properties of particulate-filled systems," *Journal of Composite Materials*. 1, pp. 100–119, 1967.

[58] S. Ray and A. J. Easteal, “Advances in Polymer-Filler Composites: Macro to Nano,” *Mater. Manuf. Process.*, vol. 22, no. 6, pp. 741–749, 2007.

[59] R. Hemanth, M. Sekar, B. Suresha, and K. S. V. K. Rao, “Effects of Fibers and Fillers on Mechanical Properties of Thermoplastic Composites,” *Environ. Heal.*, vol. 2, pp. 25–26, 2014.

[60] K. E. Prasad, B. Das, U. Maitra, U. Ramamurty, and C. N. R. Rao, “Extraordinary synergy in the mechanical properties of polymer matrix composites reinforced with 2 nanocarbons.,” *Proc. Natl. Acad. Sci. U. S. A.*, vol. 106, no. 32, pp. 13186–13189, 2009.

[61] M. Altan and H. Yildirim, “Mechanical and Morphological Properties of Polypropylene and High Density Polyethylene Matrix Composites Reinforced with Surface Modified Nano Sized TiO2 Particles,” *World Acad. Sci. Eng. Technol. Int.*, vol. 4, no. 10, pp. 231–237, 2010.

[62] N. A. M. Aridi, S. M. Sapuan, E. S. Zainudin, and F. M. AL-Oqla, “Mechanical and morphological properties of injection-molded rice husk polypropylene composites,” *Int. J. Polym. Anal. Charact.*, vol. 21, no. 4, pp. 1–9, 2016.

[63] H. . Obasi and I. O. Igwe, “Effects of Native Cassava Starch and Compatibilizer on Biodegradable and Tensile Properties of Polypropylene,” *Am. J. Eng. Res.*, no. 2, pp. 96–104, 2014.

[64] C. Maier and T. Calafut, “Polypropylene : the definitive user’s guide and databook,” *PDL Handb. Ser.*, vol. c, p. xx, 432 , 1998.

[65] A. P. Gupta and A. Alam, “Study of Flexural , Tensile , Impact properties and Morphology of Potato Starch / Polypropylene blends .,” vol. 2, no. 11, pp. 599–604, 2014.

[66] Tomé, L.C., Fernandes, S.C.M., Sadocco, P., Causio, J., Silvestre, A.J.D., Neto, C.P., Freire, C.S.R., “Antibacterial thermoplastic starch-chitosan based materials prepared by melt-mixing,” *BioResources*, vol. 7, no. 3, pp. 3398–3409, 2012.

[67] M. Liu, R. He, J. Yang, W. Zhao, and C. Zhou, “Transcrystallization at the surface of graphene-modified chitosan fibers,” *J. Phys. D. Appl. Phys.*, vol. 49, no. 26, p. 265305, 2016.

[68] S. Bloembergen, D. Lee, I. McLennan, R. Wildi and E. Egdom, "Process For Producing Biopolymer Nanoparticle Biolatex Compositions Having Enhanced Performance and Compositions Based Thereon," US 2010/0143738 A1, 2010.

[69] Y. C. Kim, “Effect of Maleated Polyethylene on the Crystallization Behavior of LLDPE/Clay Nanocomposites,” *Polym. J.*, vol. 38, no. 3, pp. 250–257, 2006.

[70] S. Azizi, W. M. Z. W. Yunus, and M. Ahmad, “Effect of polyethylene-grafted maleic anhydride on properties of high-density polyethylene and polystyrene blend/layered silicate nanocomposites,” *J. Reinf. Plast. Compos.*, vol. 30, pp. 1649–1654, 2011.

[71] K. Alfadhel, A. Al-Mulla, and B. Al-Busairi, “Development and characterization of novel polybutylene nanocomposites,” *J. Compos. Mater.*, vol. 51, no. 1, pp. 95–108, 2017.

[72] S. Chakraborty, B. Sahoo, I. Teraoka, and R. A. Gross, “Solution properties of starch nanoparticles in water and DMSO as studied by dynamic light scattering,” *Carbohydr. Polym.*, vol. 60, no. 4, pp. 475–481, 2005.

[73] H. Chiou, C. M. Fellows, R. G. Gilbert, and M. A. Fitzgerald, “Study of rice-starch structure by dynamic light scattering in aqueous solution,” *Carbohydr. Polym.*, vol. 61, no. 1, pp. 61–71, 2005.

[74] S. Wang, J. Yu, and J. Yu, “Influence of maleic anhydride on the compatibility of thermal plasticized starch and linear low-density polyethylene,” *J. Appl. Polym. Sci.*, vol. 93, no. 2, pp. 686–695, 2004.

[75] B. Duan, P. Sun, X. Wang, and C. Yang, “Preparation and properties of starch nanocrystals/carboxymethyl chitosan nanocomposite films,” *Starch/Staerke*, vol. 63, no. 9, pp. 528–535, 2011.

[76] X. Wang, L. Zhang, and D. Yue, “Nano-Starch Particles Morphology and Their Dispersion in Rubber,” *Integr. Ferroelectr.*, vol. 137, no. 1, pp. 149–155, 2012.

[77] H. Angellier, S. Molina-Boisseau, L. Lebrun, and A. Dufresne, “Processing and structural properties of waxy maize starch nanocrystals reinforced natural rubber,” *Macromolecules*, vol. 38, no. 9, pp. 3783–3792, 2005.

[78] Y. J. Wang, W. Liu, and Z. Sun, “Effects of glycerol and PE-g-MA on morphology, thermal and tensile properties of LDPE and rice starch blends,” *J. Appl. Polym. Sci.*, vol. 92, no. August, pp. 344–350, 2004.

[79] M. Pöllänen, M. Suvanto, and T. T. Pakkanen, “Cellulose reinforced high density polyethylene

composites - Morphology, Mechanical and thermal expansion properties," *Compos. Sci. Technol.*, vol. 76, pp. 21–28, 2013.

[80] H. Namazi, F. Fathi, and A. Dadkhah, "Hydrophobically modified starch using long-chain fatty acids for preparation of nanosized starch particles," *Sci. Iran.*, vol. 18, no. 3 C, pp. 439–445, 2011.

[81] M. C. Sweedman, M. J. Tizzotti, C. Schäfer, and R. G. Gilbert, "Structure and physicochemical properties of octenyl succinic anhydride modified starches: A review," *Carbohydr. Polym.*, vol. 92, no. 1, pp. 905–920, 2013.

APPENDIX

Thermal Data:

DSC Thermograms

BPE:

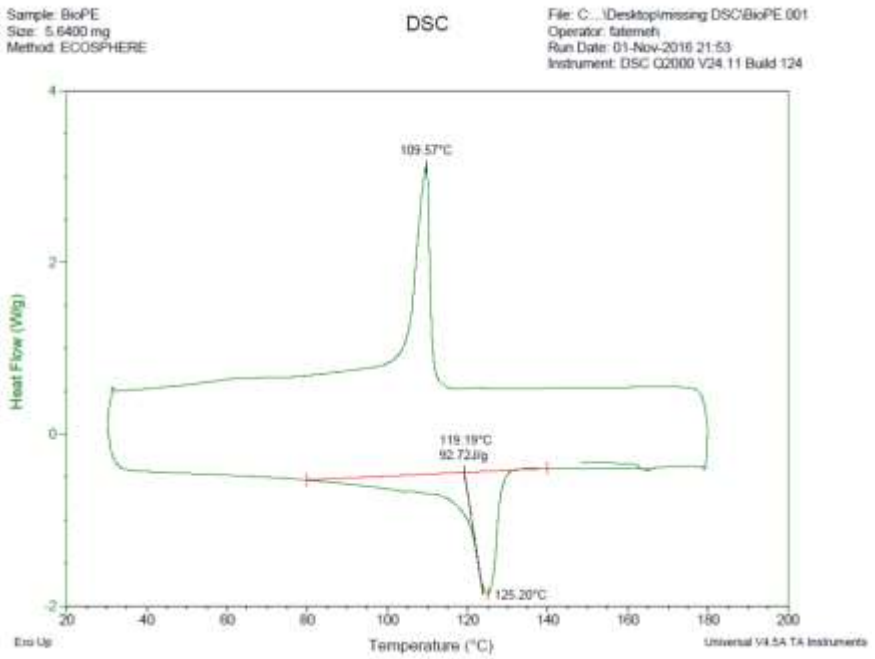

RV00

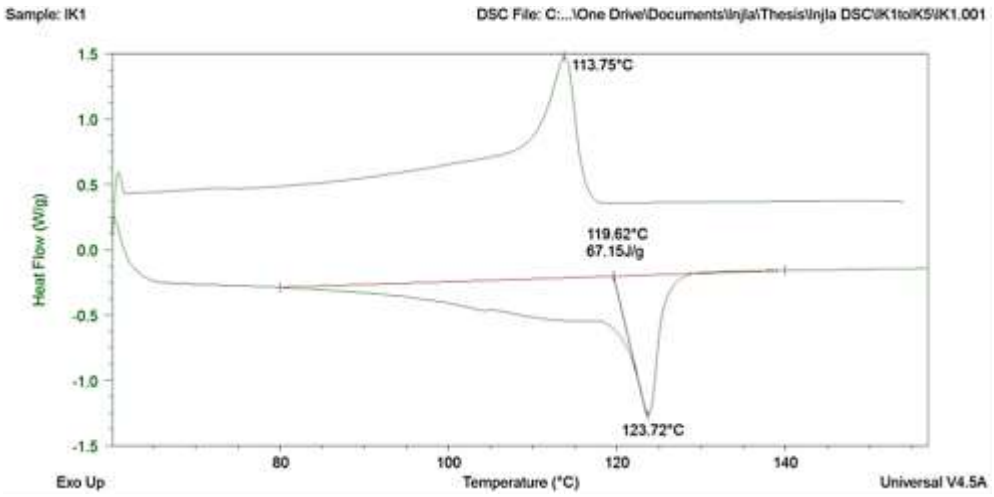

RC00

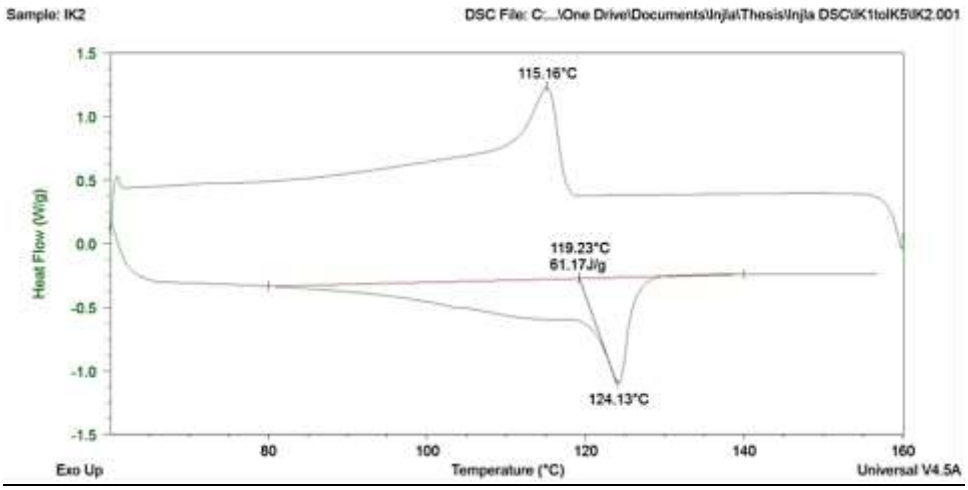
Sample: IK2
DSC File: C:...\One Drive\Documents\Injla\Thesis\Injla DSC\IK1toIK5\IK2.001
115.16°C
119.23°C
61.17J/g
124.13°C
Heat Flow (W/g)
Exo Up
Temperature (°C)
Universal V4.5A

RS00

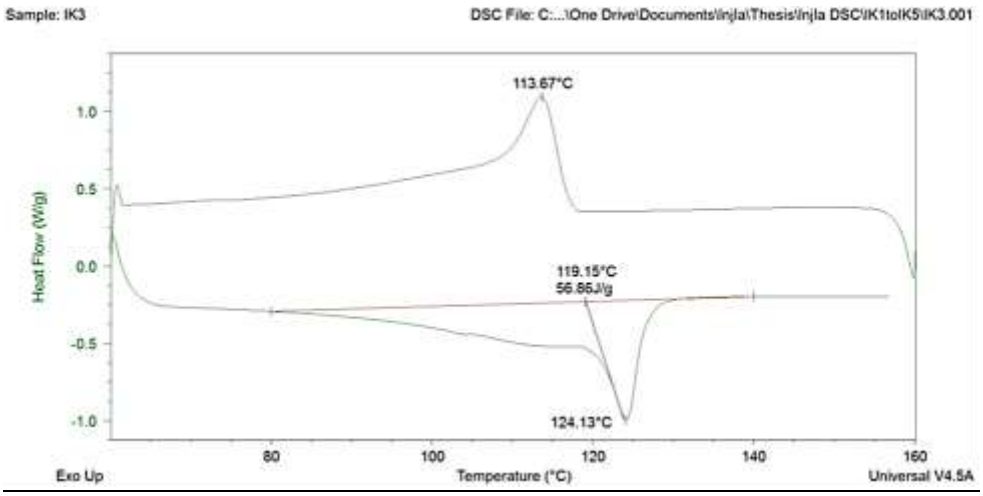
Sample: IK3
DSC File: C:...\One Drive\Documents\Injla\Thesis\Injla DSC\IK1toIK5\IK3.001
113.67°C
119.15°C
56.86J/g
124.13°C
Heat Flow (W/g)
Exo Up
Temperature (°C)
Universal V4.5A

RV0M$_L$

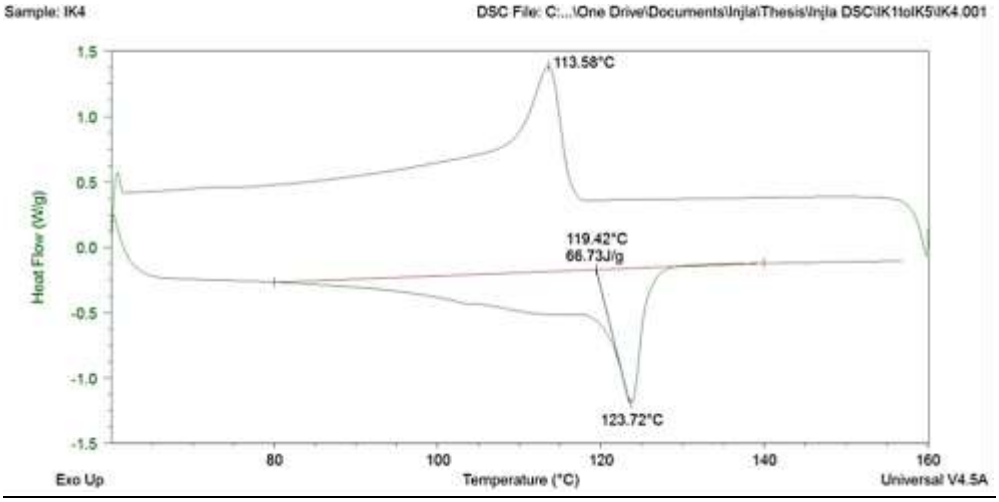
Sample: IK4
DSC File: C:...\One Drive\Documents\Injla\Thesis\Injla DSC\IK1toIK5\IK4.001
113.58°C
119.42°C
66.73J/g
123.72°C
Heat Flow (W/g)
Exo Up
Temperature (°C)
Universal V4.5A

RS0M$_L$

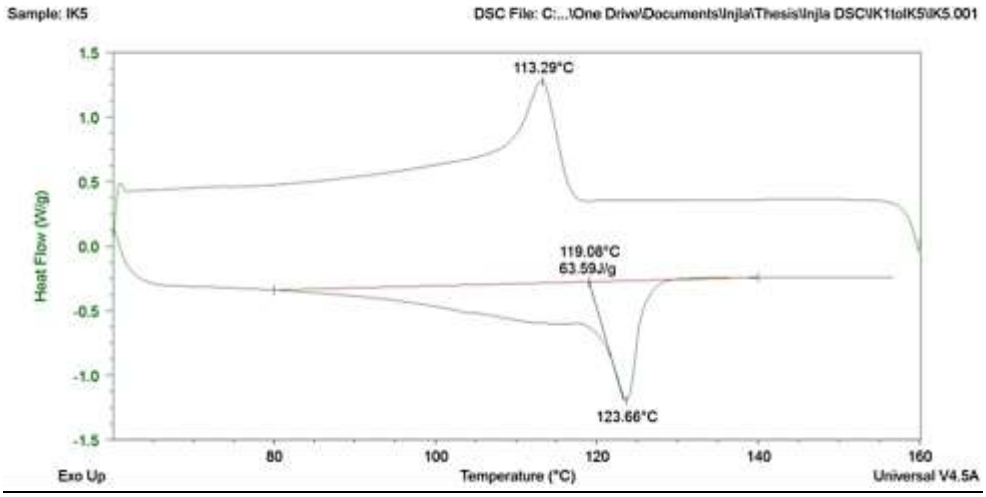
Sample: IK5
DSC File: C:...\One Drive\Documents\Injla\Thesis\Injla DSC\IK1toIK5\IK5.001
113.29°C
119.08°C
63.59J/g
123.66°C
Heat Flow (W/g)
Exo Up
Temperature (°C)
Universal V4.5A

$BS_H0M_L0.5$

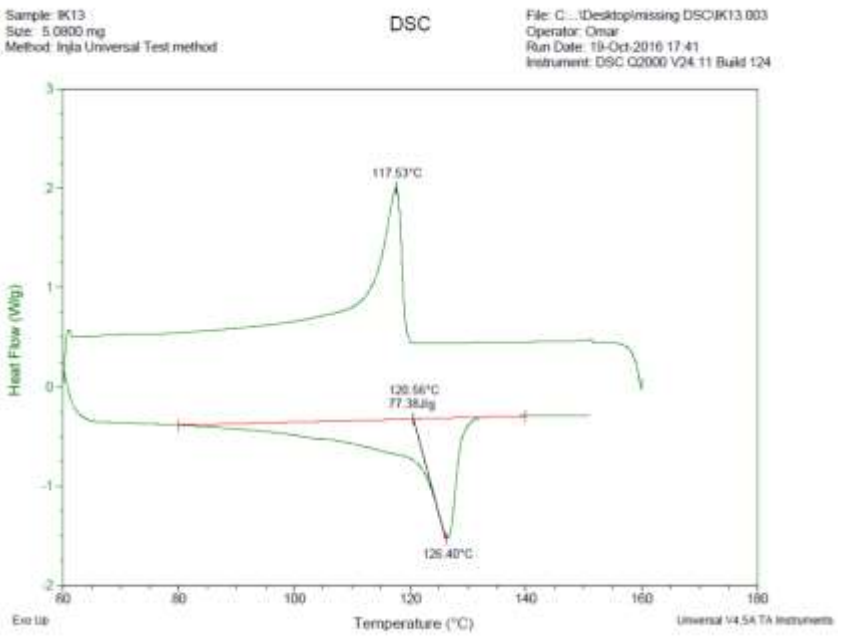

BS_H0M_L1

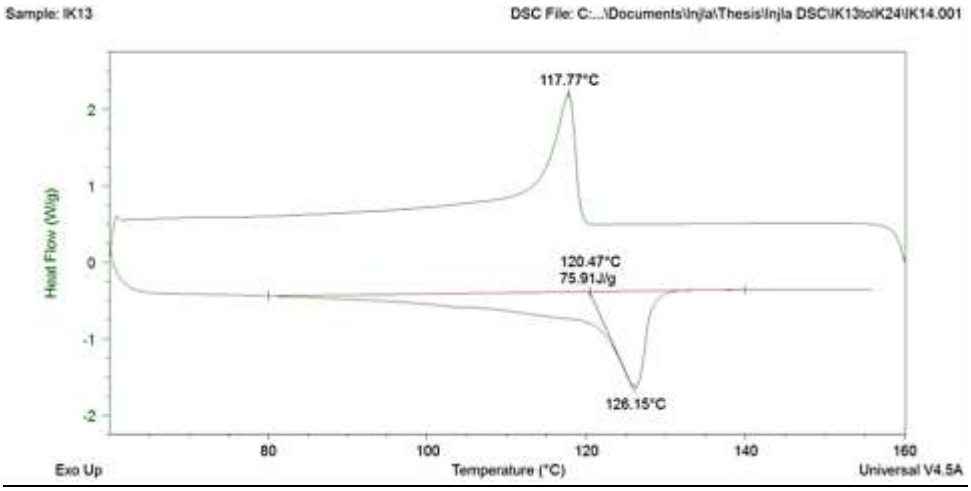

BS_H0M_L2

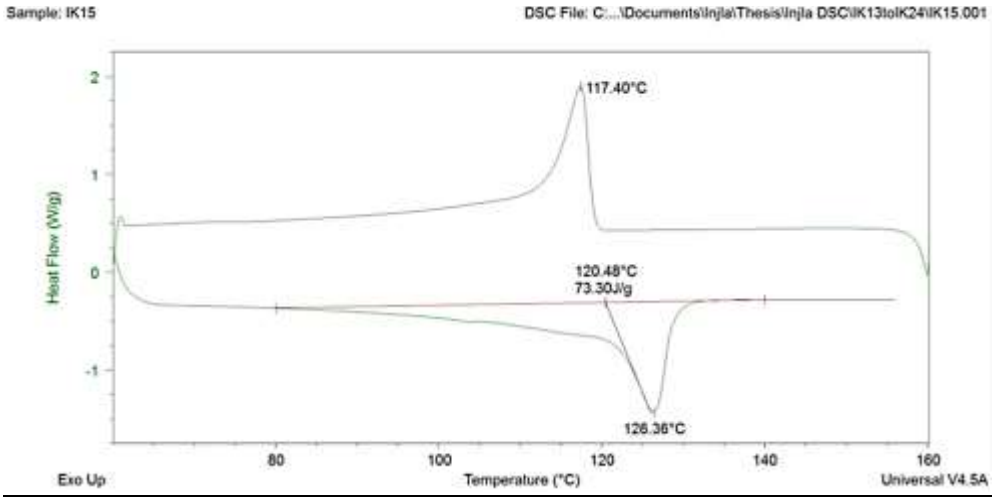

BS_H0M_L5

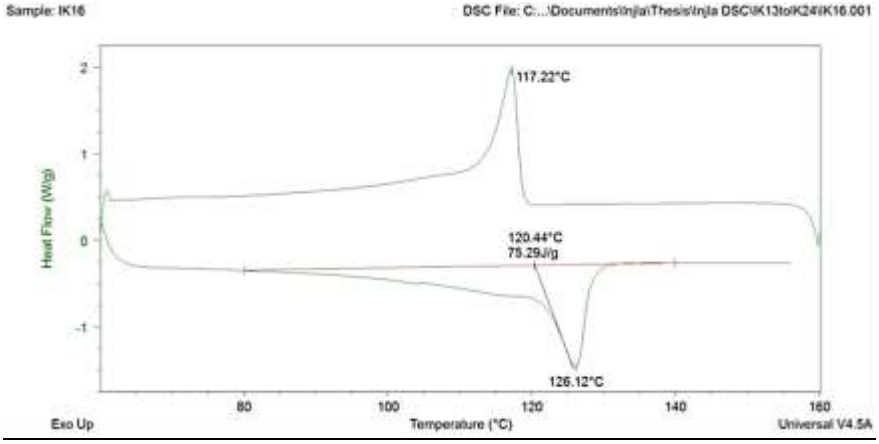

BS_H0FM_L

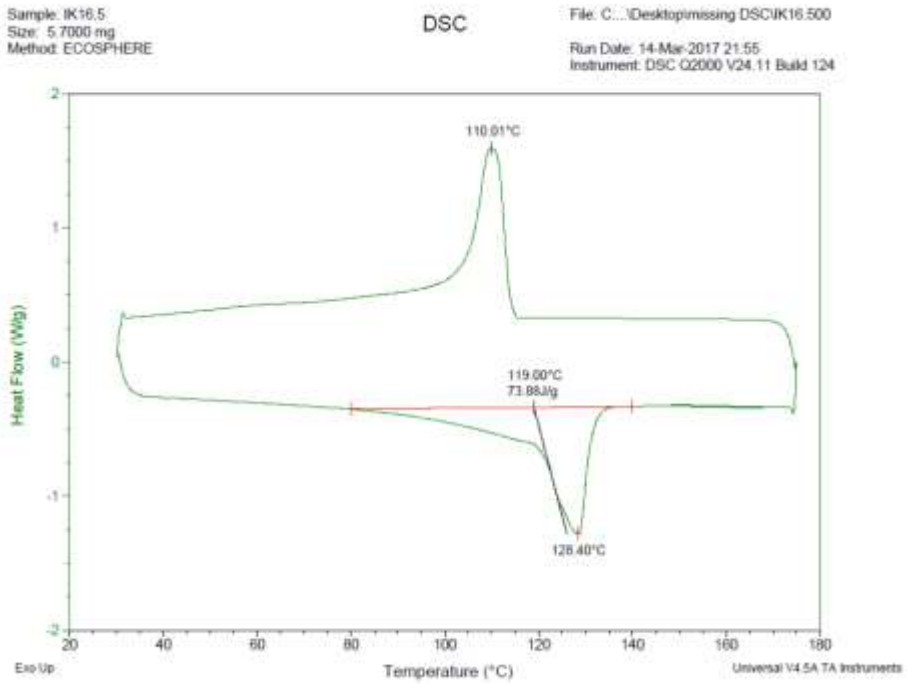

BS_H5FM_L

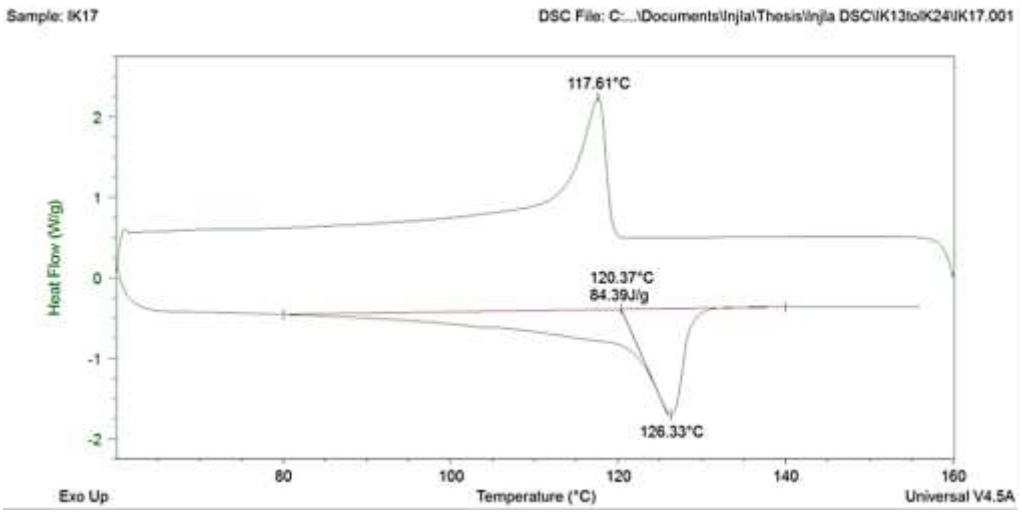

BS_H10FM_L

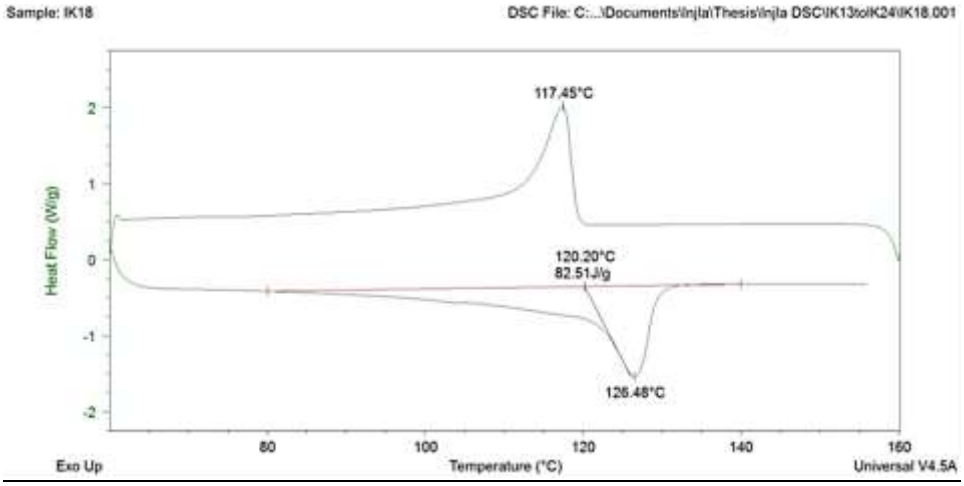

BS_H15FM_L

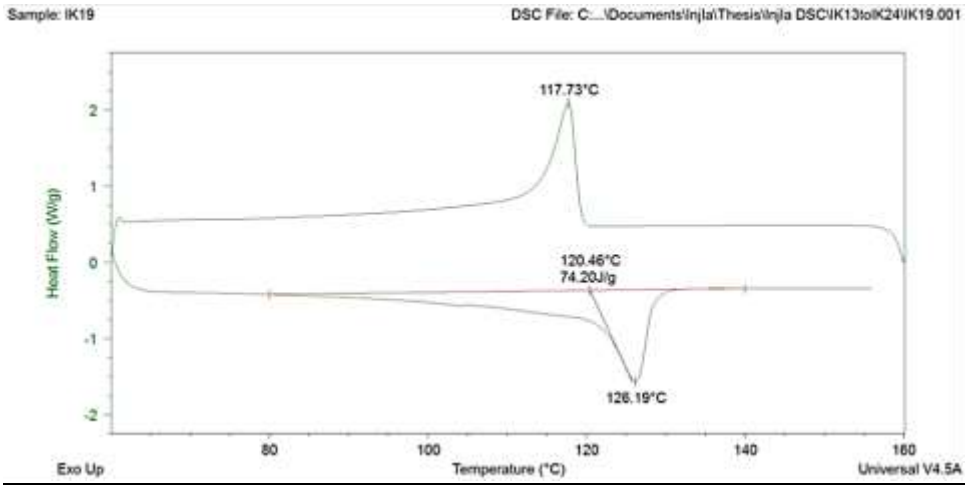

BS_H20FM_L

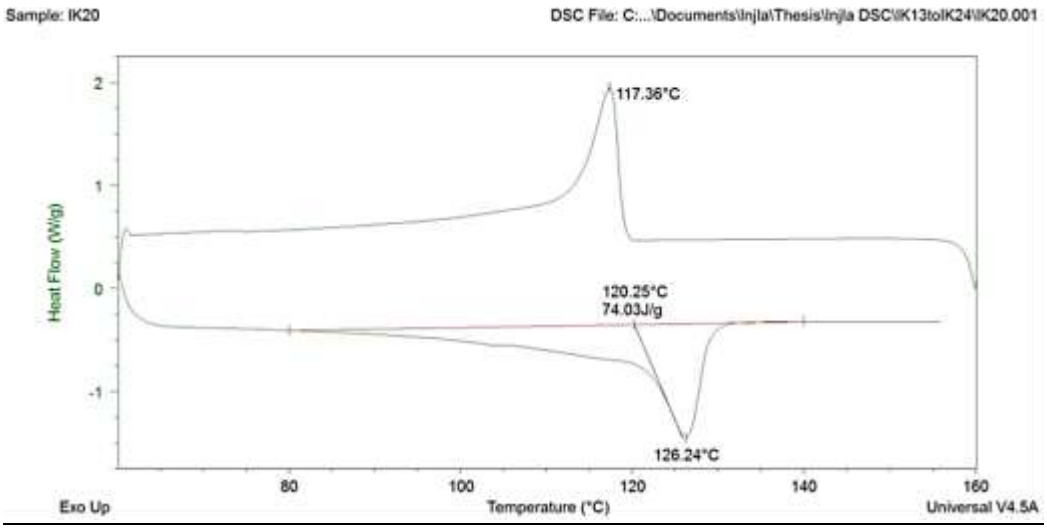

BS_HF5M_L

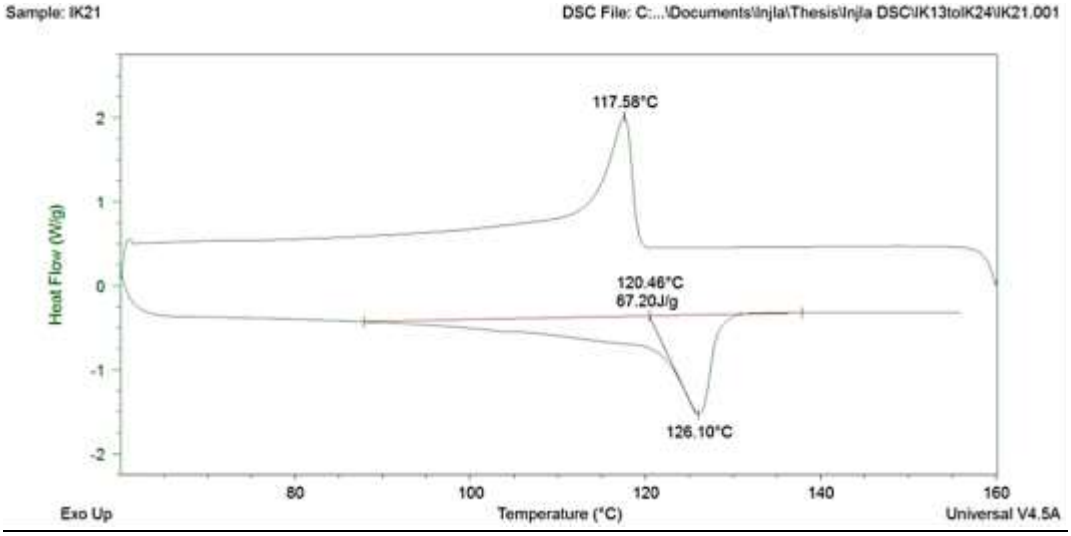

BS_HF10M_L

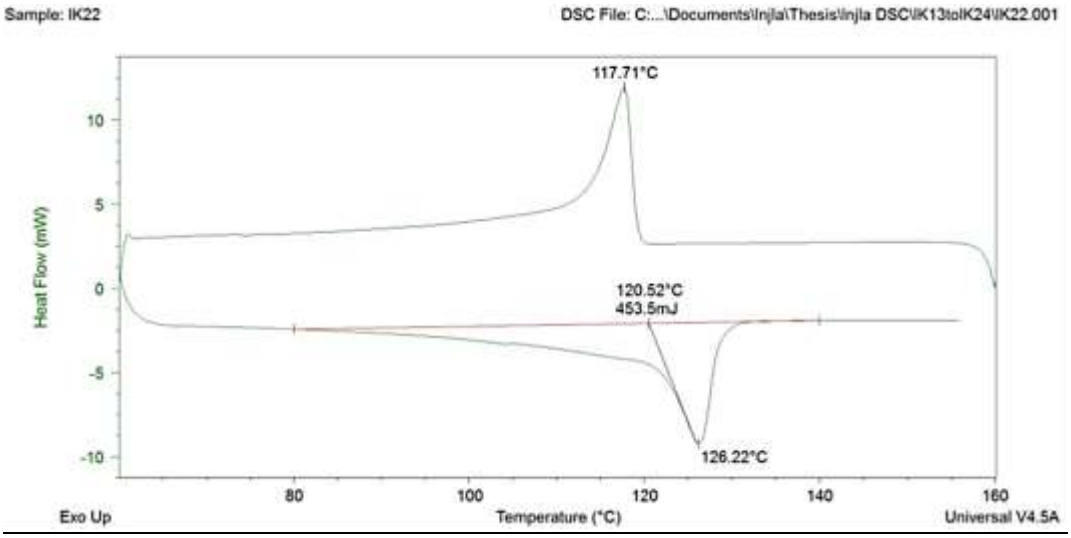

BS_HF15M_L

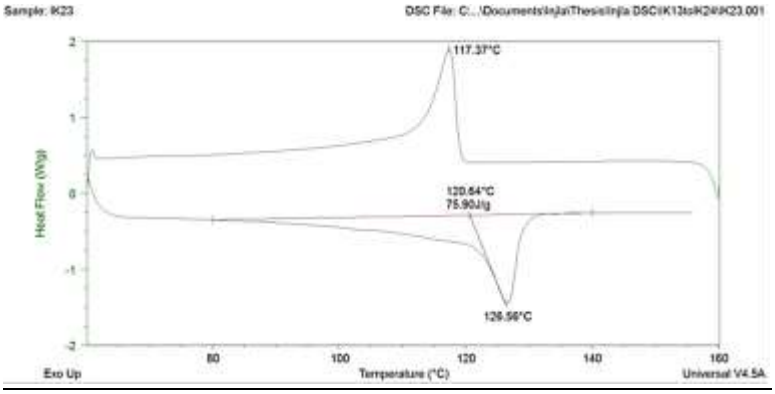

BS_HF20M_L

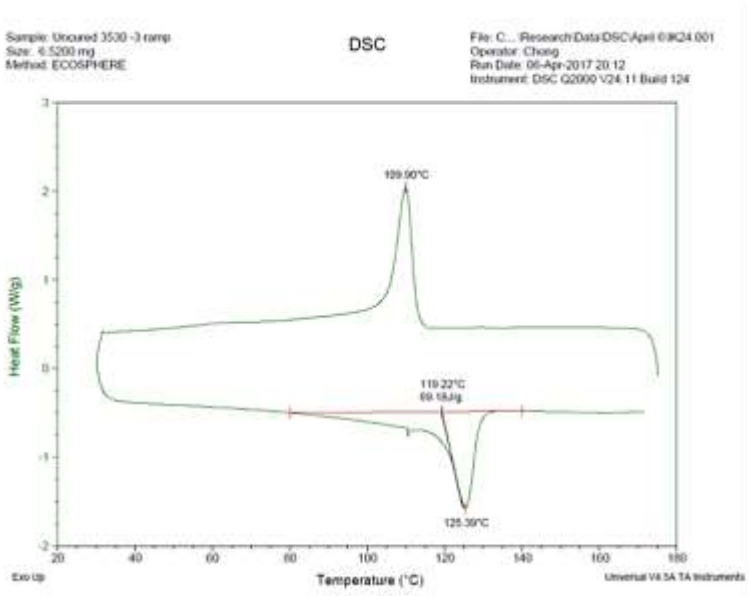

BS_HP20M_L

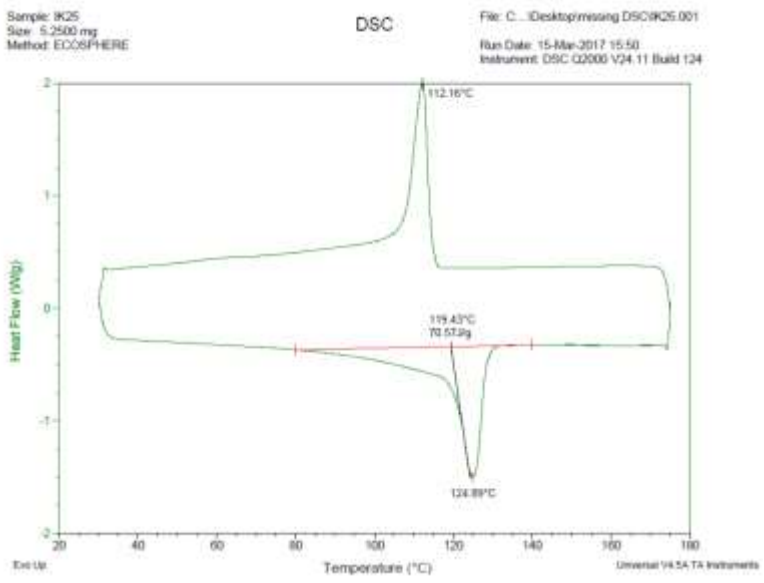

RPE

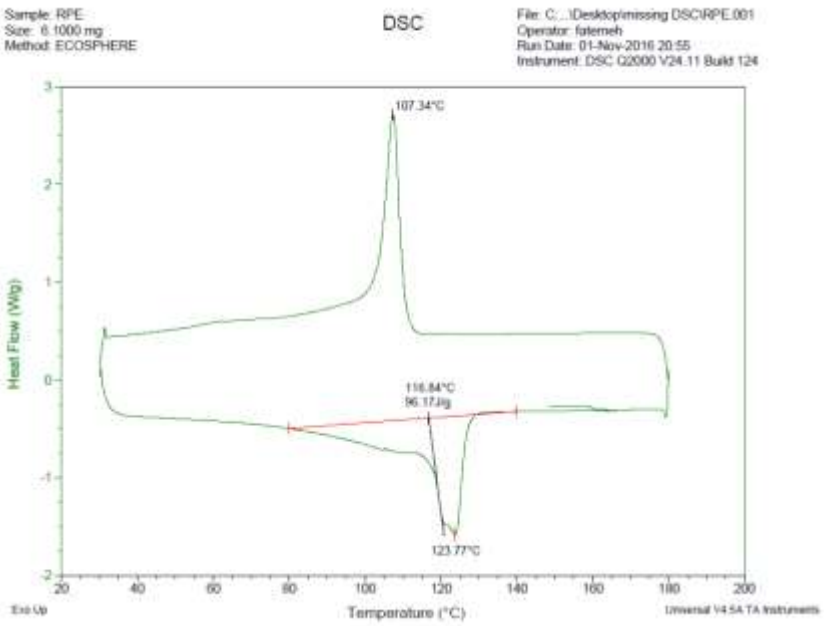

$RS_H0M_L0.5$

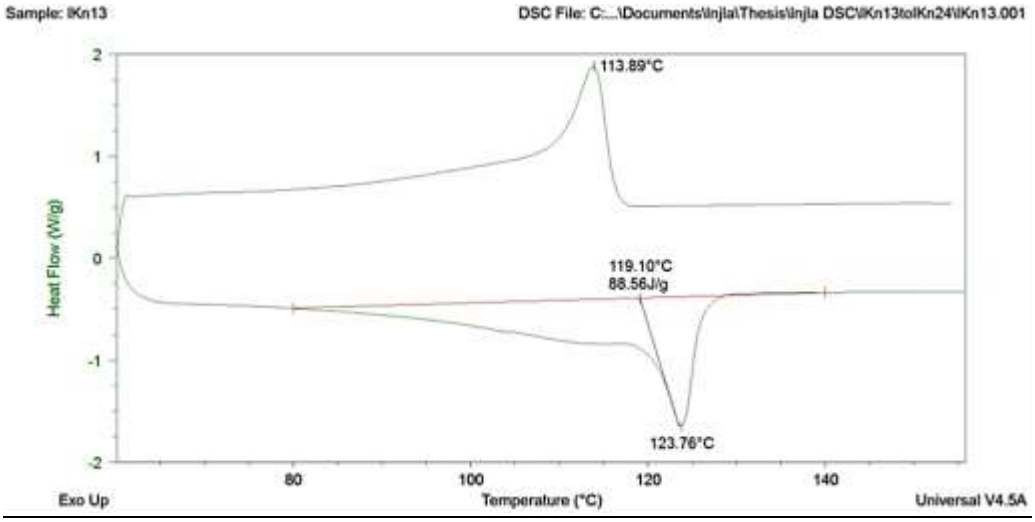

RS_H0M_L1

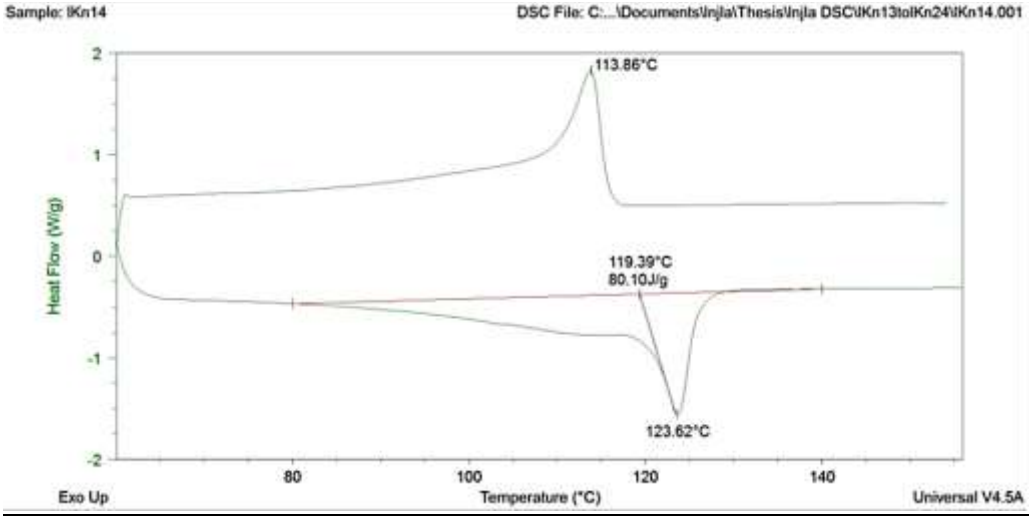

RS_H0M_L2

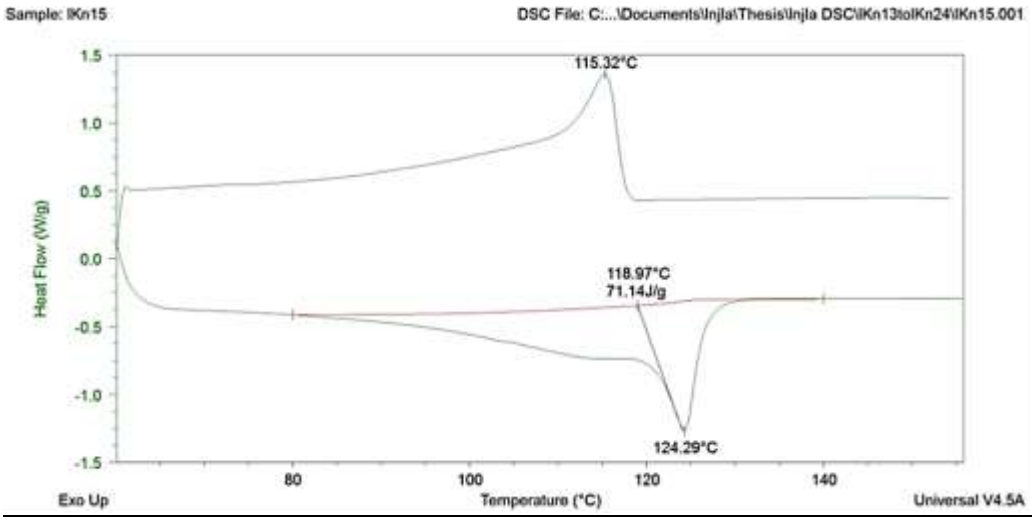

RS_H0M_L5

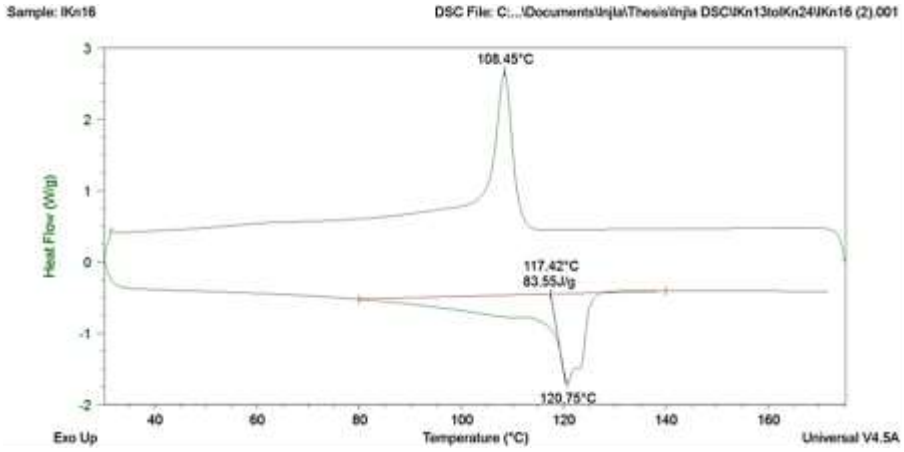

RS_H0FM_L

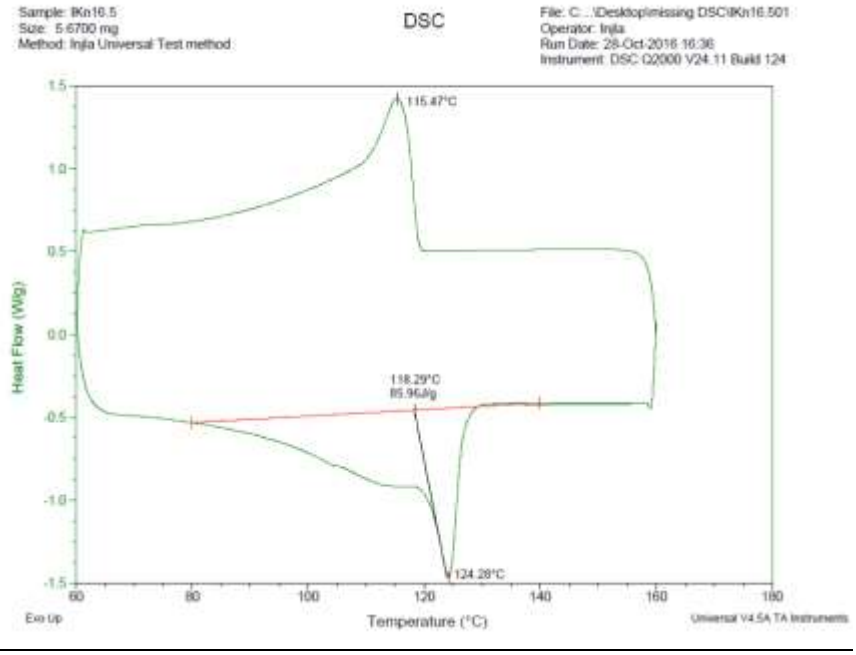

RS_H5FM_L

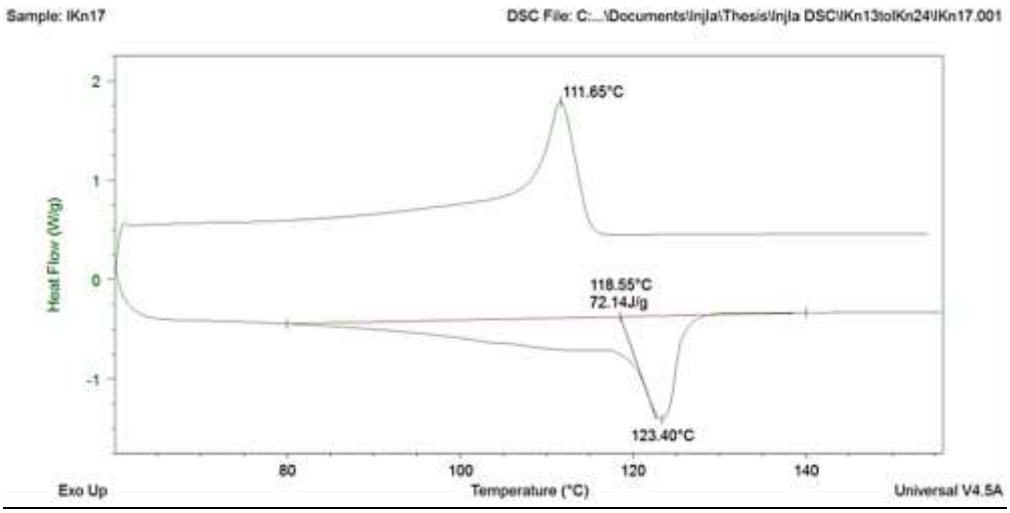

RS_H10FM_L

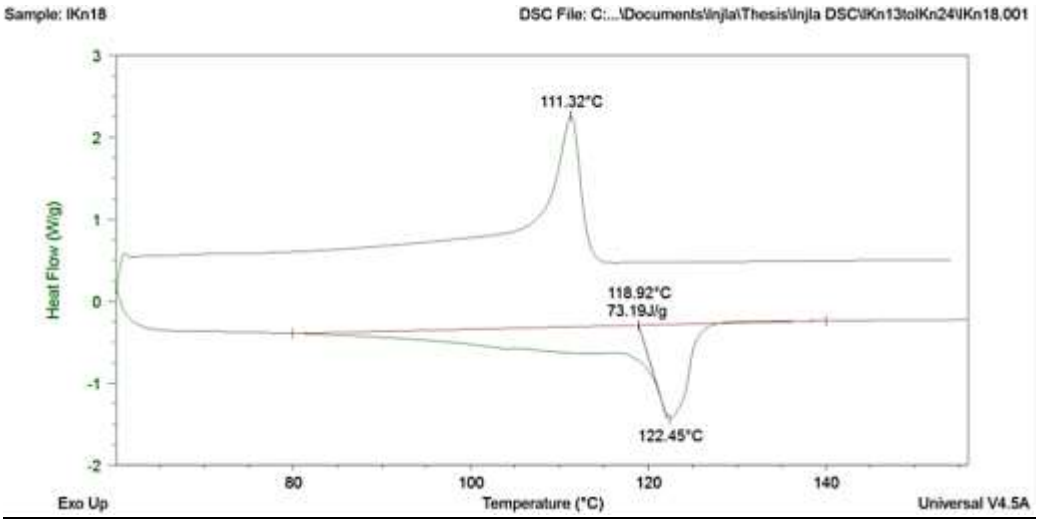

RS_H15FM_L

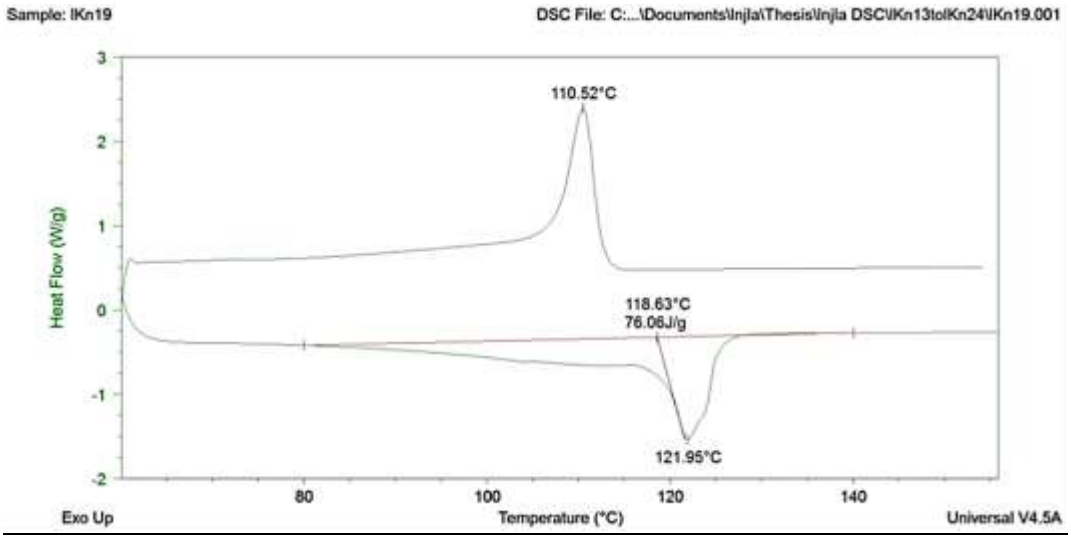

RS_H20FM_L

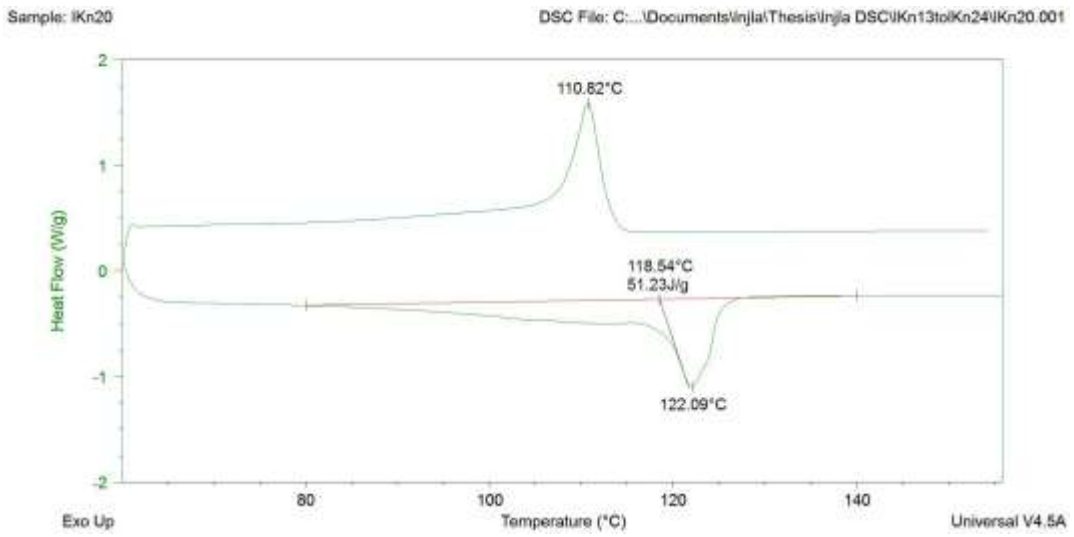

RS_HF5M_L

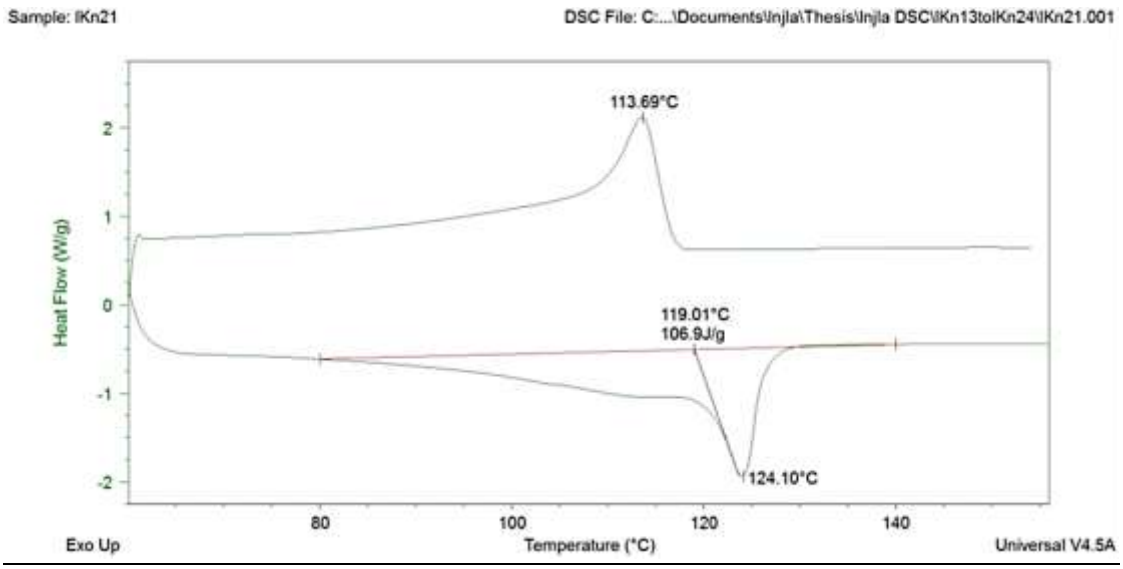

RS_HF10M_L

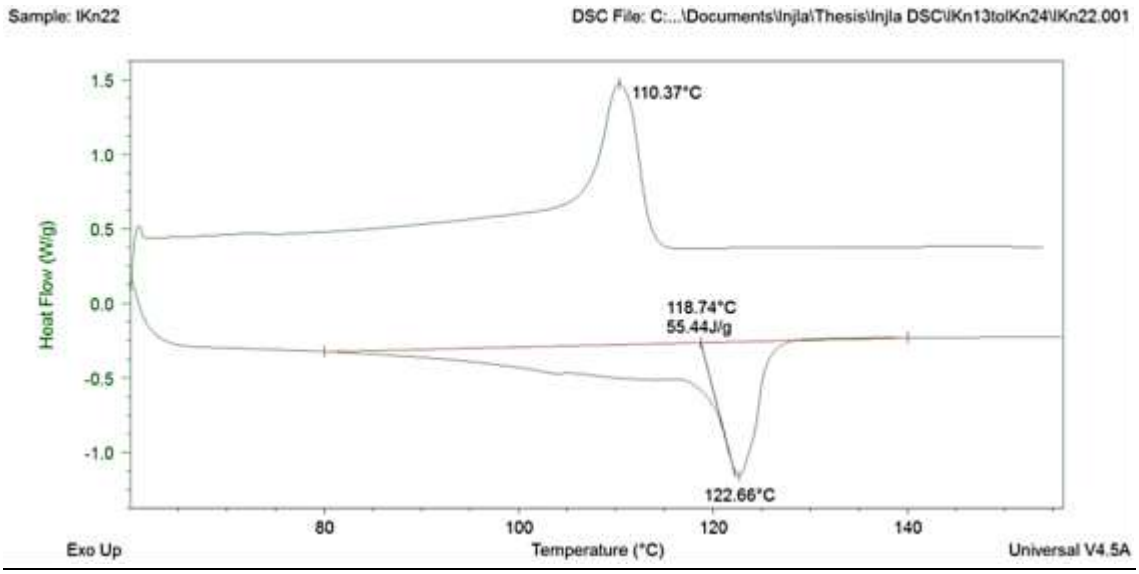

RS_HF20M_L

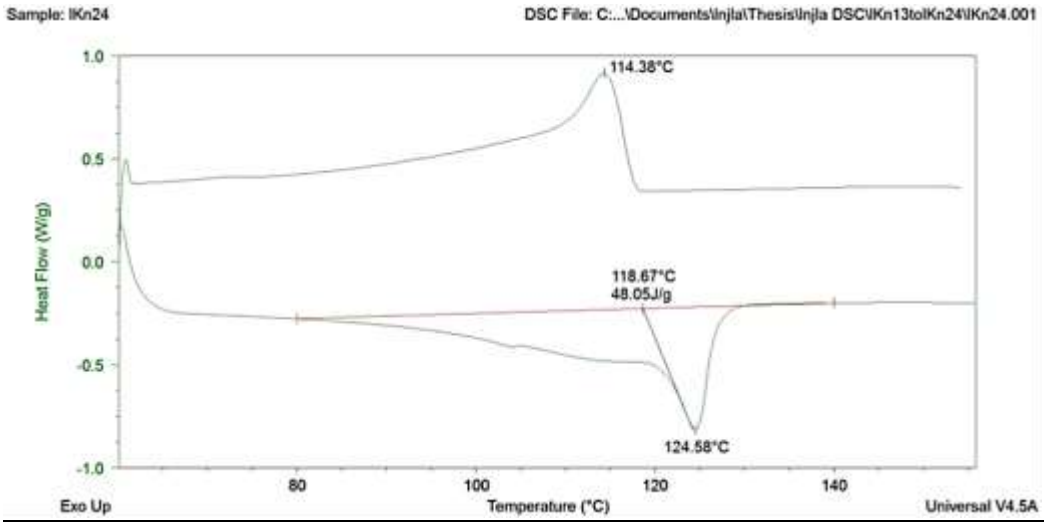

RS_HP20M_L

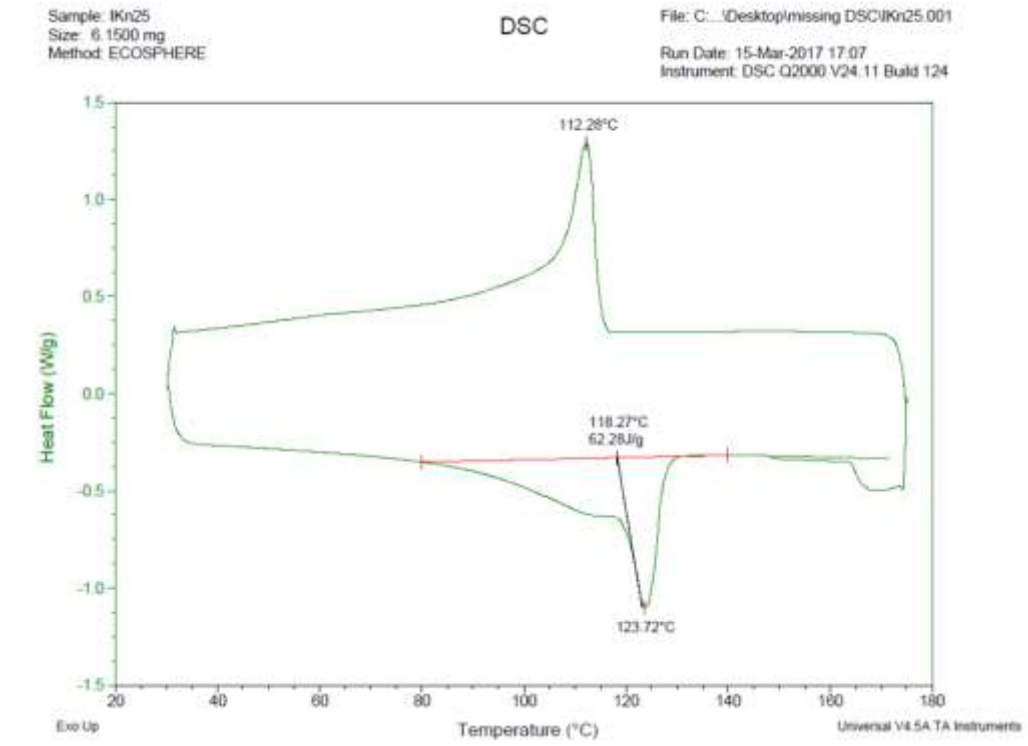

RS_HG10M_L

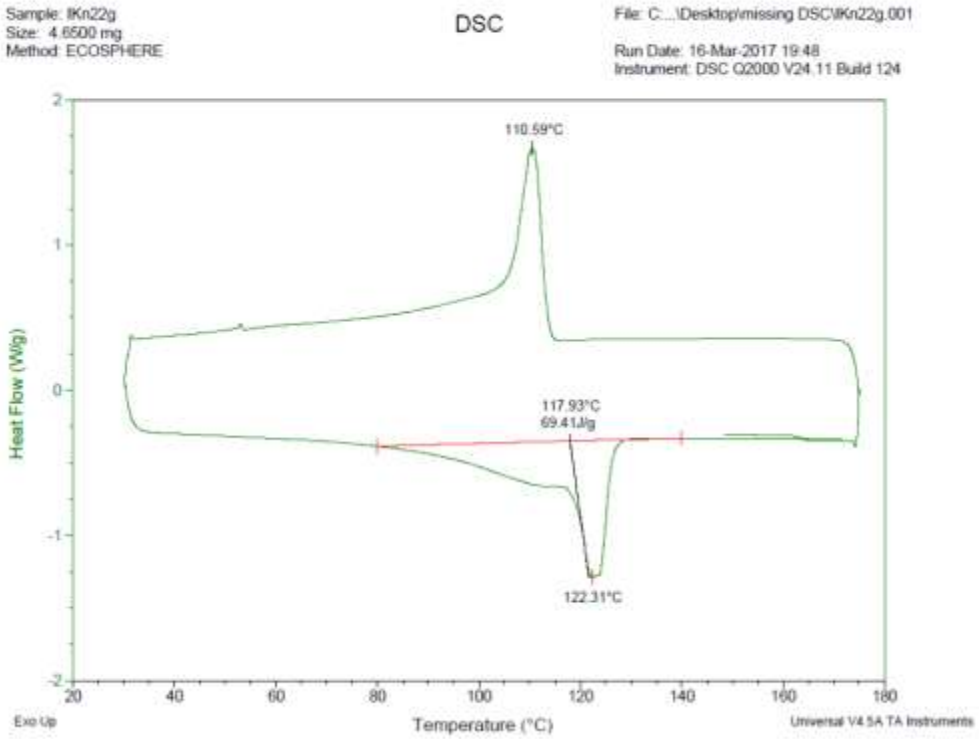
Sample: lKn22g
Size: 4.6500 mg
Method: ECOSPHERE
DSC
File: C:...\Desktop\missing DSC\lKn22g.001
Run Date: 16-Mar-2017 19:48
Instrument: DSC Q2000 V24.11 Build 124
110.59°C
117.93°C
69.41J/g
122.31°C
Heat Flow (W/g)
Exo Up
Temperature (°C)
Universal V4.5A TA Instruments

PP

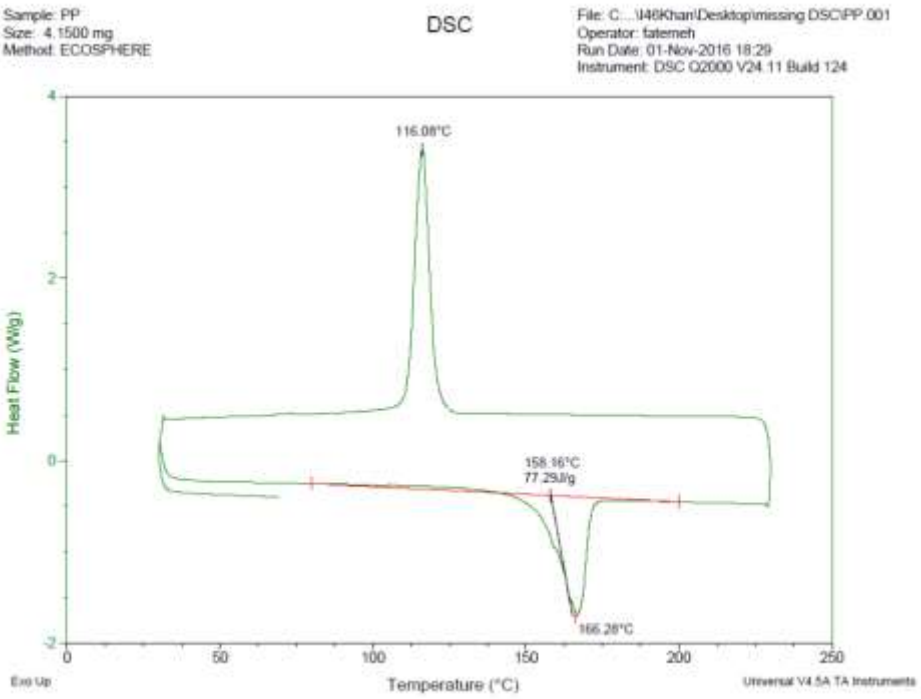
Sample: PP
Size: 4.1500 mg
Method: ECOSPHERE
DSC
File: C:...\l46Khan\Desktop\missing DSC\PP.001
Operator: fatemeh
Run Date: 01-Nov-2016 18:29
Instrument: DSC Q2000 V24.11 Build 124
116.08°C
158.16°C
77.29J/g
166.28°C
Heat Flow (W/g)
Exo Up
Temperature (°C)
Universal V4.5A TA Instruments

pS15FM$_L$

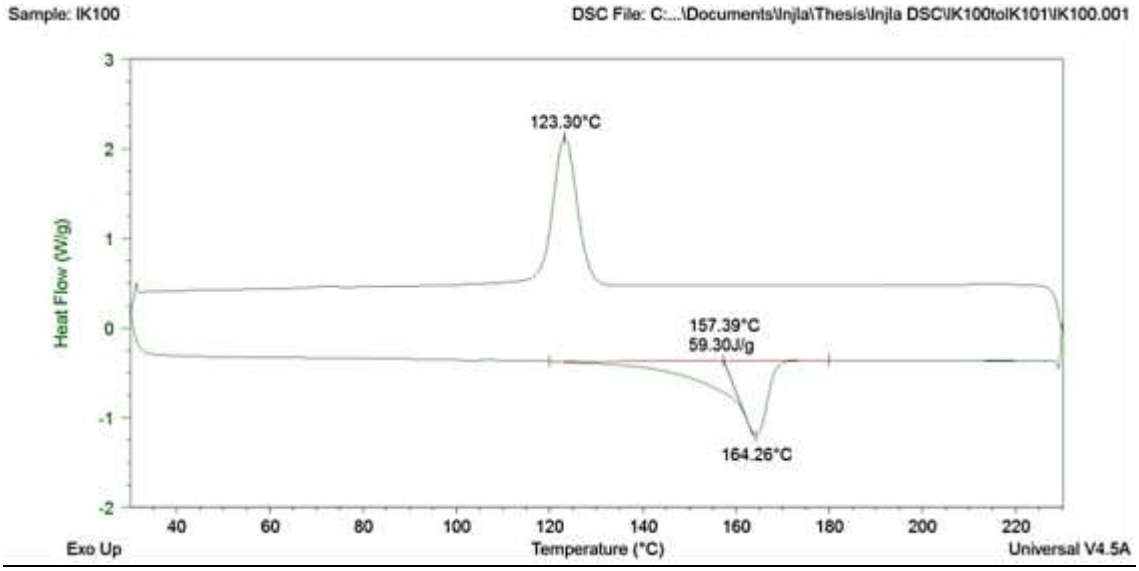

TGA Graphs:

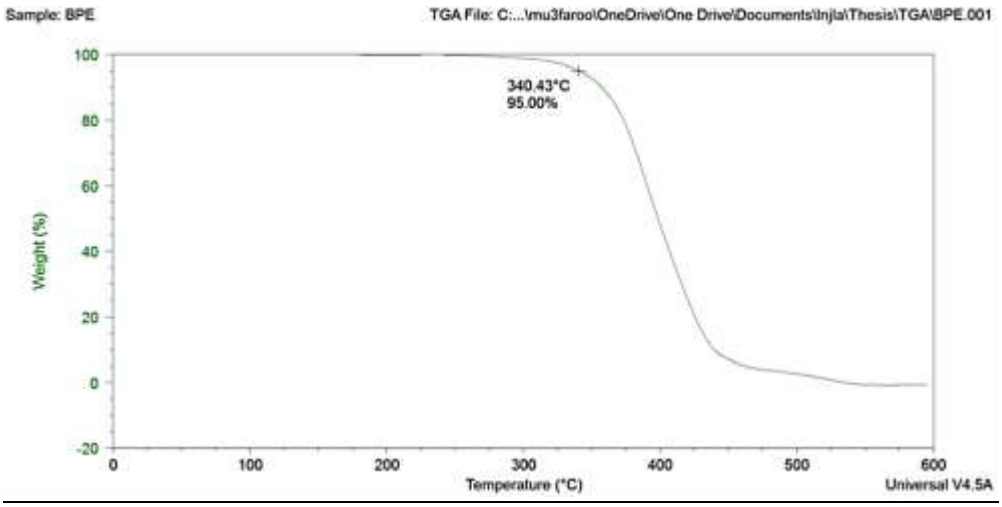

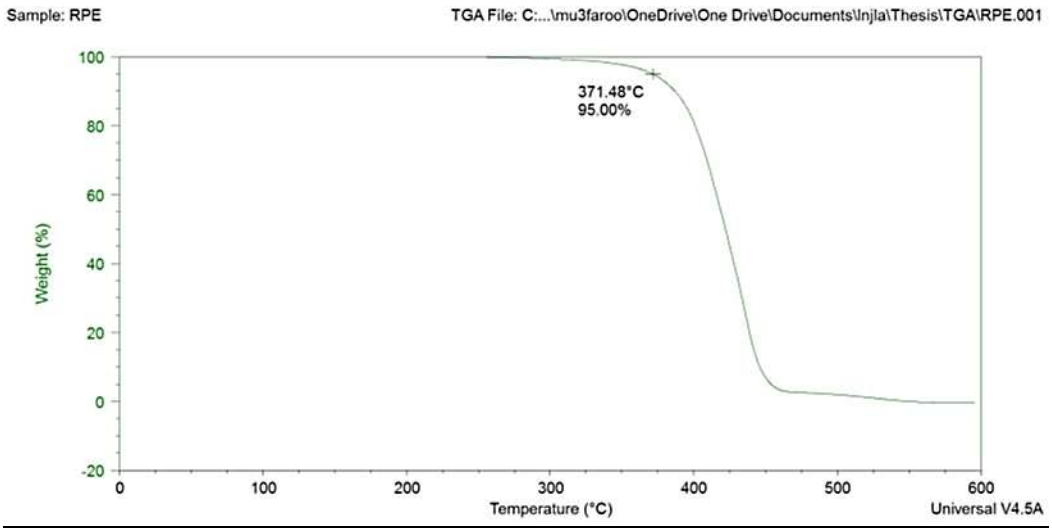
Sample: RPE
TGA File: C:...\mu3faroo\OneDrive\One Drive\Documents\Injla\Thesis\TGA\RPE.001
371.48°C
95.00%
Weight (%)
Temperature (°C)
Universal V4.5A

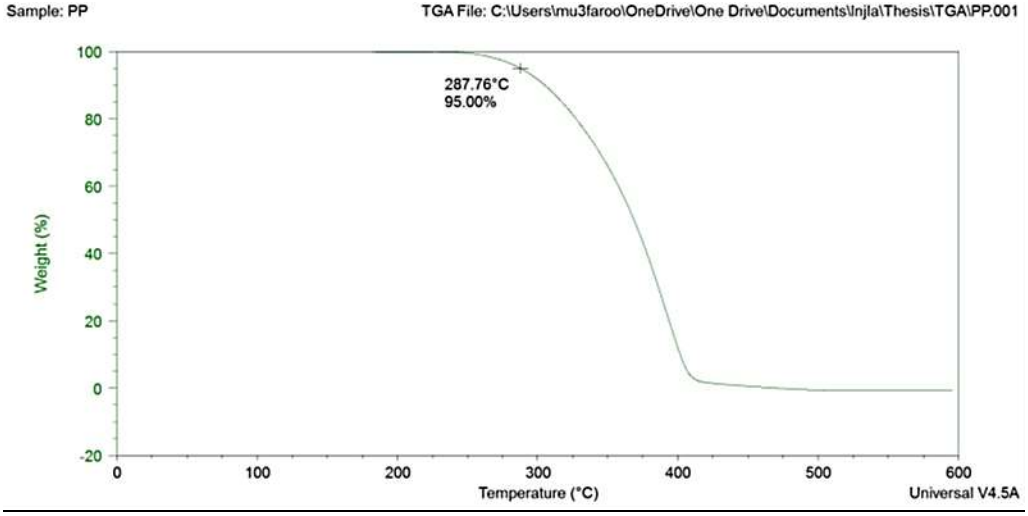
Sample: PP
TGA File: C:\Users\mu3faroo\OneDrive\One Drive\Documents\Injla\Thesis\TGA\PP.001
287.76°C
95.00%
Weight (%)
Temperature (°C)
Universal V4.5A

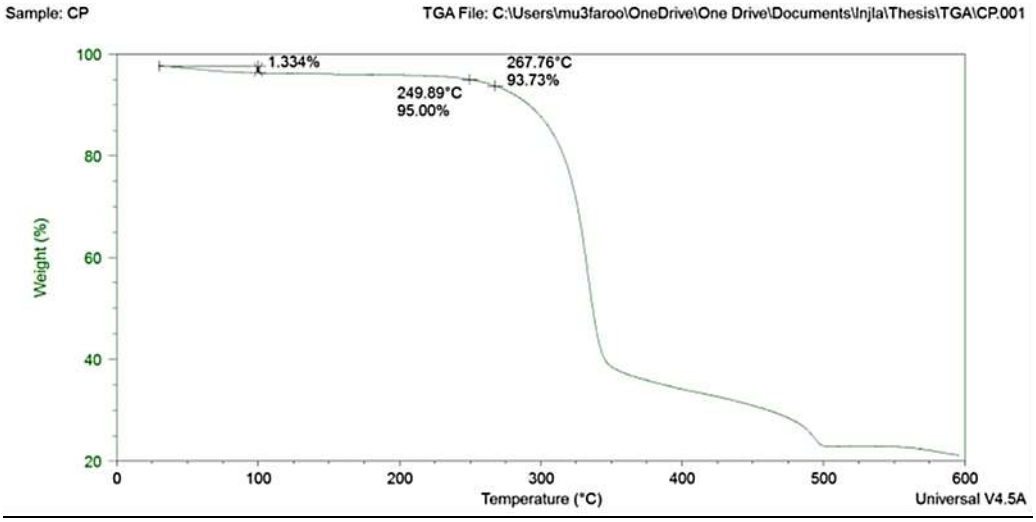
Sample: CP
TGA File: C:\Users\mu3faroo\OneDrive\One Drive\Documents\Injla\Thesis\TGA\CP.001
1.334%
267.76°C
93.73%
249.89°C
95.00%
Weight (%)
Temperature (°C)
Universal V4.5A

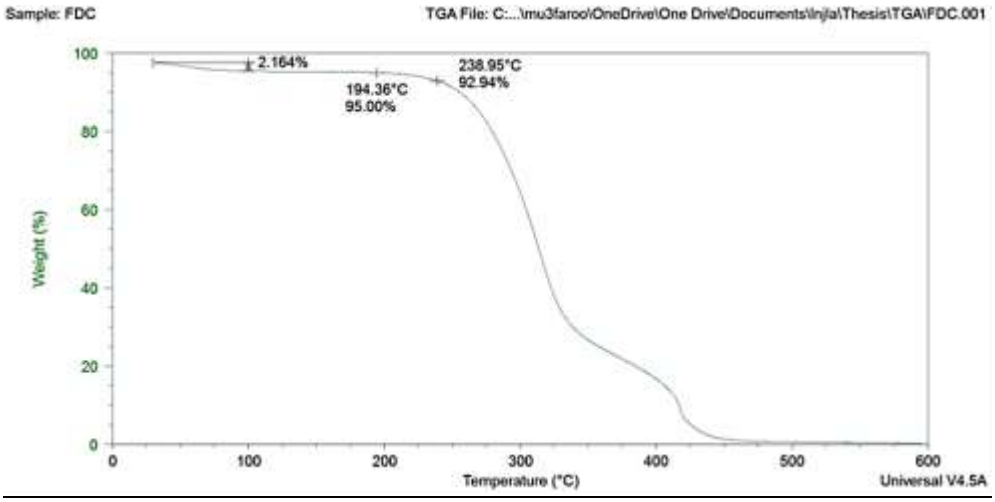
Sample: FDC
TGA File: C:...\mu3faroo\OneDrive\One Drive\Documents\Injla\Thesis\TGA\FDC.001
2.164%
194.36°C
95.00%
238.95°C
92.94%
Weight (%)
Temperature (°C)
Universal V4.5A

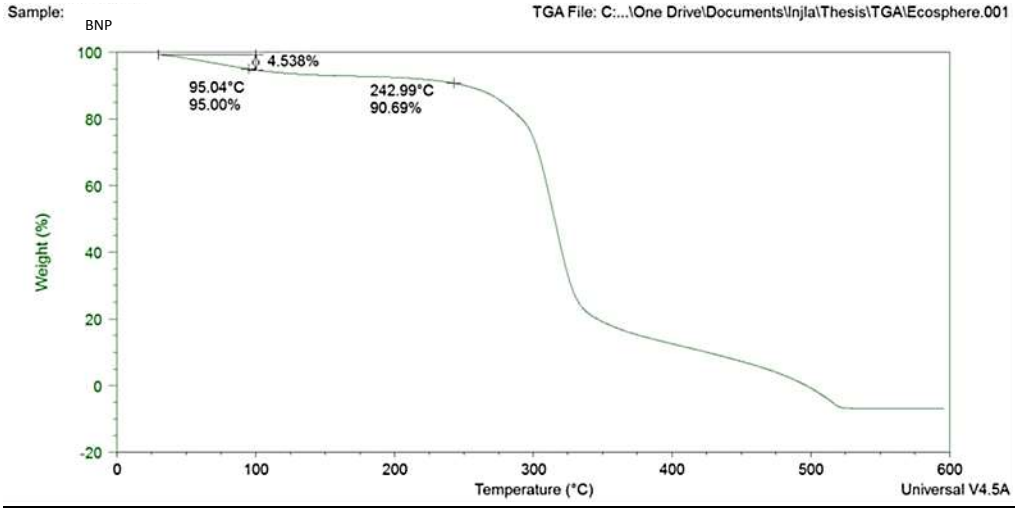
Sample:
BNP
TGA File: C:...\One Drive\Documents\Injla\Thesis\TGA\Ecosphere.001
4.538%
95.04°C
95.00%
242.99°C
90.69%
Weight (%)
Temperature (°C)
Universal V4.5A

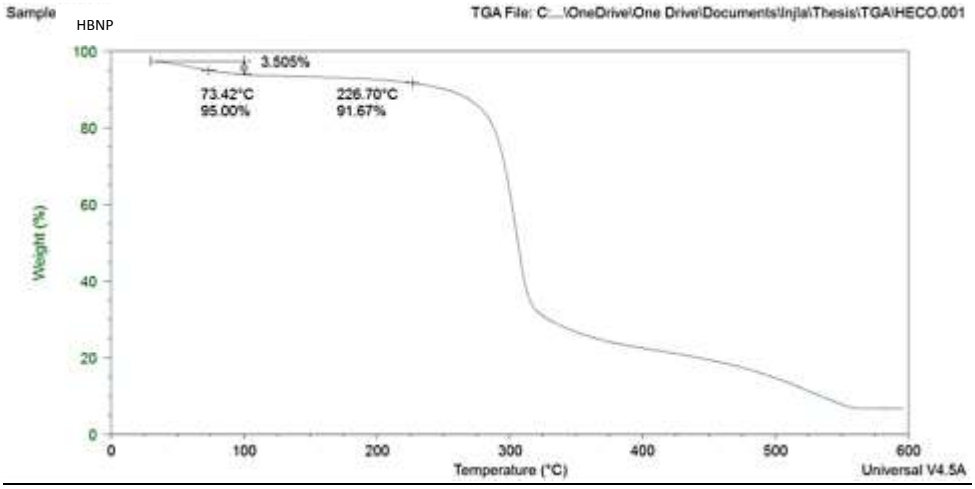
Sample
HBNP
TGA File: C:...\OneDrive\One Drive\Documents\Injla\Thesis\TGA\HECO.001
3.505%
73.42°C
95.00%
226.70°C
91.67%
Weight (%)
Temperature (°C)
Universal V4.5A

RV00

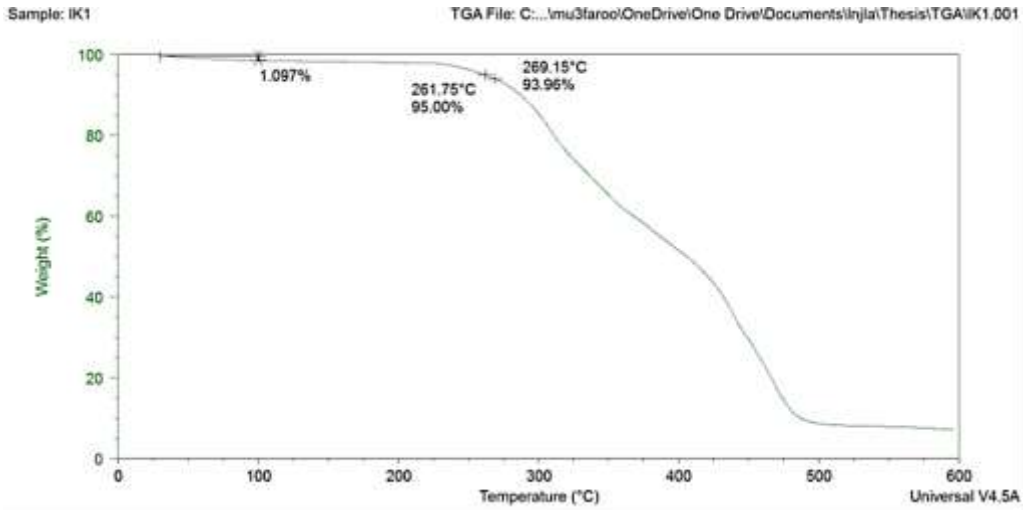
Sample: IK1
TGA File: C:...\mu3faroo\OneDrive\One Drive\Documents\Injla\Thesis\TGA\IK1.001
1.097%
261.75°C
95.00%
269.15°C
93.96%
Weight (%)
Temperature (°C)
Universal V4.5A

RC00

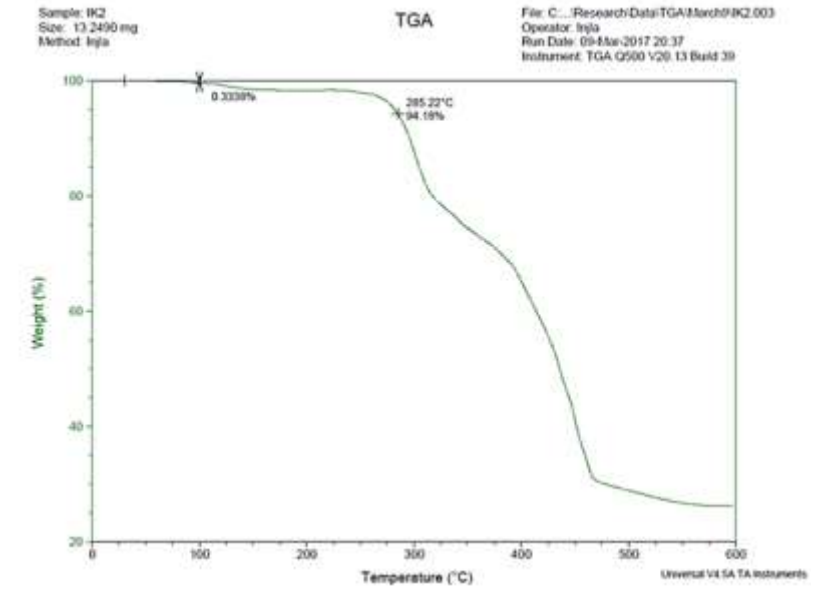
Sample: IK2
Size: 13.2490 mg
Method: Injla
TGA
File: C:...\Research\Data\TGA\March\IK2.003
Operator: Injla
Run Date: 09-Mar-2017 20:37
Instrument: TGA Q500 V20.13 Build 39
0.3338%
285.22°C
94.18%
Weight (%)
Temperature (°C)
Universal V4.5A TA Instruments

RS00

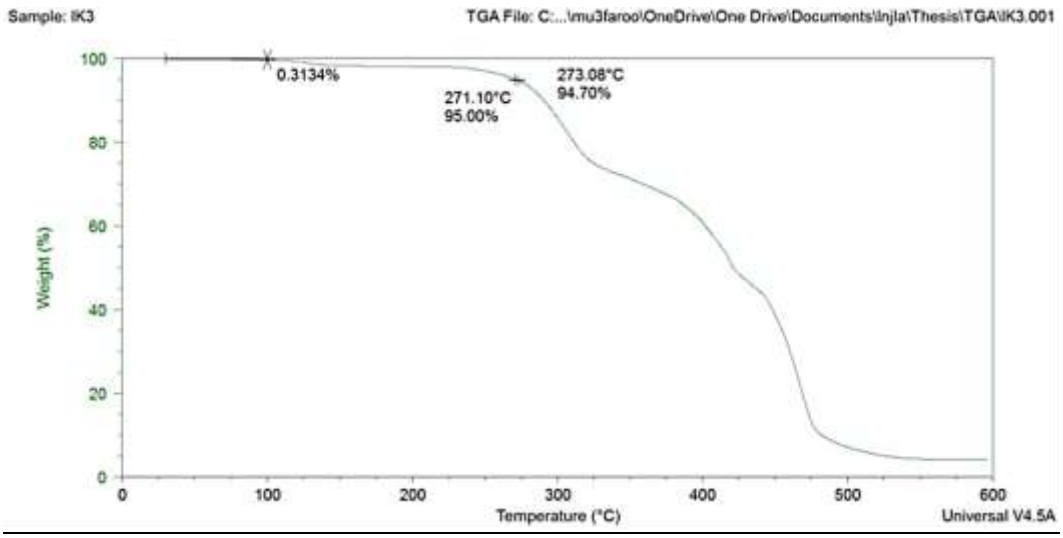
Sample: IK3
TGA File: C:...\mu3faroo\OneDrive\One Drive\Documents\Injla\Thesis\TGA\IK3.001
0.3134%
271.10°C
95.00%
273.08°C
94.70%
Weight (%)
Temperature (°C)
Universal V4.5A

RV0M$_L$

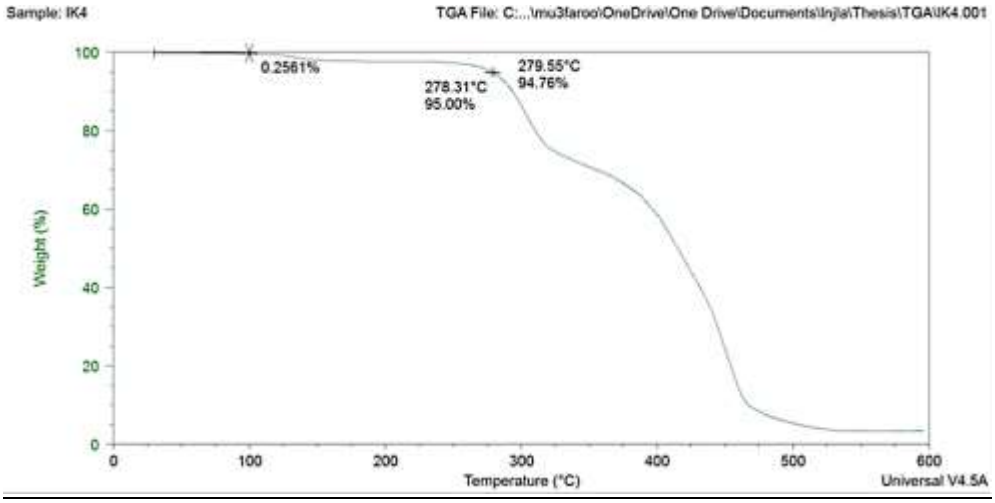
Sample: IK4
TGA File: C:...\mu3faroo\OneDrive\One Drive\Documents\Injla\Thesis\TGA\IK4.001
0.2561%
278.31°C
95.00%
279.55°C
94.76%
Weight (%)
Temperature (°C)
Universal V4.5A

RS0M$_L$

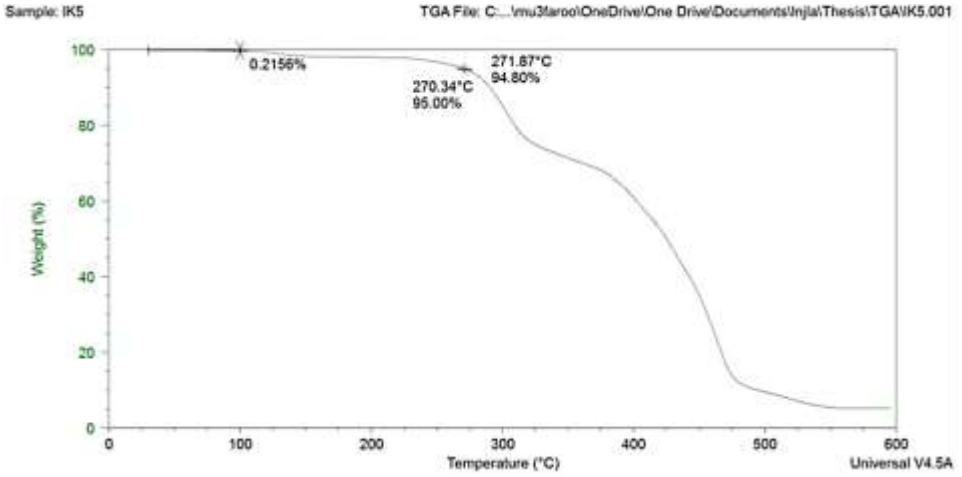

BS$_H$0M$_L$0.5

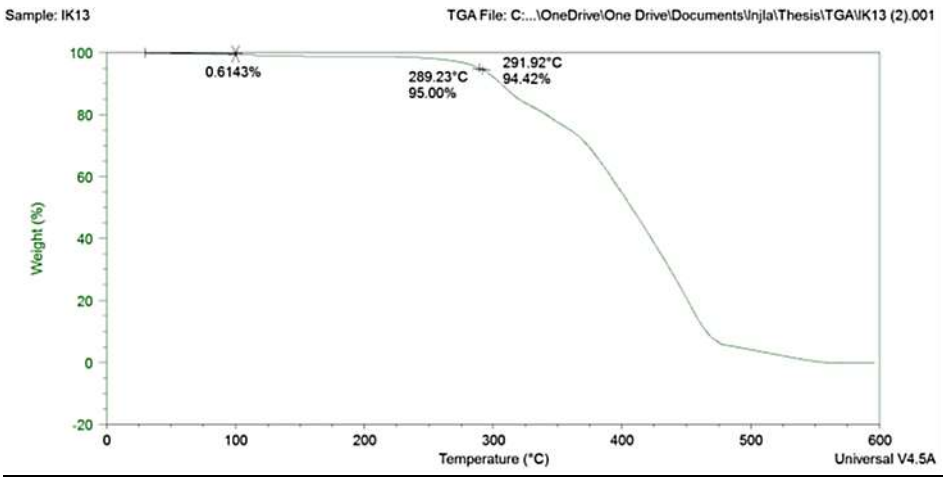

BS_H0M_L1

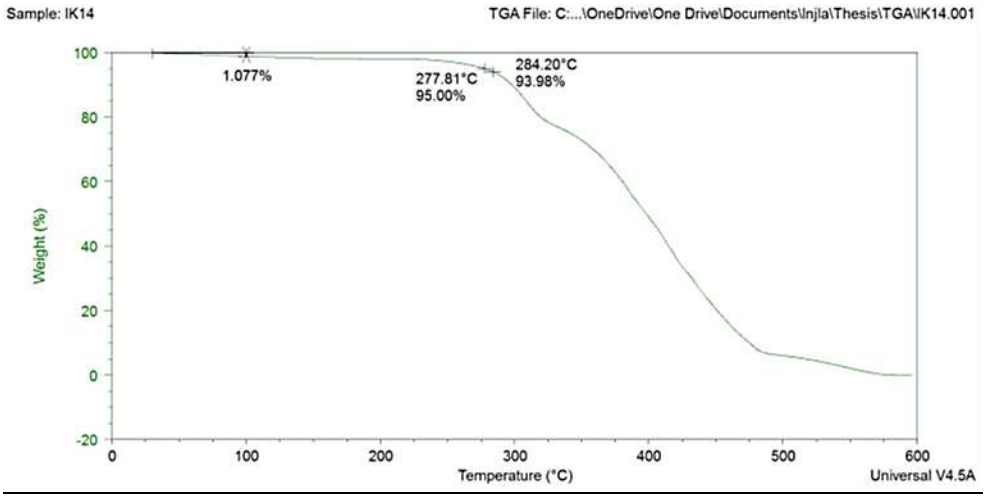

BS_H0M_L2

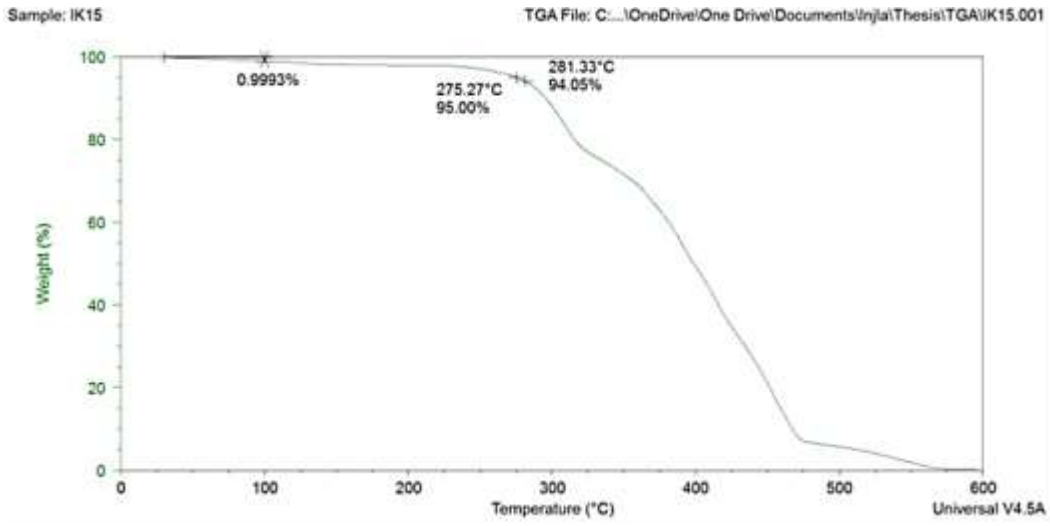

BS_H0M_L5

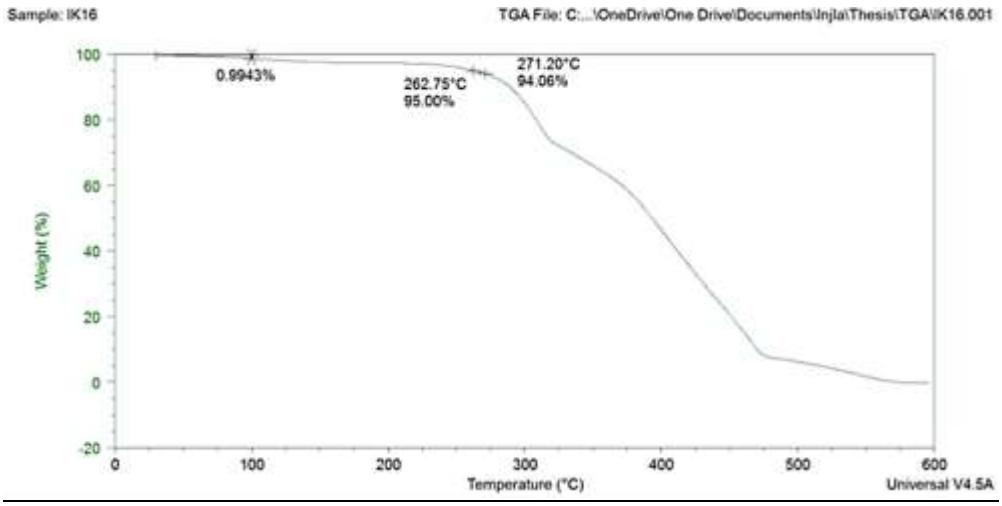

BS_H0FM_L

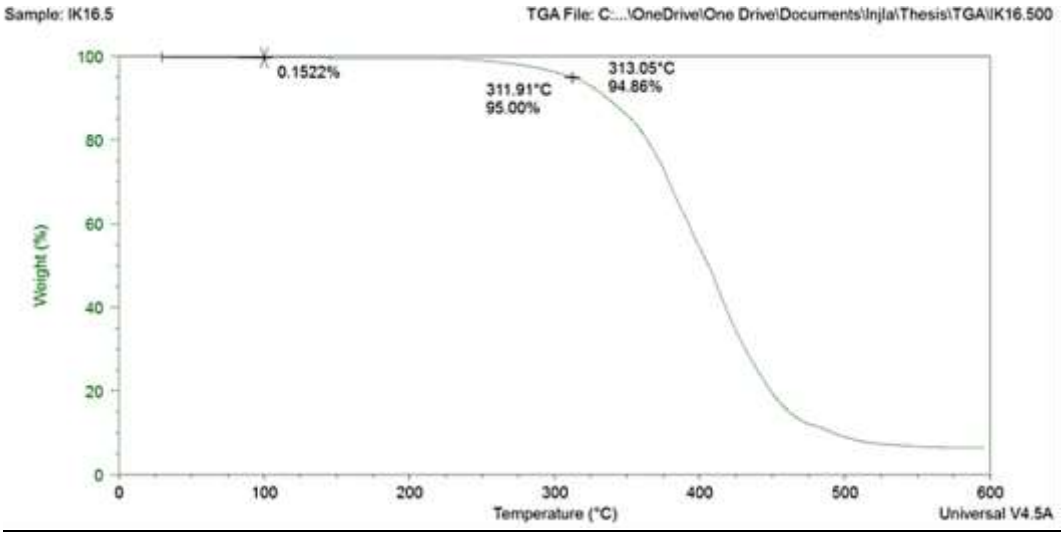

BS_H5FM_L

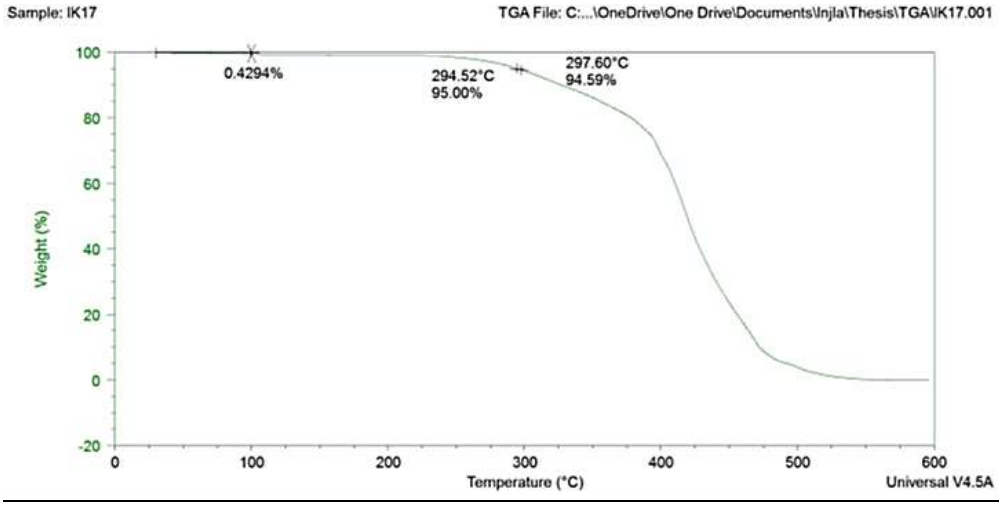

BS_H10FM_L

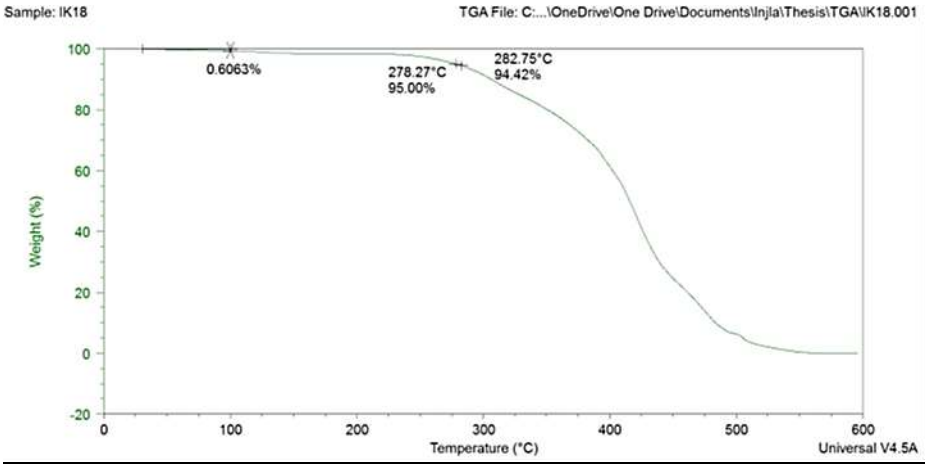

BS_H15FM_L

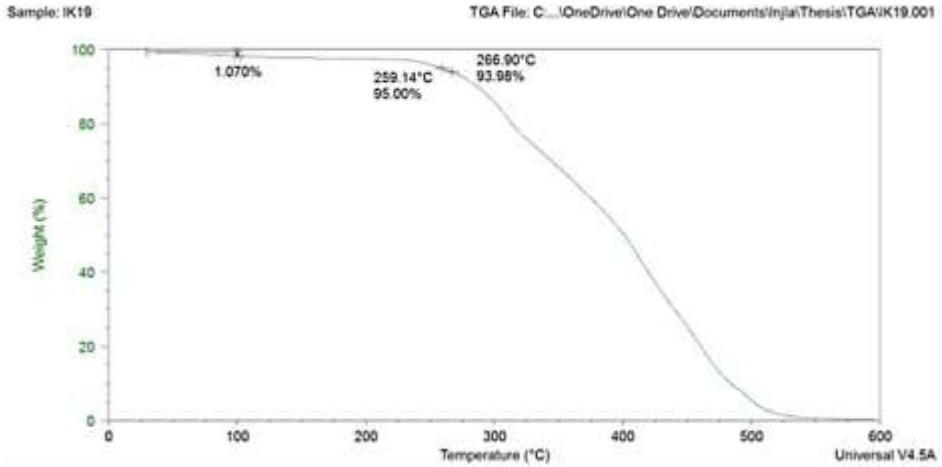

BS_H20FM_L

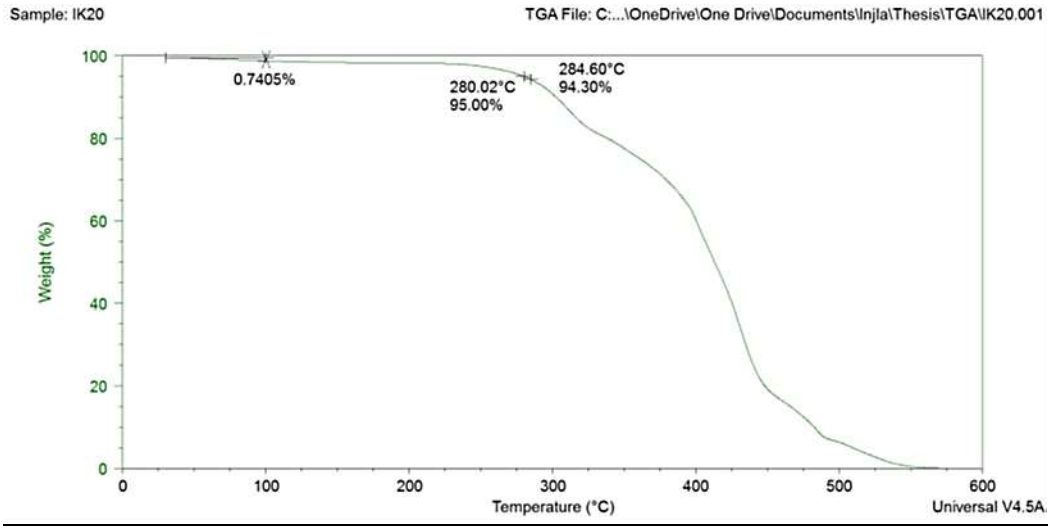

BS_HF5M_L

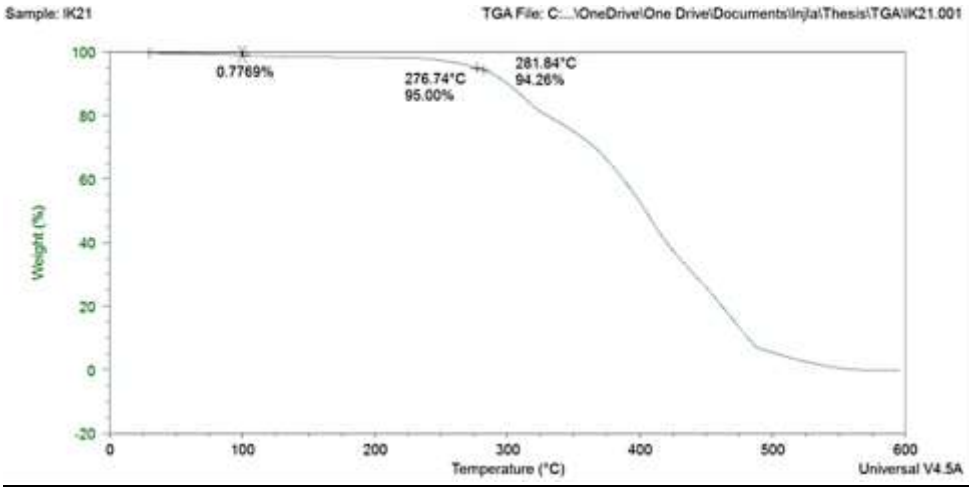

BS_HF10M_L

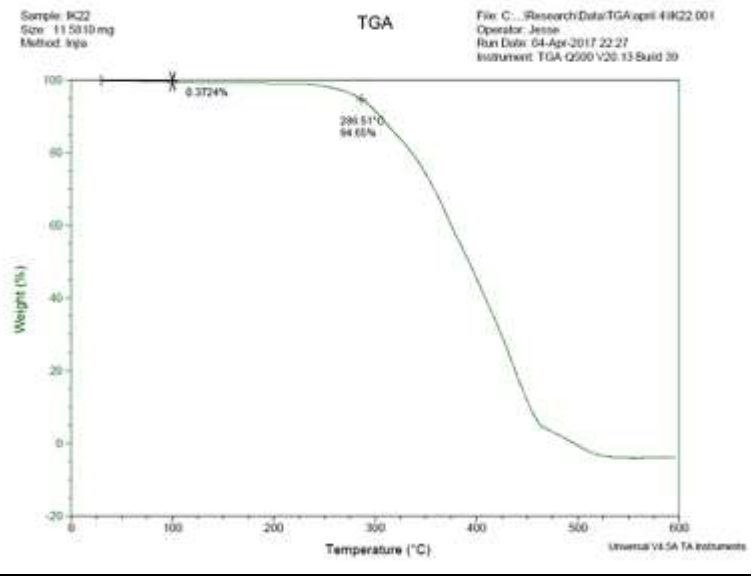

BS_HF15M_L

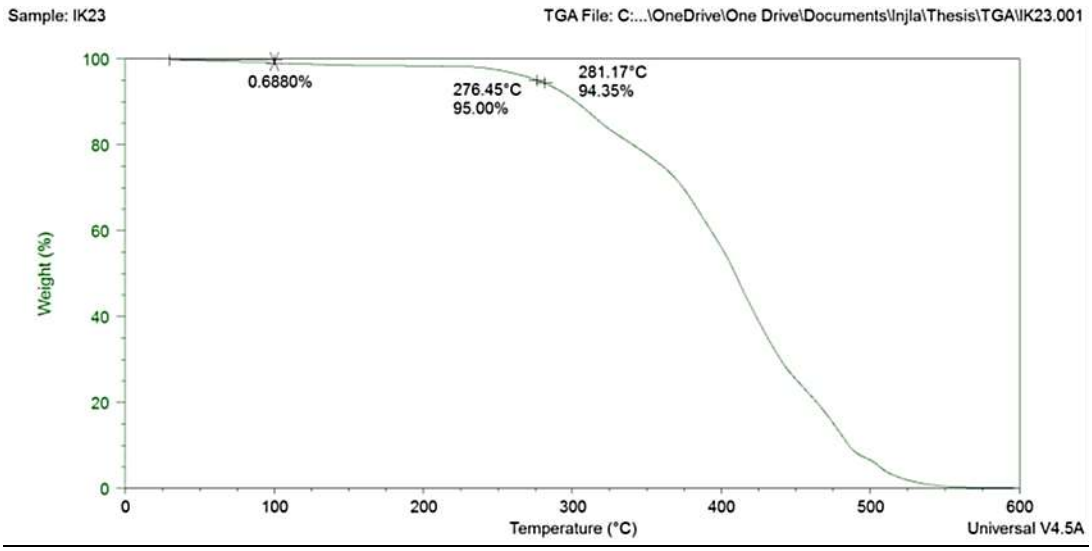

BS_HF20M_L

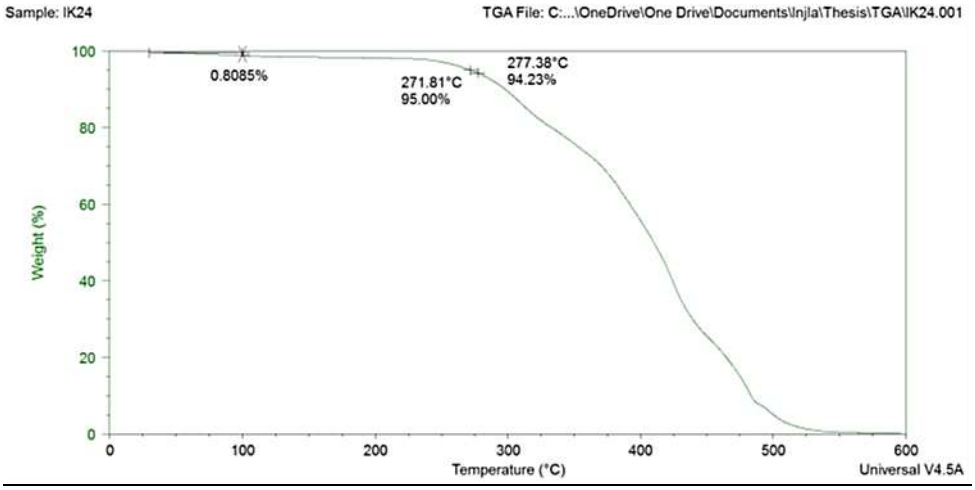

BS_HP20M_L

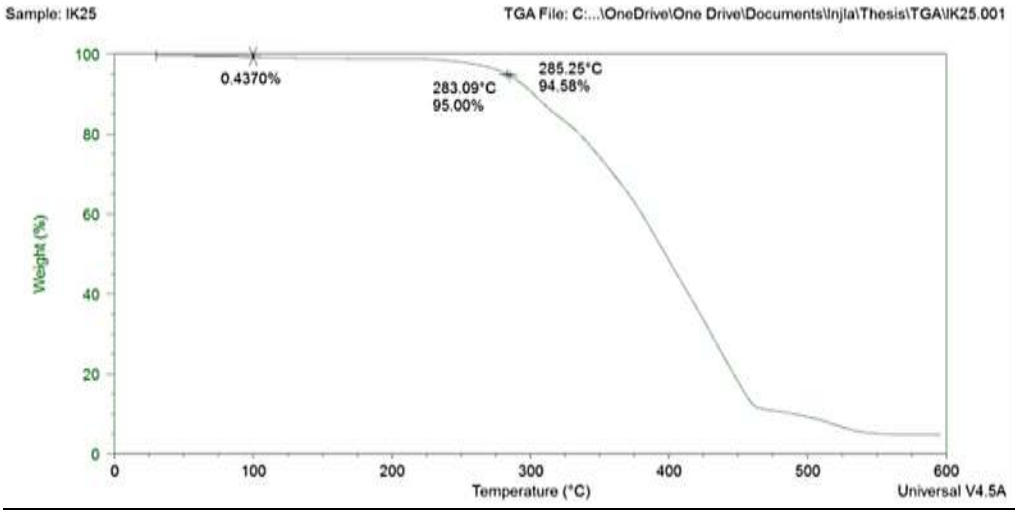

pS15FM$_L$

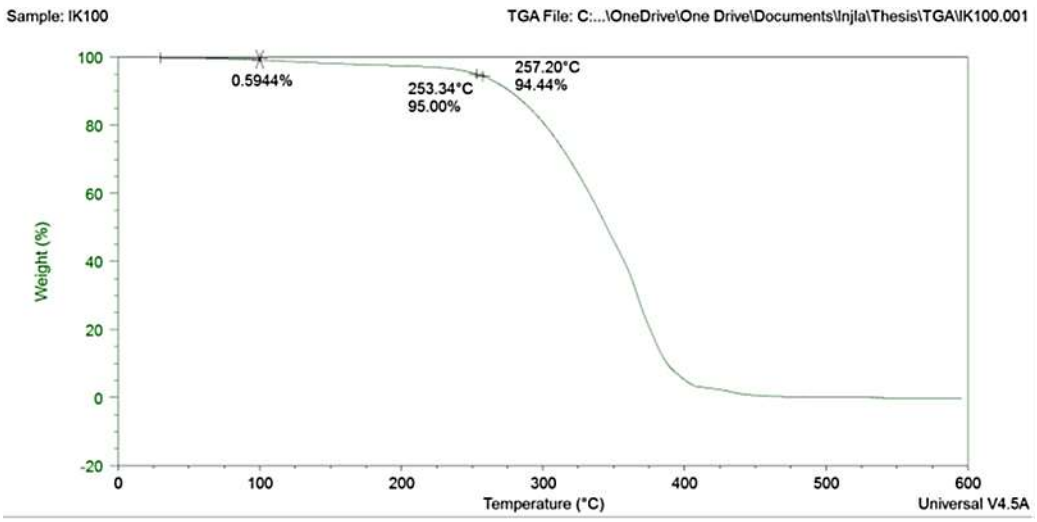

pS20FM$_L$

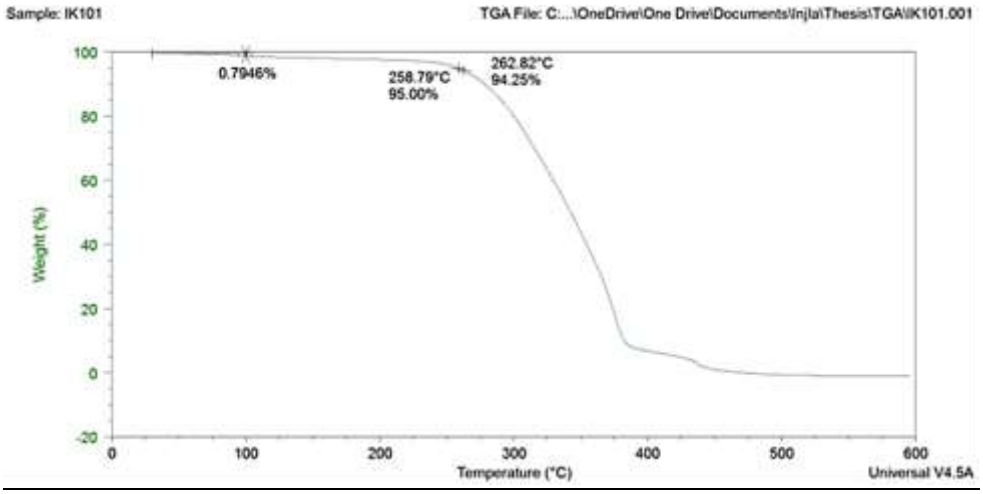

$RS_H0M_L0.5$

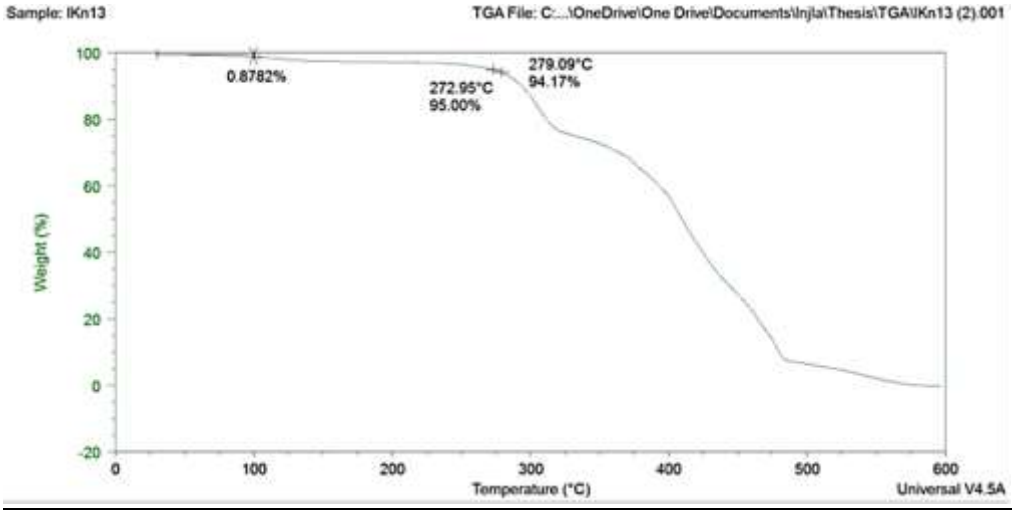

RS_H0M_L1

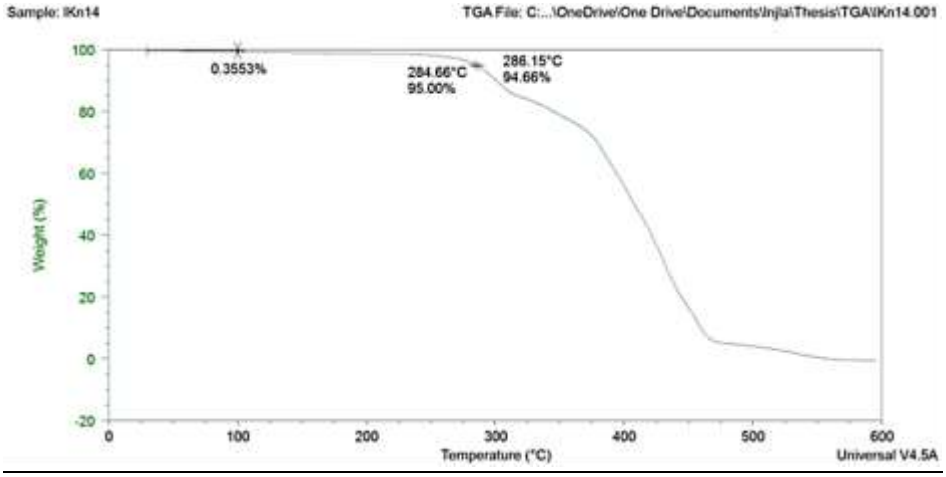

RS_H0M_L2

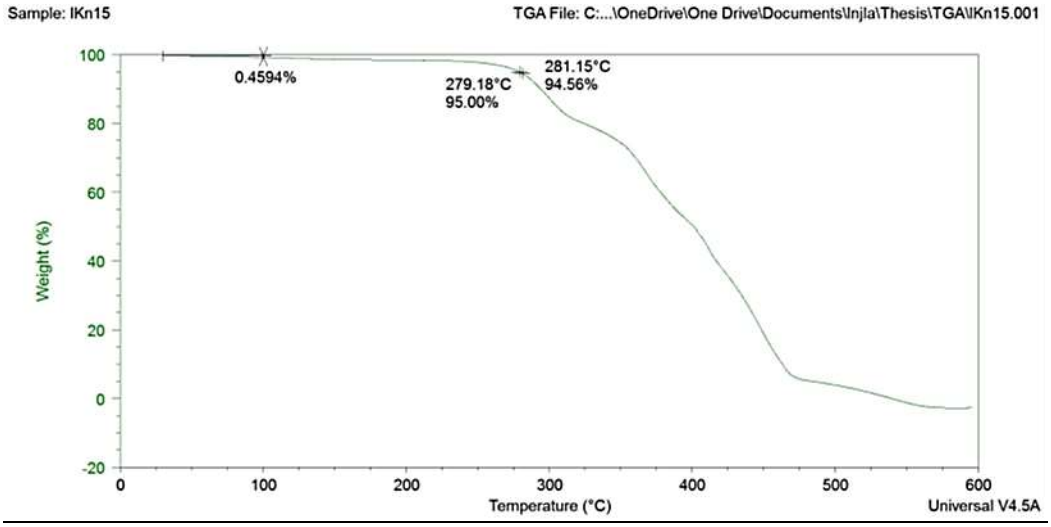

RS_H0M_L5

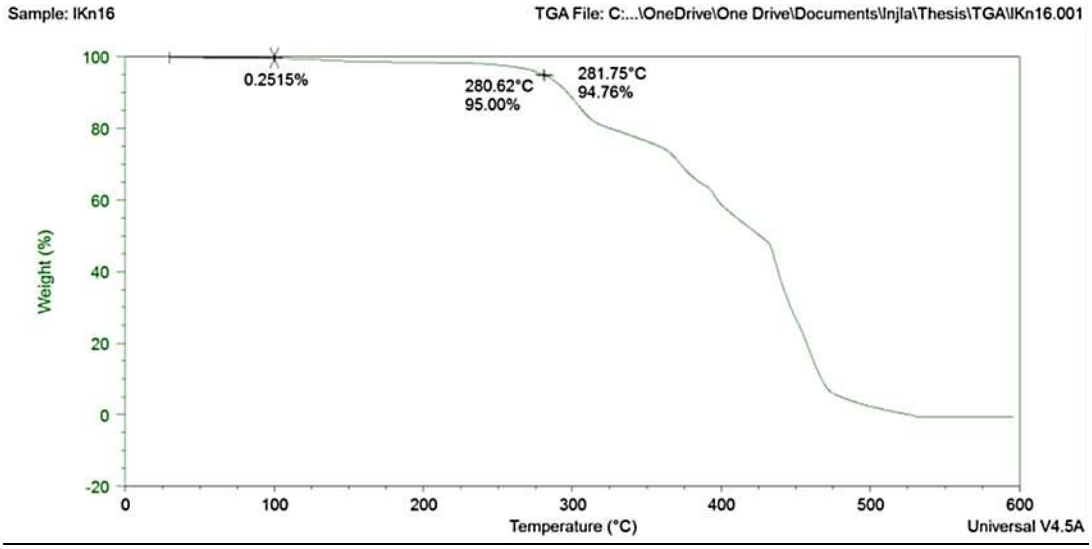

RS_H0FM_L

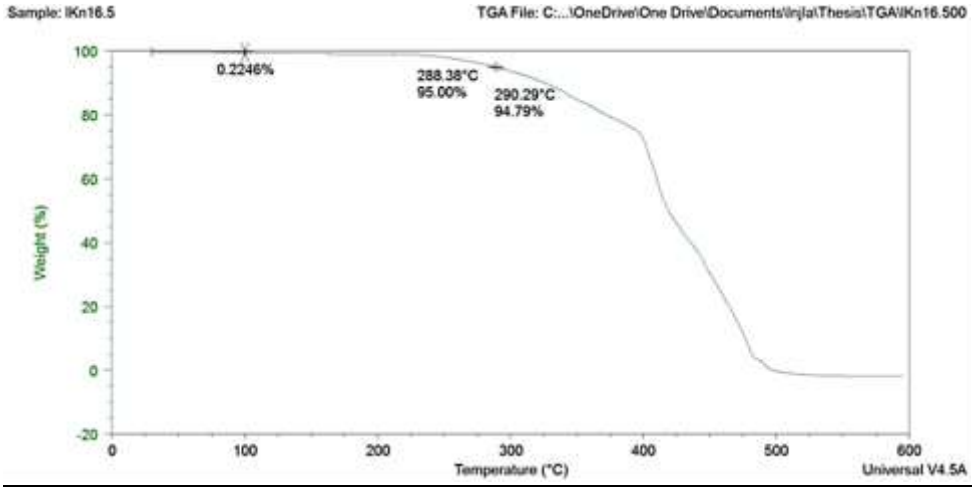

RS_H5FM_L

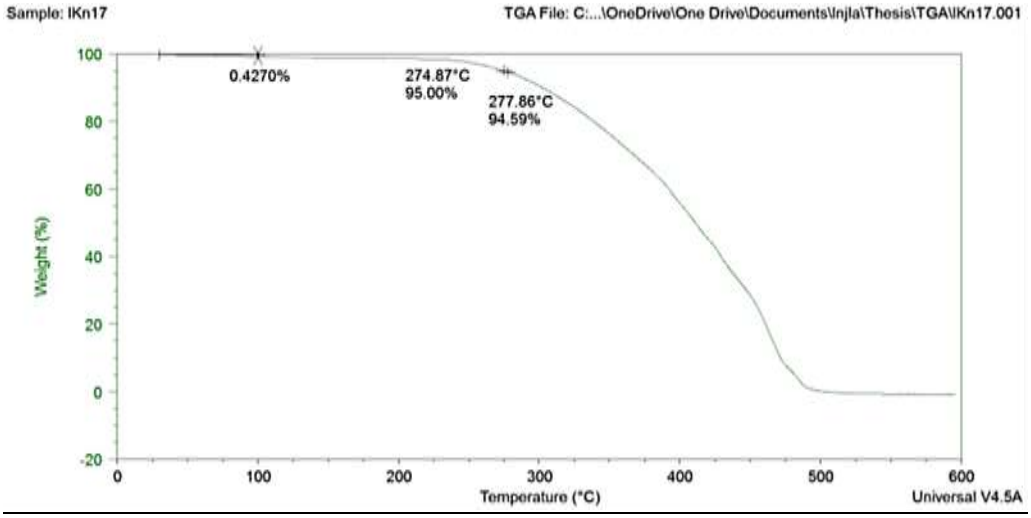

RS_H10FM_L

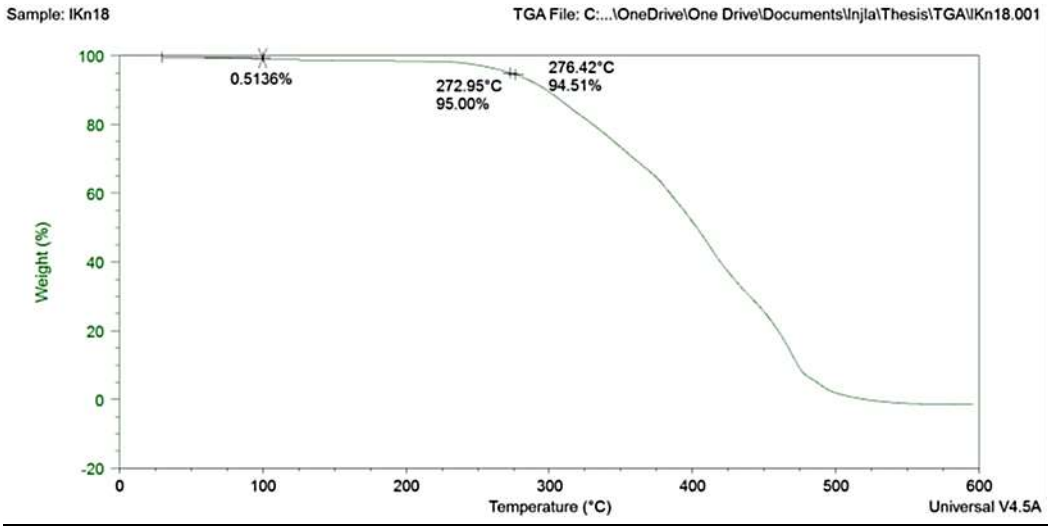

RS_H15FM_L

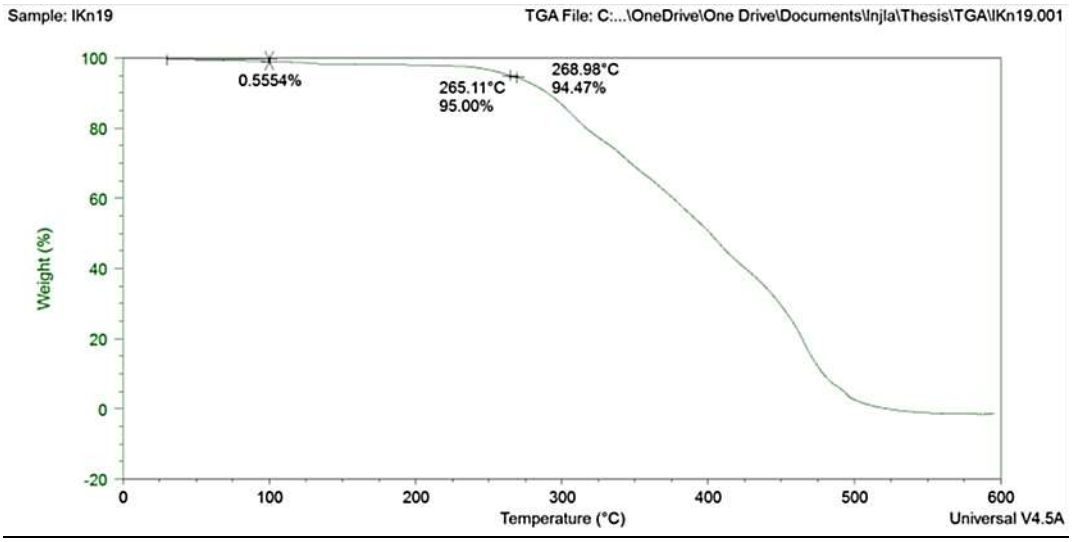

RS_H20FM_L

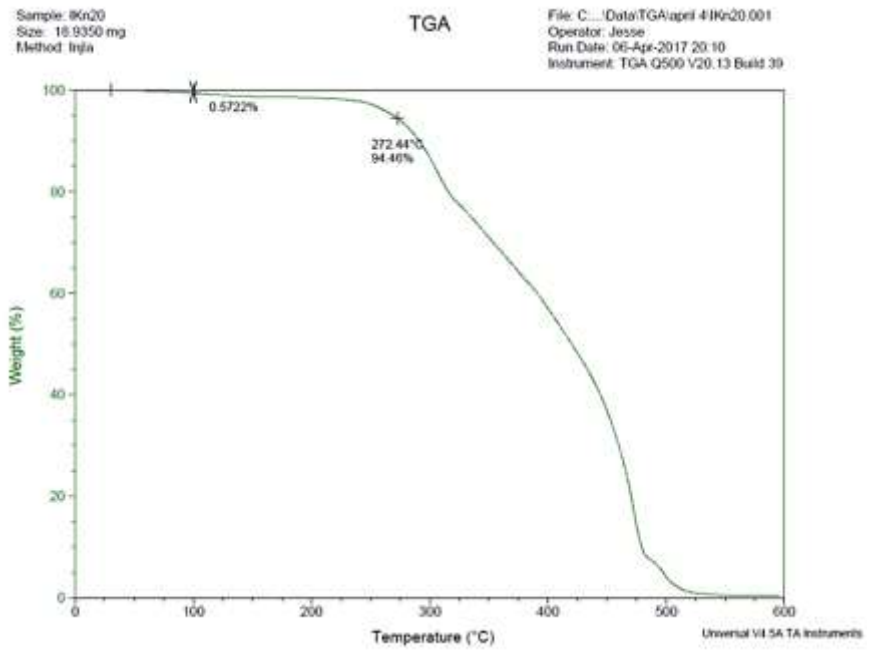

RS_HF5M_L

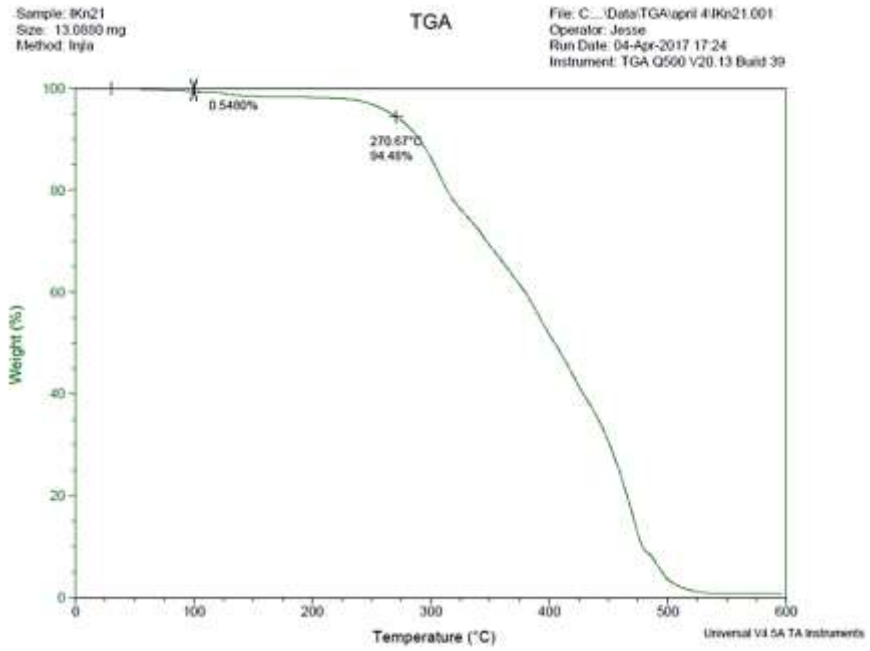

RS_HF10M_L

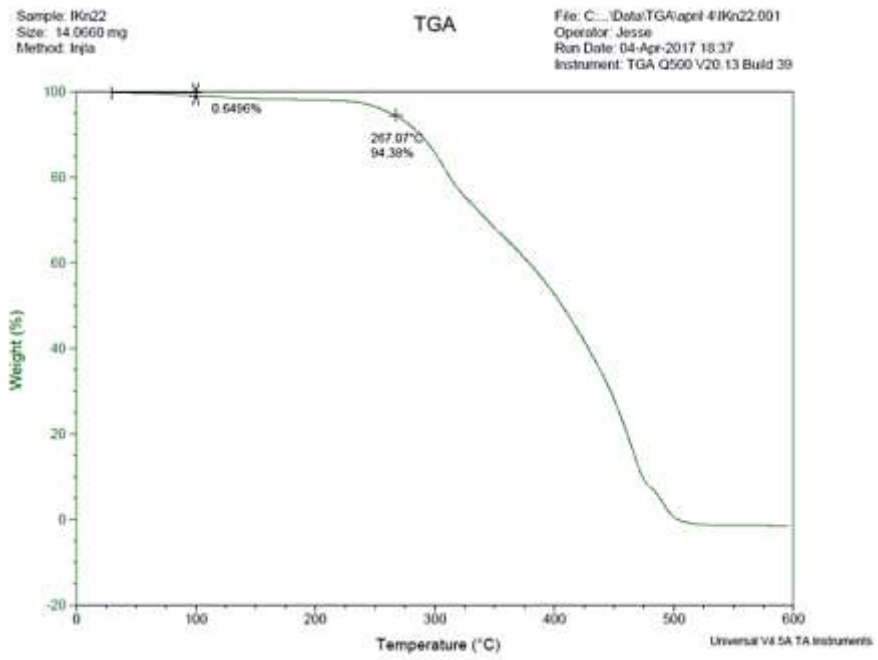

RS_HF20M_L

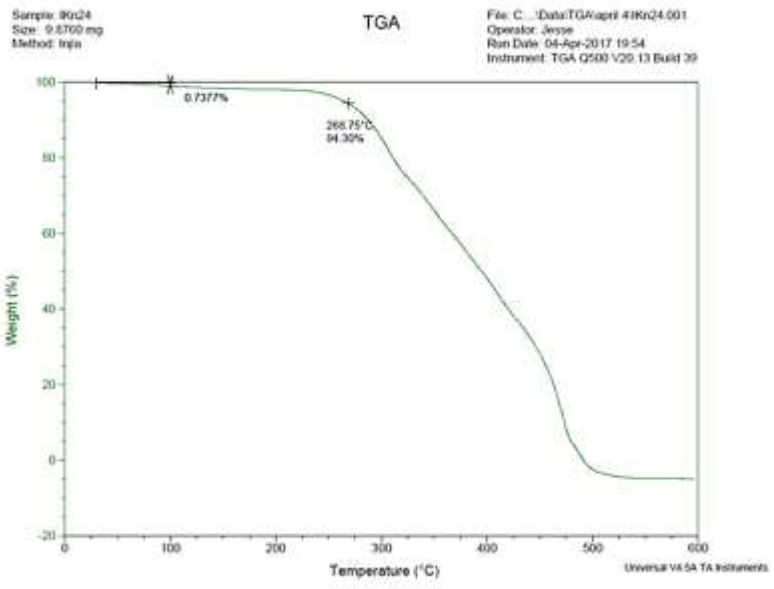

RS_HP20m_L

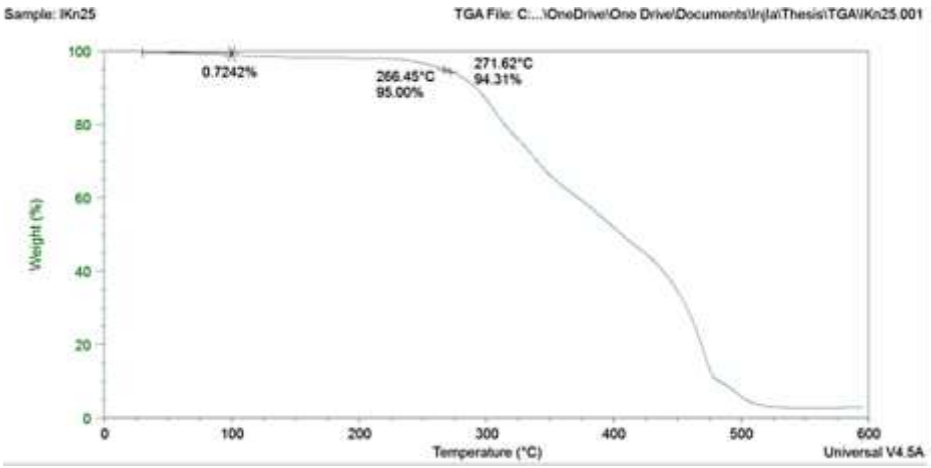

XRD

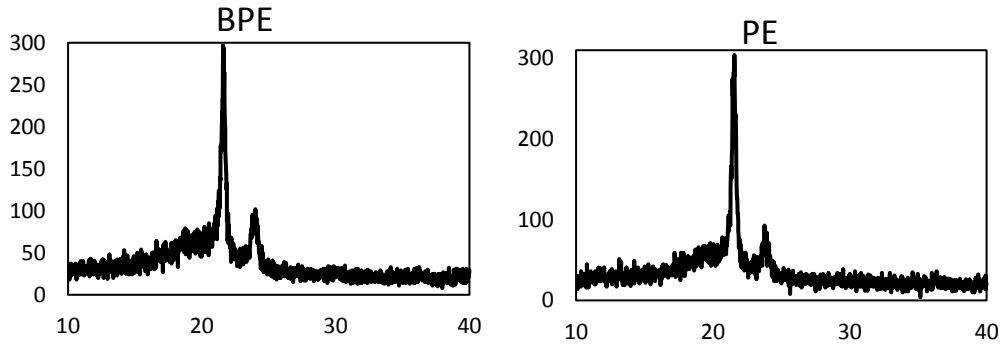

Table 14 List of work on PE/Natural Fiber Composites, Compatibilization Techniques and Results[2]

Fiber Type	Compatibilization Technique	Processing methods	Results	Reference
Wood Fiber	Silane and Isocyanate coupling	Extrusion	Increase in tensile properties after silane and isocyanate treatment	Raj et al. (1989)
Hardwood Pulp	Silane treatment, benzoyl peroxide (BPO) treatment	Barbender plasticorder	Significant increase in strength after treatment with BPO. Small improvement in strength after treatment with silane	Bataille et al. (1990)
Cellulose Fiber	Maleation of PE matrix	Internal mixer	Even slight maleation of PE increased adhesion significantly	Zhang et al. (2002b)
Wood Flour	Maleated PP	Extrusion	Coupling agent improved both stability and mechanical properties. It also improved dimensional stability of composites	Adhikari et al. (2007)
Pineapple leaf flour	Silane, Isocyanate and peroxide treatment	Solution mixing	Improved fiber-matrix interaction (after fiber treatment) produced increase in thermal stability	George et al. (1996)
Wood Flour	Coupling agent (MAPE, MAPP, acrylic acid grafted PE, maleated SEBS)	Extrusion	All compatibilizers increased tensile strength and modulus, Maleated LLDPE gave maximum tensile and impact strength	Wang et al. (2003)
Henequen	Alkalization, silane treatment, preimpregnation using dilute PE solution	Barbender intensive mixer	Alkalization and preimpregnation increased mechanical interlocking between phases. Silane treatment increased interfacial load transfer	Valadez-Gonzalez et al. (1999)
Sisal	Washing the fibers followed by treatment with 3% stearic acid	Compression molding	Pretreatment of fibers improved interfacial shear strength. Morphological observations showed less fiber pull out after treatment	Torres and Cubillas (2005)
Wood and Bagasse	Maleated coupling agent, carboxylated coupling agent, titanium derived mixture, (TDM)	Kneading in a hake rotor mixer	All compatibilizers improved compatibility between bagasse and matrix. TDM acted as lubricant in wood filled composite	Lei et al. (2007)

Caraua	Coupling Agents (maleated PE, PE (co-Vinyl acetate)	Extrusion	Maleated PE decreased thermal stability of composites more significantly than EVA	Araujo et al. (2008)
Coir	Silane, Alkalization, etherification	Heated two roll mill	Fiber treatment improved mechanical properties. Alkalization increased deformability of the composites, while silane made them more rigid.	Arrakhiz et al. (2012)